Role of tRNA methyltransferases in nervous system development and function

Jennifer L. Dumouchel

B.A. in Chemistry, Colby College, Waterville, ME. 2008.
M.S. in Chemistry, Northeastern University, Boston, MA. 2014

A dissertation submitted in partial fulfillment of the requirements for the degree of
- Doctor of Philosophy -
in the Therapeutic Sciences Graduate Program from
Brown University

Date of oral examination: May 27, 2025
Degree conferral: October 2025

Providence, RI, USA

This dissertation by Jennifer L. Dumouchel is accepted in its present form by the Therapeutic Sciences Graduate Program as satisfying the requirements for the Degree of Doctor of Philosophy.

Date:_____ _____

Kate M. O'Connor-Giles, Ph.D; Advisor

Recommended to the Graduate Council

Date:_____ _____

Nikos Tapinos, M.D./Ph.D; Committee Chair

Date:_____ _____

Erica Larschan, Ph.D; Reader

Date:_____ _____

Eric Morrow, M.D./Ph.D; Reader

Date:_____ _____

Dragony Fu, Ph.D
External Reader, University of Rochester

Approved by the Graduate Council

Date:_____ _____

Thomas A. Lewis, Ph.D; Dean of the Graduate School

Curriculum Vitae

Jennifer L. (Bushee) Dumouchel
Email: jennifer_dumouchel@brown.edu | ORCID: 0000-0001-9954-2149

EDUCATION

2019 - present	PhD Candidate, Therapeutic Sciences, Brown University
2011 - 2014	MS Chemistry, Northeastern University
2004 - 2008	BA Chemistry, Colby College

PROFESSIONAL EXPERIENCE

2019 - present	Graduate Researcher, Brown University, Providence, RI
2016 - 2019	Investigator I, Novartis, Cambridge MA
2014 - 2016	Scientist I, Novartis, Cambridge, MA
2011 - 2013	Scientific Associate II, Novartis, Cambridge, MA
2008 - 2010	Scientific Associate I, Novartis, Cambridge, MA
2007 - 2008	Undergraduate Student Research, Colby College, Waterville, ME
2006 - 2007	Summer Researcher, Pfizer, Inc. Groton, CT

RESEARCH EXPERIENCE

BROWN UNIVERSITY, Providence, RI
Therapeutic Sciences Graduate Program
Ph.D. Thesis Advisor: Dr. Kate O'Connor-Giles

- Applies genetic, behavioral, and biochemical approaches to investigate tRNA methyltransferases that regulate synapse and memory formation
- Implements multi-omic bioinformatics to study how tRNA modification dynamics influence nervous system development
- Mentors 3 junior scientists in *Drosophila* husbandry, genetics, biochemistry, behavior, and imaging studies where work is presented at scientific conferences and upcoming manuscripts

NOVARTIS INSTITUTES FOR BIOMEDICAL RESEARCH, Cambridge, MA
Departments: Metabolism & Pharmacokinetics (MAP, 2008 - 2013); Analytical Sciences and Imaging (ASI, 2014 - 2016); Pharmacokinetic Sciences (PKS, 2016 - 2019)

- Executed drug metabolism and pharmacokinetics studies for discovery chemistry teams that yielded over 40 preclinical research candidates, three investigational new drugs, and one FDA approved therapy (FABHALTA)
- Developed extrahepatic (ocular) metabolism platform as a first line screen for topical Ophthalmology programs, supported a 20% reduction of annual animal studies and improved due diligence practices
- Implemented in vitro strategies and mass spectrometry workflows to streamline early compound screening, reduce in vivo resources, improve metabolic liabilities, and mitigate toxicity and poor absorption, distribution, metabolism & excretion (ADME) properties

COLBY COLLEGE, Waterville, ME
Honors Thesis Advisor: Dr. Kevin P. Rice, Department of Chemistry

- Explored the effects of an anticancer sulfonylhydrazine on the activity of the base excision repair enzyme, apurinic endonuclease-1

PFIZER, INC., Groton, CT
Department: Pharmacokinetics Dynamics and Metabolism (PDM)

- Investigated the *in vitro/in vivo* correlation for aldehyde oxidase mediated metabolism of N-heterocyclic compounds to guide future clearance predictions for aldehyde oxidase substrates

TEACHING EXPERIENCE

BROWN UNIVERSITY

2022 - present	*Research Mentor*, O'Connor-Giles Lab *Brown University* 2024 - 2025 Kennedy Tyson, Neuroscience '26 2024 Emily Hill, MCB graduate student 2022 - 2024 William Kemball-Cook, Neuroscience '24
2025	*CIRTL Associate,* Center for the Integration of Research, Teaching, and Learning (CIRTL)
2021 - 2023	*Guest lecturer*, Physiology Pharmacology (BIOL 1260/2260)
2023	*Participant,* Sheridan Center, Teaching Consultant Program
2022	*Participant,* Sheridan Center, Reflective Teaching Certificate (Certificate I)
2021	*Teaching Assistant*, Brown/Pfizer Master's Program Physiology Pharmacology. 20 students. Responsible for discussion sections, weekly office hours, and 1 lecture
2020	*Teaching Assistant*, Physiology Pharmacology (BIOL 1260/2260) 115 students. Responsible for discussion sections, weekly office hours, and 1 lecture
2020	*Participant,* Sheridan Center, Teaching Essentials for Graduate Teaching Assistant Program

NOVARTIS

2016	*Instructor*, Bioanalysis Biotransformation workshop

COLBY COLLEGE

2008	Volunteer Scientist, Chemistry Magic Show for local 5th grade students
2006 - 2007	*Laboratory Grader*, Organic Chemistry (CH241 - CH242)
2005 - 2006	*Laboratory Assistant*, General Chemistry (CH141 - CH142)

PRESENTATIONS

2025	*A glial tRNA methyltransferase, linked to intellectual disability, coordinates neuronal development and function.* RNA Therapeutics: From Concept to Clinic. Worcester, MA.
2025	*tRNA methyltransferase in ensheathing glial modulates neuronal development and function*. Boston Area Drosophila Meeting. Boston, MA.
2022	*Exploring the novel role of a putative tRNA methyltransferase in synaptic growth and neuronal development.* TSGP T32 Retreat. Brown University, Providence, RI
2020	*Investigating the role of N6-methyl-adenoisine RNA in glioblastoma plasticity.* MPPB First Year Talks. Brown University, Providence, RI
2020	*A new vision for drug discovery: investigating ocular metabolism.* Invited Talk: Department of Chemistry Seminar Series. Colby College, Waterville, ME
2017	*Precision medicine in discovery: partnering medicinal chemistry with drug metabolism.* Invited Talk: AAPS Temple University Graduate Student Chapter Symposium – Drug Discovery and Development in the era of Precision Medicine. Temple University, Philadelphia, PA

PUBLICATIONS

*†equal contribution, *corresponding author, §co-corresponding & equal contributions*

Book Chapter

1. **Jennifer L Dumouchel*** and Valerie M. Kramlinger. *Chapter 29. Case Study 10. A case to investigate acetyl transferases kinetics.* In Enzyme Kinetics in Drug Metabolism: Fundamentals and Applications. 2nd Edition. Series: Methods in Molecular Biology. Editors: Swati Nagar, Upendra A. Argikar, and Donald Tweedie. Series Editor: John Walker. Springer / Humana Press.

Research Articles

1. Madhwani KR, Sayied S, Ogata CH, Hogan CA, Lentini JM, Mallik M, **Dumouchel JL**, Storkebaum E, Fu D, O'Connor-Giles KM. (2024) tRNA modification enzyme-dependent redox homeostasis regulates synapse formation and memory. *PNAS.* 121(46): e2317864121 PMID: 39495910
   Special Issue: RNAs & Their Intracellular Processing During Oxidative Stress
2. Hogan CA†, Gratz SJ†, and **Dumouchel JL†**, Thakur RS, Delgado A, Lentini JM, Madhawni KR, Fu D, O'Connor-Giles KM. (2023) Expanded tRNA methyltransferase family member TRMT9B regulates synaptic growth and function. *EMBO Reports.* 24: e56808. PMID: 37642556
3. Argikar UA, Blatter M, Bednarczyk D, Chen Z, Cho YS, Dore M, **Dumouchel JL**, Ho S, Hoegenauer K, Kawanami T, Mathieu S, Meredith E, Mobitz H, Murphy SK, Parthasarathy S, Pissot Soldermann C, Santos J, Silver S, Skolnik S,

Stokanovic A (2022) Paradoxical Increase of Permeability and Lipophilicity with the Increasing Topological Polar Surface Area within a Series of PRMT5 Inhibitors.
J Med Chem. 65(18):12386-12402. PMID: 36069672

4. Balhara A, Basit A, Argikar A, **Dumouchel J**, Singh S, Prasad B. (2021) Comparative proteomics analysis of the post mitochondrial supernatant fraction of human lens-free whole eye and liver. *Drug Metab Dispos*. 49(7): 592 - 600 PMID: 33952609
5. **Dumouchel JL**[§], Argikar UA[§], Adams CM, Prasanna G, Ehara T, Kim S, Breen C, Mogi M. (2020) Understanding metabolism related differences in ocular efficacy of MGV354. *Xenobiotica*. 51(1): 5-14. PMID: 32662714
[§]*co-corresponding authors & equal contributions*
6. **Dumouchel JL**, Chemuturi N, Milton MN, Camenisch G, Chastain JE, Walles M, Sasseville V, Gunduz M, Iyer G, Argikar UA. (2018) Models and approaches describing metabolism, transport, and toxicity of drugs administered by the ocular route. *Drug Metab Dispos.* 46:1670-1683. PMID: 30111625
7. Gunduz M, Argikar UA, Cirello AL, **Dumouchel JL**. (2018) New perspectives on acyl glucuronide risk assessment in drug discovery: Investigation of in vitro stability, in situ reactivity, and bioactivation. *Drug Metab Lett*. 12(2): 84-92. PMID: 29886840
8. Gunduz M, Cirello AL, Klimko P, **Dumouchel JL**, and Argikar UA. (2017) Genotoxicity of 4-(piperazine-1-yl)-8-(trifluoromethyl)pyrido[2,3-e] [1,2,4]triazole[4,30a]pyrazine, a Potent H4 Receptor Antagonist for the Treatment of Allergy: Evidence of glyoxal intermediate involvement. *Drug Metab Lett*. 11: 144-148. PMID: 29110630
9. **Dumouchel JL***, Argikar UA, Spear J, Brown A, Dunne CE, Kramlinger VM, Cirello AL, and Gunduz M. (2017) Investigation of Ocular Bioactivation Potential and the Role of Cytochrome P450 2D Enzymes in Rat. *Drug Metab Lett*. 11: 102-110. PMID: 28891437
10. Argikar UA, **Dumouchel JL**, Dunne CE, and Bushee AJ. (2017) Ocular Non-P450 oxidative, reductive, hydrolytic and conjugative drug metabolizing enzymes. *Drug Metab Reviews*. 49 (3):372-394. PMID: 28438049
11. Argikar UA, **Dumouchel JL**, Kramlinger VM, Cirello AL, Gunduz M, Dunne CE, and Sohal B. (2017) Do we need to study metabolism and distribution in the eye: Why, when, and are we there yet? *J Pharm Sci*. 106: 2276-2281. PMID: 28322939
Invited mini-review for a special issue dedicated to Prof. Yuichi Sugiyama.
12. Cirello AL, **Dumouchel JL**, Gunduz M, Dunne CE, and Argikar UA. (2017) In vitro ocular metabolism and bioactivation of ketoconazole in rat, rabbit, and human. *Drug Metab Pharmacokinet.* 32: 121-126. PMID: 28139372
13. Argikar UA, **Dumouchel JL**, Dunne CE, Saran C, Cirello AL, and Gunduz M. (2016) Ocular metabolism of levobunolol: Historic and emerging metabolic pathways. *Drug Metab Dispos.* 44:1304-1312. PMID: 27190057

14. **Bushee JL**, Dunne CE, and Argikar UA. (2015) An in vitro approach to investigate ocular metabolism of a topical, selective β1-adrenergic block agent, betaxolol. *Xenobiotica* 45(5): 396-405. PMID: 25475994
15. **Bushee JL**, Liang G, Dunne CE, Harriman SP, and Argikar UA. (2014) Identification of saturated and unsaturated fatty acids released during microsomal incubations. *Xenobiotica*. 44(8): 687-695. PMID: 24502389
16. Dunne CE[†], **Bushee JL[†]**, and Argikar UA. (2013) Metabolism of bromopride in mouse, rat, rabbit, dog, monkey, and human hepatocytes. *Drug Metab Pharmacokinet*. 28(6): 453-461. PMID: 23615565
17. Gunduz M, Argikar UA, Kamel A, Colizza K, **Bushee JL**, Cirello A, Lombardo F, and Harriman S. (2012) Oxidative *ipso* Substitution of 2,4-Difluoro-benzylphthalazines: Identification of a Rare Stable Quinone Methide and Subsequent GSH Conjugate. *Drug Metab Dispos*. 40, 2074-2080. PMID: 22851614
18. **Bushee JL** and Argikar UA. (2011) An experimental approach to enhance precursor ion fragmentation for metabolite identification studies: application of dual collision cells in an orbital trap. *Rapid Commun Mass Spectrom*. 25: 1356 - 1362. PMID: 21504000
19. Argikar UA, Liang G, **Bushee JL**, Hosagrahara V, and Lee W. (2011) Effects of pharmaceutical excipients on 4-methylumbelliferone glucuronidation: An application for compounds with low solubility. *Drug Metab Pharmacokinet*. 26: 102-106. PMID: 21084760

POSTERS

1. **Jennifer L. Dumouchel**, Emily Hill, Rajan S Thakur, Scott J Gratz, Dragony Fu, Kate M. O'Connor-Giles. A glial tRNA methyltransferase, linked to intellectual disability, coordinates neuronal development and function. RNA Therapeutics: From Concept to Clinic. June 2025, Worcester, MA.
2. **Jennifer L. Dumouchel**, Emily Hill, Sara Rios Mendez, Kimberly Rose Madhwani, Dragony Fu, Kate M. O'Connor-Giles. TRMT1, a tRNA methyltransferase linked to intellectual disability, acts in glia to promote nervous system development. Gordon Research Conference on Glia Biology & Gordon Research Seminar on Glial Biology. March 2025, Ventura, CA.
3. **Jennifer L. Dumouchel**, Emily Hill, Sara Rios Mendez, Kimberly Rose Madhwani, Dragony Fu, Kate M. O'Connor-Giles. TRMT1, a tRNA methyltransferase linked to intellectual disability, acts in glia to promote nervous system development. **Jennifer L. Dumouchel**, Sara Rios Mendez, Kimberly Rose Madhwani, Kate M. O'Connor-Giles. tRNA methyltransferase 1 promotes nervous system development. Keystone Symposia: Regulatory RNA. December 2023, Banff, Alberta, Canada.
4. **Jennifer L. Dumouchel**, Kimberly Rose Madhwani, Caley Hogan, Rajan Thakur, Scott J. Gratz, Jenna Lentini, Dragony Fu, Kate M. O'Connor-Giles. Regulation of synaptic growth through epitranscriptomic and translational changes. EMBO Practical Course Measuring translational dynamics by ribosome profiling. March 2023, EMBL Heidelberg, Germany.

5. **Jennifer L. Dumouchel**, Kimberly Rose Madhwani, Caley Hogan, Rajan Thakur, Scott J. Gratz, Jenna Lentini, Dragony Fu, Kate M. O'Connor-Giles. Exploring the novel role of a putative tRNA methyltransferase in synaptic growth and neuronal development. Drosophila Research Conference. April 2022, San Diego, CA.
6. **Jennifer L. Dumouchel**, Upendra A. Argikar, Takeru Ehara, Doug Bevan, Nan Ji, Christopher M. Adams, Muneto Mogi, and Ganesh Prasanna. Understanding differences in in vitro metabolism of MGV354 in rabbit and human. Gordon Research Conference on Drug Metabolism. July 2019, Holderness, NH.
7. Marc Vrana, Theresa Aliwarga, **Jennifer Dumouchel**, Upendra Argikar, Rheem Totah, and Bhagwat Prasad. Tissue-specific mechanisms of irinotecan metabolism. 22nd North American Meeting, International Society for the Study of Xenobiotics, July 2018, Montreal, Canada.
8. **Jennifer L. Dumouchel**, Upendra A. Argikar, and Mithat Gunduz. Analysis of physicochemical properties and ocular metabolic pathways of clinical drugs and new chemical entities: Gaps in a Drug Metabolism Tool Box for Ophthalmology. Gordon Research Conference on Drug Metabolism. July 2018, Holderness, NH.
9. Mithat Gunduz, Amanda Cirello, **Jennifer L. Dumouchel**, Dominik Hainzl, Tony D'Alessio, Carl Bialucha, Vladimir Capka and Upendra A. Argikar; In Vitro Investigation of Catabolism and Metabolism of Antibody Drug Conjugates. 21st North American ISSX Meeting. September 24-28 2017, Providence, RI.
10. **Jennifer L. Dumouchel**, Upendra A. Argikar, Adhiraj Lanba, and Christine E. Dunne. Metabolism of antiglaucoma agents by ocular N-acetyltransferases. Gordon Research Conference on Drug Metabolism. July 2017, Holderness, NH.
11. **Jennifer L. Dumouchel**, Upendra A. Argikar, and John Miners. Does CYP2C8 metabolize glucuronides? Gordon Research Conference on Drug Metabolism. July 2017, Holderness, NH.
12. Rutali Brahme, **Jennifer Dumouchel**, and Upendra Argikar. Strain and sex differences in metabolism in rats: Assessment of buspirone metabolism by high resolution LCMS/MS analysis. 65th ASMS Conference on Mass Spectrometry and Allied Topics. June 2017, Indianapolis, IN.
13. **Jennifer L. Dumouchel**, Upendra A. Argikar, and Christine E. Dunne. In Vitro Characterization of Timolol Metabolism in Rabbit Ocular and Liver S9 Fractions. Annual meeting of the American Association of Pharmaceutical Scientists. November 2016, Denver, CO.
14. Upendra A. Argikar, **Jennifer L. Dumouchel**, Christine E. Dunne, Amanda L. Cirello, Mithat Gunduz, and Valerie M. Kramlinger. Formation of active metabolites in ocular and liver S9 fractions: considerations for topical ocular route of administration. Gordon Research Conference on Drug Metabolism. July 2016, Holderness, NH.
15. **Jennifer L. Bushee**, Upendra A. Argikar, Christine E. Dunne. Assessment of active metabolites of levobunolol and betaxolol in rat, rabbit and human ocular and liver S9 fractions. Gordon Research Conference on Drug Metabolism. July 2015, Holderness, NH.

16. Upendra A. Argikar, **Jennifer L. Bushee**, Christine E. Dunne. Characterization of carteolol metabolism in rat, rabbit, and human ocular and liver S9 fractions. 250th National Meeting of American Chemical Society. August 2015, Boston, MA.
17. **Jennifer L. Bushee**, Christine E. Dunne, Upendra A. Argikar. Characterization of metipranolol metabolism in rat, rabbit, and human ocular and liver S9 fractions. 250th National Meeting of American Chemical Society. August 2015, Boston, MA.
18. **Jennifer L. Bushee**, Upendra A. Argikar, Christine E. Dunne. Assessment of active metabolites of levobunolol and betaxolol in rat, rabbit and human ocular and liver S9 fractions. 1024.5. Experimental Biology, Annual Meeting of American Society for Pharmacology and Experimental Therapeutics. April 2015, Boston, MA.
19. **Jennifer L. Bushee**, Christine E. Dunne, Upendra A. Argikar. In vitro acetylation of seven anti-glaucoma agents in rat, rabbit and human ocular and liver S9 fractions. 622.8. Experimental Biology, Annual Meeting of American Society for Pharmacology and Experimental Therapeutics. April 2015, Boston, MA.
20. Upendra A. Argikar, **Jennifer L. Bushee**, Christine E. Dunne, Amanda L. Cirello, and Mithat Gunduz. An in vitro approach to investigate ocular metabolism: Biotransformation of carteolol, pindolol, ketoconazole, and miconazole in ocular and liver S9 fractions. Gordon Research Conference on Drug Metabolism. July 2014, Holderness, NH.
21. Upendra A. Argikar, Myrtha D. Damzal, Adam Amaral, Panos Hatsis, **Jennifer L. Bushee**, Danuta Lubicka, and Suzie A. Ferreira. Optimization of CYP knock-out in vivo models – rats and mice. 10th International Society for the Study of Xenobiotics. September – October 2013, Toronto, Canada.
22. Upendra A. Argikar, **Jennifer L. Bushee**, and Amin Kamel. Glucuronidation of troglitazone in UGT1A1*1/*1, UGT1A1*1/*28 and UGT1A1*28/*28 genotyped and pooled human liver microsomes. Gordon Research Conference on Drug Metabolism. July 2013, Holderness, NH. (Invited Poster)
23. **Jennifer L. Bushee**, Christine E. Dunne, Kevin Colizza, Amanda Cirello, and Upendra A. Argikar. Characterization of bromopride and metoclopramide N-O-glucuronides in human hepatocytes by HPLC/ESI/FTMS/MS and hydrogen deuterium exchange. 61st ASMS Conference on Mass Spectrometry and Allied Topics. June 2013, Minneapolis, MN.
24. Joshua L. Johnson, Upendra Argikar, **Jennifer Bushee**, Amin Kamel and Shawn Harriman. Proteomic Characterization of Ocular S9 Fractions for Biotransformation Studies in Ophthalmic Drug Discovery. 61st ASMS Conference on Mass Spectrometry and Allied Topics. June 2013. Minneapolis, MN.
25. Christine Dunne, **Jennifer L. Bushee**, Shawn Harriman, and Upendra A. Argikar. Evaluation of Time Dependent Inactivation (TDI) of UGT1A1 by ketoprofen, ibuprofen, gemfibrozil and UGT2B7 by benoxaprofen, zomepirac, gemfibrozil. 18th North American Meeting, International Society for the Study of Xenobiotics. October 2012, Dallas, TX.
26. Mithat Gunduz, Amin Kamel, **Jennifer L. Bushee**, Upendra A. Argikar, Kevin Colizza, Amanda Cirello, Franco Lombardo, and Shawn Harriman. Investigation of the Mechanism Leading to Time Dependent Inhibition (TDI) for Compound 1, a

Candidate for Anti-Proliferative Project. 18th North American Regional ISSX Meeting. October 2012, Dallas, TX.

27. **Jennifer L. Bushee**, Guiqing Liang, Christine Dunne, Upendra A. Argikar, and Shawn Harriman. Identification of saturated and unsaturated fatty acids as microsomal degradation by-products by high resolution ESI MS/MS.18th North American Meeting, International Society for the Study of Xenobiotics, October 2012, Dallas, TX.
28. Christine Dunne, **Jennifer Bushee**, and Upendra Argikar. In vitro metabolite identification of the antiemetic drug bromopride in preclinical species and human hepatocytes using HPLC/ESI/FTMS. TP502. 60th ASMS Conference on Mass Spectrometry and Allied Topics, May 2012, Vancouver, BC, Canada.
29. Christine Dunne, **Jennifer Bushee**, and Upendra A. Argikar. In vitro metabolite identification of the antiemetic drug bromopride in rat and dog hepatocytes using HPLC/ESI/FTMS. International Conference for Young Chemists (ICYC). April 2012, at the University of Jordan, Amman, Jordan.
30. **Jennifer L. Bushee**, Mithat Gunduz, Kevin Colizza, Amin Kamel, Shawn Harriman and Upendra A. Argikar. Evaluation of broad-spectrum, irreversible CYP450 inhibitors and an inhibition cocktail for metabolite identification studies. 17th North American ISSX Meeting. October 2011, Atlanta, GA.
31. Mithat Gunduz*†*, **Jennifer L. Bushee***†*, Upendra A. Argikar, Giuliano Berellini, Kevin Colizza, Hong Jiang, Michelle Dennehy, Amanda Cirello, Nigel Waters, Amin Kamel, Franco Lombardo and Shawn Harriman. Comparative analyses of in vitro biotransformation in human liver microsomes and MetaSite based in silico predictions for 70 new chemical entities. P46. 17th North American ISSX Meeting, October 2011, Atlanta, GA.
32. Amin Kamel, Mithat Gunduz, Kevin Colizza, **Jennifer Bushee**, Upendra Argikar, Franco Lombardo and Shawn Harriman. Mechanistic studies on Nefazodone side chain cleavage using 18O2: A Baeyer-Villiger oxidation specifically catalyzed by CYP3A4 through a ferric peroxide intermediate. P254. 17th North American ISSX Meeting. October 2011, Atlanta, GA.
33. Na Pi, Shane Tichy, Adam Amaral, **Jennifer Bushee**, Upendra Argikar, Jakal Amin, and Panos Hatsis. High Resolution MS and MS/MS for Pharmacokinetics Analysis of Clozapine and Quantitation and Characterization of its Metabolite in Rat Plasma. # TP 242, 59th ASMS Conference on Mass Spectrometry and Allied Topics. June 2011, Denver, CO.
34. **Jennifer L. Bushee**, Guiqing Liang, Upendra A. Argikar and Shawn P. Harriman. Identification of fatty acids as microsomal degradation by-products in the presence and absence of bovine serum albumin by using CAD/ESI/MS/MS. The 59th ASMS Conference on Mass Spectrometry and Allied Topics. June 2011, Denver, CO.
35. Mithat Gunduz, Kevin Colizza, **Jennifer Bushee^**, Upendra A. Argikar^, Hong Jiang^, Michelle Dennehy^, Amin Kamel, Franco Lombardo and Shawn Harriman. Assessment of a human in vitro system as an alternative for S-9 fraction to predict in vivo metabolic profiles for drugs. Drug Metabolism Reviews; 42 (Suppl. 1) Published: Aug 2010. 9th International Meeting, International

Society for the Study of Xenobiotics, Sep 4 – 8, 2010. Istanbul, Turkey. (^ denotes that the authors were added after abstract submission)

36. **Jennifer L. Bushee** and Upendra A. Argikar. Experimental approach to enhance parent ion fragmentation for metabolite identification studies: Application of stepped CID and HCD in an Orbitrap-XL. 240th American Chemical Society National Meeting. August 2010, Boston, MA.
37. Upendra A. Argikar, Guiqing Liang, **Jennifer L. Bushee**, Vinayak Hosagrahara, Wendy Lee, Lipa Shah, and Sudhakar Garad. Effects of pharmaceutical excipients on 4-methyl umbelliferone glucuronidation: An application for compounds with low solubility. 240th American Chemical Society National Meeting. August 2010, Boston, MA.
38. Abbie M. Frederick, Marguerite L. Davis, **Jennifer L. Bushee**, Kristina M. Langenborg, Roxy Ghazvinian, Jessica-Ashley Williams, Krishnamurthy Shyam, Alan C. Sartorelli, and Kevin P. Rice. The consequences of carbamoylating activity from anticancer sulfonylhydrazines on the enzymes of DNA base excision repair. 100th Annual meeting of the American Association for Cancer Research. April 2009. Denver, CO.
39. Sharon L. Ripp, **Jennifer L. Bushee**, Anne E. Hagen, Thomas V. Magee, R. Scott Obach, Timothy J Strelevitz, and Alfin D N Vaz. In Vitro/In Vivo Correlation for Aldehyde Oxidase-Mediated Metabolism of N-Heterocyclic Xenobiotics. 15th North American Regional Meeting of the International Society for the Study of Xenobiotics (ISSX). October 2008, San Diego, CA.

AWARDS & COMMUNITY OUTREACH, & OUTREACH

BROWN UNIVERSITY

2025	Sigma Xi, Full Member
2025	2025 RNA Symposium Inclusivity Award
2024 - 2025	JBB Endowed Graduate Fellowship in Brain Science, Carney Institute for Brain Science
2023	Travel Grant, European Molecular Biology Organization course
2020 - 2021	NIH T32 Pharmacology Predoctoral Fellowship (5T32GM077995-10)

NOVARTIS

2018	Team Award for demonstrating creativity and the courage to take smart risks while discovering new medicines (1 of 6 global NIBR teams selected)
2017	Spotlight Award in recognition of leading Cambridge metabolism database management
2016	Spotlight Award in recognition of leadership, accountability and teamwork supporting laboratory equipment operations
2016	Fusion Team Award in recognition of effective teamwork developing a bioanalysis and biotransformation workshop

2016	Spotlight Award in recognition of laboratory management role and driving safety and compliance in accordance with Novartis laboratory policies
2015	Spotlight Awards (3) in recognition of leadership, collaboration, and use of organizational knowledge for the development of global department two-day science symposium
2013	Spotlight Award in recognition of open and inclusive collaboration within department and key partners while chairing monthly all-staff meeting

OUTREACH

2017 - 2023	*Beverly High School Career Day*, Speaker
2022 - 2023	*Sheridan Center CIRTL Working Group*, Student representative
2021 - 2022	*MPPB (now TSGP) Data Club,* Co-organizer
2015 - 2016	*Massachusetts State High School Science & Engineering Fair,* Volunteer Judge

PROFESSIONAL DEVELOPMENT

2011 - present	*Member,* Genetics Society of America (2022 - present), Society for Neuroscience (2021), American Chemical Society (2010 - 2020), American Society for Mass Spectrometry (2011 - 2019)
2023	*Participant,* Federation of American Societies for Experimental Biology (FASEB) Introduction to Science Policy & Advocacy Short Course, Virtual
2023	*Participant,* European Molecular Biology Organization (EMBO) Practical Course: Measuring translational dynamics by ribosomal profiling, Heidelberg, Germany
2023	*Participant,* Responsible Conduct of Research Refresher Course, Brown University
2012 - 2019	*Ad hoc reviewer,* American Association of Pharmaceutical Scientists (AAPS) Annual Meetings
2019	*Participant,* Responsible Conduct of Research Course, Brown University
2010 - 2018	*Participant,* Novartis Continuing Educations courses First in human clinical dose selection (2018), Molecules to Medicine (2018), DMPK Biologics (2016), Chemical Aspects of Metabolism-Related Drug Toxicity Course (2010)
2010	*Participant,* American Chemical Society, Pharmacokinetics for Chemists in Drug Discovery and Development Short Course, Boston, MA

Preface

A growing number of rare neurodevelopmental disorders linked to tRNA modifying enzymes have been reported. The underlying molecular mechanisms and reasons for the disproportionate effect on nervous system development and function are poorly understood. tRNA modification has been well studied in single-cell organisms including yeast. The family of tRNA methylation enzymes has expanded in animals and is highly conserved between Drosophila and humans, providing an exciting opportunity to study how tRNA modification is critical to nervous system development and function in a tractable *in vivo* model system.

This dissertation focuses on the investigation of two tRNA methyltransferases using Drosophila to study their *in vivo* roles in the nervous system and identify possible therapeutic targets for associated neurodevelopmental disorders. In Chapter 1, I review the role tRNA modifying enzymes play in regulating protein synthesis. I highlight tRNA modifications that impact cancer biology and neurodevelopmental disorders, along with potential therapeutics. In Chapter 2, I investigate the function of tRNA methyltransferase 9B (TRMT9B), one of two animal homologs of yeast tRNA methyltransferase 9 (Trm9), in synapse growth and function. In Chapter 3, I focus on tRNA methyltransferase 1 (TRMT1) as variants have been associated with intellectual disability and link its function in ensheathing glia to synapse development and memory recall. In Chapter 4, I explore future directions and the broader implications of tRNA modification in disease.

Acknowledgements

I'd first like to thank my mentor, Dr. Kate O'Connor-Giles. I am forever grateful that I met you at a first-year breakfast, and you told me about a mysterious tRNA methyl-transferase enriched in the brain. Your mentorship has been invaluable in my development as a scientist. I appreciate the opportunities to travel and share our science with the Drosophila and RNA biology communities. Thank you for fostering an open, inclusive environment that empowers our the lab to work collaboratively and take on challenging questions.

I'd next like to thank my committee members: Drs. Nikos Tapinos, Erica Larschan, and Eric Morrow. I appreciate your insights and helpful conversations throughout graduate school. To my external reader, Dr. Dragony Fu, thank you for expertise and collaboration to explore how RNA biology regulates nervous system development.

I am deeply grateful for the support of the Therapeutic Sciences Graduate Program (TSGP) including Dr. Diana Horrigan, Dr. Sean Lawler, Dr. Anita Zimmerman, Dr. Wayne Bowen, Dr. Elena Oancea, Dr. John Marshall, Dr. George Lisi, Dr. Nick Fawzi, Gregg Casazza, Ruth Mattson, and Jessica Bello. Thank you for the academic discussions and rotations/career advice. Being a part of the TSGP community has been a memorable journey. I appreciate the opportunity to be a part of the TSGP and value the meaningful training it has provided me as a scientist.

To the O'Connor-Giles Lab, thank you for sharing your perspectives and passion for science. Thank you to all the researchers who worked on the tRNA methyltransferase team, particularly Emily Hill, William Kemball-Cook and Kennedy Tyson. I'd also like to thank Dr. Scott Gratz and Dr. Rajan Thakur for being outstanding mentors and labmates.

I appreciate the training in all things Drosophila, molecular biology and imaging, as well as our discussion and brainstorming sessions. I'm grateful for the opportunity to work with Amanda Gratz; your mentoring and coaching pushed me to celebrate the research highs and recover from the burnout lows of graduate school. It has been wonderful working with all of you.

Thank you to the Colby Chemistry Department, particularly my first PI, Dr. Kevin Rice, and the wonderful friends who cheer each other on through all of life's milestones and marathons. To the Cornell crew, thank you for your friendship and support through virtual and in person weekends. Thank you to the colleagues I worked with before graduate school, specifically Dr. Upendra Argikar, who took a chance on hiring a recent chemistry undergraduate. I appreciate your guidance and encouragement in DMPK and beyond.

I'd like to thank my family for their unwavering support. To my parents, thank you for instilling the confidence and perseverance to take on any challenge. To my sisters, thank you for being my cheerleaders and toughest (and supportive) critics. And to my extended family the Bushees, Keegans, and Dumouchels, thank you for your love and encouragement.

Finally, I'd like to thank my husband, Matt. Thank you for always making me laugh and encouraging me to relax and sit down for a game of cribbage. I cherish all our at-home cooking and cocktail experiments, I especially appreciated you humoring my stress-induced baking while writing this dissertation. Your support through all of life's adventures means everything to me. Thank you for being my someone.

Table of Contents

List of Figures

Chapter 1

Chapter 2

Chapter 3

Chapter 4

List of Supplementary Figures

Chapter 2

Chapter 3

List of Tables

Chapter 3

List of Supplemental Tables

Chapter 3

CHAPTER 1

INTRODUCTION:

tRNA methyltransferase modifications and modifying enzymes as emerging therapeutic targets

ABSTRACT

Precise regulation of gene expression is required for proper development and cellular function. Transfer RNAs (tRNAs) function as adapters between mRNA transcripts and growing polypeptides by binding codons and amino acids to decode mRNA. Engineered tRNAs and overexpression of tRNAs are new areas of therapeutic intervention under development to correct translation. Notably, tRNAs are highly post-transcriptionally modified to promote stability and the fidelity of codon recognition. Disrupted post-transcriptional tRNA processing has been linked to numerous cancers and neurodevelopmental disorders. As the underlying cellular mechanisms disrupted in the absence of tRNA modifiers, specifically tRNA methyltransferases, are beginning to emerge, these modifying enzymes present an interesting new therapeutic target.

STATEMENT OF SIGNIFICANCE

Dynamic regulation of gene expression is required for maintenance of cellular homeostasis. The function of transfer RNAs (tRNAs) in translation is dependent on post-transcriptional modifications that promote structural stability and codon-anticodon recognition. Disrupted tRNA methyltransferases have been linked to numerous cancers and neurodevelopmental disorders. Effected tRNAs and their respective methyltransferase modifiers are potential new therapeutic targets in oncology and neurodevelopmental disorders.

INTRODUCTION

Dynamic regulation of gene expression is fundamental to development and function across species. Gene expression unpacks the storage of genetic information from DNA to messenger RNA (mRNA) before translation to protein (Chang & Qi, 2023; Crick, 1966; Diercks *et al*, 2021). Translation initiation begins a symphony of mechanisms conserved across eukaryotes where the ribosomal initiation complex binds and activates mRNA while recruiting initiator transfer RNAs (tRNA) (Brito Querido *et al*, 2024; Merrick & Pavitt, 2018). tRNAs decode mRNA, functioning as adapters between transcripts and growing polypeptides by binding both codons and the corresponding amino acid. Despite their small size (~70-90 nucleotides), these noncoding RNAs are extensively post-transcriptionally modified (Motorin & Helm, 2010). 170 tRNA modifications are known to promote their stability, folding, and precise function (Cappannini *et al*, 2024; Motorin & Helm, 2010; Rigden & Fernandez, 2024). The evolutionary conservation of many tRNA modifications between archaea, bacteria and eukaryotes highlights the fundamental significance of these modifications, promoting the development of numerous sequencing and mass spectrometry based detection methods (Jackman & Alfonzo, 2013; Kimura *et al*, 2020; Krogh & Nielsen, 2019). Improved sequencing approaches have advanced the understanding of how tRNA modifications impact health and human disease (Sarkar *et al*, 2021).

In this review, we provide a perspective on tRNA modifications that drive structure and function. We next summarize the potential of early investigations that seek to correct mistranslation through engineering synthetic tRNAs. We highlight tRNA modifications in depth and focus on four tRNA methylations that are linked to cancer and neurodevelopmental disorders, as interesting therapeutic targets.

tRNA STRUCTURE AND FUNCTION

Since the 1960s, single-cell organisms have been exceptional model systems to elucidate tRNA structure and function (Holley *et al*, 1965; Kim *et al*, 1973; Kim *et al*, 1974). Foundational research on tRNA biogenesis, transport, and enzymatic activity has been extensively conducted in yeast (Chatterjee *et al*, 2018; Kessler *et al*, 2018; Phizicky & Hopper, 2023). Briefly, precursor tRNAs are transcribed with additional 5'- and 3'-tail sequences that undergo splicing and processing in the nucleus before mature tRNAs are exported to the cytosol for continued processing. Mature tRNAs range from 70-90 nucleotides in length and have a cloverleaf secondary structure. This looped structure is comprised of five components including: (1) the acceptor stem (light blue), (2) the dihydrouridine-containing loop (D-loop, green), (3) the thymidine- pseudouridine- and cytidine-containing loop (TΨC-loop, orange), (4) the variable arm (purple) and (5) an anticodon stem-loop (blue/gray, Fig 1.1A). Common methylation modifications discussed later are highlighted in Fig 1.1A (positions noted in bold) with representative chemical structures shown in Fig 1.1B. tRNAs take on a tertiary structure described as an "L-shaped" structure shown in Fig 1.1C (Saks *et al*, 1994). At the 3'-end, the acceptor stem binds a specific amino acid supplied by an amino acid synthetase (Berg & Offengand, 1958; Carter & Wills, 2018; Pak *et al*, 2018; Rubio Gomez & Ibba, 2020). The D-loop and T-loop guide tertiary structure, stability, and interactions with the ribosomal complex (Seelam *et al*, 2017; Vare *et al*, 2017), while the anticodon loop, specifically positions 34-36, binds to a codon in mRNA through Watson-Crick base pairing (Crick, 1966; Gerber & Keller, 1999; Schaffrath & Leidel, 2017).

tRNAs decode mRNA by functioning as adapters between the mRNA and growing polypeptide chain. A brief illustration of initiated translation is presented in Fig1.1D (Blanchet & Ranjan, 2022; Dever & Green, 2012; Hinnebusch & Lorsch, 2012; Jackson

et al, 2010). In summary, a small ribosomal subunit binds mRNA of interest and assembles with a large ribosomal subunit to form a ribosomal complex. This complex is composed of three tRNA docking sites: an aminoacyl site (A-site), peptidyl site (P-site) and an exit site (E-site). These sites represent the binding sites for an initiator methionyl-tRNA or newly charged tRNA (A-site), the tRNA charged with the nascent polypeptide chain (P-site) or the uncharged (deactivated) tRNA before it leaves the ribosomal complex (E-site). After initiation of translation with the initiator tRNA, a charged tRNA enters the A-site and the tRNA anticodon loop binds with the correct mRNA codon. The amino acid is hydrolyzed to the growing polypeptide chain and the tRNA is moved to the P-site. Elongation phase continues until the mRNA is fully decoded and the terminal codon sequence is processed, the polypeptide chain is released and the ribosomal complex is recycled (Oakes *et al*, 1987; Ramakrishnan, 2002; Schultz & Kothe, 2024; Suzuki, 2021; Zaher & Green, 2009; Zhang, 2024).

tRNA THERAPEUTIC POTENTIAL

Modulating tRNA biology and translation are exciting areas of therapeutic discovery (Ward *et al*, 2024). Regulating translation through ribosomal complex can be traced back to the development of aminoglycosides, small molecule antibiotics that inhibit bacterial protein synthesis (Fan-Minogue & Bedwell, 2008). Instead of inhibiting translation, more recent research has focused on correcting and restoration of protein synthesis. Many genetic diseases, like Duchenne muscular dystrophy (DMD), are driven through inappropriate translation where nonsense mutations lead to an in-frame premature stop codon - UAG, UAA, or UGA and result in a truncated protein. Translarna (ataluren), developed by PTC Therapeutics, is a small molecular inhibitor, structurally distinct from aminoglycosides and designed to promote translation readthrough efficiency (Peltz *et al*, 2013; Welch *et al*, 2007). Translarna demonstrated dose-dependent activity in cell lines

and in a DMD-mouse model treatment over 4 weeks showed improved dystrophin protein levels and muscle strength improvement in across cardiac, lung, and leg tissues (Welch *et al.*, 2007). Studies in yeast and human cells demonstrated that Translarna has the strongest translation correction with UGA premature stop codons (Roy *et al*, 2016). While cryogenic electron microscopy and photolabeling affinity studies have demonstrated key structural-activity relationship binding sites where Translarna inhibits the release factor binding complex within the ribosome (Huang *et al*, 2022).

Other tRNA therapeutic companies, including AlltRNA, hCBioscience and Tevard Biosciences, are investigating targeted approaches to engineered tRNAs that emphasize tRNAs as a therapeutic platform which recorrect or modify translation (Dolgin, 2022). The targeted RNA platform provides alternative mechanisms to modulate underlying biology of large proteins which are often poor candidates for gene replacement therapy, like DMD. Engineered tRNAs facilitate readthrough of premature stop codons with a cognate amino acid to restore translation (Fig 1.2; (Bily *et al*, 2024; Lueck *et al*, 2019; Porter *et al*, 2021; Porter *et al*, 2024). Additional research is exploring the correction of missense mutations with engineering missense-correcting tRNAs that incorporate the correct amino into a growing peptide chain to overcome the inappropriate codon-anticodon interaction (Hou *et al*, 2024; Polikanov *et al*, 2023). Other research in cells and *in vivo* model systems focused on correcting tRNA pools. In yeast, Berg *et al* have shown increased translation readthrough through RNA polymerase III driven tRNA reexpression (Berg *et al*, 2021). In human cell lines, overexpression of mitochondrial $tRNA^{His}$ was reported to restore $tRNA^{His}$ pools, protein synthesis and mitochondrial respiration (Gong *et al*, 2020). Transgenic overexpression of $tRNA^{Gly}$ restores protein synthesis and decreased peripheral neuropathy in Charcot-Marie-Tooth models in Drosophila and mouse (Zuko *et al*, 2021). Restoration of tRNA pool or selective tRNA(s)

would serve as interesting therapeutic approaches in disease where hypo-tRNA modifications disrupt translation. While regulating translation through small molecule, engineered tRNAs, or tRNA overexpression approaches are exciting new areas of research, target tRNA modifying enzymes have been less studied as a druggable target.

DISRUPTED tRNA MODIFICATIONS IMPLICATED IN DISEASE

Maintaining tRNA pools contributes to proper maintenance of cellular homeostasis (Hanson & Coller, 2018). Stress-induced metabolic reprogramming leads to changes in protein translation and contributes to cancer diagnostic markers (Dedon & Begley, 2014). Disrupted tRNA modifications lead to uncontrolled cell proliferation and tumorigenesis (Barbieri & Kouzarides, 2020; Li *et al*, 2022). Breakdown products of tRNAs, tRNA fragments, have also been linked to numerous cancers (Cabrelle *et al*, 2024; Garcia-Vilchez *et al*, 2023).

In addition to cancers, dynamic regulation of neuronal gene expression is required for proper nervous system development and function (Klann & Dever, 2004). Careful regulation is required for circuit formation and long-term synaptic plasticity (Martin & Magistretti, 1998; Ooi & Wood, 2008; Shen, 2006). Local gene regulation and translation are implicated in memory formation (Di Liegro *et al*, 2014; Kandel, 2001; Martin *et al*, 1997; Mayford *et al*, 2012; Shrestha & Klann, 2022). In the aging nervous system, regulating oxidative stress requires regulated transcription and translation and local ribosomal assembly to maintain neuronal function (Fasnacht & Polacek, 2021; Harnett *et al*, 2022; Marini *et al*, 2018; Shigeoka *et al*, 2019; Steward, 1983). Specific disruption of post-transcriptional tRNA processing has been linked to multiple neurological diseases, including intellectual disability, Amyotrophic Lateral Sclerosis, Galloway–Mowat

syndrome, and mitochondrial disorders that disproportionately impact the brain (Ramos & Fu, 2019; Suzuki, 2021). tRNA disruptions associated with neurodevelopmental disorders range from disrupted amino acid charging (Wei *et al*, 2019) to tRNA misfolding due to hypomodifications (Davarniya *et al*, 2015; Efthymiou *et al*, 2025; Nagayoshi *et al*, 2021; Zhang *et al*, 2020) and altered codon-specific mRNA decoding (Maddirevula *et al*, 2022; Monies *et al*, 2019; Saad *et al*, 2021; Waqas *et al*, 2022; Yilmaz *et al*, 2024).

For accurate translation, the “L-shaped” tRNA structure undergoes on average 13 modifications to retain its tertiary structure, promote folding and precise function (Cappannini *et al.*, 2024; Motorin & Helm, 2010; Pan, 2018; Rigden & Fernandez, 2024). Here, we’ve focus on four methylations, mono- or di-methylations, that fall into two categories: those that occur on the tRNA body and those on the anticodon loop (Schultz & Kothe, 2024) that are implicated in health and diseases and discuss their therapeutic potential.

METTL1

In yeast, the complex comprised of tRNA methyltransferase 8 (Trm8) and tRNA methyltransferase 82 (Trm82) methylates guanosine residue 46 to a positively charged 7-methylguanosine (m7G, Fig 1.1B). This modification and tRNA modifying complex are highly conserved from yeast to humans (Alexandrov *et al*, 2005; Alexandrov *et al*, 2002). Structure-function investigations demonstrate the m7G modifications near the variable arm stabilize the “L-shaped” tertiary structure between the TΨC-loop and D-loops in temperature-dependent manner (Agris *et al*, 1986; Alexandrov *et al.*, 2005; Helm, 2006; Lorenz *et al*, 2017). m7G has been linked cellular growth impairments due to decreased $tRNA^{Tyr}$ and $tRNA^{Val}$ pools in *S. pombe* and *S. cerevisiae*, respectively, and

hypomodification activates the tRNA decay pathway (Alexandrov *et al.*, 2005; De Zoysa *et al*, 2024; De Zoysa & Phizicky, 2020).

In mammals, m7G modifications are carried out by human complex methyltransferase-like 1 (METTL1) and tRNA N7-guanosine methyltransferase (WDR4) complex. *WDR4*-associated microcephalic primordial dwarfism has been studied in yeast and human cell lines with patient mutations and demonstrated a decrease in m7G on $tRNA^{Val}$ and $tRNA^{Phe}$. Researchers hypothesize downstream impact on cellular growth mechanisms as promising future investigations (Shaheen *et al*, 2015; Trimouille *et al*, 2018). WDR4 also has been implicated as a candidate of interest for down syndrome although no mechanistic investigation of tRNA modifications have been conducted to our knowledge (Michaud *et al*, 2000; Sahun *et al*, 2014).

Overexpression of METTL1 in various cancers has led to increased m7G $tRNA^{Val}$ and $tRNA^{Pro}$ levels, increased cellular growth, and poor patient outcomes (Ma *et al*, 2021). METTL1 regulates lenvatinib resistance in hepatocellular carcinoma via epidermal growth factor receptor pathways (Huang *et al*, 2023). METTL1-associated thyroid cancers have been linked to cell proliferation via tumor necrosis factor-α pathways (Li *et al*, 2025). The growing number of cancers associated with m7G tRNA modifications are not surprising as the modification is critical for tRNA stability. *METLL1*-deficient cells interestingly show an increase of tRNA fragments which could play an important role in development of clinical cancer biomarkers to understand patient heterogeneity across multiple type of cancers (Garcia-Vilchez *et al.*, 2023).

Therapies to restore m7G modification would require careful correction of hypo- and hyper-tRNA modifications. Excitingly, for increased m7G, a METTL1 inhibitor,

STM9005, is currently in the discovery phase at Storm Therapeutics. For a tRNA methyltransferase inhibitor, standard high throughput screening small molecule approaches were taken which include triaging compounds for low nanomolar *in vitro* potency, high target selectivity, and decreased *in vitro* cell proliferation for multiple cancer cell lines. Lead candidate STM9006 decreased m7G at residue 46 tRNA levels, global proteomics changes, and *in vivo* tumor inhibition (Sapetschnig *et al*, 2024; Yankova *et al*, 2025). Modulating tRNA biology emphasizes the use and development of new RNA screening techniques such as misincorporation tRNA sequencing (Behrens *et al*, 2021). We look forward to following this first-in-class inhibitor into the clinic as it may provide an unique approach to targeting a wide variety of cancers.

ALKBH8/TRMT9B

Modifications at the anticodon wobble position, position 34 (U_{34}), that has been well studied in yeast. tRNA methyltransferase 9 (Trm9) methylates U_{34} for proper anticodon-codon interactions and protein translation (Crick, 1966; Gerber & Keller, 1999; Schaffrath & Leidel, 2017; Smith *et al*, 2024). The exact U_{34} modification pathway has been debated and to date remains incomplete (Chen *et al*, 2011). Yeast studies have shown that the elongator complex (Elp) metabolizes the first step of U_{34} to 5-carbonylmethyluridine (cm^5U) (Huang *et al*, 2005; Jablonowski *et al*, 2006). Trm9 forms a heterodimer with tRNA methyltransferase 112 (Trm112) to methylate cm^5U to 5-methyoxycarbonylmethyluridine (mcm^5U, Fig 1.1D) and further modifications occur downstream ((Kalhor & Clarke, 2003; Lentini *et al*, 2018), Fig. 1.3). *Elp* and *Trm9* deficient yeast have also been used to explore frameshift rates at ribosomal A- and P-sites for loss of each U_{34} modification (Tukenmez *et al*, 2015). Trm9 modification of U_{34} restricts wobble base pairing for $tRNA^{Arg(UCU)}$ and $tRNA^{Glu(UUC)}$ (Kalhor & Clarke, 2003).

Trm9 deficient yeast have decreased levels of proteins whose transcripts are enriched for cognate codons AGA and GGA, including proteins associated with DNA repair and cell cycle growth (Begley *et al*, 2007). Ribosomal profiling also highlighted a similar decrease in Trm9-dependent-codon-enriched mRNA translation in cells deficient of the wobble uridine modifications (Deng *et al*, 2015).

Metazoa have evolved two Trm9 homologs, ALKBH8 and TRMT9B (also known as C8ORF79, KIAA1456, and TRM9L), both enzymes encode predicted S-adenosyl methionine (SAM)-dependent Class I methyltransferases based on high conservation of class-defining sequences. ALKBH8 has evolved additional structural domains, including an RNA recognition motif (RRM) and an oxidoreductase (AlkB) domain (Fu *et al*, 2010b; Songe-Moller *et al*, 2010). ALKBH8 has been shown to drive wobble uridine metabolism to mcm^5U_{34} in flies, mice, human ALKBH8 cells (Fu *et al*, 2010a; Fu *et al.*, 2010b; Madhwani *et al*, 2024; Songe-Moller *et al.*, 2010). In mice, ALKBH8-dependent wobble uridine modifications are also required for selenoprotein synthesis as a protective mechanism against oxidative stress conditions (Leonardi *et al*, 2020; Songe-Moller *et al.*, 2010). In flies, ALKBH8 has been reported as a regulator of selenoprotein synthesis, synaptic growth and memory formation (Madhwani *et al.*, 2024). A growing number of patients have been identified with with *ALKBH8*-linked ID, including missense mutations in the methyltransferase and frameshift mutations leading to premature stop codons that lead to decreased wobble uridine modifications (Maddirevula *et al.*, 2022; Monies *et al.*, 2019; Saad *et al.*, 2021; Waqas *et al.*, 2022; Yilmaz *et al.*, 2024). Conversely, high expression of ALKBH8 has been shown to promote cancer progression and tumorigenesis in bladder cancers through c-Jun NH2 terminal kinase and p38 mitogen-activated protein kinase stress response pathways (Ohshio *et al*, 2016; Shimada *et al*, 2009).

Based on the small number of ALKBH8-modified tRNAs, overexpression tRNA selenocysteine may provide a compelling therapeutic avenue. In flies, *ALKBH8*-deficient cognitive recall was restored with media supplemented with an antioxidant, which suggests a possible interventional therapy for *ALKBH8*-associated intellectual disability patients (Madhwani *et al.*, 2024). Furthermore, understanding changes in tumor or neuronal based proteomics profiles may point towards identifying other key mechanisms to target.

Although TRMT9B is not required for the canonical Trm9 wobble uridine methylation, evolution conservation of both ALKBH8 and TRMT9B points towards deviation of substrate and function. TRMT9B is down-regulated in numerous cancers and high TRMT9B expression in lung, breast, ovarian, and colorectal cancer tumors correlated with improved patient survival (Begley *et al*, 2013; Chen *et al*, 2017; Flanagan *et al*, 2004; Voeghtly *et al*, 2012; Wang *et al*, 2018; Wang *et al*, 2017). Cancer cell lines expressing ectopic human TRMT9B showed decreased tumor growth under HIF-α hypoxic conditions and a recent study found that TRMT9B is regulated by an ERK/MAP kinase signaling cascade (Begley *et al.*, 2013; Gu *et al*, 2018). More recently TRMT9B has been studied in the nervous system, where Hogan and colleagues showed that TRMT9B has a synaptic growth methyltransferase domain-dependent mechanism and methyltransferase independent mechanism which regulates synapse function (Hogan *et al*, 2023). With relevance in cancer and neuronal development and availability of new genetic models, possible renewed interest in pursuing TRMT9B as a therapeutic target appears likely.

NSUN2

Another wobble position modification, 5-methylcytidine (m5C, Fig 1.1B) is mediated by *Saccharomyces cerevisiae* tRNA methyltransferase 4 (Trm4), which has a human ortholog NOP2/Sun methyltransferase 2 (NSUN2). Trm4 localizes to the nucleus and methylates an intron containing pre-tRNA^{Leu}. (Motorin & Grosjean, 1999). In fission yeast, Trm4a demonstrates conserved biochemical function and methylates tRNA^{Leu} at the wobble position. More broadly, m5C modifications have also been sequenced at several positions in the T-loop and variable loops (Motorin & Grosjean, 1999).

NSUN2-linked to neuronal developmental disorders are NSUN2 modifications that methylates tRNA at position 34 to m5C. Patients with *NSUN2*-associated with intellectual disability have variants that include nonsense, missense and spliced mutations, and single nucleotide deletion that leads to a premature stop codon. These variations have all reported decreased levels of m5C levels (Abbasi-Moheb *et al*, 2012; Khan *et al*, 2012; Komara *et al*, 2015; Sun *et al*, 2020). Although molecular mechanisms are unknown *NSUN2*-deficient human cell lines demonstrates changes in neuronal stem cell differential and *NSUN2*-deficient mice show depletion in tRNA^{Gly} pools that decrease global proteomic changes associated with neurotransmission and synaptic signaling (Blaze *et al*, 2021; Flores *et al*, 2017). In mice and flies, cognitive and social behavior changes are also noted in the absence of *NSUN2*-mediated tRNA modifications (Blaze *et al*, 2024; Gonskikh *et al*, 2025).

In oncology settings, hyper-m5C tRNA modifications were reported in thyroid cancers to promote tumorigenesis via anti-apoptosis pathways (Li *et al*, 2023). However, NSUN2 has multi-specific modifications, tRNA and mRNA, which further complicates narrowing down a specific molecular mechanism (Li & Huang, 2024). High m5C driven mRNA

modifications were noted in pancreatic cancer (Chen *et al*, 2022). Varying levels of NSUN2 were reported in other cancers however m5C tRNA or mRNA modifications were not measured (Okamoto *et al*, 2012). NSUN2 mediated cell proliferation in gallbladder cancer was modified through depletion of a ribosomal protein-partner, large ribosomal subunit protein 6, and not RNA modifications (Gao *et al*, 2019). Conversely, high levels of NSUN2 with low levels of insulin growth factors had improved rates of progression-free survival in ovarian cancers (Yang *et al*, 2017).

Despite a strong link in both cancer and neurodevelopmental disorders, targeting NSUN2 presents a challenge in specificity. NSUN2 can also modify mRNA and non-coding RNA (Chellamuthu & Gray, 2020; Hussain *et al*, 2013; Wang, 2016). A selective, covalent NSUN2 inhibitor was generated using an activity based proteomic profiling approach that targeted a core cysteine residue in the Class I SAM-dependent methyltransferase active site of NSUN2. This azetidine acrylamide lead candidate showed low specificity towards NSUN5-7 and effective m5C tRNA reduction in a human leukemia cell line (Tao *et al*, 2023). Preclinical and proteomic characterizations would be critical next steps in evaluating this potential drug hit and development to a lead candidate.

TRMT1

Methylation of guanosine at position 26, a hinge point between the D-loop and anticodon stem, leads to N2,2-dimethylguanosine (m2,2G, Fig 1.1B) an essential modification driven by yeast tRNA methyltransferase 1 (Trm1) (Edqvist *et al*, 1992; Ellis *et al*, 1986). Trm1 has nuclear and mitochondrial localization, and this modification can be found on most tRNAs (Ellis *et al.*, 1986). In the absence of *Trm1*, yeast show in increased

sensitivity to oxidative stress with changes in metabolic and amino acid synthesis associated with upregulation of Gcn4 (Chou *et al*, 2017). The m2,2G modification also promotes proper tRNA folding through base-pairing confirmations with five nucleosides in the D- and variable loops (Edqvist *et al.*, 1992). More recently, Bavi and colleagues have used molecular dynamics approaches to assess preferred m2,2G base pairing confirmation with adenosine and uridine (Bavi *et al*, 2013). tRNAs without the m2,2G modifications are removed through rapid tRNA decay (Dewe *et al*, 2012). Trm1 also has a non-catalytic role with tRNA chaperone La to promote tRNA maturation (Porat *et al*, 2023).

Trm1 has two mammalian orthologs, tRNA methyltransferase 1 (TRMT1) and tRNA methyltransferase like-1 (TRMT1L) (Liu & Straby, 2000). TRMT1 performs the canonical function of Trm1 and protects against oxidative stress (Dewe *et al*, 2017), while the biochemical function of TRMT1L has only been recently discovered. TRMT1L dimethylates guanosine at position 27 and is required for another tRNA modification, 3-(3-amino-3-carboyxypropyl)uridine (Hwang *et al*, 2025; Zhang *et al*, 2025). Researchers have generated human cell lines, including *TRMT1* null or patient derived mutations and observed reduced cell proliferation, m2,2G modifications, global translation rates as well as developmental delays and behavioral impairments in an *in vivo TRMT1* deficient zebrafish model (Dewe *et al.*, 2017). TRMT1 has a growing patient cohort linked to neurodevelopmental disorders and tRNA metabolism. Thirty-one patients have been identified with TRMT1-linked intellectual disability variants in a SAM-dependent methyltransferase domain, where variants include truncated proteins due to premature frame shifts/premature stops, splice variants, and missense mutations (Davarniya *et al.*, 2015; Efthymiou *et al.*, 2025; Zhang *et al.*, 2025). This tRNA body methylation is found in an extensive number of tRNAs; careful coordination of the modifications is required for

translational control (Dewe *et al.*, 2017). With the growing patient populations, available resources in cell lines and an *in vivo* model, identifying key regulators altered in *TRMT1*-translation would be attractive therapeutic candidates.

CONCLUSION

The role of tRNAs has greatly evolved from merely a small adapter which facilitates translation to a critical piece of RNA biology that promotes homeostasis and function. tRNA post-transcriptional modifications maintain structural stability, codon-anticodon recognition, tRNA charging and function. Disrupted tRNA methylation in the tRNA body or anticodon stem/loop has been linked to numerous cancers and neurodevelopmental disorders. Growing evidence indicates that the expanded tRNA modifiers, particularly, tRNA methyltransferase family has evolved in animals to regulate gene expression in new ways. Research investigating the impact of changing tRNA pool availability and translation control is an exciting new opportunity to target tRNA modifying enzymes and downstream targets in disease. Continued research is needed to understand the structure-function relationship between tRNA and ribosome and tRNA and tRNA methyltransferase. For tRNAs with conserved function across species, there are opportunities to investigate underlying molecular mechanisms traditional cell line and mice as well as non-model organisms, including zebrafish and Drosophila, may provide key mechanistic insights to downstream effects of gain- or loss-of-function of the modifying enzymes.

Chapter 1 References

Abbasi-Moheb L, Mertel S, Gonsior M, Nouri-Vahid L, Kahrizi K, Cirak S, Wieczorek D, Motazacker MM, Esmaeeli-Nieh S, Cremer K *et al* (2012) Mutations in NSUN2 cause autosomal-recessive intellectual disability. *Am J Hum Genet* 90: 847-855

Agris PF, Sierzputowska-Gracz H, Smith C (1986) Transfer RNA contains sites of localized positive charge: carbon NMR studies of [13C]methyl-enriched Escherichia coli and yeast tRNAPhe. *Biochemistry* 25: 5126-5131

Alexandrov A, Grayhack EJ, Phizicky EM (2005) tRNA m7G methyltransferase Trm8p/Trm82p: evidence linking activity to a growth phenotype and implicating Trm82p in maintaining levels of active Trm8p. *RNA* 11: 821-830

Alexandrov A, Martzen MR, Phizicky EM (2002) Two proteins that form a complex are required for 7-methylguanosine modification of yeast tRNA. *RNA* 8: 1253-1266

Barbieri I, Kouzarides T (2020) Role of RNA modifications in cancer. *Nat Rev Cancer* 20: 303-322

Bavi RS, Sambhare SB, Sonawane KD (2013) MD simulation studies to investigate iso-energetic conformational behaviour of modified nucleosides m(2)G and m(2) 2G present in tRNA. *Comput Struct Biotechnol J* 5: e201302015

Begley U, Dyavaiah M, Patil A, Rooney JP, DiRenzo D, Young CM, Conklin DS, Zitomer RS, Begley TJ (2007) Trm9-catalyzed tRNA modifications link translation to the DNA damage response. *Mol Cell* 28: 860-870

Begley U, Sosa MS, Avivar-Valderas A, Patil A, Endres L, Estrada Y, Chan CT, Su D, Dedon PC, Aguirre-Ghiso JA *et al* (2013) A human tRNA methyltransferase 9-like

protein prevents tumour growth by regulating LIN9 and HIF1-alpha. *EMBO Mol Med* 5: 366-383

Behrens A, Rodschinka G, Nedialkova DD (2021) High-resolution quantitative profiling of tRNA abundance and modification status in eukaryotes by mim-tRNAseq. *Mol Cell* 81: 1802-1815 e1807

Berg MD, Isaacson JR, Cozma E, Genereaux J, Lajoie P, Villen J, Brandl CJ (2021) Regulating Expression of Mistranslating tRNAs by Readthrough RNA Polymerase II Transcription. *ACS Synth Biol* 10: 3177-3189

Berg P, Offengand EJ (1958) An Enzymatic Mechanism for Linking Amino Acids to RNA. *Proc Natl Acad Sci U S A* 44: 78-86

Bily TMI, Heinemann IU, O'Donoghue P (2024) Missense suppressor tRNA therapeutics correct disease-causing alleles by misreading the genetic code. *Mol Ther* 32: 273-274

Blanchet S, Ranjan N (2022) Translation Phases in Eukaryotes. *Methods Mol Biol* 2533: 217-228

Blaze J, Browne CJ, Futamura R, Javidfar B, Zachariou V, Nestler EJ, Akbarian S (2024) tRNA epitranscriptomic alterations associated with opioid-induced reward-seeking and long-term opioid withdrawal in male mice. *Neuropsychopharmacology* 49: 1276-1284

Blaze J, Navickas A, Phillips HL, Heissel S, Plaza-Jennings A, Miglani S, Asgharian H, Foo M, Katanski CD, Watkins CP *et al* (2021) Neuronal Nsun2 deficiency

produces tRNA epitranscriptomic alterations and proteomic shifts impacting synaptic signaling and behavior. *Nat Commun* 12: 4913

Brito Querido J, Diaz-Lopez I, Ramakrishnan V (2024) The molecular basis of translation initiation and its regulation in eukaryotes. *Nat Rev Mol Cell Biol* 25: 168-186

Cabrelle C, Giorgi FM, Mercatelli D (2024) Quantitative and qualitative detection of tRNAs, tRNA halves and tRFs in human cancer samples: Molecular grounds for biomarker development and clinical perspectives. *Gene* 898: 148097

Cappannini A, Ray A, Purta E, Mukherjee S, Boccaletto P, Moafinejad SN, Lechner A, Barchet C, Klaholz BP, Stefaniak F *et al* (2024) MODOMICS: a database of RNA modifications and related information. 2023 update. *Nucleic Acids Res* 52: D239-D244

Carter CW, Jr., Wills PR (2018) Interdependence, Reflexivity, Fidelity, Impedance Matching, and the Evolution of Genetic Coding. *Mol Biol Evol* 35: 269-286

Chang HY, Qi LS (2023) Reversing the Central Dogma: RNA-guided control of DNA in epigenetics and genome editing. *Mol Cell* 83: 442-451

Chatterjee K, Nostramo RT, Wan Y, Hopper AK (2018) tRNA dynamics between the nucleus, cytoplasm and mitochondrial surface: Location, location, location. *Biochim Biophys Acta Gene Regul Mech* 1861: 373-386

Chellamuthu A, Gray SG (2020) The RNA Methyltransferase NSUN2 and Its Potential Roles in Cancer. *Cells* 9

Chen C, Huang B, Anderson JT, Bystrom AS (2011) Unexpected accumulation of ncm(5)U and ncm(5)S(2) (U) in a trm9 mutant suggests an additional step in the synthesis of mcm(5)U and mcm(5)S(2)U. *PLoS One* 6: e20783

Chen HM, Wang J, Zhang YF, Gao YH (2017) Ovarian cancer proliferation and apoptosis are regulated by human transfer RNA methyltransferase 9-likevia LIN9. *Oncol Lett* 14: 4461-4466

Chen SY, Chen KL, Ding LY, Yu CH, Wu HY, Chou YY, Chang CJ, Chang CH, Wu YN, Wu SR *et al* (2022) RNA bisulfite sequencing reveals NSUN2-mediated suppression of epithelial differentiation in pancreatic cancer. *Oncogene* 41: 3162-3176

Chou HJ, Donnard E, Gustafsson HT, Garber M, Rando OJ (2017) Transcriptome-wide Analysis of Roles for tRNA Modifications in Translational Regulation. *Mol Cell* 68: 978-992 e974

Crick FH (1966) Codon--anticodon pairing: the wobble hypothesis. *J Mol Biol* 19: 548-555

Davarniya B, Hu H, Kahrizi K, Musante L, Fattahi Z, Hosseini M, Maqsoud F, Farajollahi R, Wienker TF, Ropers HH *et al* (2015) The Role of a Novel TRMT1 Gene Mutation and Rare GRM1 Gene Defect in Intellectual Disability in Two Azeri Families. *PLoS One* 10: e0129631

De Zoysa T, Hauke AC, Iyer NR, Marcus E, Ostrowski SM, Stegemann F, Ermolenko DN, Fay JC, Phizicky EM (2024) A connection between the ribosome and two S.

pombe tRNA modification mutants subject to rapid tRNA decay. *PLoS Genet* 20: e1011146

De Zoysa T, Phizicky EM (2020) Hypomodified tRNA in evolutionarily distant yeasts can trigger rapid tRNA decay to activate the general amino acid control response, but with different consequences. *PLoS Genet* 16: e1008893

Dedon PC, Begley TJ (2014) A system of RNA modifications and biased codon use controls cellular stress response at the level of translation. *Chem Res Toxicol* 27: 330-337

Deng W, Babu IR, Su D, Yin S, Begley TJ, Dedon PC (2015) Trm9-Catalyzed tRNA Modifications Regulate Global Protein Expression by Codon-Biased Translation. *PLoS Genet* 11: e1005706

Dever TE, Green R (2012) The elongation, termination, and recycling phases of translation in eukaryotes. *Cold Spring Harb Perspect Biol* 4: a013706

Dewe JM, Fuller BL, Lentini JM, Kellner SM, Fu D (2017) TRMT1-Catalyzed tRNA Modifications Are Required for Redox Homeostasis To Ensure Proper Cellular Proliferation and Oxidative Stress Survival. *Mol Cell Biol* 37

Dewe JM, Whipple JM, Chernyakov I, Jaramillo LN, Phizicky EM (2012) The yeast rapid tRNA decay pathway competes with elongation factor 1A for substrate tRNAs and acts on tRNAs lacking one or more of several modifications. *RNA* 18: 1886-1896

Di Liegro CM, Schiera G, Di Liegro I (2014) Regulation of mRNA transport, localization and translation in the nervous system of mammals (Review). *Int J Mol Med* 33: 747-762

Diercks CS, Dik DA, Schultz PG (2021) Adding New Chemistries to the Central Dogma of Molecular Biology. *Chem* 7: 2883-2895

Dolgin E (2022) tRNA therapeutics burst onto startup scene. *Nat Biotechnol* 40: 283-286

Edqvist J, Grosjean H, Straby KB (1992) Identity elements for N2-dimethylation of guanosine-26 in yeast tRNAs. *Nucleic Acids Res* 20: 6575-6581

Efthymiou S, Leo CP, Deng C, Lin SJ, Maroofian R, Lin R, Karagoz I, Zhang K, Kaiyrzhanov R, Scardamaglia A *et al* (2025) Bi-allelic pathogenic variants in TRMT1 disrupt tRNA modification and induce a neurodevelopmental disorder. *Am J Hum Genet* 112: 1117-1138

Ellis SR, Morales MJ, Li JM, Hopper AK, Martin NC (1986) Isolation and characterization of the TRM1 locus, a gene essential for the N2,N2-dimethylguanosine modification of both mitochondrial and cytoplasmic tRNA in Saccharomyces cerevisiae. *J Biol Chem* 261: 9703-9709

Fan-Minogue H, Bedwell DM (2008) Eukaryotic ribosomal RNA determinants of aminoglycoside resistance and their role in translational fidelity. *RNA* 14: 148-157

Fasnacht M, Polacek N (2021) Oxidative Stress in Bacteria and the Central Dogma of Molecular Biology. *Front Mol Biosci* 8: 671037

Flanagan JM, Healey S, Young J, Whitehall V, Trott DA, Newbold RF, Chenevix-Trench G (2004) Mapping of a candidate colorectal cancer tumor-suppressor gene to a 900-kilobase region on the short arm of chromosome 8. *Genes Chromosomes Cancer* 40: 247-260

Flores JV, Cordero-Espinoza L, Oeztuerk-Winder F, Andersson-Rolf A, Selmi T, Blanco S, Tailor J, Dietmann S, Frye M (2017) Cytosine-5 RNA Methylation Regulates Neural Stem Cell Differentiation and Motility. *Stem Cell Reports* 8: 112-124

Fu D, Brophy JA, Chan CT, Atmore KA, Begley U, Paules RS, Dedon PC, Begley TJ, Samson LD (2010a) Human AlkB homolog ABH8 Is a tRNA methyltransferase required for wobble uridine modification and DNA damage survival. *Mol Cell Biol* 30: 2449-2459

Fu Y, Dai Q, Zhang W, Ren J, Pan T, He C (2010b) The AlkB domain of mammalian ABH8 catalyzes hydroxylation of 5-methoxycarbonylmethyluridine at the wobble position of tRNA. *Angew Chem Int Ed Engl* 49: 8885-8888

Gao Y, Wang Z, Zhu Y, Zhu Q, Yang Y, Jin Y, Zhang F, Jiang L, Ye Y, Li H *et al* (2019) NOP2/Sun RNA methyltransferase 2 promotes tumor progression via its interacting partner RPL6 in gallbladder carcinoma. *Cancer Sci* 110: 3510-3519

Garcia-Vilchez R, Anazco-Guenkova AM, Dietmann S, Lopez J, Moron-Calvente V, D'Ambrosi S, Nombela P, Zamacola K, Mendizabal I, Garcia-Longarte S *et al* (2023) METTL1 promotes tumorigenesis through tRNA-derived fragment biogenesis in prostate cancer. *Mol Cancer* 22: 119

Gerber AP, Keller W (1999) An adenosine deaminase that generates inosine at the wobble position of tRNAs. *Science* 286: 1146-1149

Gong S, Wang X, Meng F, Cui L, Yi Q, Zhao Q, Cang X, Cai Z, Mo JQ, Liang Y *et al* (2020) Overexpression of mitochondrial histidyl-tRNA synthetase restores mitochondrial dysfunction caused by a deafness-associated tRNA(His) mutation. *J Biol Chem* 295: 940-954

Gonskikh Y, Tirrito C, Bommisetti P, Mendoza-Figueroa MS, Stoute J, Kim J, Wang Q, Song Y, Liu KF (2025) Spatial regulation of NSUN2-mediated tRNA m5C installation in cognitive function. *Nucleic Acids Res* 53

Gu C, Ramos J, Begley U, Dedon PC, Fu D, Begley TJ (2018) Phosphorylation of human TRM9L integrates multiple stress-signaling pathways for tumor growth suppression. *Sci Adv* 4: eaas9184

Hanson G, Coller J (2018) Codon optimality, bias and usage in translation and mRNA decay. *Nat Rev Mol Cell Biol* 19: 20-30

Harnett D, Ambrozkiewicz MC, Zinnall U, Rusanova A, Borisova E, Drescher AN, Couce-Iglesias M, Villamil G, Dannenberg R, Imami K *et al* (2022) A critical period of translational control during brain development at codon resolution. *Nat Struct Mol Biol* 29: 1277-1290

Helm M (2006) Post-transcriptional nucleotide modification and alternative folding of RNA. *Nucleic Acids Res* 34: 721-733

Hinnebusch AG, Lorsch JR (2012) The mechanism of eukaryotic translation initiation: new insights and challenges. *Cold Spring Harb Perspect Biol* 4

Hogan CA, Gratz SJ, Dumouchel JL, Thakur RS, Delgado A, Lentini JM, Madhwani KR, Fu D, O'Connor-Giles KM (2023) Expanded tRNA methyltransferase family member TRMT9B regulates synaptic growth and function. *EMBO Rep* 24: e56808

Holley RW, Everett GA, Madison JT, Zamir A (1965) Nucleotide Sequences in the Yeast Alanine Transfer Ribonucleic Acid. *J Biol Chem* 240: 2122-2128

Hou Y, Zhang W, McGilvray PT, Sobczyk M, Wang T, Weng SHS, Huff A, Huang S, Pena N, Katanski CD *et al* (2024) Engineered mischarged transfer RNAs for correcting pathogenic missense mutations. *Mol Ther* 32: 352-371

Huang B, Johansson MJ, Bystrom AS (2005) An early step in wobble uridine tRNA modification requires the Elongator complex. *RNA* 11: 424-436

Huang M, Long J, Yao Z, Zhao Y, Zhao Y, Liao J, Lei K, Xiao H, Dai Z, Peng S *et al* (2023) METTL1-Mediated m7G tRNA Modification Promotes Lenvatinib Resistance in Hepatocellular Carcinoma. *Cancer Res* 83: 89-102

Huang S, Bhattacharya A, Ghelfi MD, Li H, Fritsch C, Chenoweth DM, Goldman YE, Cooperman BS (2022) Ataluren binds to multiple protein synthesis apparatus sites and competitively inhibits release factor-dependent termination. *Nat Commun* 13: 2413

Hussain S, Sajini AA, Blanco S, Dietmann S, Lombard P, Sugimoto Y, Paramor M, Gleeson JG, Odom DT, Ule J *et al* (2013) NSun2-mediated cytosine-5 methylation of vault noncoding RNA determines its processing into regulatory small RNAs. *Cell Rep* 4: 255-261

Hwang SP, Liao H, Barondeau K, Han X, Herbert C, McConie H, Shekar A, Pestov DG, Limbach PA, Chang JT *et al* (2025) TRMT1L-catalyzed m(2)(2)G27 on tyrosine tRNA is required for efficient mRNA translation and cell survival under oxidative stress. *Cell Rep* 44: 115167

Jablonowski D, Zink S, Mehlgarten C, Daum G, Schaffrath R (2006) tRNAGlu wobble uridine methylation by Trm9 identifies Elongator's key role for zymocin-induced cell death in yeast. *Mol Microbiol* 59: 677-688

Jackman JE, Alfonzo JD (2013) Transfer RNA modifications: nature's combinatorial chemistry playground. *Wiley Interdiscip Rev RNA* 4: 35-48

Jackson RJ, Hellen CU, Pestova TV (2010) The mechanism of eukaryotic translation initiation and principles of its regulation. *Nat Rev Mol Cell Biol* 11: 113-127

Kalhor HR, Clarke S (2003) Novel methyltransferase for modified uridine residues at the wobble position of tRNA. *Mol Cell Biol* 23: 9283-9292

Kandel ER (2001) The molecular biology of memory storage: a dialogue between genes and synapses. *Science* 294: 1030-1038

Kessler AC, Silveira d'Almeida G, Alfonzo JD (2018) The role of intracellular compartmentalization on tRNA processing and modification. *RNA Biol* 15: 554-566

Khan MA, Rafiq MA, Noor A, Hussain S, Flores JV, Rupp V, Vincent AK, Malli R, Ali G, Khan FS *et al* (2012) Mutation in NSUN2, which encodes an RNA methyltransferase, causes autosomal-recessive intellectual disability. *Am J Hum Genet* 90: 856-863

Kim SH, Quigley GJ, Suddath FL, McPherson A, Sneden D, Kim JJ, Weinzierl J, Rich A (1973) Three-dimensional structure of yeast phenylalanine transfer RNA: folding of the polynucleotide chain. *Science* 179: 285-288

Kim SH, Sussman JL, Suddath FL, Quigley GJ, McPherson A, Wang AH, Seeman NC, Rich A (1974) The general structure of transfer RNA molecules. *Proc Natl Acad Sci U S A* 71: 4970-4974

Kimura S, Dedon PC, Waldor MK (2020) Comparative tRNA sequencing and RNA mass spectrometry for surveying tRNA modifications. *Nat Chem Biol* 16: 964-972

Klann E, Dever TE (2004) Biochemical mechanisms for translational regulation in synaptic plasticity. *Nat Rev Neurosci* 5: 931-942

Komara M, Al-Shamsi AM, Ben-Salem S, Ali BR, Al-Gazali L (2015) A Novel Single-Nucleotide Deletion (c.1020delA) in NSUN2 Causes Intellectual Disability in an Emirati Child. *J Mol Neurosci* 57: 393-399

Krogh N, Nielsen H (2019) Sequencing-based methods for detection and quantitation of ribose methylations in RNA. *Methods* 156: 5-15

Lentini JM, Ramos J, Fu D (2018) Monitoring the 5-methoxycarbonylmethyl-2-thiouridine (mcm5s2U) modification in eukaryotic tRNAs via the gamma-toxin endonuclease. *RNA* 24: 749-758

Leonardi A, Kovalchuk N, Yin L, Endres L, Evke S, Nevins S, Martin S, Dedon PC, Melendez JA, Van Winkle L *et al* (2020) The epitranscriptomic writer ALKBH8 drives tolerance and protects mouse lungs from the environmental pollutant naphthalene. *Epigenetics* 15: 1121-1138

Li J, Zhang H, Wang H (2022) N(1)-methyladenosine modification in cancer biology: Current status and future perspectives. *Comput Struct Biotechnol J* 20: 6578-6585

Li P, Huang D (2024) NSUN2-mediated RNA methylation: Molecular mechanisms and clinical relevance in cancer. *Cell Signal* 123: 111375

Li P, Wang W, Zhou R, Ding Y, Li X (2023) The m(5) C methyltransferase NSUN2 promotes codon-dependent oncogenic translation by stabilising tRNA in anaplastic thyroid cancer. *Clin Transl Med* 13: e1466

Li W, Xie R, Chen H, Lin J, Zhong M, Zhang J, Zheng S, Jiang C, Chen X, Xu S (2025) METTL1-mediated m(7)G tRNA modification drives papillary thyroid cancer progression and metastasis by regulating the codon-specific translation of TNF-alpha. *Cell Death Dis* 16: 378

Liu J, Straby KB (2000) The human tRNA(m(2)(2)G(26))dimethyltransferase: functional expression and characterization of a cloned hTRM1 gene. *Nucleic Acids Res* 28: 3445-3451

Lorenz C, Lunse CE, Morl M (2017) tRNA Modifications: Impact on Structure and Thermal Adaptation. *Biomolecules* 7

Lueck JD, Yoon JS, Perales-Puchalt A, Mackey AL, Infield DT, Behlke MA, Pope MR, Weiner DB, Skach WR, McCray PB, Jr. *et al* (2019) Engineered transfer RNAs for suppression of premature termination codons. *Nat Commun* 10: 822

Ma J, Han H, Huang Y, Yang C, Zheng S, Cai T, Bi J, Huang X, Liu R, Huang L *et al* (2021) METTL1/WDR4-mediated m(7)G tRNA modifications and m(7)G codon

usage promote mRNA translation and lung cancer progression. *Mol Ther* 29: 3422-3435

Maddirevula S, Alameer S, Ewida N, de Sousa MML, Bjoras M, Vagbo CB, Alkuraya FS (2022) Insight into ALKBH8-related intellectual developmental disability based on the first pathogenic missense variant. *Hum Genet* 141: 209-215

Madhwani KR, Sayied S, Ogata CH, Hogan CA, Lentini JM, Mallik M, Dumouchel JL, Storkebaum E, Fu D, O'Connor-Giles KM (2024) tRNA modification enzyme-dependent redox homeostasis regulates synapse formation and memory. *Proc Natl Acad Sci U S A* 121: e2317864121

Marini A, Rotblat B, Sbarrato T, Niklison-Chirou MV, Knight JRP, Dudek K, Jones C, Bushell M, Knight RA, Amelio I *et al* (2018) TAp73 contributes to the oxidative stress response by regulating protein synthesis. *Proc Natl Acad Sci U S A* 115: 6219-6224

Martin JL, Magistretti PJ (1998) Regulation of gene expression by neurotransmitters in the central nervous system. *Eur Neurol* 39: 129-134

Martin KC, Casadio A, Zhu H, Yaping E, Rose JC, Chen M, Bailey CH, Kandel ER (1997) Synapse-specific, long-term facilitation of aplysia sensory to motor synapses: a function for local protein synthesis in memory storage. *Cell* 91: 927-938

Mayford M, Siegelbaum SA, Kandel ER (2012) Synapses and memory storage. *Cold Spring Harb Perspect Biol* 4

Merrick WC, Pavitt GD (2018) Protein Synthesis Initiation in Eukaryotic Cells. *Cold Spring Harb Perspect Biol* 10

Michaud J, Kudoh J, Berry A, Bonne-Tamir B, Lalioti MD, Rossier C, Shibuya K, Kawasaki K, Asakawa S, Minoshima S *et al* (2000) Isolation and characterization of a human chromosome 21q22.3 gene (WDR4) and its mouse homologue that code for a WD-repeat protein. *Genomics* 68: 71-79

Monies D, Vagbo CB, Al-Owain M, Alhomaidi S, Alkuraya FS (2019) Recessive Truncating Mutations in ALKBH8 Cause Intellectual Disability and Severe Impairment of Wobble Uridine Modification. *Am J Hum Genet* 104: 1202-1209

Motorin Y, Grosjean H (1999) Multisite-specific tRNA:m5C-methyltransferase (Trm4) in yeast Saccharomyces cerevisiae: identification of the gene and substrate specificity of the enzyme. *RNA* 5: 1105-1118

Motorin Y, Helm M (2010) tRNA stabilization by modified nucleotides. *Biochemistry* 49: 4934-4944

Nagayoshi Y, Chujo T, Hirata S, Nakatsuka H, Chen CW, Takakura M, Miyauchi K, Ikeuchi Y, Carlyle BC, Kitchen RR *et al* (2021) Loss of Ftsj1 perturbs codon-specific translation efficiency in the brain and is associated with X-linked intellectual disability. *Sci Adv* 7

Oakes M, Scheinman A, Rivera M, Soufer D, Shankweiler G, Lake J (1987) Evolving ribosome structure and function: rRNA and the translation mechanism. *Cold Spring Harb Symp Quant Biol* 52: 675-685

Ohshio I, Kawakami R, Tsukada Y, Nakajima K, Kitae K, Shimanoe T, Saigo Y, Hase H, Ueda Y, Jingushi K *et al* (2016) ALKBH8 promotes bladder cancer growth and progression through regulating the expression of survivin. *Biochem Biophys Res Commun* 477: 413-418

Okamoto M, Hirata S, Sato S, Koga S, Fujii M, Qi G, Ogawa I, Takata T, Shimamoto F, Tatsuka M (2012) Frequent increased gene copy number and high protein expression of tRNA (cytosine-5-)-methyltransferase (NSUN2) in human cancers. *DNA Cell Biol* 31: 660-671

Ooi L, Wood IC (2008) Regulation of gene expression in the nervous system. *Biochem J* 414: 327-341

Pak D, Kim Y, Burton ZF (2018) Aminoacyl-tRNA synthetase evolution and sectoring of the genetic code. *Transcription* 9: 205-224

Pan T (2018) Modifications and functional genomics of human transfer RNA. *Cell Res* 28: 395-404

Peltz SW, Morsy M, Welch EM, Jacobson A (2013) Ataluren as an agent for therapeutic nonsense suppression. *Annu Rev Med* 64: 407-425

Phizicky EM, Hopper AK (2023) The life and times of a tRNA. *RNA* 29: 898-957

Polikanov YS, Etheve-Quelquejeu M, Micura R (2023) Synthesis of Peptidyl-tRNA Mimics for Structural Biology Applications. *Acc Chem Res* 56: 2713-2725

Porat J, Vakiloroayaei A, Remnant BM, Talebi M, Cargill T, Bayfield MA (2023) Crosstalk between the tRNA methyltransferase Trm1 and RNA chaperone La influences eukaryotic tRNA maturation. *J Biol Chem* 299: 105326

Porter JJ, Heil CS, Lueck JD (2021) Therapeutic promise of engineered nonsense suppressor tRNAs. *Wiley Interdiscip Rev RNA* 12: e1641

Porter JJ, Ko W, Sorensen EG, Lueck JD (2024) Optimization of ACE-tRNAs function in translation for suppression of nonsense mutations. *Nucleic Acids Res* 52: 14112-14132

Ramakrishnan V (2002) Ribosome structure and the mechanism of translation. *Cell* 108: 557-572

Ramos J, Fu D (2019) The emerging impact of tRNA modifications in the brain and nervous system. *Biochim Biophys Acta Gene Regul Mech* 1862: 412-428

Rigden DJ, Fernandez XM (2024) The 2024 Nucleic Acids Research database issue and the online molecular biology database collection. *Nucleic Acids Res* 52: D1-D9

Roy B, Friesen WJ, Tomizawa Y, Leszyk JD, Zhuo J, Johnson B, Dakka J, Trotta CR, Xue X, Mutyam V *et al* (2016) Ataluren stimulates ribosomal selection of near-cognate tRNAs to promote nonsense suppression. *Proc Natl Acad Sci U S A* 113: 12508-12513

Rubio Gomez MA, Ibba M (2020) Aminoacyl-tRNA synthetases. *RNA* 26: 910-936

Saad AK, Marafi D, Mitani T, Du H, Rafat K, Fatih JM, Jhangiani SN, Coban-Akdemir Z, Baylor-Hopkins Center for Mendelian G, Gibbs RA *et al* (2021)

Neurodevelopmental disorder in an Egyptian family with a biallelic ALKBH8 variant. *Am J Med Genet A* 185: 1288-1293

Sahun I, Marechal D, Pereira PL, Nalesso V, Gruart A, Garcia JM, Antonarakis SE, Dierssen M, Herault Y (2014) Cognition and hippocampal plasticity in the mouse is altered by monosomy of a genomic region implicated in Down syndrome. *Genetics* 197: 899-912

Saks ME, Sampson JR, Abelson JN (1994) The transfer RNA identity problem: a search for rules. *Science* 263: 191-197

Sapetschnig A, Thomas B, Yankova E, Fischl H, Azevedo A, Bucknell S, Fosbeary R, Sawyer S, Evans S, Livi C *et al* (2024) 105P Targeting the tRNA methyltransferase METTL1 with small molecule inhibitors in cancer. *ESMO Open* 9

Sarkar A, Gasperi W, Begley U, Nevins S, Huber SM, Dedon PC, Begley TJ (2021) Detecting the epitranscriptome. *Wiley Interdiscip Rev RNA* 12: e1663

Schaffrath R, Leidel SA (2017) Wobble uridine modifications-a reason to live, a reason to die?! *RNA Biol* 14: 1209-1222

Schultz SK, Kothe U (2024) RNA modifying enzymes shape tRNA biogenesis and function. *J Biol Chem* 300: 107488

Seelam PP, Sharma P, Mitra A (2017) Structural landscape of base pairs containing post-transcriptional modifications in RNA. *RNA* 23: 847-859

Shaheen R, Abdel-Salam GM, Guy MP, Alomar R, Abdel-Hamid MS, Afifi HH, Ismail SI, Emam BA, Phizicky EM, Alkuraya FS (2015) Mutation in WDR4 impairs tRNA m(7)G46 methylation and causes a distinct form of microcephalic primordial dwarfism. *Genome Biol* 16: 210

Shen K (2006) Think globally, act locally: local translation and synapse formation in cultured Aplysia neurons. *Neuron* 49: 323-325

Shigeoka T, Koppers M, Wong HH, Lin JQ, Cagnetta R, Dwivedy A, de Freitas Nascimento J, van Tartwijk FW, Strohl F, Cioni JM *et al* (2019) On-Site Ribosome Remodeling by Locally Synthesized Ribosomal Proteins in Axons. *Cell Rep* 29: 3605-3619 e3610

Shimada K, Nakamura M, Anai S, De Velasco M, Tanaka M, Tsujikawa K, Ouji Y, Konishi N (2009) A novel human AlkB homologue, ALKBH8, contributes to human bladder cancer progression. *Cancer Res* 69: 3157-3164

Shrestha P, Klann E (2022) Spatiotemporally resolved protein synthesis as a molecular framework for memory consolidation. *Trends Neurosci* 45: 297-311

Smith TJ, Giles RN, Koutmou KS (2024) Anticodon stem-loop tRNA modifications influence codon decoding and frame maintenance during translation. *Semin Cell Dev Biol* 154: 105-113

Songe-Moller L, van den Born E, Leihne V, Vagbo CB, Kristoffersen T, Krokan HE, Kirpekar F, Falnes PO, Klungland A (2010) Mammalian ALKBH8 possesses tRNA methyltransferase activity required for the biogenesis of multiple wobble

uridine modifications implicated in translational decoding. *Mol Cell Biol* 30: 1814-1827

Steward O (1983) Polyribosomes at the base of dendritic spines of central nervous system neurons--their possible role in synapse construction and modification. *Cold Spring Harb Symp Quant Biol* 48 Pt 2: 745-759

Sun S, Chen L, Wang Y, Wang J, Li N, Wang X (2020) Further delineation of autosomal recessive intellectual disability syndrome caused by homozygous variant of the NSUN2 gene in a chinese pedigree. *Mol Genet Genomic Med* 8: e1518

Suzuki T (2021) The expanding world of tRNA modifications and their disease relevance. *Nat Rev Mol Cell Biol* 22: 375-392

Tao Y, Felber JG, Zou Z, Njomen E, Remsberg JR, Ogasawara D, Ye C, Melillo B, Schreiber SL, He C *et al* (2023) Chemical Proteomic Discovery of Isotype-Selective Covalent Inhibitors of the RNA Methyltransferase NSUN2. *Angew Chem Int Ed Engl* 62: e202311924

Trimouille A, Lasseaux E, Barat P, Deiller C, Drunat S, Rooryck C, Arveiler B, Lacombe D (2018) Further delineation of the phenotype caused by biallelic variants in the WDR4 gene. *Clin Genet* 93: 374-377

Tukenmez H, Xu H, Esberg A, Bystrom AS (2015) The role of wobble uridine modifications in +1 translational frameshifting in eukaryotes. *Nucleic Acids Res* 43: 9489-9499

Vare VY, Eruysal ER, Narendran A, Sarachan KL, Agris PF (2017) Chemical and Conformational Diversity of Modified Nucleosides Affects tRNA Structure and Function. *Biomolecules* 7

Voeghtly LM, Mamula K, Campbell JL, Shriver CD, Ellsworth RE (2012) Molecular alterations associated with breast cancer mortality. *PLoS One* 7: e46814

Wang S, Liu X, Huang J, Zhang Y, Sang C, Li T, Yuan J (2018) Expression of KIAA1456 in lung cancer tissue and its effects on proliferation, migration and invasion of lung cancer cells. *Oncol Lett* 16: 3791-3795

Wang SL, Huang JA, Liu XQ (2017) Mechanism of action of KIAA1456 gene on the proliferation and apoptosis of alveolar epithelial cells. *Eur Rev Med Pharmacol Sci* 21: 600-605

Wang W (2016) mRNA methylation by NSUN2 in cell proliferation. *Wiley Interdiscip Rev RNA* 7: 838-842

Waqas A, Nayab A, Shaheen S, Abbas S, Latif M, Rafeeq MM, Al-Dhuayan IS, Alqosaibi AI, Alnamshan MM, Sain ZM *et al* (2022) Case Report: Biallelic Variant in the tRNA Methyltransferase Domain of the AlkB Homolog 8 Causes Syndromic Intellectual Disability. *Front Genet* 13: 878274

Ward C, Beharry A, Tennakoon R, Rozik P, Wilhelm SDP, Heinemann IU, O'Donoghue P (2024) Mechanisms and Delivery of tRNA Therapeutics. *Chem Rev* 124: 7976-8008

Wei N, Zhang Q, Yang XL (2019) Neurodegenerative Charcot-Marie-Tooth disease as a case study to decipher novel functions of aminoacyl-tRNA synthetases. *J Biol Chem* 294: 5321-5339

Welch EM, Barton ER, Zhuo J, Tomizawa Y, Friesen WJ, Trifillis P, Paushkin S, Patel M, Trotta CR, Hwang S *et al* (2007) PTC124 targets genetic disorders caused by nonsense mutations. *Nature* 447: 87-91

Yang JC, Risch E, Zhang M, Huang C, Huang H, Lu L (2017) Association of tRNA methyltransferase NSUN2/IGF-II molecular signature with ovarian cancer survival. *Future Oncol* 13: 1981-1990

Yankova E, Sapetschnig A, Thomas B, Evans S, Eleftheriou M, Russell J, Tandon V, Webster N, Fischl H, Bucknell S *et al* (2025) Abstract 1768: Pharmacological inhibition of METTL1 as a novel therapeutic strategy against aggressive malignancies. *Cancer Research* 85: 1768-1768

Yilmaz M, Kamasak T, Terali K, Cebi AH, Turkyilmaz A (2024) The first Turkish family with a novel biallelic missense variant of the ALKBH8 gene: A study on the clinical and variant spectrum of ALKBH8-related intellectual developmental disorders. *Am J Med Genet A* 194: e63535

Zaher HS, Green R (2009) Fidelity at the molecular level: lessons from protein synthesis. *Cell* 136: 746-762

Zhang J (2024) Recognition of the tRNA structure: Everything everywhere but not all at once. *Cell Chem Biol* 31: 36-52

Zhang K, Lentini JM, Prevost CT, Hashem MO, Alkuraya FS, Fu D (2020) An intellectual disability-associated missense variant in TRMT1 impairs tRNA modification and reconstitution of enzymatic activity. *Hum Mutat* 41: 600-607

Zhang K, Manning AC, Lentini JM, Howard J, Dalwigk F, Maroofian R, Efthymiou S, Chan P, Eliseev SI, Yang Z *et al* (2025) Human TRMT1 and TRMT1L paralogs ensure the proper modification state, stability, and function of tRNAs. *Cell Rep* 44: 115092

Zuko A, Mallik M, Thompson R, Spaulding EL, Wienand AR, Been M, Tadenev ALD, van Bakel N, Sijlmans C, Santos LA *et al* (2021) tRNA overexpression rescues peripheral neuropathy caused by mutations in tRNA synthetase. *Science* 373: 1161-1166

Chapter 1 Figures

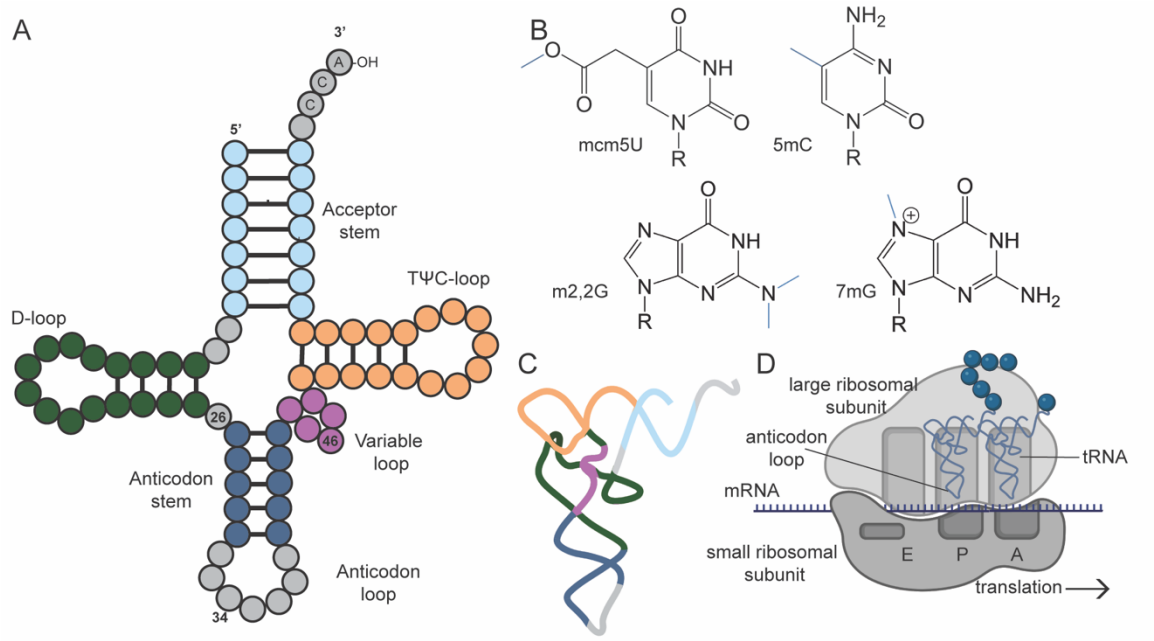

Figure 1.1. tRNAs mediate translation

A-B. Graphical illustration of tRNA cloverleaf structure (A) with representative modified positions discussed are numbered (bold font) with (B) representative chemical structures of nucleoside methylations (blue), where R equals the ribose. tRNA modification abbreviations - mcm5U: 5-methyoxycarbonyl-methyluridine; m5C: 5-methylcytidine; m7G: 7-methylguanine; m2,2G: N2,N2-dimethylguanosine.

C-D. Tertiary tRNA structure (C) adopted from (Suzuki, 2021) highlighting acceptor stem (light blue), D-loop (green), anticodon stem and loop (dark blue and gray respectively), variable loop (purple), T-loop (orange) and (D) charged tRNAs in translation. Panels C and D were created in BioRender (https://BioRender.com).

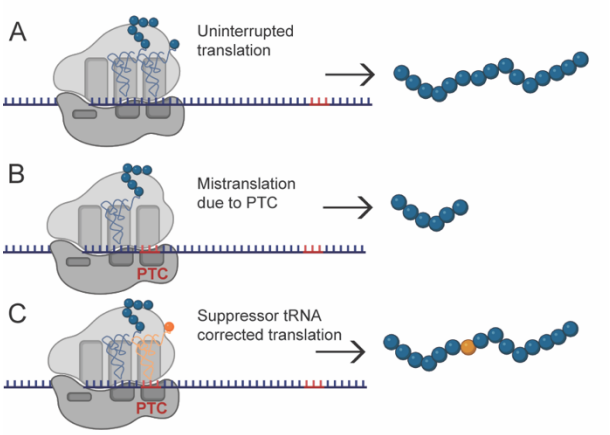

Figure 1.2. Illustration of suppressor tRNAs function

Graphical representation of (A) uninterrupted translations which generates a fully formed polypeptide chain, (B) interrupted translation due to a premature stop codon (PTC, red) that results in a truncated protein and (C) corrected mistranslation with the addition of an engineered suppressor tRNA (orange, charged tRNA with amino acid) that stabilizes the PTC (red) and results in a fully formed polypeptide chain. Figure adapted from (Porter *et al.*, 2021) and created in BioRender (https://BioRender.com).

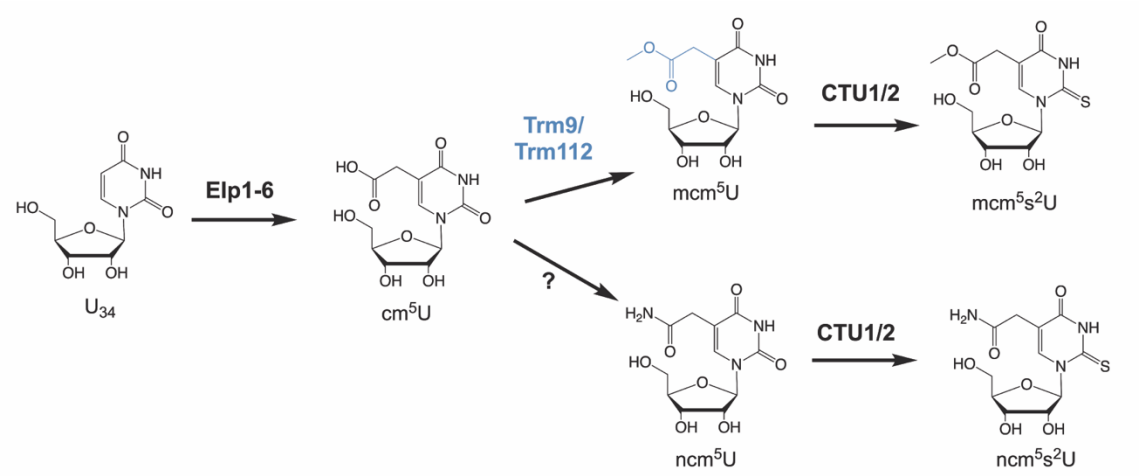

Figure 1.3. Wobble uridine (U_{34}) methylation in yeast adapted from (Hogan *et al.*, 2023). Abbreivations - Elp: elongator complex; cm^5U: 5-carbonylmethyluridine; Trm9: tRNA methyltransferase 9; Trm112: tRNA methyltransferase 112; mcm^5U: 5-methyoxy-carbonylmethyluridine; CTU: cytosolic thiouridylase; mcm^5s^2U: 5-methoxy-carbonylmethyl-2-thiouridine; ncm^5U: 5-carbamoylmethyluridine; ncm^5s^2U: 5-carbamoylmethyl-2-thiouridine

CHAPTER 2

Expanded tRNA methyltransferase family member TRMT9B regulates synaptic growth and function

Adapted from Hogan CA**,** Gratz, SJ and Dumouchel JL *et al* (2023) **EMBO Rep** 24(10): e56808. PMID: 37642556

Caley A Hogan[1*], Scott J. Gratz[2*], **Jennifer L. Dumouchel[3*]**, Ambar Delgado[2*], Jenna M. Lentini[4*], Kimberly R. Madhwani[5*], Rajan S. Thakur[2*], Dragony Fu[4], and Kate M. O'Connor-Giles[2,6#]

[1]Genetics Training Program, University of Wisconsin-Madison, Madison, WI
[2]Department of Neuroscience, Brown University, Providence, RI
[3]Therapeutic Sciences Graduate Program, Brown University, Providence, RI
[4]Department of Biology, Center for RNA Biology, University of Rochester, Rochester, NY
[5]Neuroscience Graduate Training Program, Brown University, Providence, RI
[6]Carney Institute for Brain Science, Providence, RI

*Equal contribution
[#]Corresponding author: Kate M. O'Connor-Giles; email: oconnorgiles@brown.edu

The authors declare no competing interests.

Keywords: TRMT9B, synapse, neurotransmitter release, tRNA methyltransferase, *Drosophila*

Author contributions:
Conceptualization: CAH, SJG, DF, KOCG; Investigation: CAH, SJG, JLD, AD, JL, KRM, RT; Formal Analysis: CAH, SJG, JLD, AD, JL, KRM, RT, DF, KOCG; Writing – Original Draft Preparation: CAH, KOCG; Writing – Review & Editing: CAH, SJG, JLD, AD, JL, KRM, DF, KOCG; Visualization - CAH, SJG, JLD, JL, RT, DF, KOCG; Project Administration - KOCG, DF; Funding Acquisition - KOCG, DF.

ABSTRACT

Nervous system function rests on the formation of functional synapses between neurons. We have identified TRMT9B as a new regulator of synapse formation and function in Drosophila. TRMT9B has been studied for its role as a tumor suppressor and is one of two metazoan homologs of yeast tRNA methyltransferase 9 (Trm9), which methylates tRNA wobble uridines. Whereas Trm9 homolog ALKBH8 is ubiquitously expressed, TRMT9B is enriched in the nervous system. However, in the absence of animal models, TRMT9B's role in the nervous system has remained unstudied. Here, we generate null alleles of *TRMT9B* and find it acts postsynaptically to regulate synaptogenesis and promote neurotransmission. Through liquid chromatography-mass spectrometry, we find that ALKBH8 catalyzes canonical tRNA wobble uridine methylation, raising the question of whether TRMT9B is a methyltransferase. Structural modeling studies suggest TRMT9B retains methyltransferase function. *In vivo*, disruption of key methyltransferase residues blocks TRMT9B's ability to rescue synaptic overgrowth, but not neurotransmitter release. These findings reveal distinct roles for TRMT9B in the nervous system and highlight the significance of tRNA methyltransferase family diversification in metazoans.

INTRODUCTION

Complex nervous systems are composed of thousands to billions of neurons connected through synapses in neural circuits that control behavior and thought. To achieve this functional organization, neurons must form synaptic connections in appropriate numbers and strength during development. Synapse number and strength are also substrates for the neuronal plasticity that underlies experience-dependent changes to brain function (Citri & Malenka, 2008). Dysregulation of synapse formation and plasticity have been broadly linked to neurodevelopmental disorders, including autism spectrum disorder and other forms of intellectual disability (Guang *et al*, 2018; Zoghbi & Bear, 2012). While we have learned a great deal about a small subset of genes underlying neurodevelopmental disorders, a recent study found that the majority of genes in the human genome are understudied – including those associated with human disorders (Stoeger *et al*, 2018). With the increasingly broad application of clinical sequencing in individuals with neurodevelopmental delay, new genes whose function in the nervous system remains unknown are being uncovered. A lack of foundational understanding of synaptic gene function is a significant obstacle for translating clinical identification of causative variants into effective treatments for neurodevelopmental disorders.

To uncover conserved, uncharacterized genes with roles in the formation of functional synapses, we first looked for genes expressed 'in the right place at the right time.' Using ModENCODE data (Brown *et al*, 2014; Graveley *et al*, 2011) we observed that many Drosophila synaptic genes exhibit a unique spatio-temporal transcriptional profile during development. Expression is enriched in the nervous system and transcription is generally low with peaks during each of the two periods of extensive synaptogenesis, late embryonic and pupal (Fig. 2.S1). We reasoned that uncharacterized genes with this expression pattern might be enriched for genes involved in synapse formation and/or

function and compared the expression pattern of every gene in the genome with this profile. Focusing on genes with the highest correlation coefficients that were uncharacterized and conserved in mammals, we began generating CRISPR loss-of-function and endogenously tagged alleles to assess potential roles in synapse development at the well-characterized glutamatergic neuromuscular junction (NMJ). Computed Gene 42261 (CG42261) emerged as a potential negative regulator of synaptic growth. CG42261, which was also identified in an RNAi screen as a potential regulator of thermal nociception and named *fire dancer* (Honjo *et al*, 2016), encodes the Drosophila homolog of human TRMT9B. TRMT9B has been studied for its role as a tumor suppressor and is downregulated in colorectal, breast, bladder, cervical, ovarian and testicular carcinomas (Begley *et al*, 2013; Chen *et al*, 2017; Flanagan *et al*, 2004; Wang *et al*, 2018). TRMT9B is one of two metazoan homologs of yeast tRNA methyltransferase 9 (Trm9), which methylates tRNA wobble uridines (Begley *et al*, 2007; Begley *et al.*, 2013; Fu *et al*, 2010a; Kalhor & Clarke, 2003; Songe-Moller *et al*, 2010). Trm9 homolog ALKBH8 has a demonstrated role in catalyzing tRNA wobble uridine methylation in mammals (Fu *et al.*, 2010a; Songe-Moller *et al.*, 2010), whereas it has remained unknown if TRMT9B plays a similar role despite years of study. Intriguingly, an emerging body of work demonstrates that enzymes in the expanded metazoan tRNA methyltransferase family have evolved to methylate new substrates, including rRNAs, mRNAs and proteins (Abbasi-Moheb *et al*, 2012; Chellamuthu & Gray, 2020; Chen *et al*, 2011; Xu *et al*, 2017). Methylation of each of these substrates provides a reversible level of regulation that modulates biological processes ranging from transcription to splicing to translation to protein interactions, pointing to diverse regulatory roles for these tRNA methyltransferases (Greenberg & Bourc'his, 2019; Murn & Shi, 2017; Zhou *et al*, 2020).

Here, we detail the first animal model of *TRMT9B* to investigate its biological role in the nervous system. Using endogenously tagged lines, we find that TRMT9B is expressed in neuronal, glial and muscle cell bodies, and at synapses. At the NMJ, TRMT9B functions postsynaptically to regulate synaptic growth and promote neurotransmitter release. Through quantitative RNA mass spectrometry, we determined that TRMT9B is dispensable for baseline tRNA wobble uridine methylation, raising the possibility that it has evolved a new function. Our modeling studies and genetic rescue experiments suggest that TRMT9B regulates synapse formation through a methyltransferase-dependent mechanism whereas its role in neurotransmission appears to be independent of enzymatic function. Together our findings highlight the expanding roles of the tRNA methyltransferase family in animals and reveal critical requirements for TRMT9B in nervous system development.

RESULTS

TRMT9B negatively regulates synaptic growth

As part of an ongoing effort to identify and characterize new regulators of synapse formation and function, we used ModENCODE developmental RNA-Seq data to identify uncharacterized, conserved neuronal genes whose expression in Drosophila corresponds to periods of synaptogenesis (Graveley *et al.*, 2011). We then began generating CRISPR alleles of top candidate genes (Dietzl *et al*, 2007; Hu *et al*, 2017; Ni *et al*, 2011) and investigating synapse number at glutamatergic motor synapses. As detailed below, loss of CG42261, which encodes one of two Drosophila homologs of yeast wobble uridine methyltransferase Trm9, resulted in significant ectopic synapse formation. CG42261 was also identified in an RNAi screen for candidate regulators of thermal nociception and named *fire dancer (fid)*; (Honjo *et al.*, 2016). Here, we follow

recently established nomenclature for members of the tRNA methyltransferase family and refer to CG42261/Fid as TRMT9B (Tweedie *et al*, 2021).

We used CRISPR-based gene editing to generate two independent null alleles: (1) *TRMT9B*^{KO}, in which the exons coding for 1366/1391 amino acids are removed and replaced with a visible marker and attP landing site and (2) *TRMT9B*$^{HA+IC}$, in which an HA peptide tag and a cassette encoding a visible marker flanked by piggyBac inverted terminal repeat sequences is inserted after the sole *TRMT9B* translational start site (Fig. 2.1A). The visible marker cassette disrupts the open reading frame to generate a null allele, and its subsequent removal by piggyBac transposase yields an in-frame epitope-tagged allele (Bruckner *et al*, 2017).

At well-characterized Drosophila larval NMJs, individual motorneurons form tens to hundreds of glutamatergic synapses with postsynaptic muscle targets in a stereotyped manner. We quantified synaptic growth by counting synaptic boutons at the highly stereotyped NMJ 4 formed between motorneuron 4-1b and muscle 4. We observed a significant increase in bouton number in homozygous *TRMT9B*^{KO}, homozygous *TRMT9B*$^{HA+IC}$, and heteroallelic *TRMT9B*$^{KO/HA+IC}$ mutants (Fig. 2.1B-E,G). All three *TRMT9B* allelic combinations exhibited a 30-35% increase in bouton number relative to control. We observe similar synaptic overgrowth in *TRMT9B*^{KO} over a deficiency and in a line with artificial stop codons (*TRMT9B*$^{MiMIC\text{-}STOP}$) that is partially restored to wild type when one copy of the stop cassette is replaced with GFP (*TRMT9B*$^{MiMIC\text{-}GFP}$, Fig. 2.S2A; (Nagarkar-Jaiswal *et al*, 2015; Venken *et al*, 2011). We also observe synaptic overgrowth at NMJ 6/7 (Fig. 2.S2B), consistent with a broader role in restraining synapse formation.

To further confirm loss of *TRMT9B* as the cause of synaptic overgrowth, we restored gene function under endogenous control by removing the interfering cassette in *TRMT9B*$^{HA+IC}$ to generate N-terminally tagged *TRMT9B*^{HA}. Bouton number at *TRMT9B*^{HA} NMJs was restored to near control levels, suggesting the endogenous tag may have a minor effect on protein function (Fig. 2.1F,G). Together, these findings reveal a requirement for TRMT9B in restraining synaptic growth.

TRMT9B promotes neurotransmitter release

To investigate the impact of loss of TRMT9B on nervous system function, we assessed neurotransmission at *TRMT9B* null NMJs. To assess neurotransmission in our mutants, we measured spontaneous and evoked synaptic potentials through current clamp recordings at muscle 6, which is innervated by one type Ib and one type Is motorneuron. We observed significantly reduced excitatory junction potentials (EJPs) together with normal miniature EJP (mEJP) amplitude (quantal size) in *TRMT9B* null mutants (Fig. 2.2A-E). These findings indicate a 51% decrease in neurotransmitter release (quantal content; Fig. 2.2F). Restoration of endogenous *TRMT9B* function through removal of the *TRMT9B*$^{HA+IC}$ interfering cassette fully rescued EJPs (Fig. 2.2C,D, *TRMT9B*^{HA}). mEJPs were slightly increased and, thus, quantal content was not fully restored to wild-type levels (Fig. 2.2C,E,F), suggesting again that the endogenous tag may have a small effect on TRMT9B function. Thus, in addition to its role in restraining synaptic growth, TRMT9B promotes synaptic function.

TRMT9B is expressed in neurons, glia and muscle

Consistent with its roles in synapse development, *TRMT9B* is enriched in Drosophila and mammalian nervous systems in contrast to ALKBH8, which is ubiquitously expressed across species (Brown *et al.*, 2014; GTEx, 2015; Uhlén *et al*, 2015; Yue *et al*,

2014). To investigate the cellular and subcellular expression of TRMT9B in the nervous system and at the NMJ, we turned to our endogenously tagged alleles. In N-terminally tagged *TRMT9B*^{sfGFP}, we observe expression in neuronal cell bodies (Fig. 2.3A) and the synaptic neuropil of the larval ventral ganglion as indicated by colocalization with active zone protein Brp (Fig. 2.3B). To determine which cell types express TRMT9B in the nervous system, we conducted colocalization studies with the neuronal marker Elav and glial marker Repo. We found that TRMT9B is strongly expressed in neuronal as well as glia cell bodies (Fig. 2.3C). TRMT9B is also expressed in muscle, where it is broadly cytoplasmic with peri-nuclear accumulation (Fig. 2.3D). Finally, we observe TRMT9B at the NMJ where it primarily colocalizes presynaptically with the neuronal membrane marker HRP. In contrast, we do not observe expression at the postsynaptic density (Fig. 2.3D). While we cannot rule out the possibility that the tag has a minor effect on subcellular localization, we observe a similar expression pattern, albeit at lower levels, in *TRMT9B*^{HA}, which largely rescues synaptic growth and function (Fig. 2.S3A-C; See Figs 1 and 2), indicating that tagged alleles localize similarly in the nervous system. TRMT9B's broad cellular and subcellular expression pattern in neurons, glia and muscle raises the intriguing possibility of a role for TRMT9B in methylating different substrates in distinct cells and subcellular locations, including at synapses.

TRMT9B functions postsynaptically to regulate synaptic growth

Synapse formation involves a complex interplay between pre- and postsynaptic cells, both of which express TRMT9B. Our endogenous rescue system offers the advantage of driving expression at biological levels, but does not allow spatial control of gene expression. To determine the site of TRMT9B function in regulating motor synapse formation, we conducted cell-specific rescue using *C155-Gal4* and *24B-Gal4* to drive expression of a full-length *TRMT9B* transgene in presynaptic neurons and postsynaptic

muscle, respectively. We found that muscle, but not neuronal, expression of *TRMT9B* fully rescues synaptic growth at the NMJ (Fig. 2.4A-H). Thus, TRMT9B acts postsynaptically to attenuate synaptic growth.

We next quantified individual active zones labeled with Brp and found that the number of active zones per NMJ is wild type in *TRMT9B* mutants due to a decrease in active zone number per bouton that offsets the increase in bouton number (Fig. 2.4I-L). This indicates that a previously described homeostatic mechanism for maintaining overall active zone number at NMJs (Goel *et al*, 2019) is intact in the absence of TRMT9B. Coupled with the decrease in neurotransmitter release, this further suggests that individual *TRMT9B* synapses are impaired. Thus, TRMT9B regulates both NMJ growth and the formation of functional synapses – defining fundamental neurodevelopmental roles for this member of the expanded family of tRNA methyltransferases.

Wobble uridine methylation in the absence of TRMT9B

We next sought to determine whether TRMT9B retains canonical tRNA methyltransferase function. Both TRMT9B and its paralog ALKBH8 are homologous to yeast Trm9, yet it has remained unknown if both proteins methylate wobble uridines. Of the two metazoan homologs, TRMT9B has a domain structure more similar to Trm9 with a well-conserved Class I SAM-dependent methyltransferase domain (Fig. 2.5A). In contrast, ALKBH8, in addition to a conserved methyltransferase domain, contains an RNA-binding motif and a 2OG-Fe (II) oxygenase domain that catalyzes an animal-specific tRNA modification (Fig. 2.5A, (Fu *et al*, 2010b; van den Born *et al*, 2011). Mouse and human ALKBH8 have been shown to methylate tRNA wobble uridines (Fu *et al.*, 2010a; Songe-Moller *et al.*, 2010), whereas TRMT9B's biochemical function has remained unknown in the absence of animal models. To investigate the respective roles

of the two Drosophila Trm9 paralogs in tRNA methylation, we generated a null allele of Drosophila *ALKBH*8, currently identified as CG17807. To our knowledge, this is the first animal model in which both paralogs have been knocked out, allowing us to investigate the molecular function of each protein.

Most of our understanding of tRNA wobble uridine modification comes from studies in yeast (Schaffrath & Leidel, 2017). In one branch of the wobble uridine modification pathway, the Elongator complex is thought to act first to generate 5-carbonylmethyluridine (cm5U, Fig. 2.5B, purple). Trm9 then acts in concert with obligate cofactor Trm112 to add a second methyl group and generate 5-methoxycarbonylmethyluridine (mcm5U, Fig. 2.5B, pink). Further modification by the Ncs2-Ncs6 thiolase complex generates a terminal mcm5s2U modification (Fig. 2.5B, green). In a second branch, wobble uridines in certain tRNAs are converted to the amide modification ncm5U by an unknown enzyme (Fig. 5B, orange (Johansson *et al*, 2008).

To analyze tRNA wobble uridine modification in our null alleles, we conducted quantitative liquid chromatography-mass spectrometry (LC-MS). Briefly, total RNA isolated from heads of mated male and female control, *TRMT9B*^{KO}, and *ALKBH8*^{KO} flies was nuclease digested and dephosphorylated to generate individual ribonucleosides followed by LC-MS analysis of nucleoside modifications (Cai *et al*, 2015; Dewe *et al*, 2017; Fu *et al.*, 2010a). We found that the mcm5s2U modifications, which is tRNA specific and in yeast depends on Trm9, is present in nucleosides isolated from control and *TRMT9B*^{KO} flies, but reduced to near background levels in *ALKBH8*^{KO} flies (Fig. 2.5C). Similarly, mcm5U, which is the terminal modification for a single tRNA and thus present at low levels near our resolution of detection, was observed at similar levels in control and *TRMT9B*^{KO} flies (control: 92.13 $\pm$ 14.59, *TRMT9B*^{KO}: 101.70 $\pm$ 26.45,

P=0.92) and not detected in the absence of ALKBH8. Notably, we detected an increase in the accumulation of ncm5U and ncm5S2U in *ALKBH8*^{KO} flies, but not control or *TRMT9B* flies (Fig. 2.5C, D). These findings are consistent with studies in yeast showing that loss of Trm9 leads to loss of mcm5s2U concomitant with the accumulation of amide intermediates (Chen *et al.*, 2011). Based on these findings, we conclude that ALKBH8 methylates tRNA wobble uridines independently of TRMT9B under basal conditions.

We next explored the possibility that TRMT9B catalyzes a different tRNA methylation – a possibility hinted at in previous overexpression studies (Begley *et al.*, 2013). Specifically, we investigated a panel of well-characterized tRNA modifications at multiple tRNA sites, the majority involving methylation. Further confirming our results above, we found that mcm5s2U was decreased to near background levels in *ALKBH8*^{KO} flies while no major change in mcm5s2U was detected in *TRMT9B*^{KO} flies (Fig. 2.5D). For the remaining modifications with levels within a quantifiable range, we observed a slight variation in levels for a subset of nucleosides isolated from the *ALKBH8*^{KO} flies when compared to control flies, suggesting that loss of ALKBH8-catalyzed wobble uridine modifications could impact other tRNA modifications. In contrast, no modification exhibited more than a 2-fold change in the *TRMT9B*^{KO} compared to control.

Finally, we explored the possibility that TRMT9B has a developmental role in tRNA wobble uridine modification by analyzing wobble uridine modifications in third-instar larvae. We isolated the nervous system and body walls to assess both neuronal and muscle roles. Again, we found that mcm5s2U is lost while ncm5U and ncm5S2U are increased in *ALKBH8*, but not *TRMT9B*, mutants (Fig. 2.5E). While our findings do not rule out the possibility that TRMT9B plays a conditional role in tRNA wobble uridine methylation or methylates a small subset of tRNAs not detectable by bulk analysis, these

observations indicate that ALKBH8 is the primary paralog carrying out the canonical Trm9 tRNA wobble uridine methyltransferase role and suggest a new role for TRMT9B.

TRMT9B has a structurally conserved methyltransferase domain

This finding raises the question of whether TRMT9B has maintained function as a methyltransferase or evolved a non-enzymatic role. To investigate TRMT9B's potential role as a methyltransferase, we first aligned the predicted methyltransferase domains of yeast Trm9 with Drosophila and human TRMT9B (Fig. 2.6A). Although methyltransferases are not generally well conserved at the level of primary sequence (Martin & McMillan, 2002), we observe conservation throughout the methyltransferase domain, including residues known to be important for methyltransferase function. The defining sequence features of Class I SAM-dependent methyltransferase are (1) an acidic residue at the end of the first beta strand and (2) a GxGxG SAM-binding motif – both of which are critical for SAM binding and conserved in yeast Trm9 and fly and human TRMT9B (Fig. 2.6A, blue boxed residues; (Kozbial & Mushegian, 2005; Martin & McMillan, 2002). Additional acidic residues in beta strands 2, 3 and 4 and glycines in beta strand 5 that are highly conserved across Class I SAM-dependent methyltransferases are also present in fly and human TRMT9B (Fig. 2.6A, blue residues; (Kozbial & Mushegian, 2005). We next assessed residues found to be critical for SAM binding and enzymatic activity in a comprehensive mutational analysis of yeast Trm9 (Létoquart *et al*, 2015), and found that these residues are also highly conserved in Drosophila and human TRMT9B and ALKBH8 (Fig. 2.6A, black and red boxed residues). Together, these observations are consistent with the model that both paralogs retain methyltransferase function.

To investigate tertiary structure, we generated structural homology models of the methyltransferase domains of Drosophila and human TRMT9B and ALKBH8. For an unbiased approach, we used Modeller to model the methyltransferase domains against known crystal structures reported in the RCSB Protein Data Bank (Pieper *et al*, 2014), and identified Trm9 as a match for each enzyme, lending further support for the hypothesis that both TRMT9B and ALKBH8 maintain methyltransferase function. To evaluate structural conservation, we used Chimera to compare our Drosophila TRMT9B methyltransferase domain model to the yeast Trm9 structure determined by X-ray diffraction of *Yarrowia lipolytica* Trm9 and its obligate co-factor Trm112 (Fig. 2.6B; (Létoquart *et al.*, 2015). Class I methyltransferases form a seven-stranded beta sheet flanked by alpha helices. In our model, this folded structure is maintained and key residues are superimposed (Fig. 2.6B, orange ribbon). We observed similar structural conservation between yeast Trm9 and our model of human TRMT9B (Fig. 2.S4A). We next overlaid our models of TRMT9B with Drosophila and human ALKBH8 and observed significant structural conservation between the four methyltransferase domains (Fig. 2.6C). Finally, we assessed the predicted structure of the Drosophila TRMT9B methyltransferase domain using AlphaFold (Jumper *et al*, 2021; Varadi *et al*, 2022). Strong alignment was observed between the AlphaFold predicted model, the Drosophila TRMT9B model predicted using Modeller, and the yeast Trm9 crystal structure (Fig. 2.S4B). Thus, multiple independent *in silico* modeling approaches support structural conservation of TRMT9B's methyltransferase domain across species, suggesting TRMT9B functions as a methyltransferase in flies and humans.

Disruption of TRMT9B's methyltransferase domain blocks rescue of synaptic growth

To experimentally determine if TRMT9B functions as a methyltransferase, we sought to generate a methyltransferase-dead rescue construct for expression under GAL4 control and compared its ability to rescue synaptic growth deficits in *TRMT9B* mutants to wild-type rescue constructs. To disrupt methyltransferase function, we replaced two residues identified by Létoquart and colleagues as critical for SAM substrate binding and catalytic activity in Trm9 with alanines (See Fig. 6A, red boxed residues; (Létoquart *et al.*, 2015). Absent a known substrate for TRMT9B, we cannot biochemically assess the disruption of methyltransferase function, so we confirmed that the residues correspond in our structural alignments and modeled the effect of alanine substitutions on protein structure to confirm that tertiary protein structure remains intact, consistent with prior studies (Fig. 2.7A; (Létoquart *et al.*, 2015). We integrated wild-type (*UAS-TRMT9B*) and methyltransferase-dead (*UAS-TRMT9B*^{MTD}) transgenes at the same genomic site and expressed each transgene under the control of *24B-Gal4* in *TRMT9B* nulls. While expression of wild-type *TRMT9B* fully rescued synaptic overgrowth as observed above, expression of *TRMT9B*^{MTD} failed to rescue (Fig. 2.7B-F), consistent with the conclusion that methyltransferase activity is required for TRMT9B's role in regulating synaptic growth. To confirm proper translation and localization of methyltransferase-dead TRMT9B, we generated V5-tagged versions of the wild-type and methyltransferase-dead transgenes and confirmed expression of the correct size proteins at comparable levels by western blot (Fig. S5A, B) and similar localization patterns when expressed in neurons or muscle (Fig. 2.S5C-H). Consistent with our sequence and structural analyses, these data provide additional support for the model that TRMT9B functions through a methyltransferase-dependent mechanism to regulate synaptic growth.

TRMT9B regulates neurotransmitter release through a distinct mechanism

Our findings indicate that TRMT9B promotes neurotransmitter release independently of its role in regulating synapse number. To determine if methyltransferase function is also required for TRMT9B's role in neurotransmission, we first conducted cell-specific rescue and found that postsynaptic expression of TRMT9B fully rescues neurotransmitter release (Fig. 2.8A-D, H-J). In contrast, presynaptic expression of TRMT9B fails to rescue (*TRMT9B*$^{KO/HA+IC}$ vs. *C155; TRMT9B*^{KO}*/UAS-TRMT9B, TRMT9B*$^{HA+IC}$: P=0.408, ANOVA followed by Tukey's test). We next attempted to rescue synaptic function with *TRMT9B*^{MTD} and found that methyltransferase-dead TRMT9B also restores neurotransmitter release (Fig. 2.8E, H-J). We assessed neurotransmission upon postsynaptic overexpression of either methyltransferase-dead or wild-type TRMT9B and observed no effect (Fig. 2.8F,G H-J), ruling out additive effects. Thus, TRMT9B can promote neurotransmitter release independently of its methyltransferase function. These findings indicate diverse functions for TRMT9B in synaptogenesis and neurotransmitter release and underscore the important role of the expanded tRNA methyltransferase family in the nervous system.

DISCUSSION

We hypothesized that we could identify new, conserved regulators of synapse formation among uncharacterized genes whose transcription specifically correlates with peak periods of synaptogenesis during Drosophila embryonic and adult nervous system development. This otherwise unbiased approach led to the surprise discovery of a member of the tRNA methyltransferase family. Through biochemical, structural modeling and genetic studies, we found that TRMT9B regulates synaptogenesis through a methyltransferase-dependent mechanism and may have evolved in animals to methylate

a novel substrate. Our data also suggest that TRMT9B can promote neurotransmitter release through a non-enzymatic mechanism. These findings highlight both the important regulatory role of methylation in the nervous system and the expanding functions of tRNA methyltransferase family members.

In Drosophila, *TRMT9B* transcription peaks in late embryogenesis shortly before synaptogenesis begins in the developing nervous system. *TRMT9B* is primarily expressed in the nervous system, with lower levels of expression in carcass (muscle and epidermis), fat body, imaginal discs, and testes (Brown *et al.*, 2014). Similarly, mouse and human *TRMT9B* are highly expressed in the nervous system, including the cerebellum, visual cortex, hippocampus and cerebral cortex (GTEx, 2015; Uhlén *et al.*, 2015; Yue *et al.*, 2014). Nonetheless, to date TRMT9B has only been studied in the context of non-neuronal cancers, although a recent study found that TRMT9B expression is significantly increased along with a host of gene regulatory proteins during NeuroD1-mediated conversion of astrocytes to neurons (Ma *et al*, 2022). An RNAi screen in Drosophila identified a putative role for Drosophila *TRMT9B* in promoting dendrite outgrowth in class IV multidendritic sensory neurons and in thermal nociception (Honjo *et al.*, 2016). We find that TRMT9B negatively regulates synaptogenesis at the NMJ and *TRMT9B* mutants display significant impairment in neurotransmitter release. While bouton number is increased in *TRMT9B* mutants, a homeostatic decrease in the number of active zones per bouton normalizes synapse number per NMJ. This indicates that abnormal synaptic transmission in *TRMT9B* mutants is due to functional impairment of the individual synapses that compose the NMJ rather than altered synapse number, pointing to a requirement for TRMT9B in regulating both synapse number and the formation of functional synapses.

In 2004, TRMT9B was first identified as a potential tumor suppressor in colorectal cancer (Flanagan *et al.*, 2004). Since that time, reduced TRMT9B expression due to genomic rearrangements or epigenetic silencing has been observed in ovarian, lung, and other carcinomas (Begley *et al.*, 2013; Chen *et al.*, 2017; Flanagan *et al.*, 2004; Wang *et al.*, 2018). Restoration of TRMT9B expression in colon, lung, and ovarian cancer cells reduces proliferation and significantly reduces colon tumor growth *in vivo*, confirming an important tumor suppressor role for TRMT9B (Blanco *et al*, 2014; Chen *et al.*, 2017; Wang *et al.*, 2018). Despite the numerous links to cancer, the biological role of TRMT9B function has remained unknown. Although insight into TRMT9B's biochemical role has been limited by the lack of an animal model, a gain-of-function study found that TRMT9B promotes expression of tumor suppressor LIN9, a core member of the DREAM complex that represses cell cycle-dependent gene expression, and blocks HIF1-α-dependent adaptation to a hypoxia (Begley *et al.*, 2013). A more recent study found that stress-dependent phosphorylation modulates TRMT9B's interactions with the 14-3-3 gamma, epsilon, and eta signaling molecules and its ability to suppress proliferation and hypoxic adaptation (Gu *et al*, 2018).

The tRNA methyltransferase (Trm) family of enzymes has expanded from 18 Trm proteins that form 15 holoenzymes in yeast to 34 Trm homologs in humans, with all yeast tRNA methyltransferases represented in animals and more than half represented by two or more paralogs in humans (Towns & Begley, 2012). Many of the additional family members in animals are yet to be characterized, raising the question of whether they maintain redundant roles as canonical tRNA methyltransferases or have evolved new functions. Of the two metazoan homologs of yeast Trm9, mammalian ALKBH8 has been shown to methylate tRNA wobble uridines (Fu *et al.*, 2010a; Kalhor & Clarke, 2003; Songe-Moller *et al.*, 2010). Our quantitative mass spectrometry studies demonstrate that

ALKBH8 is similarly responsible for the methylation of tRNA wobble uridines in Drosophila. Interestingly, ALKBH8 has recently been linked to intellectual disability in several families, and, we have found, acts through a tRNA methyltransferase-dependent mechanism to regulate nervous system development (Maddirevula *et al*, 2022; Monies *et al*, 2019; Saad *et al*, 2021).

In contrast, we find that TRMT9B is either dispensable for tRNA wobble uridine methylation or plays a conditional role not detected in our analysis. Our findings are consistent with the previous observation that ALKBH8, but not TRMT9B, can rescue tRNA methylation in a yeast deletion of Trm9 (Begley *et al.*, 2013) and suggest TRMT9B may have evolved a new function. TRMT9B might also function as a tRNA wobble uridine methyltransferase under specific conditions or methylate only one or a few, possibly brain-enriched, tRNAs as has recently been demonstrated for a mammalian homolog of yeast Trm140, which methylates tRNAs in the anticodon loop (Xu *et al.*, 2017). This possibility would be consistent with the recent finding that overexpression of TRMT9B leads to subtle, but significant changes in tRNAs with an mcm5U terminal modification, although mcm5S2U levels remain unchanged (Jungfleisch *et al*, 2022).

To explore how TRMT9B might function biochemically, we investigated TRMT9B's sequence and structural homology with SAM-dependent methyltransferases. Several lines of evidence suggest that TRMT9B retains methyltransferase function: (1) residues required for enzymatic function in yeast are highly conserved, including the canonical Class I SAM-dependent methyltransferase GxGxG motif and acidic amino acid at the end of the second beta strand, both of which mediate SAM binding; (2) structural modeling reveals remarkable similarity between the methyltransferase domains of yeast Trm9 and fly and human TRMT9B and ALKBH8; and (3) disruption of two residues

critical for methyltransferase function in yeast eliminates the ability of a TRMT9B transgene to rescue synaptic growth without disrupting its ability to fold or localize properly. Although these highly conserved residues appear to be critical for methyltransferase function in Drosophila *TRMT9B*, without a substrate we cannot confirm this biochemically. In contrast to synaptic growth, we found that *TRMT9B*^{MTD} restores neurotransmitter release in *TRMT9B* mutants. Thus, TRMT9B appears to have evolved an entirely novel methyltransferase-independent role, possibly as a scaffolding protein or competitive interactor of TRM112. Future genetic and biochemical studies to identify functional interactors will be important.

Another major next step will be identifying TRMT9B's substrate(s). A previous study identified changes to a number of tRNA modifications upon expression of TRMT9B (Begley *et al.*, 2013). However, it is unclear if any of these modifications are direct targets of TRMT9B as many tRNA modifications depend on prior modifications. To investigate the possibility that TRMT9B catalyzes a distinct modification on tRNAs, we assessed a panel of tRNA post-transcriptional modifications in our mutants via quantitative mass spectrometry. We did not identify a TRMT9B-dependent modification among our panel, which includes nine of the 12 modifications affected in the Begley et al. (Begley *et al.*, 2013) study. However, it remains possible that TRMT9B catalyzes a modification we were unable to evaluate, including an animal-specific tRNA modification yet to be identified. As most of our understanding of tRNA methylation comes from studies in single-cell organisms, it would not be surprising if additional tRNA modifications specific to animals, and possibly enriched in specific tissues such as the nervous system, remain undiscovered. Another possibility is that TRMT9B methylates a non-tRNA substrate. In fact, several members of the expanded metazoan tRNA methyltransferase family methylate non-tRNA substrates. For example, the NSUN family

of yeast Trm4 homologs, methylate not only tRNAs, but mRNA, rRNA, and noncoding RNAs, and have important roles in both cancer and neurodevelopment (Abbasi-Moheb *et al.*, 2012; Chellamuthu & Gray, 2020; Chen *et al*, 2021). Intriguingly, we have found that both fly and human TRMT9B immunoprecipitate TRMT112, the homolog of obligate yeast Trm9 co-factor Trm112, in IP-LC-MS/MS experiments (2 unique peptides, 11% peptide coverage; (Gu *et al.*, 2018), respectively). TRMT112 promotes the methylation of diverse substrates as an obligate cofactor for several tRNA, rRNA, and protein methyltransferases – an indication of the expansive landscape of potential TRMT9B substrates (Gao *et al*, 2020; Garcia *et al*, 2021; Guy & Phizicky, 2014; van Tran *et al*, 2019; Yang *et al*, 2021). A recent study of the Trm112 interactome in Archaea identified a similarly broad array of interacting methyltransferases as well as small molecule methyltransferases involved in steroid and vitamin biosynthesis (van Tran *et al*, 2018), raising still more diverse possibilities. Especially exciting is the possibility hinted at by its endogenous expression pattern that TRMT9B methylates distinct targets in different cellular and sub-cellular contexts, including synaptic targets. Given TRMT9B's fundamental roles as a regulator of synapse formation and function and a tumor suppressor, it will be of great interest and clinical significance to identify target(s) of TRMT9B methylation in future studies.

MATERIALS AND METHODS

Drosophila genetics and gene editing

The following stocks used in this study are available through the Bloomington Drosophila Stock Center (BDSC): *w*^{1118} (RRID:BDSC_5905), *vasa-Cas9* (RRID:BDSC_51324), piggyBac transposase (RRID:BDSC_8283), *attP2* (RRID:BDSC_25710), *elav*^{c155} *Gal4* (RRID:BDSC_458), *24B Gal4* (RRID:BDSC_92172). y^{1} w*; Mi(mod *et al*)fid^{MI13909}

(*TRMT9B MiMIC*^{Stop}) and *y*^{1} *w***; Mi{PT-GFSTF.1}dfid*$^{MI13909\text{-}GFSTF.1}$ (*TRMT9B MiMIC*^{GFP}) were generated through the Gene Disruption Project and obtained from the BDSC (RRID:BDSC_59229 and RRID:BDSC_66771) (Nagarkar-Jaiswal *et al.*, 2015; Venken *et al.*, 2011). All crosses were set up with 10 males and 10 females in 25ºC incubators with humidity control and 12h light/dark cycles.

CRISPR-based homology directed repair strategies were used to generate knockouts and in-frame endogenous tags. Target sites were selected using CRISPR Optimal Target Finder program (http://targetfinder.flycrispr.neuro.brown.edu; (Gratz *et al*, 2014)). The following gRNAs were used: TRMT9B^{KO}: 5′-AATCCATCGTCCTGAAATAG-3′, 5’-AGTCTATTACTCTAGTCGGC-3’; TRMT9B^{HA+IC}: 5′-CGACGGCTTTGTTGAATGCG-3′. gRNA and donor plasmids were generated as described in (Gratz *et al.*, 2014). *Vasa-Cas9* embryos were injected with a mixture of two gRNA plasmids (100ng/µL, each) and a double stranded DNA donor plasmid (500ng/µL) by BestGene, Inc., crossed to *w*^{1118} flies after eclosion, and progeny screened for DsRed expression in the eye. Knock-out alleles were generated by replacing the majority of the endogenous locus with a visible marker and attP landing site (Gratz *et al*, 2013). Endogenously tagged alleles were created using a scarless CRISPR-piggyBac approach (https://flycrispr.org; (Bruckner *et al.*, 2017)). An HA or superfolder GFP (sfGFP) tag flanked by flexible linkers and a visible marker flanked by piggyBac inverted terminal repeat sequences were inserted immediately downstream of the sole *TRMT9B* or ALKBH8 (CG17807) translational start sites. This generates null alleles due stop codons in the inverted repeat sequences. TRMT9B lines were crossed to piggyBac transposase to remove the marker cassette and generate in-frame tags. All engineered lines were confirmed by PCR and Sanger sequencing.

UAS rescue lines were generated by cloning full-length Drosophila and human TRMT9B coding sequence into pUAST-C5 (Drosophila Genomics Resource Center #1261). To generate methyltransferase-dead Drosophila TRMT9B, mutations to critical residues in the methyltransferase domain were introduced via KLD reaction. Specifically, we mutated codon 417 (GAG to GCC) and codon 693 (CAC to GCC) to introduce E139A and H231A mutations. These amino acids correspond to yeast residues D72 and H116, which were identified as critical for methyltransferase function (Létoquart *et al.*, 2015). In parallel, we generated V5 tagged wild-type and methyltransferase-dead Drosophila TRMT9B transgenes to confirm localization. All transgenes were integrated into the attP2 landing site by BestGene, Inc. (Groth *et al*, 2004).

Immunostaining and confocal imaging

Male third instar larvae were dissected in Ca^{2+}-free saline and fixed for 10 minutes with 4% paraformaldehyde in PBS. Dissected larvae were washed and permeabilized in PBS with 0.1% Triton-X then blocked overnight at 4℃ in PBS containing 0.1% Triton-X and 1% BSA. Dissected larvae were incubated with primary antibodies for two hours at room temperature and secondary antibodies for one hour at room temperature, then mounted in Vectashield (Vector Laboratories). For localization studies, male third-instar larvae were dissected in ice-cold Ca^{2+}-free saline and fixed for 6 min in Bouin's Fixative. Dissected larvae were washed and permeabilized in PBS with 0.1% Triton-X then blocked overnight at 4℃ in PBS containing 0.1% Triton-X, 5%NGS and 1% BSA, followed by overnight incubation with primary and secondary antibodies, then mounted in Vectashield (Vector Laboratories). The following antibodies were used at the indicated concentrations: mouse anti-Bruchpilot (Brp) at 1:100 (Developmental Studies Hybridoma Bank (DSHB) #nc82; RRID: AB_2314866), rabbit anti-HA at 1:500 (Cell Signaling Technology C29F4), mouse anti-V5 (1:500, ThermoFisher Scientific #R960-25;

RRID:AB_2556564), anti-HRP conjugated to Alexa Fluor 647 at 1:500 (Jackson ImmunoResearch Laboratories, Inc., #123-605-021; RRID:AB_2338967), rabbit anti-GFP conjugated to AlexaFluor 488 at 1:500 (Thermo Fisher Scientific, #A-21311; RRID:AB_221477), and secondary antibodies Alexa Fluor 488, Alexa Fluor 568, and Alexa Fluor 647 at 1:500 (Thermo Fisher Scientific). Images were obtained on a Nikon A1R HD confocal microscope with Plan Apo 40x and 60X oil-immersion objectives.

Electrophysiology

Electrophysiological baseline readings were performed on male third instar larvae. Larvae were dissected in low Ca^{2+} modified hemolymph-like saline (HL3 in mM: 70 NaCl, 5 KCl, 20 $MgCl_2$, 10 $NaHCO_3$, 115 sucrose, 5 trehalose, 5 HEPES and 0.2 Ca^{2+}, pH 7.2). Excitatory junction potentials were recorded using 1.0MM x 0.58MM, 4” borosilicate glass sharp electrode (electrode resistance between 10 and 15 MΩ) filled with 3M KCl. Recordings were performed in hemolymph-like saline solution containing 0.6 mM Ca^{2+} on muscle 6 of abdominal segments A3 and A4. A 1.5MM x 1.12MM, 4” borosilicate polished glass electrode was used to suction nerves. Recordings were performed on a Nikon FN1 microscope using a 40x (0.80 NA) water-dipping objective, and acquired using an AxoClamp 900A amplifier, Axon Digidata 1550B low-noise data acquisition system, and pClamp 11.0.3 software (Molecular Devices). Electrophysiological sweeps were digitized at 10 kHz, and filtered at 0.1 kHz. Miniature excitatory junctional potentials (mEJPs) were recorded with no external stimulation. For each recording, at least 100 mEJPs were analyzed using Mini Analysis (Synaptosoft) to obtain a mean mEJP amplitude value per muscle. Cut motor axons of each segment were stimulated for 0.5ms with an A-M Systems Isolated pulse stimulator to elicit EJPs. Stimulus intensity was adjusted to consistently elicit compound responses from both type Ib and Is motorneurons. At least 30 consecutive EJPs were recorded for each cell and analyzed in

pClamp to obtain mean amplitude. Quantal content (QC) was determined for each recording by calculating the ratio of mean EJP amplitude to mean mEJP amplitude then averaging recordings across all NMJs for a given genotype. Muscle input resistance (Rin) and resting membrane potential (V_{rest}) were monitored during each experiment. Recordings were only performed if the V_{rest} was between -50 and -80 mV and membrane resistance was 4 MΩ or higher.

Sequence alignment, phylogeny, and homology modeling

Alignments of the methyltransferase domains as defined by Pfam (Mistry *et al*, 2021) were conducted using T-Coffee (Notredame *et al*, 2000) using the following UniProt sequences: P49957 (*Saccharomyces cerevisiae* Trm9), Q9VBJ3 (Drosophila TRMT9B), Q9P272 (human TRMT9B), Q9W232 (Drosophila ALKBH8), and Q96BT7 (human ALKBH8). A phylogenetic tree was determined by PhyML maximum likelihood and visualized with TreeDyn in phylogeny.fr (Dereeper *et al*, 2008; Lemoine *et al*, 2019). Template-based structural homology models of the methyltransferase domains of Drosophila and human TRMT9B and ALKBH8 were performed using Modeller (Pieper *et al.*, 2014) through the ModWeb online service (https://modbase.compbio.ucsf.edu/modweb). Best scoring models for all four proteins included *Yarrowia lipolytica* Trm9, obtained from 2.5 Å X-ray diffraction of Trm9-Trm112, PDB: 5CM2 chain Z (Létoquart *et al.*, 2015). All homology models built with PDB 5CM2 chain Z were reliable with GA341 score of >0.99989 and normalized DOPE (zDOPE) score < 0). Drosophila and human TRMT9B models were built with residues 39 to 160 of *Y. lipolytica*, with 39% and 46% sequence identity, respectively. The Drosophila ALKBH8 model was built with residues 39 to 191 with 40% sequence identity and the human ALKBH8 model was built with residues 16 to 174 with 46% sequence identity. To model the mutations in methyltransferase-dead TRMT9B, we again used residues 39 to 160.

Additional details on the best scoring models can be found in the protein data bank files ((Hogan *et al*, 2023) Supplemental Files S1-S5). Models were visualized and compared to PDB 5CM2 chain Z using UCSF ChimeraX (Pettersen *et al*, 2021). A template-free model for Drosophila TRMT9B was obtained from AlphaFold version 1 predictions and is provided in the supplemental files ((Hogan *et al*, 2023), Supplemental Files S6 from (Jumper *et al.*, 2021; Varadi *et al.*, 2022). The AlphaFold model confidently predicted (pLDDT > 70) the methyltransferase domain, residues 123-278, although a biological function was not defined. Confidence scores for critical methyltransferase activity including the GxGxG domain, the acidic residue, and SAM binding histidine were very high (pLDDT between 89.8 - 95.7).

Liquid chromatography-mass spectrometry of RNA modifications

Vials containing adult fly heads were flash frozen in liquid nitrogen and stored at −80°C. Twenty-five milligrams of frozen adult flies were homogenized with a plastic pestle in a 1.5 mL microfuge tube while adding 250 µL of TRIzol reagent at a time until 1 mL was added. RNA was then extracted via an adapted TRIzol extraction protocol (Bogart & Andrews, 2006). RNA was resuspended in RNase-free ddH_2O. Total RNA was processed and analyzed by LC-MS as previously described (Su *et al*, 2014; Zhang *et al*, 2020). Briefly, total RNA (20 ug) was digested and dephosphorylated with Benzonase, Phosphodiesterase, and Calf Intestinal phosphatase for 3 hours at 37°C. Enzymes and undigested RNAs were removed using a 10,000-Da MWCO spin filter (Amicon) and purified ribonucleosides were stored at -80°C until further analysis. For fly larval preparations, wandering third instar larvae were dissected in HL3 with RNAse and paraformaldehyde free tools. The CNS and body walls were manually homogenized with a plastic pestle in 200uL TRIzol reagent, frozen and stored at -80ºC before extraction

using the Direct-zol RNA micropep kit (Zymo Research), and processed as described above. Ribonucleosides were separated using a Hypersil GOLD™ C18 Selectivity Column (Thermo Scientific) followed by nucleoside analysis using a Q Exactive Plus Hybrid Quadrupole-Orbitrap. The modification difference ratio was calculated using the m/z intensity values of each modified nucleoside between control and mutants following normalization to the sum of intensity values for the canonical nucleosides A, U, G and C.

IP-MS analysis of TRMT9B-interacting proteins

We pulled down endogenous TRMT9B protein and interacting proteins in *y^1 w^*; Mi{PT-GFSTF.1}dfid$^{MI13909\text{-}GFSTF.1}$*, in which TRMT9B is tagged with GFP and FLAG (Nagarkar-Jaiswal *et al.*, 2015). Whole adult flies were flash frozen in liquid nitrogen and manually homogenized. Cells were then lysed in lysis buffer (50 mM Tris-HCl, pH 7.5, 150 mM NaCl, 1 mM EDTA, 1% Triton X-100 supplemented with a protease inhibitor cocktail). Lysates were cleared by centrifugation and immunoprecipitated with anti- FLAG-antibody-conjugated agarose beads. Beads were washed three times with FLAG-wash buffer (50mM Tris-HCl, pH 7.5, 500mM NaCl, 1mM EDTA, 1% Triton X-100) and twice with TBS buffer (50 mM Tris-HCl, pH 7.5, 150 mM NaCl). EGFP-FlAsH-StrepII-3xFLAG -tagged TRMT9B was eluted with 100 µg/ml of 3×FLAG peptide in TBS buffer. As a control, an identical purification was performed in w1118 control flies. A silver stain was performed to confirm the presence of proteins in the eluted fractions, which were then subjected to trypsin digestion and tandem mass spectrometry. We used a 1% false discovery rate peptide threshold and 99% protein threshold to identify interacting proteins identified by at least two unique peptides.

Western blots

Protein samples were prepared from wandering third instar larvae in the 2X Laemmli buffer followed by boiling at 95°C for 5 min. The following antibodies were used: mouse anti-V5 (1:5000, RRID:AB_2556564,ThermoFisher Scientific # R960-25) and mouse anti-tubulin (1:4000, RRID: AB_2315513, Developmental Studies Hybridoma Bank #E7c). Secondary antibodies (Jackson Immunochemicals) were used at 1:10000. Quantification was performed using Image J software.

Experimental Design and Statistical Analysis

Quantifications were conducted blind to genotype. Sample sizes were based on prior published studies. Statistical analyses were conducted in GraphPad Prism 8 and 9. One-way ANOVA followed by Tukey's test was used for multiple comparisons of normally distributed data with equal variance. Multiple comparisons of non-normally distributed data were performed using the Kruskal-Wallis test followed by Dunn's multiple comparisons test. Significance is reported as values less than 0.05, 0.01, 0.001, and 0.0001 represented by one, two, three, or four stars, respectively. Unless otherwise indicated, significance refers to the indicated genotype compared to control. Error bars represent the mean ± s.e.m. or standard deviation as indicated.

DATA AVAILABILITY

Source data for all figures are at the Harvard Dataverse repository. https://dataverse.harvard.edu/privateurl.xhtml?token=2e306968-cd38-4ba9-aa9a-68c2c3d909d1

For supplemental PDB files, refer to supplemental files provided in the online version of (Hogan *et al* 2023).

ACKNOWLEDGEMENTS

This work was supported by a grant from the NIH National Institute of Neurological Disorders and Stroke (NINDS) to K.M.O.-G. and D.F. (R01 NS117068) and trainee support from the National Institute of General Medical Sciences to C.A.H and K.R.M through the University of Wisconsin Predoctoral Training Program in Genetics (T32GM007133) and J.L.D through the Brown University Predoctoral Training Program in Trans-disciplinary Pharmacological Sciences (T32 GM077995). J.M.L and D.F were additionally supported by NSF CAREER Award 1552126 and K.R.M. by NINDS F99NS129128. We thank Sina Ghaemmaghami and the Mass Spectrometry Resource Lab at the University of Rochester; the Biotechnology Center Mass Spectrometry/Proteomics Facility at the University of Wisconsin-Madison; the Laboratories of Genetics and Cell and Molecular Biology at the University of Wisconsin-Madison where a subset of this work was completed; and the Developmental Studies Hybridoma Bank and Bloomington Drosophila Stock Center for providing antibodies and fly stocks. We thank Sebastien Santini (CNRS/AMU IGS UMR7256) and the PACA Bioinfo platform (supported by IBISA) for the availability and management of the phylogeny.fr website used for phylogeny and sequence alignment. We thank James Kentro for making Figure EV1. Molecular graphics images were created using the UCSF Chimera package from the Resource for Biocomputing, Visualization, and Informatics at the University of California, San Francisco (supported by NIH P41 RR001081). We are grateful to the O'Connor-Giles and Fu labs and Heather Broihier for critical feedback on the work and manuscript.

Disclosure and competing interests statement

The authors declare that they have no conflict of interest.

Chapter 2 References

Abbasi-Moheb L, Mertel S, Gonsior M, Nouri-Vahid L, Kahrizi K, Cirak S, Wieczorek D, Motazacker MM, Esmaeeli-Nieh S, Cremer K *et al* (2012) Mutations in NSUN2 cause autosomal-recessive intellectual disability. *Am J Hum Genet* 90: 847-855

Begley U, Dyavaiah M, Patil A, Rooney JP, DiRenzo D, Young CM, Conklin DS, Zitomer RS, Begley TJ (2007) Trm9-catalyzed tRNA modifications link translation to the DNA damage response. *Mol Cell* 28: 860-870

Begley U, Sosa MS, Avivar-Valderas A, Patil A, Endres L, Estrada Y, Chan CT, Su D, Dedon PC, Aguirre-Ghiso JA *et al* (2013) A human tRNA methyltransferase 9-like protein prevents tumour growth by regulating LIN9 and HIF1-alpha. *EMBO Mol Med* 5: 366-383

Blanco S, Dietmann S, Flores JV, Hussain S, Kutter C, Humphreys P, Lukk M, Lombard P, Treps L, Popis M *et al* (2014) Aberrant methylation of tRNAs links cellular stress to neuro-developmental disorders. *EMBO J* 33: 2020-2039

Bogart K, Andrews J (2006) Extraction of Total RNA from Drosophila. *CGB Technical Report 2006-10*

Brown JB, Boley N, Eisman R, May GE, Stoiber MH, Duff MO, Booth BW, Wen J, Park S, Suzuki AM *et al* (2014) Diversity and dynamics of the Drosophila transcriptome. *Nature* 512: 393-399

Bruckner JJ, Zhan H, Gratz SJ, Rao M, Ukken F, Zilberg G, O'Connor-Giles KM (2017) Fife organizes synaptic vesicles and calcium channels for high-probability neurotransmitter release. *J Cell Biol* 216: 231-246

Cai WM, Chionh YH, Hia F, Gu C, Kellner S, McBee ME, Ng CS, Pang YL, Prestwich EG, Lim KS *et al* (2015) A Platform for Discovery and Quantification of Modified Ribonucleosides in RNA: Application to Stress-Induced Reprogramming of tRNA Modifications. *Methods Enzymol* 560: 29-71

Chellamuthu A, Gray SG (2020) The RNA Methyltransferase NSUN2 and Its Potential Roles in Cancer. *Cells* 9

Chen C, Huang B, Anderson JT, Byström AS (2011) Unexpected accumulation of ncm(5)U and ncm(5)S(2) (U) in a trm9 mutant suggests an additional step in the synthesis of mcm(5)U and mcm(5)S(2)U. *PLoS One* 6: e20783

Chen HM, Wang J, Zhang YF, Gao YH (2017) Ovarian cancer proliferation and apoptosis are regulated by human transfer RNA methyltransferase 9-likevia LIN9. *Oncol Lett* 14: 4461-4466

Chen YS, Yang WL, Zhao YL, Yang YG (2021) Dynamic transcriptomic m(5) C and its regulatory role in RNA processing. *Wiley Interdiscip Rev RNA* 12: e1639

Citri A, Malenka RC (2008) Synaptic plasticity: multiple forms, functions, and mechanisms. *Neuropsychopharmacology* 33: 18-41

Dereeper A, Guignon V, Blanc G, Audic S, Buffet S, Chevenet F, Dufayard JF, Guindon S, Lefort V, Lescot M *et al* (2008) Phylogeny.fr: robust phylogenetic analysis for the non-specialist. *Nucleic Acids Res* 36: W465-469

Dewe JM, Fuller BL, Lentini JM, Kellner SM, Fu D (2017) TRMT1-Catalyzed tRNA Modifications Are Required for Redox Homeostasis To Ensure Proper Cellular Proliferation and Oxidative Stress Survival. *Mol Cell Biol* 37

Dietzl G, Chen D, Schnorrer F, Su KC, Barinova Y, Fellner M, Gasser B, Kinsey K, Oppel S, Scheiblauer S *et al* (2007) A genome-wide transgenic RNAi library for conditional gene inactivation in Drosophila. *Nature* 448: 151-156

Flanagan JM, Healey S, Young J, Whitehall V, Trott DA, Newbold RF, Chenevix-Trench G (2004) Mapping of a candidate colorectal cancer tumor-suppressor gene to a 900-kilobase region on the short arm of chromosome 8. *Genes Chromosomes Cancer* 40: 247-260

Fu D, Brophy JA, Chan CT, Atmore KA, Begley U, Paules RS, Dedon PC, Begley TJ, Samson LD (2010a) Human AlkB homolog ABH8 Is a tRNA methyltransferase required for wobble uridine modification and DNA damage survival. *Mol Cell Biol* 30: 2449-2459

Fu Y, Dai Q, Zhang W, Ren J, Pan T, He C (2010b) The AlkB domain of mammalian ABH8 catalyzes hydroxylation of 5-methoxycarbonylmethyluridine at the wobble position of tRNA. *Angew Chem Int Ed Engl* 49: 8885-8888

Gao J, Wang B, Yu H, Wu G, Wan C, Liu W, Liao S, Cheng L, Zhu Z (2020) Structural insight into HEMK2-TRMT112-mediated glutamine methylation. *Biochem J* 477: 3833-3838

Garcia BCB, Horie M, Kojima S, Makino A, Tomonaga K (2021) BUD23-TRMT112 interacts with the L protein of Borna disease virus and mediates the chromosomal tethering of viral ribonucleoproteins. *Microbiol Immunol* 65: 492-504

Goel P, Dufour Bergeron D, Bohme MA, Nunnelly L, Lehmann M, Buser C, Walter AM, Sigrist SJ, Dickman D (2019) Homeostatic scaling of active zone scaffolds maintains global synaptic strength. *J Cell Biol* 218: 1706-1724

Gratz SJ, Ukken FP, Rubinstein CD, Thiede G, Donohue LK, Cummings AM, O'Connor-Giles KM (2014) Highly specific and efficient CRISPR/Cas9-catalyzed homology-directed repair in Drosophila. *Genetics* 196: 961-971

Gratz SJ, Wildonger J, Harrison MM, O'Connor-Giles KM (2013) CRISPR/Cas9-mediated genome engineering and the promise of designer flies on demand. *Fly (Austin)* 7: 249-255

Graveley BR, Brooks AN, Carlson JW, Duff MO, Landolin JM, Yang L, Artieri CG, van Baren MJ, Boley N, Booth BW *et al* (2011) The developmental transcriptome of Drosophila melanogaster. *Nature* 471: 473-479

Greenberg MVC, Bourc'his D (2019) The diverse roles of DNA methylation in mammalian development and disease. *Nat Rev Mol Cell Biol* 20: 590-607

Groth AC, Fish M, Nusse R, Calos MP (2004) Construction of transgenic Drosophila by using the site-specific integrase from phage phiC31. *Genetics* 166: 1775-1782

GTEx (2015) Human genomics. The Genotype-Tissue Expression (GTEx) pilot analysis: multitissue gene regulation in humans. *Science* 348: 648-660

Gu C, Ramos J, Begley U, Dedon PC, Fu D, Begley TJ (2018) Phosphorylation of human TRM9L integrates multiple stress-signaling pathways for tumor growth suppression. *Sci Adv* 4: eaas9184

Guang S, Pang N, Deng X, Yang L, He F, Wu L, Chen C, Yin F, Peng J (2018) Synaptopathology Involved in Autism Spectrum Disorder. *Front Cell Neurosci* 12: 470

Guy MP, Phizicky EM (2014) Two-subunit enzymes involved in eukaryotic post-transcriptional tRNA modification. *RNA Biol* 11: 1608-1618

Honjo K, Mauthner SE, Wang Y, Skene JH, Tracey WD, Jr. (2016) Nociceptor-Enriched Genes Required for Normal Thermal Nociception. *Cell Rep* 16: 295-303

Hu Y, Comjean A, Roesel C, Vinayagam A, Flockhart I, Zirin J, Perkins L, Perrimon N, Mohr SE (2017) FlyRNAi.org-the database of the Drosophila RNAi screening center and transgenic RNAi project: 2017 update. *Nucleic Acids Res* 45: D672-D678

Johansson MJ, Esberg A, Huang B, Bjork GR, Bystrom AS (2008) Eukaryotic wobble uridine modifications promote a functionally redundant decoding system. *Mol Cell Biol* 28: 3301-3312

Jumper J, Evans R, Pritzel A, Green T, Figurnov M, Ronneberger O, Tunyasuvunakool K, Bates R, Žídek A, Potapenko A *et al* (2021) Applying and improving AlphaFold at CASP14. *Proteins* 89: 1711-1721

Jungfleisch J, Bottcher R, Tallo-Parra M, Perez-Vilaro G, Merits A, Novoa EM, Diez J (2022) CHIKV infection reprograms codon optimality to favor viral RNA translation by altering the tRNA epitranscriptome. *Nat Commun* 13: 4725

Kalhor HR, Clarke S (2003) Novel methyltransferase for modified uridine residues at the wobble position of tRNA. *Mol Cell Biol* 23: 9283-9292

Kozbial PZ, Mushegian AR (2005) Natural history of S-adenosylmethionine-binding proteins. *BMC Struct Biol* 5: 19

Lemoine F, Correia D, Lefort V, Doppelt-Azeroual O, Mareuil F, Cohen-Boulakia S, Gascuel O (2019) NGPhylogeny.fr: new generation phylogenetic services for non-specialists. *Nucleic Acids Res* 47: W260-w265

Létoquart J, van Tran N, Caroline V, Aleksandrov A, Lazar N, van Tilbeurgh H, Liger D, Graille M (2015) Insights into molecular plasticity in protein complexes from Trm9-Trm112 tRNA modifying enzyme crystal structure. *Nucleic Acids Res* 43: 10989-11002

Ma NX, Puls B, Chen G (2022) Transcriptomic analyses of NeuroD1-mediated astrocyte-to-neuron conversion. *Dev Neurobiol* 82: 375-391

Maddirevula S, Alameer S, Ewida N, de Sousa MML, Bjoras M, Vagbo CB, Alkuraya FS (2022) Insight into ALKBH8-related intellectual developmental disability based on the first pathogenic missense variant. *Hum Genet* 141: 209-215

Martin JL, McMillan FM (2002) SAM (dependent) I AM: the S-adenosylmethionine-dependent methyltransferase fold. *Curr Opin Struct Biol* 12: 783-793

Mistry J, Chuguransky S, Williams L, Qureshi M, Salazar GA, Sonnhammer ELL, Tosatto SCE, Paladin L, Raj S, Richardson LJ *et al* (2021) Pfam: The protein families database in 2021. *Nucleic Acids Res* 49: D412-d419

mod EC, Roy S, Ernst J, Kharchenko PV, Kheradpour P, Negre N, Eaton ML, Landolin JM, Bristow CA, Ma L *et al* (2010) Identification of functional elements and regulatory circuits by Drosophila modENCODE. *Science* 330: 1787-1797

Monies D, Vagbo CB, Al-Owain M, Alhomaidi S, Alkuraya FS (2019) Recessive Truncating Mutations in ALKBH8 Cause Intellectual Disability and Severe Impairment of Wobble Uridine Modification. *Am J Hum Genet* 104: 1202-1209

Murn J, Shi Y (2017) The winding path of protein methylation research: milestones and new frontiers. *Nat Rev Mol Cell Biol* 18: 517-527

Nagarkar-Jaiswal S, DeLuca SZ, Lee PT, Lin WW, Pan H, Zuo Z, Lv J, Spradling AC, Bellen HJ (2015) A genetic toolkit for tagging intronic MiMIC containing genes. *Elife* 4

Ni JQ, Zhou R, Czech B, Liu LP, Holderbaum L, Yang-Zhou D, Shim HS, Tao R, Handler D, Karpowicz P *et al* (2011) A genome-scale shRNA resource for transgenic RNAi in Drosophila. *Nat Methods* 8: 405-407

Notredame C, Higgins DG, Heringa J (2000) T-Coffee: A novel method for fast and accurate multiple sequence alignment. *J Mol Biol* 302: 205-217

Pettersen EF, Goddard TD, Huang CC, Meng EC, Couch GS, Croll TI, Morris JH, Ferrin TE (2021) UCSF ChimeraX: Structure visualization for researchers, educators, and developers. *Protein Sci* 30: 70-82

Pieper U, Webb BM, Dong GQ, Schneidman-Duhovny D, Fan H, Kim SJ, Khuri N, Spill YG, Weinkam P, Hammel M *et al* (2014) ModBase, a database of annotated comparative protein structure models and associated resources. *Nucleic Acids Res* 42: D336-346

Saad AK, Marafi D, Mitani T, Du H, Rafat K, Fatih JM, Jhangiani SN, Coban-Akdemir Z, Baylor-Hopkins Center for Mendelian G, Gibbs RA *et al* (2021)

Neurodevelopmental disorder in an Egyptian family with a biallelic ALKBH8 variant. *Am J Med Genet A* 185: 1288-1293

Schaffrath R, Leidel SA (2017) Wobble uridine modifications-a reason to live, a reason to die?! *RNA Biol* 14: 1209-1222

Songe-Moller L, van den Born E, Leihne V, Vagbo CB, Kristoffersen T, Krokan HE, Kirpekar F, Falnes PO, Klungland A (2010) Mammalian ALKBH8 possesses tRNA methyltransferase activity required for the biogenesis of multiple wobble uridine modifications implicated in translational decoding. *Mol Cell Biol* 30: 1814-1827

Stoeger T, Gerlach M, Morimoto RI, Nunes Amaral LA (2018) Large-scale investigation of the reasons why potentially important genes are ignored. *PLoS Biol* 16: e2006643

Su D, Chan CT, Gu C, Lim KS, Chionh YH, McBee ME, Russell BS, Babu IR, Begley TJ, Dedon PC (2014) Quantitative analysis of ribonucleoside modifications in tRNA by HPLC-coupled mass spectrometry. *Nat Protoc* 9: 828-841

Towns WL, Begley TJ (2012) Transfer RNA methytransferases and their corresponding modifications in budding yeast and humans: activities, predications, and potential roles in human health. *DNA Cell Biol* 31: 434-454

Tweedie S, Braschi B, Gray K, Jones TEM, Seal RL, Yates B, Bruford EA (2021) Genenames.org: the HGNC and VGNC resources in 2021. *Nucleic Acids Res* 49: D939-d946

Uhlén M, Fagerberg L, Hallström BM, Lindskog C, Oksvold P, Mardinoglu A, Sivertsson Å, Kampf C, Sjöstedt E, Asplund A *et al* (2015) Proteomics. Tissue-based map of the human proteome. *Science* 347: 1260419

van den Born E, Vagbo CB, Songe-Moller L, Leihne V, Lien GF, Leszczynska G, Malkiewicz A, Krokan HE, Kirpekar F, Klungland A *et al* (2011) ALKBH8-mediated formation of a novel diastereomeric pair of wobble nucleosides in mammalian tRNA. *Nat Commun* 2: 172

van Tran N, Ernst FGM, Hawley BR, Zorbas C, Ulryck N, Hackert P, Bohnsack KE, Bohnsack MT, Jaffrey SR, Graille M *et al* (2019) The human 18S rRNA m6A methyltransferase METTL5 is stabilized by TRMT112. *Nucleic Acids Res* 47: 7719-7733

van Tran N, Muller L, Ross RL, Lestini R, Letoquart J, Ulryck N, Limbach PA, de Crecy-Lagard V, Cianferani S, Graille M (2018) Evolutionary insights into Trm112-methyltransferase holoenzymes involved in translation between archaea and eukaryotes. *Nucleic Acids Res* 46: 8483-8499

Varadi M, Anyango S, Deshpande M, Nair S, Natassia C, Yordanova G, Yuan D, Stroe O, Wood G, Laydon A *et al* (2022) AlphaFold Protein Structure Database: massively expanding the structural coverage of protein-sequence space with high-accuracy models. *Nucleic Acids Res* 50: D439-d444

Venken KJ, Schulze KL, Haelterman NA, Pan H, He Y, Evans-Holm M, Carlson JW, Levis RW, Spradling AC, Hoskins RA *et al* (2011) MiMIC: a highly versatile transposon insertion resource for engineering Drosophila melanogaster genes. *Nat Methods* 8: 737-743

Wang S, Liu X, Huang J, Zhang Y, Sang C, Li T, Yuan J (2018) Expression of KIAA1456 in lung cancer tissue and its effects on proliferation, migration and invasion of lung cancer cells. *Oncol Lett* 16: 3791-3795

Xu L, Liu X, Sheng N, Oo KS, Liang J, Chionh YH, Xu J, Ye F, Gao YG, Dedon PC *et al* (2017) Three distinct 3-methylcytidine (m(3)C) methyltransferases modify tRNA and mRNA in mice and humans. *J Biol Chem* 292: 14695-14703

Yang WQ, Xiong QP, Ge JY, Li H, Zhu WY, Nie Y, Lin X, Lv D, Li J, Lin H *et al* (2021) THUMPD3-TRMT112 is a m2G methyltransferase working on a broad range of tRNA substrates. *Nucleic Acids Res* 49: 11900-11919

Yue F, Cheng Y, Breschi A, Vierstra J, Wu W, Ryba T, Sandstrom R, Ma Z, Davis C, Pope BD *et al* (2014) A comparative encyclopedia of DNA elements in the mouse genome. *Nature* 515: 355-364

Zhang K, Lentini JM, Prevost CT, Hashem MO, Alkuraya FS, Fu D (2020) An intellectual disability-associated missense variant in TRMT1 impairs tRNA modification and reconstitution of enzymatic activity. *Hum Mutat* 41: 600-607

Zhou Y, Kong Y, Fan W, Tao T, Xiao Q, Li N, Zhu X (2020) Principles of RNA methylation and their implications for biology and medicine. *Biomed Pharmacother* 131: 110731

Zoghbi HY, Bear MF (2012) Synaptic dysfunction in neurodevelopmental disorders associated with autism and intellectual disabilities. *Cold Spring Harb Perspect Biol* 4

Chapter 2 Figures

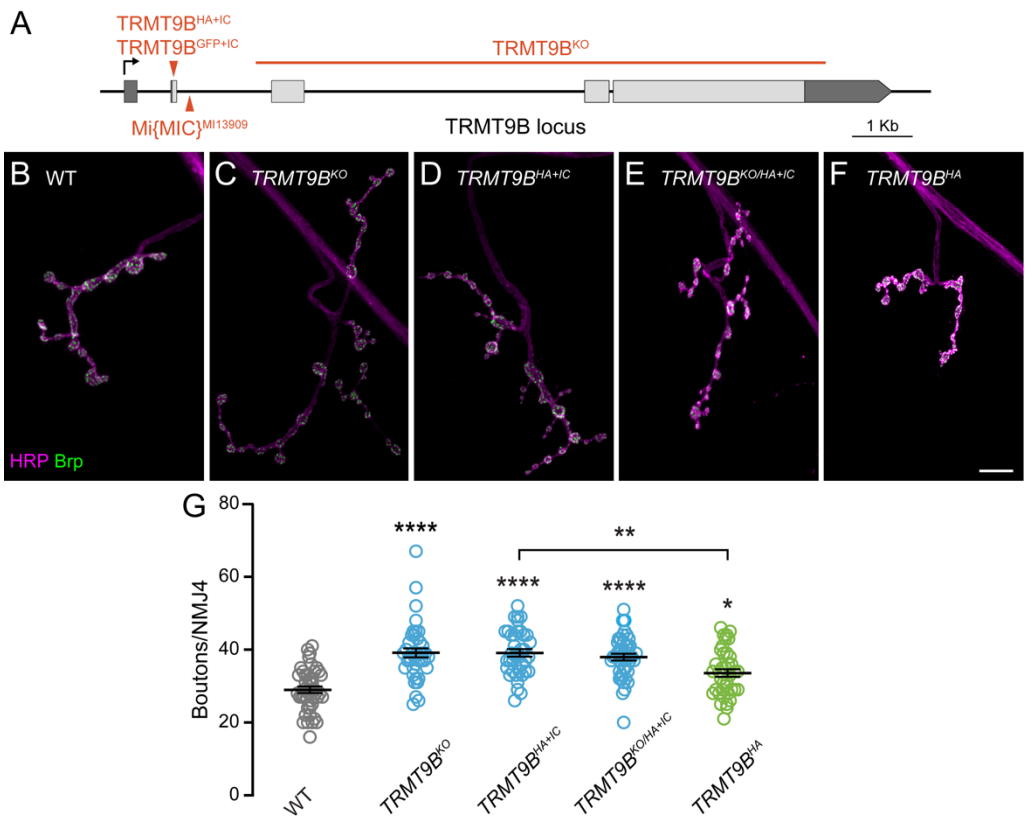

Figure 2.1. TRMT9B attenuates synaptic growth

A. Schematic of the *TRMT9B* locus with alleles used in this study. Red triangles represent insertion alleles and the red line delineates the extent of the deletion in the *TRMT9B*^{KO}.

B-F. Representative confocal images of NMJ4 in wild type (grey), three allelic combinations of *TRMT9B* null mutants (blue), and rescue (green). Scale bar: 10 μm.

G. Quantification of bouton number per NMJ4 from B-F. Data points represent individual NMJs (*w*^{1118}: 44, *TRMT9B*^{KO}: 40, *TRMT9B*$^{HA+IC}$: 39, *TRMT9B*$^{KO/HA+IC}$: 42; *TRMT9B*^{HA}: 39) from 8-10 biological replicates per genotype. Mean ± s.e.m is indicated. Kruskal-Wallis

test followed by Dunn's multiple comparisons test. ****$P<0.0001$, **$P = 0.004$, *$P = 0.034$.

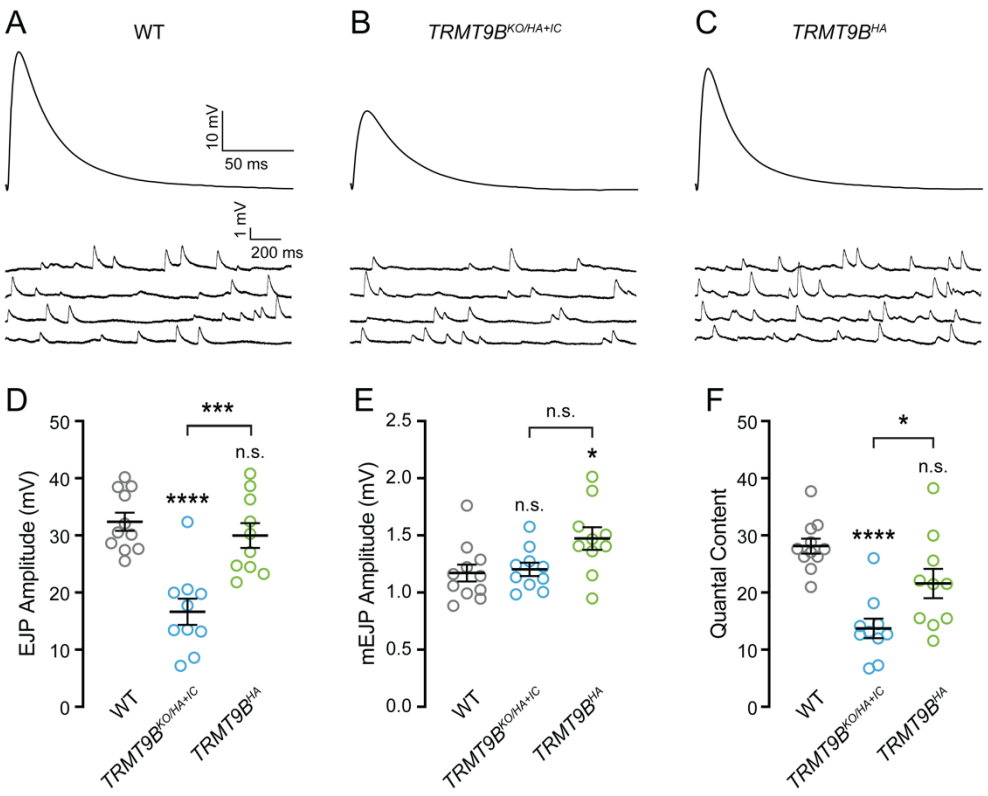

Figure 2.2 TRMT9B promotes neurotransmitter release

A-C. Representative traces of EJPs and mEJPs from current clamp recordings at muscle 6 in wild type (grey), *TRMT9B* null (blue), and rescue (green). Stimulus artifacts have been removed from EJPs for clarity.

D-F. Quantification of average mEJP amplitude, EJP amplitude, and quantal content for genotypes in A-C. Data points represent individual NMJs (w^{1118}: 11, $TRMT9B^{KO/HA+IC}$: 10; $TRMT9B^{HA}$: 10) from 5-8 biological replicates per genotype. Mean ± s.e.m is indicated. ANOVA followed by Tukey's test. ****P<0.0001, ***P=0.0002, *P<0.05.

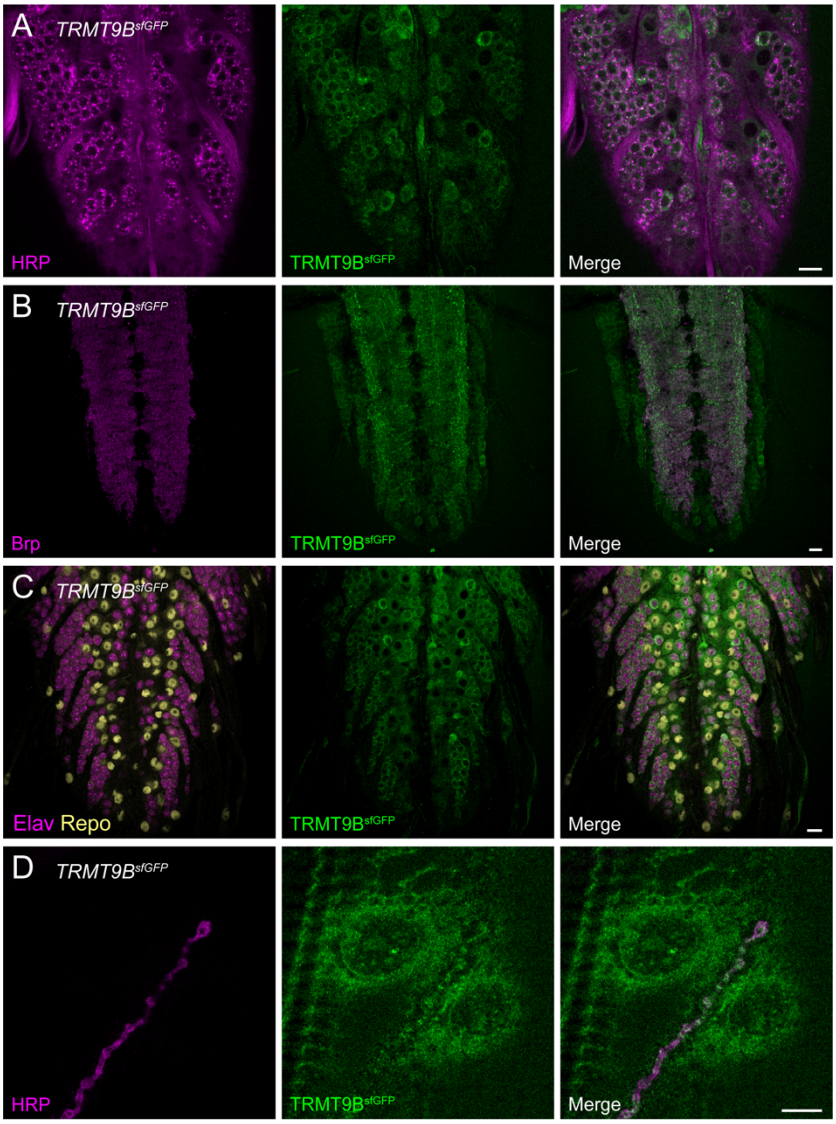

Figure 2.3. TRMT9B is expressed in neuronal, glial, and muscle cell bodies and at synapses

A. Confocal Z-projections of a *TRMT9B*^{sfGFP} larval ventral ganglion co-labeled with antibodies against GFP (green) and the neuronal membrane marker HRP (magenta) showing expression in cell bodies.

B. Confocal Z-projections of a *TRMT9B*^{sfGFP} larval ventral ganglion co-labeled with antibodies against GFP (green) and the synaptic marker Brp (magenta) showing expression in the synaptic neuropil. C. Confocal Z-projections of a *TRMT9B*^{sfGFP} larval

ventral ganglia co-labeled with antibodies against GFP (green) and neuronal marker Elav (magenta) or glial marker Repo (yellow) showing expression in neurons and glia. D. Confocal Z-projections of a *TRMT9B*^{sfGFP} NMJ/muscle co-labeled with antibodies against GFP (green) and neuronal membrane marker HRP (magenta) showing expression in boutons and muscle with perinuclear accumulation. Scale bars for A-D: 10 μm.

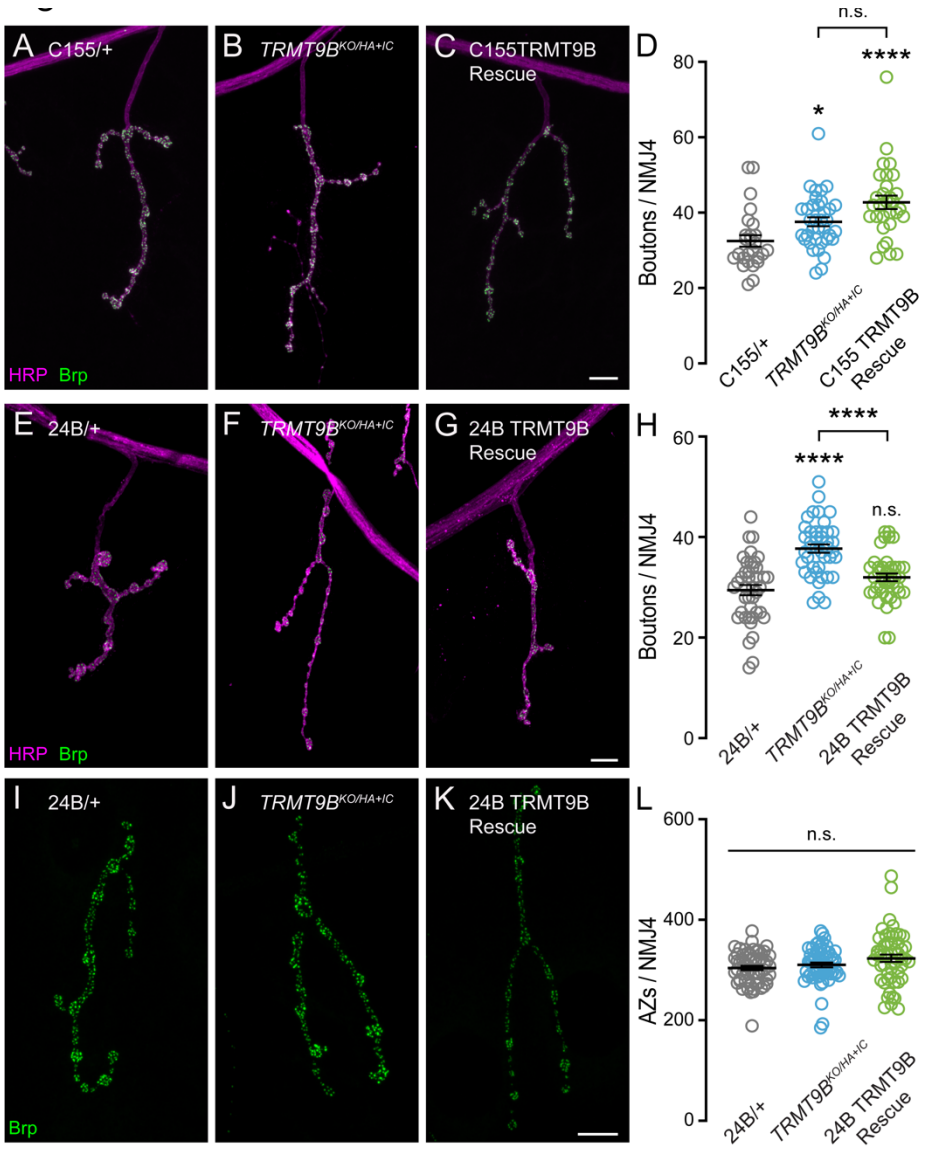

Figure 2.4. TRMT9B functions postsynaptically to regulate synaptic growth

A-C. Representative confocal images of NMJ4 in control (grey), *TRMT9B* null (blue), and presynaptic rescue (green).

D. Quantification of bouton number per NMJ4 from A-C. Data points represent individual NMJs (*C155 Gal4/+*: 26, *C155 Gal4/+; TRMT9B$^{KO/HA+IC}$*: 36; *C155-Gal4; TRMT9B^{KO}/UAS-TRMT9B, TRMT9B^{HA+IC}*: 30) from 10 biological replicates per genotype.

E-G. Representative confocal images of NMJ4 in control (grey), *TRMT9B* null (blue), and postsynaptic rescue (green).

H. Quantification of bouton number per NMJ4 from E-G. Data points represent individual NMJs (*24B-Gal4/+*: 41, *24B-Gal4, TRMT9B$^{KO/HA+IC}$*: 42; *24B-Gal4, TRMT9B^{KO}/UAS-TRMT9B, TRMT9B^{HA+IC}*: 40) from 8-10 biological replicates per genotype.

I-K. Representative high-resolution confocal images of NMJs with individual active zones labeled with Brp in in control (grey) and *TRMT9B* null (blue).

L. Quantification of active zone (AZ) number per NMJ4 from I-K. Data points represent individual NMJs (*24B-Gal4/+*: 59, *24B-Gal4/+, TRMT9B$^{KO/HA+IC}$*: 59; *24B-Gal4, TRMT9B^{KO}/UAS-TRMT9B, TRMT9B^{HA+IC}*: 53) from 10 biological replicates per genotype.

Data Information: Mean ± s.e.m is indicated. Kruskal-Wallis test followed by Dunn's multiple comparisons test. ****P<0.0001, *P=0.02. Scale bars: 10 μm.

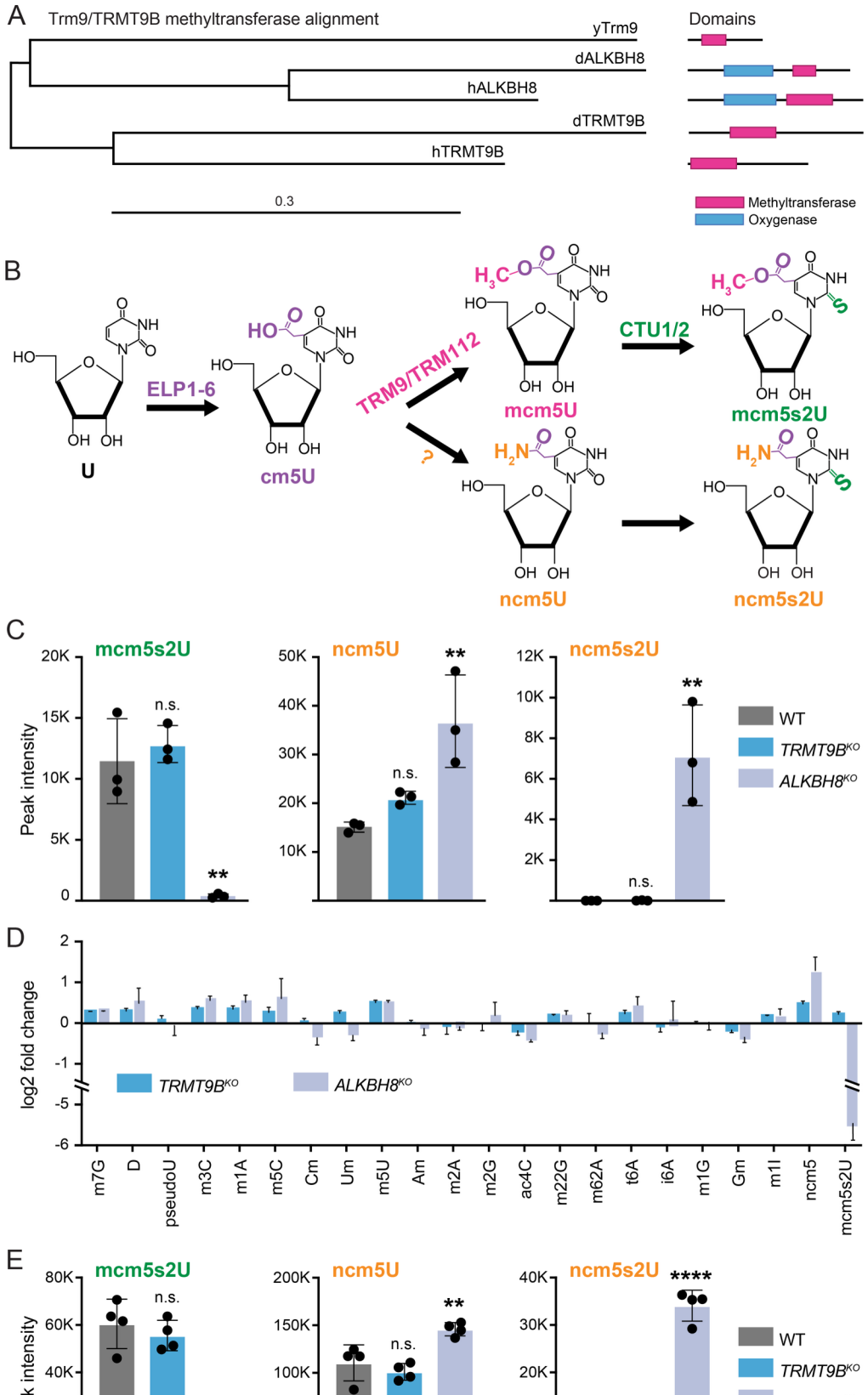
A
Trm9/TRMT9B methyltransferase alignment
yTrm9
dALKBH8
hALKBH8
dTRMT9B
hTRMT9B
0.3
Domains
Methyltransferase
Oxygenase
B
U
ELP1-6
cm5U
TRM9/TRM112
mcm5U
CTU1/2
mcm5s2U
ncm5U
ncm5s2U
C
mcm5s2U
ncm5U
ncm5s2U
Peak intensity
n.s.
**
WT
TRMT9B^KO
ALKBH8^KO
D
log2 fold change
m7G
D
pseudoU
m3C
m1A
m5C
Cm
Um
m5U
Am
m2A
m2G
ac4C
m22G
m62A
t6A
i6A
m1G
Gm
m1I
ncm5
mcm5s2U
E
****

Figure 2.5. TRMT9B is not required for baseline tRNA wobble uridine methylation

A. Phylogenetic tree of yeast Trm9, fly and human TRMT9B, and fly and human ALKBH8 determined by maximum likelihood from alignments of their methyltransferase domains.

B. Yeast wobble uridine methylation pathway.

C. Peak intensity areas of modified uridines normalized to the canonical nucleosides A, U, G, and C measured by liquid chromatography-mass spectrometry (LC-MS) in total RNA isolated from w^{1118}, $TRMT9B^{KO}$ and $ALKBH8^{KO}$ heads (three biological replicates).

D. Log2 fold change in the levels of the indicated tRNA modification in $TRMT9B^{KO}$ and $ALKBH8^{KO}$ heads relative to w^{1118} control.

E. Peak intensity areas of modified uridines normalized to the canonical nucleosides A, U, G, and C measured by LC-MS in total RNA isolated from w^{1118}, $TRMT9B^{KO}$ and $ALKBH8^{KO}$ larval nervous system and body walls (four biological replicates).

Data Information: Mean ± standard deviation is indicated. Kruskal-Wallis test followed by Dunn's multiple comparisons test. ****P<0.0001, **P<0.01, *P=0.039.

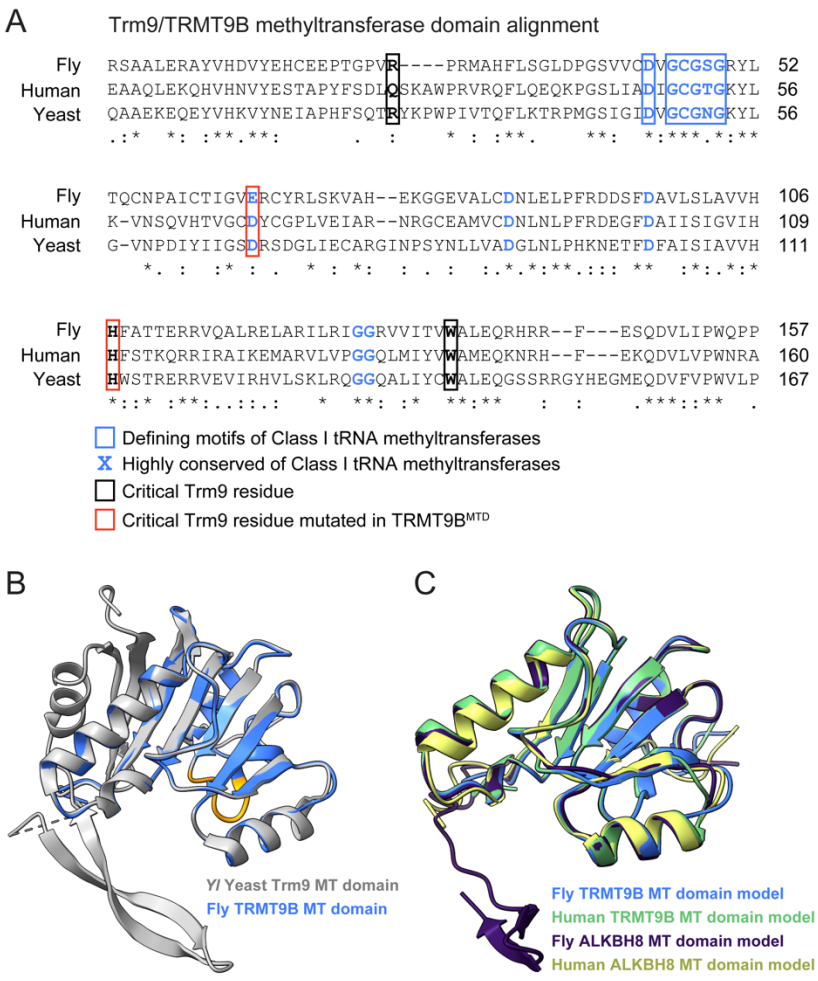

Figure 2.6. TRMT9B encodes a conserved methyltransferase

A. Sequence alignment of yeast Trm9, *Drosophila* TRMT9B, and human TRMT9B methyltransferase domains. Class I methyltransferase defining sequences are blue and boxed. Additional residues highly conserved across class I methyltransferases are indicated in blue. Critical residues identified in yeast by Létoquart et al. 2015 are boxed in black or red, with red indicating the amino acids mutated in our methyltransferase-dead transgene. Identical amino acids are marked with asterisks, conserved substitutions are marked with two dots, and semi-conserved substitutions with single dots.

B. Structural homology model of the *Drosophila* TRMT9B methyltransferase domain (blue) with yeast Trm9 structure (gray, PBD ID: 5CM2 chain Z). The class I methyltransferase GxGxG motif (orange) is in conserved positions across species. C. Extension of the homology model shows conserved tertiary structure between *Drosophila* (blue) and human (green) TRMT9B and *Drosophila* (purple) and human (yellow) ALKBH8 methyltransferase domains.

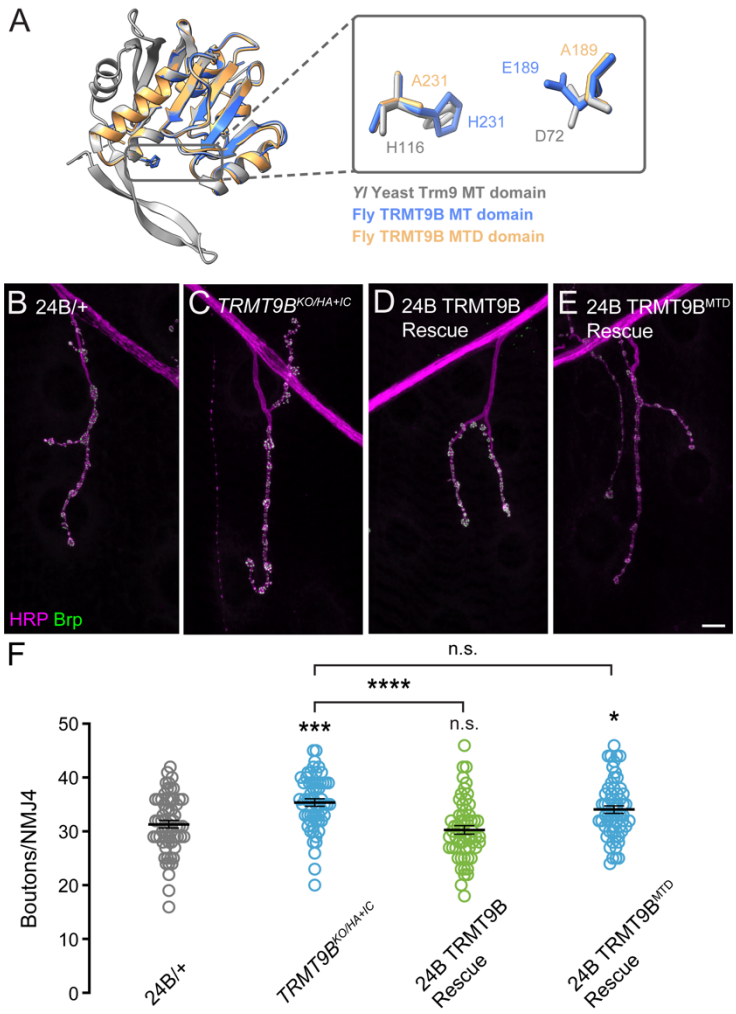

Figure 2.7. TRMT9B regulation of synaptic growth requires methyltransferase function

A. Homology model of TRMT9B with methyltransferase-disrupting mutations. Superimposition of wild-type (blue) and methyltransferase-dead (MTD, light orange) TRMT9B methyltransferase domain models with yeast Trm9 structure (gray, PBD ID: 5CM2 chain Z) indicates the preservation of tertiary structure in TRMT9B^{MTD}. Insert shows mutated residues in TRMT9B^{MTD}.

B-E. Representative confocal images of NMJ4 in control (grey), *TRMT9B* null (blue), postsynaptic TRMT9B rescue (green), and postsynaptic TRMT9B^{MTD} rescue (blue). Scale bar: 10 μm.

F. Quantification of bouton number per NMJ4 from B-E. Data points represent individual NMJs (*24B-Gal4/+*: 60, *24B-Gal4, TRMT9B$^{KO/HA+IC}$*: 59; *24B-Gal4, TRMT9B^{KO}/UAS-TRMT9B, TRMT9B^{HA+IC}*: 57; *24B-Gal4, TRMT9B^{KO}/UAS-TRMT9B^{MTD}, TRMT9B^{HA+IC}*) from 10 biological replicates per genotype. Mean ± s.e.m is indicated. ANOVA followed by Tukey's multiple comparisons test. ****P<0.0001, ***P= 0.0003, *P=0.03.

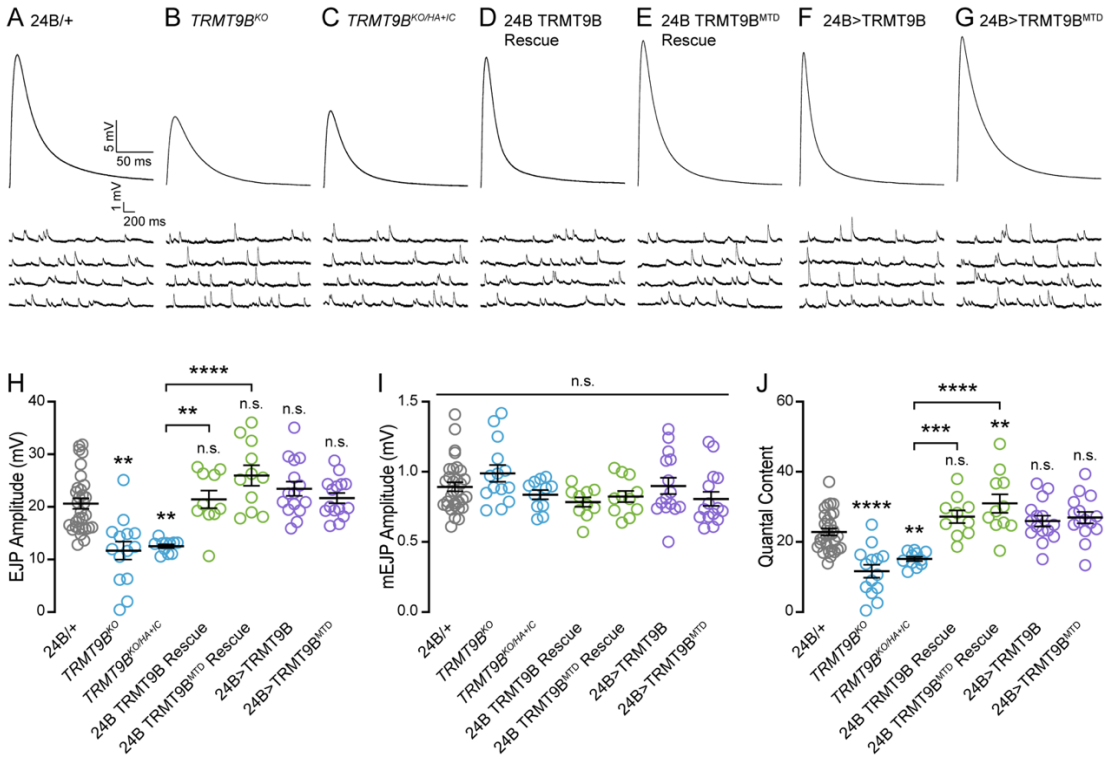

Figure 2.8. TRMT9B regulates neurotransmitter release through a distinct mechanism

A-G. Representative traces of EJPs and mEJPs from current clamp recordings at muscle 6 in control (grey), two *TRMT9B* null alleles (blue), TRMT9B and TRMT9B^{MTD} rescue (green), and overexpression (purple). Stimulus artifacts have been removed from EJPs for clarity.

H-J. Quantification of average mEJP amplitude, EJP amplitude, and quantal content for genotypes in A-G. Data points represent individual NMJs (*24B-Gal4/+*: 31, *TRMT9B^{KO}*: 14, TRMT9B$^{KO/HA+IC}$: 11; *24B-Gal4, TRMT9B^{KO}/UAS-TRMT9B, TRMT9B^{HA+IC}*: 10; *24B-Gal4, TRMT9B^{KO}/UAS-TRMT9B^{MTD}, TRMT9B^{HA+IC}*: 11 from 4-11 biological replicates per genotype. Mean ± s.e.m is indicated. Kruskal-Wallis non-parametric test followed by Dunn's multiple comparisons test for EJPs and mEJPs. ANOVA followed by Tukey's test for normally distributed QC. ****P<0.0001, ***P<0.001, **P<0.01.

Chapter 2 Supplemental Figures

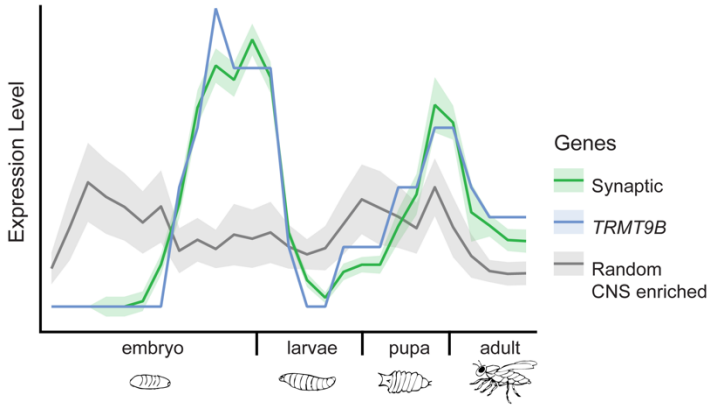

Figure 2.S1. Developmental transcriptional profile of representative synaptic genes and TRMT9B. Temporal transcriptional profiles of 10 representative synaptic genes (green), *TRMT9B* (blue), and 10 random non-synaptic CNS-enriched genes (grey) throughout development reveals characteristic peaks of synaptic and *TRMT9B* gene expression during embryonic and adult nervous system development. Analysis of ModENCODE data (Graveley *et al.*, 2011).

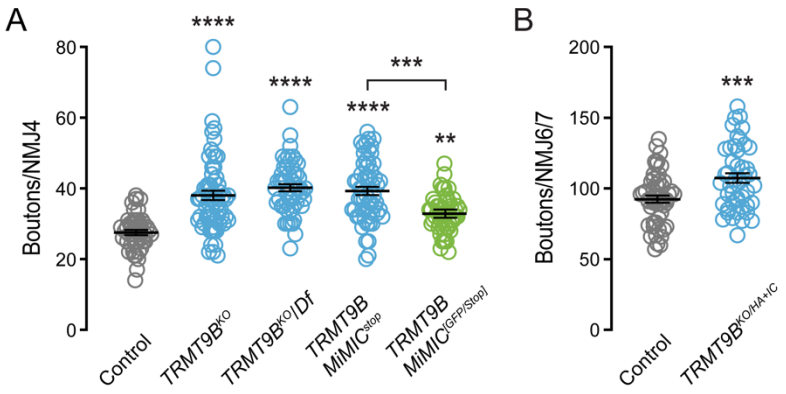

Figure 2.S2. TRMT9B attenuates synaptic growth

A. Quantification of bouton number per NMJ4 in wild type (grey), three allelic combinations of *TRMT9B* null mutants (blue), and rescue (green). Data points represent individual NMJs (w^{1118}: 46, $TRMT9B^{KO}$: 66, $TRMT9B^{KO}/Df$: 53, *TRMT9B* $MiMIC^{STOP}$: 58; *TRMT9B* $MiMIC^{GFP/STOP}$: 49) from 11-16 biological replicates per genotype. Mean ± s.e.m is indicated. Kruskal-Wallis test followed by Dunn's multiple comparisons test. ****P<0.0001, ***P=0.0005, **P=0.0037.

B. Quantification of bouton number per NMJ6/7 in wild type (grey) and *TRMT9B* null mutants (blue). Data points represent individual NMJs (control: 52, $TRMT9B^{KO/HA+IC}$: 46) from 13 biological replicates per genotype. Mean ± s.e.m is indicated. Unpaired t-test, *P*=0.0005.

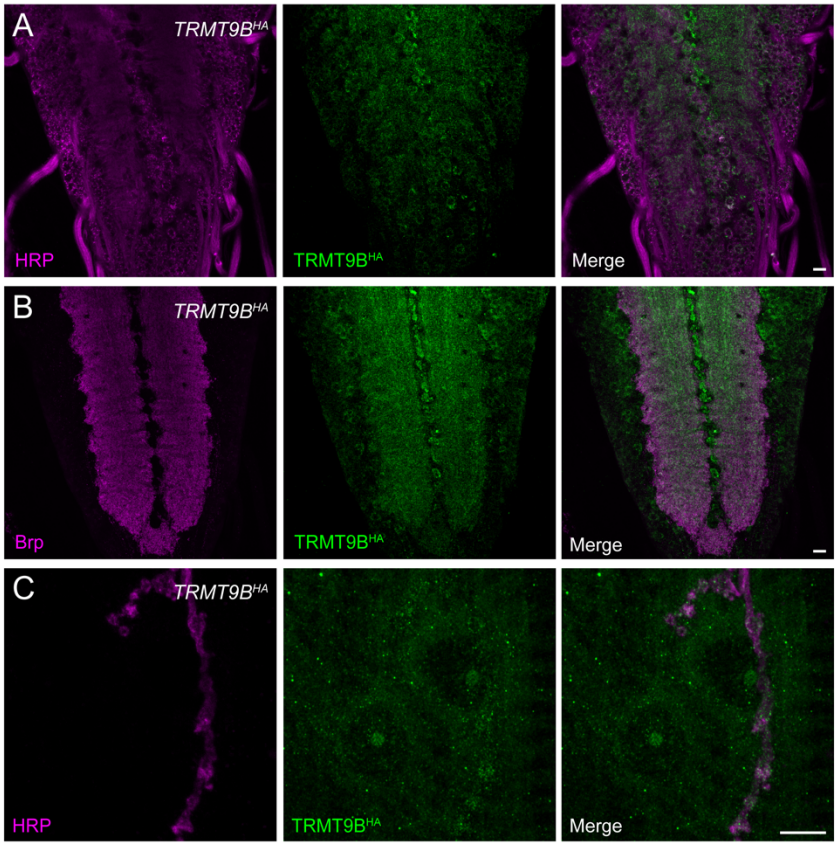

Figure 2.S3. TRMT9B expression in *TRMT9B^{HA}*. (**A-C**) Confocal Z-projections of *TRMT9B^{HA}* larval ventral ganglia or NMJ/muscle co-labeled with antibodies against HA (green) and the neuronal membrane marker HRP (magenta) or synaptic marker Brp (magenta). Scale bars: 10 μm.

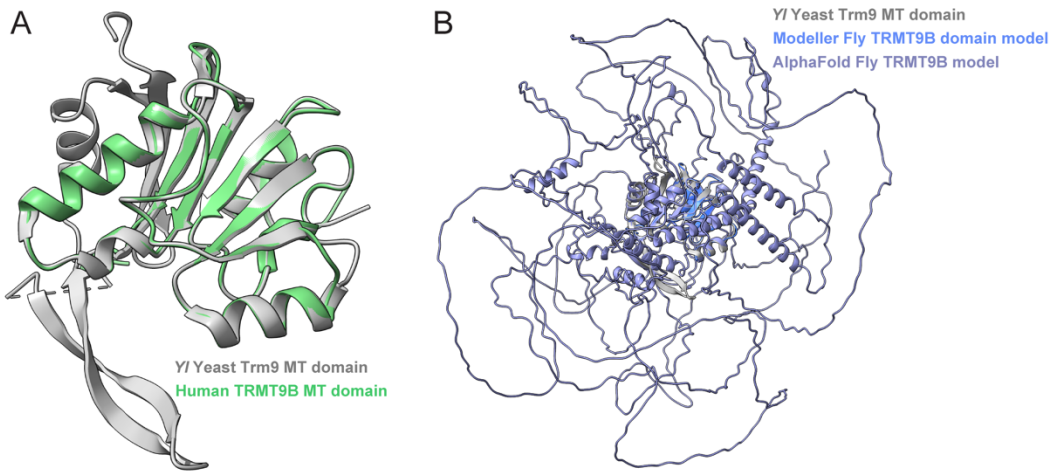

Figure 2.S4. Structural models of TRMT9B and yeast Trm9

A. Structural homology model of the human TRMT9B methyltransferase domain (green) with yeast Trm9 structure (gray, PBD ID: 5CM2 chain Z).

B. Superimposition of the predicted AlphaFold *Drosophila* TRMT9B model (purple) with the Modeller-predicted *Drosophila* TRMT9B model (blue) and yeast Trm9 structure (gray, PBD ID: 5CM2 chain Z).

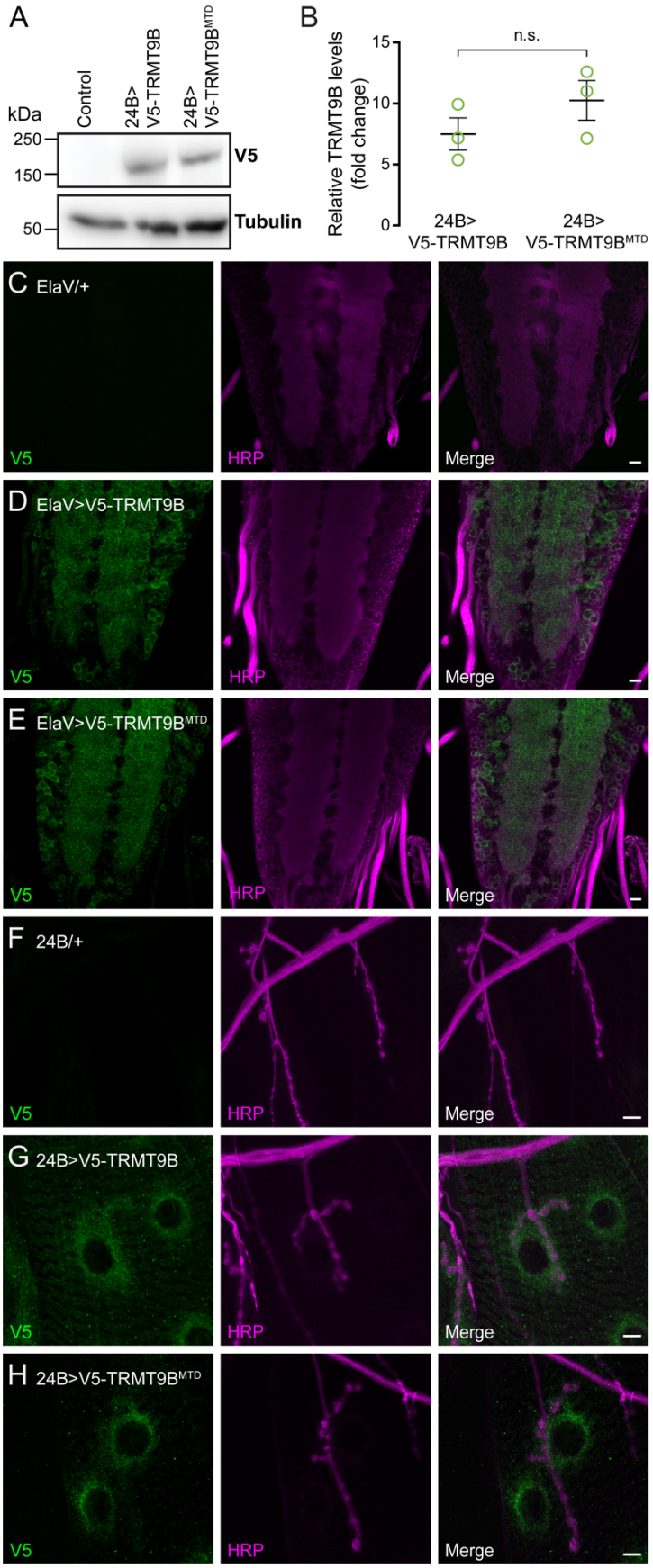
A
Control
24B> V5-TRMT9B
24B> V5-TRMT9B^MTD
kDa
250
150
50
V5
Tubulin
B
Relative TRMT9B levels (fold change)
15
10
5
0
n.s.
24B> V5-TRMT9B
24B> V5-TRMT9B^MTD
C ElaV/+
D ElaV>V5-TRMT9B
E ElaV>V5-TRMT9B^MTD
F 24B/+
G 24B>V5-TRMT9B
H 24B>V5-TRMT9B^MTD
V5
HRP
Merge

Figure 2.S5. Expression of wild-type and methyltransferase-dead TRMT9B transgenes.

A. Representative western blot images of third instar larval extracts from *24B-Gal4/+* control, *24B-Gal4>UAS-V5::TRMT9B* and *24B-Gal4>UAS-V5::TRMT9B^{MTD}* stained for V5 and Tubulin.

B. Quantification of postsynaptic expression of V5-tagged TRMT9B transgenes (3 biological replicates). Mean ± s.e.m is indicated. Welch's t-test, *P*=0.261 (n.s.).

C-E. Confocal Z-projections of larval ventral ganglia in *24B-Gal4/+* control, *24B-Gal4>UAS-V5::TRMT9B* and *24B-Gal4>UAS-V5::TRMT9B^{MTD}* co-labeled with antibodies against V5 (green) and the neuronal membrane marker Hrp (magenta).

F-H. Confocal Z-projections of larval NMJs in *24B-Gal4/+* control, *24B-Gal4>UAS-V5::TRMT9B* and *24B-Gal4>UAS-V5::TRMT9B^{MTD}* co-labeled with antibodies against V5 (green) and the neuronal membrane marker Hrp (magenta).

Scale bars for C-H: 10 μm.

CHAPTER 3

tRNA methyltransferase in ensheathing glia modulates synaptic growth and memory

Jennifer L. Dumouchel[1], Rajan S. Thakur[2], Emily Hill[3], Scott J. Gratz[2], Dragony Fu[4], and Kate M. O'Connor-Giles[2,5#]

[1]Therapeutic Sciences Graduate Program, Brown University, Providence, RI

[2]Department of Neuroscience, Brown University, Providence, RI

[3]Molecular Biology, Cell Biology, and Biochemistry Graduate Program, Brown University, Providence, RI

[4]Department of Biology, Center for RNA Biology, University of Rochester, Rochester, NY

[5]Carney Institute for Brain Science, Brown University, Providence, RI

[#]Corresponding author: Kate M. O'Connor-Giles; email: oconnorgiles@brown.edu

Keywords: tRNA methyltransferase, Drosophila, synapse, ensheathing glia, intellectual disability

Author Contributions:

- J.L.D. composed text, tables and figures, generated phylogenetic tree, homology modeling and methyltransferase domain alignment for Fig 3.1 and 3.S1.; dissections and adult fly head isolate for mass spectrometry experiments and data analysis Fig 3.2 and 3.8.; dissections, confocal imaging and analysis for Fig 3.3, 3.6A-D, 3.7B-F; 3.S2, S5C-G, 3.S6; short term memory behavioral studies and analysis Fig 3.4, 3.6E, 3.7G, 3.S3, S3.5H; dissections for SoRA imaging Fig 3.5C-D; western blot experiments and analysis Fig 3.S4A and 3.5SA-B.
- R.S.T contributed to experimental design, *TRMT1*^{RNAi} validation imaging and western blot experiments Fig 3.5A-D and TRMT1 super resolution SoRA imaging Fig 3.5C-D.
- E.H. assisted with dissection and bouton counting analysis for Fig 3.S5F and assisted with dissections for Fig 3.7B.
- S.J.G. contributed to experimental design, endogenous CRISPR tag design, active zone analysis in Fig 3.2E, and figure assembly.
- D.F. isolated total RNA, LC-MS/MS assessment and visualization for Fig 3.2
- K.O.C.G. contributed to project conception, experimental design, endogenous tag CRISPR design, assembling figures, tables, and manuscript writing.

ABSTRACT

Precise and dynamic regulation of protein expression is critical for nervous system development and function, and disruption of these processes is linked to diverse neurological disorders. Transfer RNAs (tRNAs) are extensively modified to maintain structural stability and ensure efficient and accurate mRNA decoding during protein synthesis. Human tRNA methyltransferase 1 (TRMT1), which dimethylates guanosine 26 to N2,N2-dimethylguanosine (m2,2G), has been linked to a rare form of intellectual disability; however, how the loss of this modification disrupts the nervous system remains unknown. We used CRISPR gene editing to generate a Drosophila model and show that loss of *TRMT1* leads to reduced synapse formation at the glutamatergic larval neuromuscular junction and memory impairment. TRMT1 is primarily expressed in glia and muscle nuclei and, interestingly, reexpression of TRMT1 specifically in ensheathing glia fully restores both synapse formation and memory impairment. Global nervous system proteomic changes in the absence of *TRMT1* demonstrate dysregulation of translation for glial pathways including metabolic homeostasis and phagocytosis. Overall, our findings demonstrate Drosophila as a tractable *in vivo* model system to understand TRMT1's role in the nervous system and suggest glia-neuron interactions underlie *TRMT1*-associated intellectual disability, with promise of identifying future therapeutic targets.

INTRODUCTION

Precise regulation of gene expression is required for proper nervous system development and cellular function (Klann & Dever, 2004). Proper translation control influences neuronal differentiation and function, including synapse formation, maturation and elimination and directly reflects memory formation and storage (Flavell & Greenberg, 2008; Holt & Schuman, 2013; Sossin & Costa-Mattioli, 2019). Transfer RNAs (tRNAs) function as adapters between mRNA transcripts and growing polypeptides by binding both codons and amino acids to decode mRNA. To promote stability and the fidelity of codon recognition, tRNAs are highly post-transcriptionally modified, with over 170 modifications reported (Agris *et al*, 2017; Cappannini *et al*, 2024; Jackman & Alfonzo, 2013; Lei *et al*, 2023; Motorin & Helm, 2010; Rigden & Fernandez, 2024). Extensive foundational research on tRNA biogenesis, transport, and enzymatic activity has been conducted over the past 60 years, primarily in single cell organisms (Phizicky & Hopper, 2015). More recently, inappropriate tRNA modifications have been associated with human disorders and classified as “tRNA modopathies” (Chujo & Tomizawa, 2025; Suzuki, 2021). Increasing evidence indicates that careful regulation of post-transcriptional tRNA modifications, particularly where and when these modifications occur across development, drives function. Disrupted post-transcriptional tRNA processing has been linked to multiple neurodevelopmental diseases, underscoring their importance in the brain (Chujo & Tomizawa, 2025). Mutations in tRNA synthetases, which attach amino acids to tRNAs, decrease protein synthesis and lead to peripheral neuropathy (Blocquel *et al*, 2019; Sauter *et al*, 2015; Storkebaum, 2016; Wei *et al*, 2019). Variants in the enzymes that catalyze a number of modifications on the tRNA anticodon loop and tRNA body have been linked to intellectual disability (Abbasi-Moheb *et al*, 2012; Alazami *et al*, 2013; Monies *et al*, 2019; Nagayoshi *et al*, 2021; Shaheen *et*

al, 2016; Zhang *et al*, 2020). Despite these growing links, the roles of tRNA modifying enzymes in the nervous system are not well studied.

A growing number of human genetic studies are identifying genes linked to rare forms of intellectual disability (Najmabadi *et al*, 2011). Variants in tRNA methyltransferase 1 (TRMT1) have been identified in patients with autosomal recessive intellectual disability, (Fig S3.1, (Davarniya *et al*, 2015; Efthymiou *et al*, 2025; Zhang *et al.*, 2020). Human TRMT1 is an ortholog of yeast tRNA methyltransferase 1 (Trm1) (Ellis *et al*, 1986; Hopper *et al*, 1982; Phillips & Kjellin-Straby, 1967). Trm1 is known to methylate guanosine at position 26 in the tRNA body to generate N2,N2- dimethylguanosine (m2,2G) and support proper tRNA structure and function (Adler *et al*, 1958; Bromberg *et al*, 1957; Liu & Straby, 2000). In *Trmt1*-deficient human cells and patient-derived cell lines demonstrate absence of m2,2G tRNA modifications, protein synthesis and cell proliferation (Dewe *et al*, 2017; Efthymiou *et al.*, 2025; Zhang *et al.*, 2020). In a neuroblastoma cell line, high-potassium induced depolarization induces a relocalization of TRMT1 to the nucleus, where TRMT1 modifies cytosolic tRNAs (Jonkhout *et al*, 2021; Pogodalla *et al*, 2021). In *Trmt1* deficient mice and zebrafish, changes in exploratory motor behaviors (Vauti *et al*, 2007) and hyperactivity have been observed (Efthymiou *et al.*, 2025), respectively. This growing body of research reveals the importance of studying how tRNA modification impacts the nervous system.

To study the nervous system role of TRMT1 *in vivo*, we used CRISPR gene editing to generate a Drosophila loss-of-function model and an endogenously tagged allele. Consistent with human cell- based $TRMT1^{KO}$ models and patient cells, m2,2G is absent in *TRMT1* null flies. Using the well-characterized glutamatergic larval neuromuscular junction model synapse, we found that loss of *TRMT1* disrupts synapse formation.

TRMT1 null flies also exhibit impaired memory formation. Notably, we find that TRMT1 is primarily expressed in glia and muscle nuclei and cell-specific expression of TRMT1 in phagocytic ensheathing glia, but not muscle, neurons or other glial cell types, fully restores both synapse formation and memory impairment. We conducted whole-brain proteomics in the absence of *TRMT1* and identified dysregulation of proteins in glial pathways, including the innate immune system. Overall, our findings demonstrate that TRMT1 plays a critical role in the development and function of the nervous system and point to glia-neuron interactions that may provide mechanistic insight into *TRMT1*-associated intellectual disability.

RESULTS

TRMT1 catalyzes the m2,2G base modification in Drosophila tRNAs

To evaluate using Drosophila as a model system to study TRMT1, we assessed the conservation of TRMT1 sequence and structure across species. TRMT1 is responsible for the addition of two methyl groups on guanosine at position 26 to N2,N2-dimethylguanosine (m2,2G) and is a homolog of yeast Trm1 (Ellis *et al.*, 1986; Hopper *et al.*, 1982; Niederberger *et al*, 1999; Phillips & Kjellin-Straby, 1967). Similar to yeast Trm1, mouse and human TRMT1 contain a catalytically active Class I S-adenosyl-L-methionine dependent methyltransferase domain that drives canonical function, and additionally contain nuclear and mitochondrial targeting signals (Fig. 3.1A, (Dewe *et al.*, 2017)). Vertebrate genomes also encode a paralog, tRNA methyltransferase like (TRMT1L) gene, which contain a methyltransferase domain and has been recently shown to be responsible for the dimethylation of guanosine at residue 27 and maintenance of 3-(3-amino-3carboypropyl)uridine levels (Zhang *et al.*, 2020; Zhang *et al*, 2025). Drosophila TRMT1 includes a methyltransferase domain and nuclear localization

signal, but lacks a mitochondrial targeting signal (Fig 3.1A). Primary sequence analysis of the Drosophila TRMT1 methyltransferase domain shows a 39% and 60% sequence identity and similarity, respectively, with yeast Trm1 methyltransferase domain and 49% and 64% sequence identity and similarity, respectively, with human TRMT1 methyltransferase domain (Fig 3.S1). We next turned to homology modeling to investigate tertiary structure using Modeller through Chimera (Pettersen *et al*, 2021; Pieper *et al*, 2009; Sali & Blundell, 1993) to compare the yeast, fly, mouse, and human TRMT1 methyltransferase domains against the best predicted template, a crystal structure of Trm1 from *Pyrococcus horikoshii* (PDB:2EJT (Ihsanawati *et al*, 2008)). Our model (Fig 3.1B) indicates high structural conservation across all species.

Given the conservation of TRMT1 across species, we generated a null allele of Drosophila *TRMT1* (CG6388) using a CRISPR-gene editing approach (Bruckner *et al*, 2017; Gratz *et al*, 2019) for *in vivo* studies. Briefly, an interfering cassette containing a sfGFP and a visible marker flanked with piggyBac inverted repeat sequences was inserted immediately downstream of the *TRMT1* AUG start site (Fig 3.1C). Disruption of the open reading frame by the inserted cassette generates a null allele ($TRMT1^{KO}$) and cassette removal by piggyBac transposase restores the reading frame to generate an endogenously tagged allele ($TRMT1^{sfGFP}$).

TRMT1 is responsible for the addition of two methyl groups on guanosine at position 26 to m2,2G and is a homolog of yeast Trm1 (Fig 3.2A (Ellis *et al.*, 1986; Hopper *et al.*, 1982; Niederberger *et al.*, 1999; Phillips & Kjellin-Straby, 1967). Previously, primer extension and TRMT1 RNAi knock down studies conducted in S2R+ cells demonstrate conserved TRMT1 biochemical function in flies (Funk *et al*, 2020). To measure methyltransferase activity *in vivo* in the absence of TRMT1, we conducted quantitative

nucleoside liquid chromatography mass spectrometry (LC-MS). Bulk RNA from control, *TRMT1*^{KO}, and *TRMT1*^{sfGFP} was isolated from adult heads. RNA was digested and dephosphorylated before isolating small RNAs before nucleosides were analyzed by LC-MS. We found that m2,2G was absent in adult flies deficient in *TRMT1* (Fig 3.2B). We also observed complete restoration of wild-type levels of m2,2G in our *TRMT1*^{sfGFP} endogenous rescue line. No other significant changes to nucleoside modifications were observed (Fig 3.2C). Our findings demonstrate Drosophila TRMT1 has conserved enzymatic function and confirm we've generated both a null allele and a biologically active endogenously tagged allele.

TRMT1 promotes synaptic growth

To investigate the neurodevelopmental role of TRMT1, we turned to the Drosophila larval neuromuscular junction (NMJ), a well-characterized glutamatergic model system in which single motor neurons innervate a single postsynaptic muscle. Each motor neuron forms a stereotyped number of boutons, which contain ~10 individual synapses. We can readily identify and quantify synaptic boutons and individual synapses using the neuronal membrane marker Horseradish peroxidase (HRP) and the presynaptic active zone marker, Bruchpilot (Brp), respectively. In the absence of *TRMT1*, we observed a 26% decrease in boutons per NMJ4 (Fig 3.3A-B,D). We observed similar synaptic undergrowth in male and female *TRMT1*^{KO} flies and in *TRMT1*^{KO} over a deficiency (Fig 3.S2). Restoration of endogenous TRMT1 returned bouton number to control levels (Fig 3.3C-D). The number of synapses per bouton was increased, leaving the total number of synapses unchanged (Fig 3.3E). This likely reflects a compensatory homeostatic mechanism as previously observed at the Drosophila NMJ (Goel *et al*, 2019).

TRMT1 promotes short-term memory

A growing number of variants have been associated with *TRMT1*-linked intellectual disability, however underlying mechanisms that explore synapse and cognitive function are unclear. TRMT1-variants were all identified in the methyltransferase domain and 7 of 11 missense mutations are in amino acids conserved in Drosophila (Fig 3.S1, (Davarniya *et al.*, 2015; Efthymiou *et al.*, 2025; Zhang *et al.*, 2020). Drosophila serves as an excellent model to investigate the potential behavioral consequences of an impaired nervous system (Abbasi-Moheb *et al.*, 2012; Coll-Tane *et al*, 2019; Madhwani *et al*, 2024). We turned to an aversive gustatory memory assay to assess short-term memory formation (Abbasi-Moheb *et al.*, 2012; Amrein & Thorne, 2005; Coll-Tane *et al.*, 2019; Keene & Waddell, 2007; Madhwani *et al.*, 2024; Scott, 2005). Taste aversion assays assess how starved, 1 week old adult flies learn to associate the presentation of a sweet tastant (sucrose) to taste receptors on their tarsi (legs) with presentation of a bitter tastant (quinine) to the proboscis (mouth) by monitoring the proboscis extension response (PER) (Fig 3.4A, (Keene & Waddell, 2007; Kirkhart & Scott, 2015; Masek & Keene, 2016; Masek & Scott, 2010)). Under basal conditions, flies demonstrate a strong preference for sweet tastants compared to bitter tastants (Fig 3.S3A-B). In *TRMT1*^{KO} flies, PER suppression was minimal, consistent with impaired learning and/or memory formation compared to wild-type (Fig 3.4B). Similarly, we also observed impaired memory in *TRMT1*^{KO} over a deficiency (Fig 3.S3C). Finally, restoration of endogenous TRMT1 restores averse taste memory to wild-type levels (Fig 3.4B). These findings support Drosophila as a tractable system for uncovering the molecular and cellular mechanisms underlying *TRMT1*-associated intellectual disability.

TRMT1 is expressed in glia and muscle

TRMT1 localization has been characterized in human cells where it localizes in the mitochondria and nucleus (Dewe *et al.*, 2017; Jonkhout *et al.*, 2021). To investigate where TRMT1 is expressed in the nervous system under baseline conditions, we used our endogenously tagged allele. TRMT1 endogenous tag size was confirmed by western blot (Fig 3.S4A). We first looked at the expression of N-terminally tagged *TRMT1*^{sfGFP} (green) in the larval ventral nerve cord to determine which cell types express TRMT1. We observe striking colocalization with a pan-glial nuclear marker Repo (Fig 3.5A) and surprisingly, we do not observe colocalization with neuronal nuclei, marked with the pan-neuronal marker Elav (magenta; Fig 3.5B). Although Drosophila TRMT1 lacks a mitochondrial localization signal, by super resolution microscopy we find the endogenous TRMT1 may localize with mitochondria, marked with the ATP synthase complex ATP5A, near glial nuclei (Fig 3.5C-D). We also observe TRMT1 expression in muscle nuclei and not muscle mitochondria (Fig 3.S4B-C).

TRMT1 functions in glial to promote synaptogenesis and memory

To evaluate where TRMT1 function is required to promote synapse formation and memory, we first used a cell-specific screening approach using an independent TRMT1 RNAi line (*TRMT1*^{RNAi}, (Perkins *et al*, 2015)). First, *TRMT1*^{RNAi} was validated by measuring TRMT1 protein knockdown. We measured GFP levels in flies expressing one copy of our *TRMT*^{sfGFP} with and without *TRMT1*^{RNAi} expressed in all glia using the *repo*-Gal4 driver. We observed a decrease in 60% and 70% in adult heads (Fig 3.S5A-B) and larval ventral nerve cord (Fig 3.S5C-E), respectively. To determine where TRMT1 functions, we drove RNAi expression using a ubiquitous (act5C), pan-neuronal (elav, (Robinow & White, 1988)), pan-glial (repo, (Sepp *et al*, 2001)), or pan-muscle (24B, (Brand & Perrimon, 1993)) Gal4 driver and assessed bouton number at NMJ4.

Ubiquitous and pan-glial knockdown of TRMT1 resulted in a decrease of boutons by 27% and 30%, respectively, compared to their individual Gal4 controls (Fig 3.5SF). Surprisingly, we observed no effect on NMJ growth when TRMT1 was knocked down in all neurons or muscle (Fig 3.5SF). These findings suggest TRMT1 functions in glial cells to regulate synaptic growth.

To validate the hypothesis that TRMT1 plays a neurodevelopmental role in glial cells, we conducted cell-specific rescue using *repo-Gal4* to drive a full-length *TRMT1* transgene in all glial cells. We found that expressing *TRMT1* in all glial cells restores synaptic growth at the NMJ4 (Fig 3.6A-D). Overexpression of *TRMT1* or an N-terminal tagged *V5-TRMT1* in glial cells showed no effect on bouton number (Fig 3.5SG). Thus, we conclude that TRMT1 acts in glial cells to promote NMJ development.

Next, we sought to investigate if TRMT1 also functions in glial cells to promote memory. We again used repo-Gal4 to restore TRMT1 in all glial cells and observed full restoration of memory impairment (Fig 3.6E). All lines exhibit normal basal preferences for sucrose and quinine (Fig 3.S5H). Together, our findings demonstrate that TRMT1 functions in glia to promote synapse formation and memory.

TRMT1 acts in ensheathing glia to regulate synaptic growth and memory

Drosophila glial subtypes are well defined based on morphology and function in larval and adult nervous systems (Bittern *et al*, 2021; Coutinho-Budd *et al*, 2024; Freeman, 2015; Ito *et al*, 1995; Lee & Sun, 2015; Yildirim *et al*, 2019). In third instar larvae, glial cells that associate with the neuropil include astrocyte-like, cortex, and ensheathing glia, while the perineurial and subperineurial glia cells form the blood brain barrier (Fig 3.7A,(Bittern *et al.*, 2021)). We hypothesized that reduction of TRMT1 in one or more

glial subtypes might phenocopy the neuronal results. To test this, we knocked down *TRMT1* in five previously characterized subtype-specific glial drivers and assessed synaptic growth at NMJ4. Ensheathing glial knockdown of TRMT1 using the *56F03E12*-Gal4 driver (Kremer *et al*, 2017; Stahl *et al*, 2018) resulted in a 32% decrease in boutons number compared to control (Fig 3.7B). In contrast, we observed no effect on bouton number when TRMT1 was knocked down in perineurial (*c527*-gal4 driver (Hummel *et al*, 2002)), subperineurial (*moody.SPG*-gal4 (Bainton *et al*, 2005; Padiath *et al*, 2006)), cortex (*55B12*-gal4 (Jenett *et al*, 2012)), and astrocyte-like glial cells (*alrm*-gal4 (Doherty *et al*, 2009), Fig 3.7B)). To confirm our findings, we used a second, more specific ensheathing glial Gal4 line, *83E12*-Gal4 (Pogodalla *et al.*, 2021), and again phenocopied pan-glial knockdown with a -24% reduction in boutons per NMJ4 compared to controls (Fig 3.7B). Thus, we hypothesize that TRMT1 functions in ensheathing glia to promote NMJ development.

To validate this hypothesis, we conducted cell-specific rescue using both ensheathing glial Gal4 drivers. We again found that expressing TRMT1 in all ensheathing glial cells restores synaptic growth at the NMJ4 (Fig 3.7C-F, Fig 3.S6). We next investigated TRMT1's role in memory and found that restoration of TRMT1 specifically in ensheathing glial cells restores memory impairments (Fig 3.7G).

TRMT1-dependent modifications regulate the nervous system proteome

To understand how TRMT1 might function in glia, we conducted global proteomics in the larval and adult nervous system. We isolated total protein from the larval CNS and body wall or adult heads of control and $TRMT1^{KO}$ animals (4 independent replicates/genotype/tissue). Unlabeled proteomics was performed by high resolution liquid chromatography with tandem MS (LC-MS/MS) using a Thermo Scientific Orbitrap

Astral MS. We quantified 7922 and 6698 proteins in the larval and adult *TRMT1*^{KO} nervous system, respectively. To identify differentially expressed proteins, proteins were narrowed based on adjusted p-value < 0.05 and log2fold change (log2FC), where upregulated proteins (orange) are 663 in larva and 65 in adult (larval, log2FC > 1.3; adult, log2FC > 1) and downregulated proteins (blue) are 388 in larval and 66 in adult (larval, log2FC < -1.3; adult, log2FC < -1, Fig 3.8A,D).

We conducted GeneOntology to investigate enrichment of biological processes and molecular function in the absence of TRMT1. In larval and adult, we observed downregulation of muscle and myofibril components (Fig 3.8B,E). In parallel, upregulation of metabolic and oxidoreductase activity were seen at both developmental stages (Fig 3.8C,F). While top Gene Ontology categories indicated dysregulation of metabolism, we also were interested in known synaptic proteins based on our robust synaptic phenotypes studied. Manual assessment of proteomics dataset, postsynapse scaffolding proteins including Dlg1 (log2FC -0.54) and calcium channel subunits Cac (log2FC +0.45) and Stj (log2FC +0.43) showed minor changes at the protein level.

We used STRING-DB analysis to evaluate protein-protein association networks shared across the larval and adult development stages. To understand altered pathways in *TRMT1*^{KO} larval and adult, we investigated the 41 differentially expressed proteins at the intersection of the two datasets (Fig 3.8G). Enrichment of glial processes included phagocytosis (NimC1, Eater, TotA, SPE, GNBP3), and metabolism/transport (MDR, SLC22A, GSTD2-3, CYP9C1, CYP9B2; SLC22A; CNT2, Adgf-D, Adk, and Veil; Fig 3.8H). We are currently investigating the role of these pathways in TRMT1 phenotypes through genetic interaction studies. Together, our findings suggest a model where TRMT1 dimethylates guanosine at position 26 in tRNAs to ensure proper protein

translation in glia and downstream regulation of these proteins promotes synaptic bouton growth and memory retention.

DISCUSSION

We generated a *TRMT1 loss-of-function* model in Drosophila to gain new insights to its role in the intact nervous system. Through biochemical, structural modeling, and imaging studies, we found that TRMT1 carries out the conserved methyltransferase function and is expressed in glial and muscle nuclei. Rigorous genetic studies indicate that TRMT1 acts in ensheathing glia to promote synaptic growth and memory. Our proteomics data raises the possibility that loss of *TRMT1* may lead to the dysregulation of phagocytosis as well as xenobiotic and adenosine metabolism. These findings highlight Drosophila as a versatile model to gain mechanistic insight into *TRMT1*-associated intellectual disability and identify protein-based therapeutic targets.

Cross-talk between glial cells and neurons is an exciting and continuously evolving field of cell-to-cell communication building on evolutionary conservation (Fields & Stevens-Graham, 2002; Freeman & Doherty, 2006; Lyons & Talbot, 2014) and human models of neurodevelopment and neurodegenerative disorders (Lee & Sun, 2015). Drosophila glial cells regulate synapse formation, function, the blood brain barrier, and response to injury and have been well reviewed by others (Bittern *et al.*, 2021; Yildirim *et al.*, 2019). Ensheathing glial cells establish a barrier between the neuropil to help maintain homeostasis (Flores-Valle *et al*, 2025). This specialized cell type comprises transporters, lipids, cytoskeletal components including β_{heavy} Spectrin (Pogodalla *et al.*, 2021). Other functions include regulation of metabolic homeostasis and neuronal activity through glutamate homeostasis driven by mitochondrial sulfite oxidase *Shopper* (Otto *et al*,

2018). We find metabolic dysregulation at the protein level including regulators of adenosine metabolism (Lee *et al*, 2018; Singer *et al*, 2012; Theparambil *et al*, 2024) and multiple transporters that are critical to maintenance of the blood brain barrier (Gai *et al*, 2016; Hindle & Bainton, 2014). Our model supports the absence of *TRMT1* in ensheathing glial leads to impaired cognitive function as seen in zebrafish and human (Davarniya *et al.*, 2015; Efthymiou *et al.*, 2025; Zhang *et al.*, 2020). Although Drosophila lack myelin, ensheathing glia wrap around the neuropil region and those that wrap axons are also known as wrapping glia; together these cells modulate immune response through phagocytosis, similar to mammalian oligodendrocytes and microglia (Freeman & Doherty, 2006), respectively. Continued generation of ensheathing and wrapping glia genetic reagents would be helpful to differentiate their functions (Kottmeier *et al*, 2020). Phagocytic receptors such as Draper and SIMU have been investigated in Drosophila in response to injury and axon degeneration (Hilu-Dadia *et al*, 2018; Logan *et al*, 2012; Lu *et al*, 2017; Macdonald *et al*, 2013; McLaughlin *et al*, 2019; Purice *et al*, 2017). Synapse pruning is an important function between ensheathing (Leier *et al*, 2025) and astrocyte-like glial (Ackerman *et al*, 2021) and neurons to remove dying neurons, maintains homeostasis during critical periods (Hilu-Dadia *et al.*, 2018; Jindal *et al*, 2023; Manaka *et al*, 2004; McLaughlin *et al.*, 2019; Nelson *et al*, 2025). Our proteomics dataset points toward the upregulation of the immune system and specifically two phagocytic receptors, NimC1 and Eater. Immune responses were also upregulated in a *TRMT1* zebrafish model (Efthymiou *et al.*, 2025). TRMT1 has also been shown to be cleaved and inactivated by the SARS-Cov2 protease, although an underlying mechanism of how decreased TRMT1-mediated translation contributes to viral pathogenesis is unknown (D'Oliviera *et al*, 2025; Li *et al*, 2021; Lu & Zhou, 2023; Zhang *et al*, 2024). Post-mortem brain tissue from patients with COVID-19 and brain organoids infected with COVID-19 demonstrated increased synapse elimination drive by microglia phagocytosis and

synaptic signaling (Partiot *et al*, 2024; Samudyata *et al*, 2022; Yang *et al*, 2021). Further investigation is required and of great interest to understand the role of TRMT1-mediated translation and synapse formation and function with respect to the innate immune response in the brain.

Complementing work done in other model systems, our data supports Drosophila TRMT1 dimethylates m2,2G (Davarniya *et al.*, 2015; Dewe *et al.*, 2017; Efthymiou *et al.*, 2025; Ellis *et al.*, 1986; Funk *et al.*, 2020; Hopper *et al.*, 1982; Niederberger *et al.*, 1999; Phillips & Kjellin-Straby, 1967; Vauti *et al.*, 2007; Zhang *et al.*, 2020; Zhang *et al.*, 2025). TRMT1 is a primary tRNA modifier and has been shown to methylate 12 total tRNAs cytosolic and mitochondrial to maintain proper tRNA structure and function (Dewe *et al.*, 2017; Zhang *et al.*, 2025). Generation of the methyltransferase domain mutations would allow for future *in vivo* studies to explore the non-catalytic activity of *Trm1* observed in yeast (Porat *et al*, 2023). We observed impaired synaptic function and builds on *in vitro* findings that TRMT1 has altered *in vitro* sub-cellular expression under stressed, neuronal cell culture conditions (Jonkhout *et al.*, 2021). TRMT1 has been shown to be ubiquitously expressed in Drosophila, mice, pigs, and human (Brown *et al*, 2014; Sjostedt *et al*, 2020; Tushaus *et al*, 2023) across development but disproportionate loss of TRMT1 in the brain has led to intellectual disability in humans (Davarniya *et al.*, 2015; Efthymiou *et al.*, 2025; Zhang *et al.*, 2020). Future studies to investigate global changes in protein synthesis (Dewe *et al.*, 2017; Efthymiou *et al.*, 2025; Zhang *et al.*, 2020) mitochondrial versus cytosolic translation (Kimura *et al*, 2022) in the absence or overexpression of TRMT1 as well as cell-specific ribosomal profiling (Chen & Dickman, 2021; Thomas *et al*, 2012) will provide greater insight on the role of TRMT1 in the brain.

Numerous tRNA modifying enzymes have been linked to rare neurodevelopmental disorders (Ramos & Fu, 2019; Suzuki, 2021). Recent reports have called for an increase in the number of genetic tools, access to therapeutic intervention outside of gene therapy, and greater understanding of the underlying molecular mechanisms for rare genetic diseases (Fox & Booth, 2024; Sankar *et al*, 2024). Thirty-one patients have been identified with *TRMT1*-linked intellectual disability. Variants identified are all in the methyltransferase domain and include shifts/premature stops, splice variants, and missense mutations, 7 of 11 of which are in amino acids conserved in Drosophila (Davarniya *et al.*, 2015; Efthymiou *et al.*, 2025; Zhang *et al.*, 2020). Studies in cells with patient mutations reveal both loss of m2,2G modifications and decreased protein translation (Efthymiou *et al.*, 2025; Zhang *et al.*, 2020). An *in vivo TRMT1* zebrafish knockout model similarly shows decreased m2,2G modification as well as changes in activity levels, locomotion, and immune function (Efthymiou *et al.*, 2025). Our studies provide an additional *in vivo* model and reveal impaired synapse development and memory formation. Our studies further demonstrate that TRMT1 is highly expressed in glia and regulates these functions through a role in ensheathing glia, which have been well characterized for their role in phagocytosis. Interestingly, our nervous system-wide proteomics data reveals differential expression of proteins involved in phagocytosis in the absence of TRMT1, suggesting potential protein therapeutic targets. These data also highlight changes in xenobiotic enzymes and transporters in the brain, which should be carefully assessed for small molecule therapeutic approaches. These findings provide a foundation for further investigation of the pathology behind *TRMT1*-associated intellectual disability and new insights into potential avenues for the development of therapeutics.

Materials and Methods

Drosophila genetics and gene editing

All fly experiments were performed at 25°C in an incubator (60% humidity, 12 h light/dark cycle; Darwin Chambers, St Louis, MO) using a molasses-based media in narrow vials (Fly Food R, Lab Express, Catalog #7003-NV) unless noted otherwise. Independent crosses were flipped every 2-3 days and performed under non-crowding conditions for both third wandering instar larvae and adult experiments. Stocks obtained from the Bloomington Drosophila Stock Center (BDSC, NIH P40OD018537) include the following: w^{1118} (RRID:BDSC_5905), *piggyBac transposase* (RRID: BDSC_8283), *TRMT1 deficiency* (RRID: BDSC_7516;(Parks *et al*, 2004)), *UAS-TRMT1*^{RNAi} (RRID: BSDC_603563, (Perkins *et al.*, 2015)). For RNAi screening and UAS/Gal4 follow up approaches the following fly lines were used: *act5C-Gal4* (ubiquitous expression, RRID: BDSC_3954), *elav*^{C155}*-Gal4* (pan-neuronal expression, RRID: BDSC_458, (Robinow & White, 1988)), *24B-Gal4* (pan-muscle expression, RRID: BDSC_92172, (Brand & Perrimon, 1993)), *repo-Gal4* (pan-glial expression, RRID: BDSC_7415, (Sepp *et al.*, 2001)), *alrm-Gal4* (astrocyte-like glia expression, RRID:BDSC_67032, (Doherty *et al.*, 2009)), *83E12-Gal4* (ensheathing glia expression, RRID:BDSC_40363, (Pogodalla *et al.*, 2021), *56F03-Gal4* (ensheathing glia expression, RRID: BDSC_39157, (Kremer *et al.*, 2017; Stahl *et al.*, 2018)), *55B12-Gal4* (cortex glia expression, RRID:BDSC_39103, (Jenett *et al.*, 2012)), *moody-Gal4* (subperineurial glia expression, RRID:BDSC_90883, (Bainton *et al.*, 2005; Padiath *et al.*, 2006)), and *c527-Gal4* (perineurial glia expression, RRID:BDSC_90391, (Hummel *et al.*, 2002)). A detailed description of BDSC stocks are included in Table 3.1. In addition to this study, the following genetic lines were generated: *TRMT1*^{KO}, *UAS-TRMT1*, and *UAS-V5-TRMT1*.

A CRISPR approach using homology-directed repair was used to generate a null and an in-frame endogenous tagged allele. Target sites were selected using CRISPR Optimal Target Finder program (http://targetfinder.flycrispr.neuro.brown.edu) and a gRNA (*TRMT1*^{KO}: 5'-TTAACTCATCCAAATGGAAG-3') was generated using methods described in (Gratz *et al*, 2014). Vasa-Cas9 embryos were injected with gRNA plasmids (100 ng/uL) and a double stranded donor plasmid (500 ng/uL) by BestGene, Inc. Post eclosion, flies were crossed to w1118 flies and progeny were screened for the visible marker, DsRed, expressed in the eye. An endogenously tagged allele was created using a scarless CRISPR-piggyBac approach (https://flycrispr.org; (Bruckner *et al.*, 2017)). A sfGFP (5' -

GTGTCCAAGGGCGAGGAGCTGTTCACCGGCGTGGTGCCCATCCTGGTGGAGCTG
GATGGCGACGTGAACGGCCACAAGTTCAGCGTGCGCGGCGAGGGCGAGGGCGAC
GCCACCAACGGCAAGCTGACCCTGAAGTTCATCTGCACCACCGGCAAGCTGCCCG
TGCCCTGGCCCACCCTGGTGACCACCCTGACCTACGGCGTGCAGTGCTTCAGCCG
CTACCCCGATCACATGAAGCAGCACGATTTCTTCAAGAGCGCCATGCCCGAGGGC
TACGTGCAGGAGCGCACCATCAGCTTCAAGGATGACGGCACCTACAAGACCCGCG
CCGAGGTGAAGTTCGAGGGCGATACCCTGGTGAACCGCATCGAGCTGAAGGGCAT
CGATTTCAAGGAGGATGGCAACATCCTGGGCCACAAGCTGGAGTACAACTTCAACA
GCCACAACGTGTACATCACCGCCGATAAGCAGAAGAACGGCATCAAGGCCAACTT
CAAGATCCGCCACAATGTGGAGGATGGCTCCGTGCAGCTGGCCGATCACTACCAG
CAGAACACCCCCATCGGCGACGGCCCAGTGCTGCTGCCCGATAACCACTACCTGA
GCACCCAGAGCGTGCTGTCCAAGGACCCCAACGAGAAGCGCGATCACATGGTGCT
GCTGGAGTTCGTGACCGCCGCCGGCATCACCCTGGGCATGGATGAGCTGTACAAG
- 3') tag flanked by flexible linkers and a visible marker flanked by piggyBac inverted terminal repeat sequences were inserted immediate downstream of the TRMT1 translation start site. The insertion generated a null allele (*TRMT1*^{KO}). To generate an

endogenously N-terminal sfGFP tagged line, piggyBac transposase was used to remove the inserted marker cassette. Lines were molecularly verified by Sanger sequencing.

Generation of UAS lines

UAS fly lines were generated by cloning untagged TRMT1 coding sequence into a pUAST-C5 vector. An N-terminal V5 tagged TRMT1 transgene was similarly generated to assess localization. Best Gene, Inc inserted the transgenes into the attP2 site landing site according to published methods (Groth *et al*, 2004). Plasmids were validated by Sanger sequencing and fly lines were validated by Sanger sequencing, western blot and immunostaining.

Immunostaining and confocal imaging

Third-instar larvae (male and female mixed, unless otherwise noted) were dissected in Ca^{2+}-free saline and fixed with Bouin's fluids for 6 min. Fixed tissues were washed and permeabilized in 1X phosphate buffered saline (PBS) with 0.1% triton X-100, blocked with PBS containing 1% bovine serum albumin and 0.1% triton X-100 for 1 h at room temperature or overnight at 4°C, followed by primary antibodies overnight at 4°C, secondary antibodies incubated at 4 h at room temperature and mounted in VectaShield, and cured overnight. Primary antibodies include mouse anti-bruchpilot, mouse anti-repo, rat anti-elaV, mouse anti-ATP5A, mouse anti-V5 tag, while secondary include goat anti-species specific antibodies conjugated with either Alexa Fluor 488, 567, or 647. Complete antibodies details and concentrations used are provided in Table 3.1. For localization studies, the block also contained 5% normal goat serum to reduce nonspecific binding. Superresolution studies were mounted with ProLongGlass Antifade Mountant or Fluoromont-G.

Images were acquired on a Nikon A1R HD confocal microscope with a Plan-Apo 60X 1.49 NA oil-immersion objective at a pixel resolution of 100 nm. Superresolution images were acquired on a Nikon CSU-W1 SoRA (Spinning Disk Super Resolution by Optical Pixel Reassignment) with a Photometrics Prime BSI sCMOS camera and a 60x 1.49 NA oil-immersion objective, where images were acquired using a Richardson-Lucy deconvolution with 15-20 iterations. Image analysis was performed using ImageJ and Nikon Elements General Analysis software. Representative images were background subtracted using a roll ball method and equally adjusted for brightness and contacts for all genotypes.

Sequence alignment, phylogeny, homology modeling

Alignment of the Pfam defined methyltransferase domains (Mistry *et al*, 2021) were performed using T-Coffee (Notredame *et al*, 2000) for the following UniProt identifying sequences: P15565 (yeast Trm1), Q9VK89 (Drosophila TRMT1), Q3TX08 (mouse TRMT1), A2RSY6 (mouse TRM1L), Q9NXH9 (human TRMT1) and Q7X2T5 (human TRM1L). Phylogenetic tree was generated using phyloTv2 (https://phylot.biobyte.de/). Mitochondrial targeting sequence searches were performed with DeepMito (Savojardo *et al*, 2020) and Motofates (Fukasawa *et al*, 2015). Nuclear localization signal search was performed with NLStradamus (Nguyen Ba *et al*, 2009) Homology modeling of the methyltransferase domains of yeast, Drosophila, mouse and human TRMT1 was conducted using Modeller (Pieper *et al.*, 2009) using ChimeraX (Pettersen *et al.*, 2021; Sali & Blundell, 1993). Models were built using the best scored template, the methyltransferase domain of *Pyrococcus horikoshii* Trm1 (PDB: 2EJT, (Ihsanawati *et al.*, 2008), methyltransferase domain residues 43-489 (yeast), 18-451 (Drosophila), 56-498 (mouse) and 43-499 (human) that resulted in best fit models with e-values < 1.64E-37 and scores > 142.

Mass spectrometry centered analysis

For mass spectrometry studies, third wandering instar larvae were dissected in PBS, cleaned to retain cuticle (body wall) and larval brain (N = 6/genotype; 4 biological replicates), flash frozen under liquid nitrogen, and at -80°C. Adult flies (mixed gender, 3 – 5 days post eclosure, nucleotide analysis: N = 300/genotype; proteomics N = 100/genotype, 4 biological replicates per experiment) were briefly anesthetized and sorted on a fly pad. Flies were flash frozen under liquid nitrogen. Adult heads (250 µm) were separated from whole bodies at the cuticle by shaking over dry ice pellets and sorted from bodies (710 µm) and wings and legs (53 µm) using a three-tiered sieve and stored at -80°C.

RNA modifications – Adult fly heads (~25 mg) were manually homogenized with a plastic pestle in 1.5 mL microcentrifuge tubes in 250 µL of TRIzol Reagent and subsequent 250 µL aliquots were added until TRIzol reached 1 mL total volume. Total RNA was extracted as previously described (Bogart K, 2006) and resuspended in RNase-free water. Total RNA (20 µg) was treated with benzonase, phosphodiesterase, and calf-intestinal phosphatase for 3 h at 37°C to digest and dephosphorylate. Digested samples were filtered with a 10,000-Da MWCO spin filter (Amicon) and undigested RNA were stored at -80°C until use. Using a Hypersil^{TM} GOLD C18 Selectivity Column (Thermo Scientific), ribonucleosides were separated and analyzed on a Q Exactive Plus Hybrid Quadrupole Orbitrap. The ratio of modified to unmodified nucleoside was calculated using the mass to charge (m/z) intensity between control and *TRMT1*^{KO} and ratios were normalized to the sum intensity values for the canonical nucleosides (A,U,G, and C).

Proteomics – Tissues, larva (brain and body wall) and adult heads, were lysed, protein concentration was measured by BCA (Thermo Fisher Scientific) and sample lysates were cleaned using S-Trap columns (Protiff LLC). Cleaned, digested, label-free samples were run on an Orbitrap Astral Mass Spectrometer (Thermo Fisher Scientific, Waltham, MA). Samples were analyzed using Proteome Discoverer software platform (Thermo Fisher Scientific) using Sequest-HT search algorithms against the Drosophila melanogaster RefSeq protein database. Proteomics datasets were narrowed to peptides > 3 in two or more replicates, statistically significant proteins (p-value < 0.05), and differentially expressed proteins were narrowed by p-value < 0.05 and log2foldchange (log2FC), to determine upregulated (log2FC > 1 for adult heads; > 1.3 for larva) and downregulated (log2FC < -1 for adult head; < -1.3 for larva) proteins. Statistically significant proteins were trimmed using REVIGO ((Supek *et al*, 2011); http://revigo.irb.hr/) and Gene Ontology enrichment of molecular function, cellular component, and biological processes was assessed through gProfiler (Kolberg *et al*, 2023; Reimand *et al*, 2007) using R Studio 2024.12.1+. Protein-protein interactions were assessed with StringDB (Snel *et al*, 2000; Szklarczyk *et al*, 2023) and the intersection of differentially expressed proteins between development stages was completed using Venny2.0 (https://bioinfogp.cnb.csic.es/tools/venny/).

Western blots

Protein samples were prepared from adult fly heads (N = 20 heads/genotype/replicate) by homogenizing tissue with plastic pestles in lysis buffer consisting of 2x Laemmli buffer and 2-mercaptoethanol. Tissue homogenates were boiled at 95°C for 5 min and centrifuged at 8,000 rpm for 6 min to remove tissue debris. Protein samples were run on a stacking gel at 50V for 30 min and run on a 10% SDS-PAGE gel at 90 V until the protein ladder was resolved. Gels were transferred onto a nitrocellulose membrane (BIO

RAD Catalog # 162-0116) at 15V for 30 min. Membranes were briefly stained with Ponceau-S staining solution to assess relative transfer efficiency and washed in PBS before being blocked in freshly prepared 5% (w/v) bovine serum albumin in PBS with 0.1% Tween-20 at room temperature for 30 min. Primary antibodies include rabbit anti-GFP and mouse-anti-syntaxin and affiniPure goat anti-species specific secondary antibodies; all vendor details and dilutions are included in Table 3.1. Briefly, primary antibodies were prepared in 5% bovine serum albumin in PBS with 0.1% tween-20 and incubated overnight at 4°C. Blots were washed in PBS with 0.1% tween-20 for 30 min before incubation with secondary in PBS with 0.1% tween-20 for 2 h at room temperature. Blots were washed in PBS with 0.1% tween-20 for 30 min and then in PBS for 10 min. Blots were developed with SuperSignal™ West Femto Maximum Sensitivity Substrate (Thermo Fisher Scientific) developing solution and imaged on a ChemiDoc MP Imaging System (BIO RAD). Before reprobing for loading control proteins, blots were stripped at room temperature in 3% acetic acid for 45 min and washed in PBS for 30 min. Quantification was performed using ImageJ software. Net protein bands were calculated as mean value - average background value; protein bands were then normalized to respective loading controls. *TRMT1*^{RNAi} knockdown efficiency percent was calculated by dividing the endogenously tagged TRMT1 protein levels with pan-glial TRMT1 knockdown by the TRMT1 protein levels in an heterozygous endogenously tagged TRMT1.

Behavior and development experiments

Taste Preference – To test preference to sweet or bitter tastants, assays were adapted from (Kirkhart & Scott, 2015; Masek & Keene, 2016). One-week old mated female flies (N >19/genotype/experiment) were starved in narrow vials (Lab Express, Cat #8002-5) with water (750 µL milliQ-water on 2.5cm x 4 cm filter paper) for 24 h incubated at 25°C,

before mounting on microscope slides (5 flies/row, 2 rows/slide, Fisher Scientific Cat # 12-550-143) and acclimated upright in a dark, humid chamber for 2.5 h before testing. Solutions were administered using a 1 mL syringe (VWR, Cat # BD-309628) fitted with a 20 µL pipette tip (RAININ, Cat # 30389291). Flies were sasitated with milliQ-water post acclimation. Flies were presented with freshly prepared tastants, 500 mM sucrose (sweet tastant, Fisher Scientific, Cat # BP220-212) or 50 mM quinine (bitter tastant, Sigma Aldrich, Cat # Q1125-5G) on their tarsi for 2-3 sec in triplicate with 10 sec between tests. Number of proboscis extension reflexes (PER) were recorded. Flies were washed with a droplet of water and recovered for 2 min between tastant trials. PER was calculated as the number of proboscis extensions by the number of tasting presentations. Mean PERs for each solution were calculated from three independent, biological replicates.

Taste Aversion – Taste aversion studies were prepared as described for taste preference and followed previously reported protocols (Kirkhart & Scott, 2015; Masek & Keene, 2016). Following acclimation, flies (one-week old, mated female flies, n >25 /genotype/gender) were given water until satiated and pre-tested to measure PER with three applications of 500 mM sucrose to their tarsi in 10 s intervals. Flies with < 3 PER responses were excluded from training. Flies were trained with paired sweet/bitter tastants, where 500 mM sucrose was presented to their tarsi and 50 mM quinine to their proboscis for 2-3 sec. Flies were washed with a droplet of water and recovered for 2 min between sessions, three total. After the final training, flies were given 5 min rest. To test memory formation, flies were exposed to sucrose on their tarsi and the number of PER were recorded. Suppression of PER was calculated one minus the percentage of proboscis extension by the number of tasting presentations. Mean suppression of PER for three biological replicates was reported.

Experimental design and statistical analysis

Samples were masked to genotype. All experiments were conducted in triplicate with all crosses set up at least twice to obtain results from independent replicates. Statistical differences were calculated using GraphPad Prism 10. Repeated measures and multiple comparisons will be evaluated for distribution and variance. Normally distributed datasets with equal variance were analyzed with one-way ANOVA with Tukey's post hoc multiple comparisons. Non-normally distributed datasets were analyzed using Kruskal-Wallis test with Dunn's post hoc multiple comparisons. Error bars report mean ± standard mean error (SEM) unless otherwise noted. Statistical details and sample sizes are listed in each figure legend and full genotypes are reported in Table 3.S1-S2.

ACKNOWLEDGEMENTS

This work was supported by a grant from the NIH National Institute of Neurological Disorders and Stroke to K.M.O.-G. and D.F. (R01 NS117068) and trainee support from the National Institute of General Medical Sciences to J.L.D through the Brown University Predoctoral Training Program in Trans-disciplinary Pharmacological Sciences (T32 GM077995) and the Brown University Carney Institute for Brain Science JBB Endowed Graduate Fellowship. The Nikon SoRa microscope was provided by the Neurobiology of Cells and Circuits/Center for Translational Neuroscience Microscopy Committee, Carney Institute for Brain Science. This research has been facilitated by the services at the University of Rochester Mass Spectrometry Resource Laboratory, and we thank Sina Ghaemmaghami and Kevin Welle for their support. We thank FlyBase (FB2025_02; (Jenkins *et al*, 2022; Ozturk-Colak *et al*, 2024), Developmental Studies Hybridoma Bank, Drosophila Genomics Resource Center, and Bloomington Drosophila Stock Center (NIH

P40OD018537) for database, antibodies, plasmid and fly stock resources. We thank Sebastien Santini (CNRS/AMU IGS UMR7256) and the PACA Bioinfo platform (supported by IBISA) for the availability and management of the phylogeny.fr website used for phylogeny and sequence alignment. Molecular graphics images were created using the UCSF Chimera package from the Resource for Biocomputing, Visualization, and Informatics at the University of California, San Francisco (supported by NIH P41 RR001081). We are grateful to the O'Connor-Giles and Fu labs for critical feedback on the work and manuscript; and are grateful for James Kentro's assistance in the GeneOntology R Studio code.

Disclosure and competing interests statement

The authors declare that they have no conflict of interest.

Chapter 3 Reference

Abbasi-Moheb L, Mertel S, Gonsior M, Nouri-Vahid L, Kahrizi K, Cirak S, Wieczorek D, Motazacker MM, Esmaeeli-Nieh S, Cremer K *et al* (2012) Mutations in NSUN2 cause autosomal-recessive intellectual disability. *Am J Hum Genet* 90: 847-855

Ackerman SD, Perez-Catalan NA, Freeman MR, Doe CQ (2021) Astrocytes close a motor circuit critical period. *Nature* 592: 414-420

Adler M, Weissmann B, Gutman AB (1958) Occurrence of methylated purine bases in yeast ribonucleic acid. *J Biol Chem* 230: 717-723

Agris PF, Narendran A, Sarachan K, Vare VYP, Eruysal E (2017) The Importance of Being Modified: The Role of RNA Modifications in Translational Fidelity. *Enzymes* 41: 1-50

Alazami AM, Hijazi H, Al-Dosari MS, Shaheen R, Hashem A, Aldahmesh MA, Mohamed JY, Kentab A, Salih MA, Awaji A *et al* (2013) Mutation in ADAT3, encoding adenosine deaminase acting on transfer RNA, causes intellectual disability and strabismus. *J Med Genet* 50: 425-430

Amrein H, Thorne N (2005) Gustatory perception and behavior in Drosophila melanogaster. *Curr Biol* 15: R673-684

Bainton RJ, Tsai LT, Schwabe T, DeSalvo M, Gaul U, Heberlein U (2005) moody encodes two GPCRs that regulate cocaine behaviors and blood-brain barrier permeability in Drosophila. *Cell* 123: 145-156

Bittern J, Pogodalla N, Ohm H, Bruser L, Kottmeier R, Schirmeier S, Klambt C (2021) Neuron-glia interaction in the Drosophila nervous system. *Dev Neurobiol* 81: 438-452

Blocquel D, Sun L, Matuszek Z, Li S, Weber T, Kuhle B, Kooi G, Wei N, Baets J, Pan T *et al* (2019) CMT disease severity correlates with mutation-induced open

conformation of histidyl-tRNA synthetase, not aminoacylation loss, in patient cells. *Proc Natl Acad Sci U S A* 116: 19440-19448

Bogart K AJ (2006) Extraction of total RNA from Drosophila. CGB Technical Report 2006-10.

Brand AH, Perrimon N (1993) Targeted gene expression as a means of altering cell fates and generating dominant phenotypes. *Development* 118: 401-415

Bromberg PA, Gutman AB, Weissmann B (1957) The purine bases of human urine. I. Separation and identification. *J Biol Chem* 224: 407-422

Brown JB, Boley N, Eisman R, May GE, Stoiber MH, Duff MO, Booth BW, Wen J, Park S, Suzuki AM *et al* (2014) Diversity and dynamics of the Drosophila transcriptome. *Nature* 512: 393-399

Bruckner JJ, Zhan H, Gratz SJ, Rao M, Ukken F, Zilberg G, O'Connor-Giles KM (2017) Fife organizes synaptic vesicles and calcium channels for high-probability neurotransmitter release. *J Cell Biol* 216: 231-246

Cappannini A, Ray A, Purta E, Mukherjee S, Boccaletto P, Moafinejad SN, Lechner A, Barchet C, Klaholz BP, Stefaniak F *et al* (2024) MODOMICS: a database of RNA modifications and related information. 2023 update. *Nucleic Acids Res* 52: D239-D244

Chen X, Dickman D (2021) Tissue-Specific Ribosome Profiling in Drosophila. *Methods Mol Biol* 2252: 175-188

Chujo T, Tomizawa K (2025) Mitochondrial tRNA modifications: functions, diseases caused by their loss, and treatment strategies. *RNA* 31: 382-394

Coll-Tane M, Krebbers A, Castells-Nobau A, Zweier C, Schenck A (2019) Intellectual disability and autism spectrum disorders 'on the fly': insights from Drosophila. *Dis Model Mech* 12

Coutinho-Budd J, Freeman MR, Ackerman S (2024) Glial Regulation of Circuit Wiring, Firing, and Expiring in the Drosophila Central Nervous System. *Cold Spring Harb Perspect Biol* 16

D'Oliviera A, Dai X, Mottaghinia S, Olson S, Geissler EP, Etienne L, Zhang Y, Mugridge JS (2025) Recognition and cleavage of human tRNA methyltransferase TRMT1 by the SARS-CoV-2 main protease. *Elife* 12

Davarniya B, Hu H, Kahrizi K, Musante L, Fattahi Z, Hosseini M, Maqsoud F, Farajollahi R, Wienker TF, Ropers HH *et al* (2015) The Role of a Novel TRMT1 Gene Mutation and Rare GRM1 Gene Defect in Intellectual Disability in Two Azeri Families. *PLoS One* 10: e0129631

Dewe JM, Fuller BL, Lentini JM, Kellner SM, Fu D (2017) TRMT1-Catalyzed tRNA Modifications Are Required for Redox Homeostasis To Ensure Proper Cellular Proliferation and Oxidative Stress Survival. *Mol Cell Biol* 37

Doherty J, Logan MA, Tasdemir OE, Freeman MR (2009) Ensheathing glia function as phagocytes in the adult Drosophila brain. *J Neurosci* 29: 4768-4781

Efthymiou S, Leo CP, Deng C, Lin SJ, Maroofian R, Lin R, Karagoz I, Zhang K, Kaiyrzhanov R, Scardamaglia A *et al* (2025) Bi-allelic pathogenic variants in TRMT1 disrupt tRNA modification and induce a neurodevelopmental disorder. *Am J Hum Genet* 112: 1117-1138

Ellis SR, Morales MJ, Li JM, Hopper AK, Martin NC (1986) Isolation and characterization of the TRM1 locus, a gene essential for the N2,N2-dimethylguanosine modification of both mitochondrial and cytoplasmic tRNA in Saccharomyces cerevisiae. *J Biol Chem* 261: 9703-9709

Fields RD, Stevens-Graham B (2002) New insights into neuron-glia communication. *Science* 298: 556-562

Flavell SW, Greenberg ME (2008) Signaling mechanisms linking neuronal activity to gene expression and plasticity of the nervous system. *Annu Rev Neurosci* 31: 563-590

Flores-Valle A, Vishniakou I, Seelig JD (2025) Dynamics of glia and neurons regulate homeostatic rest, sleep and feeding behavior in Drosophila. *Nat Neurosci*

Fox TA, Booth C (2024) Improving access to gene therapy for rare diseases. *Dis Model Mech* 17

Freeman MR (2015) Drosophila Central Nervous System Glia. *Cold Spring Harb Perspect Biol* 7

Freeman MR, Doherty J (2006) Glial cell biology in Drosophila and vertebrates. *Trends Neurosci* 29: 82-90

Fukasawa Y, Tsuji J, Fu SC, Tomii K, Horton P, Imai K (2015) MitoFates: improved prediction of mitochondrial targeting sequences and their cleavage sites. *Mol Cell Proteomics* 14: 1113-1126

Funk HM, Zhao R, Thomas M, Spigelmyer SM, Sebree NJ, Bales RO, Burchett JB, Mamaril JB, Limbach PA, Guy MP (2020) Identification of the enzymes responsible for m2,2G and acp3U formation on cytosolic tRNA from insects and plants. *PLoS One* 15: e0242737

Gai Y, Liu Z, Cervantes-Sandoval I, Davis RL (2016) Drosophila SLC22A Transporter Is a Memory Suppressor Gene that Influences Cholinergic Neurotransmission to the Mushroom Bodies. *Neuron* 90: 581-595

Goel P, Khan M, Howard S, Kim G, Kiragasi B, Kikuma K, Dickman D (2019) A Screen for Synaptic Growth Mutants Reveals Mechanisms That Stabilize Synaptic Strength. *J Neurosci* 39: 4051-4065

Gratz SJ, Goel P, Bruckner JJ, Hernandez RX, Khateeb K, Macleod GT, Dickman D, O'Connor-Giles KM (2019) Endogenous Tagging Reveals Differential Regulation

of Ca(2+) Channels at Single Active Zones during Presynaptic Homeostatic Potentiation and Depression. *J Neurosci* 39: 2416-2429

Gratz SJ, Ukken FP, Rubinstein CD, Thiede G, Donohue LK, Cummings AM, O'Connor-Giles KM (2014) Highly specific and efficient CRISPR/Cas9-catalyzed homology-directed repair in Drosophila. *Genetics* 196: 961-971

Groth AC, Fish M, Nusse R, Calos MP (2004) Construction of transgenic Drosophila by using the site-specific integrase from phage phiC31. *Genetics* 166: 1775-1782

Hilu-Dadia R, Hakim-Mishnaevski K, Levy-Adam F, Kurant E (2018) Draper-mediated JNK signaling is required for glial phagocytosis of apoptotic neurons during Drosophila metamorphosis. *Glia* 66: 1520-1532

Hindle SJ, Bainton RJ (2014) Barrier mechanisms in the Drosophila blood-brain barrier. *Front Neurosci* 8: 414

Holt CE, Schuman EM (2013) The central dogma decentralized: new perspectives on RNA function and local translation in neurons. *Neuron* 80: 648-657

Hopper AK, Furukawa AH, Pham HD, Martin NC (1982) Defects in modification of cytoplasmic and mitochondrial transfer RNAs are caused by single nuclear mutations. *Cell* 28: 543-550

Hummel T, Attix S, Gunning D, Zipursky SL (2002) Temporal control of glial cell migration in the Drosophila eye requires gilgamesh, hedgehog, and eye specification genes. *Neuron* 33: 193-203

Ihsanawati, Nishimoto M, Higashijima K, Shirouzu M, Grosjean H, Bessho Y, Yokoyama S (2008) Crystal structure of tRNA N2,N2-guanosine dimethyltransferase Trm1 from Pyrococcus horikoshii. *J Mol Biol* 383: 871-884

Ito K, Urban J, Technau GM (1995) Distribution, classification, and development ofDrosophila glial cells in the late embryonic and early larval ventral nerve cord. *Rouxs Arch Dev Biol* 204: 284-307

Jackman JE, Alfonzo JD (2013) Transfer RNA modifications: nature's combinatorial chemistry playground. *Wiley Interdiscip Rev RNA* 4: 35-48

Jenett A, Rubin GM, Ngo TT, Shepherd D, Murphy C, Dionne H, Pfeiffer BD, Cavallaro A, Hall D, Jeter J *et al* (2012) A GAL4-driver line resource for Drosophila neurobiology. *Cell Rep* 2: 991-1001

Jenkins VK, Larkin A, Thurmond J, FlyBase C (2022) Using FlyBase: A Database of Drosophila Genes and Genetics. *Methods Mol Biol* 2540: 1-34

Jindal DA, Leier HC, Salazar G, Foden AJ, Seitz EA, Wilkov AJ, Coutinho-Budd JC, Broihier HT (2023) Early Draper-mediated glial refinement of neuropil architecture and synapse number in the Drosophila antennal lobe. *Front Cell Neurosci* 17: 1166199

Jonkhout N, Cruciani S, Santos Vieira HG, Tran J, Liu H, Liu G, Pickford R, Kaczorowski D, Franco GR, Vauti F *et al* (2021) Subcellular relocalization and nuclear redistribution of the RNA methyltransferases TRMT1 and TRMT1L upon neuronal activation. *RNA Biol* 18: 1905-1919

Keene AC, Waddell S (2007) Drosophila olfactory memory: single genes to complex neural circuits. *Nat Rev Neurosci* 8: 341-354

Kimura Y, Saito H, Osaki T, Ikegami Y, Wakigawa T, Ikeuchi Y, Iwasaki S (2022) Mito-FUNCAT-FACS reveals cellular heterogeneity in mitochondrial translation. *RNA* 28: 895-904

Kirkhart C, Scott K (2015) Gustatory learning and processing in the Drosophila mushroom bodies. *J Neurosci* 35: 5950-5958

Klann E, Dever TE (2004) Biochemical mechanisms for translational regulation in synaptic plasticity. *Nat Rev Neurosci* 5: 931-942

Kolberg L, Raudvere U, Kuzmin I, Adler P, Vilo J, Peterson H (2023) g:Profiler-interoperable web service for functional enrichment analysis and gene identifier mapping (2023 update). *Nucleic Acids Res* 51: W207-W212

Kottmeier R, Bittern J, Schoofs A, Scheiwe F, Matzat T, Pankratz M, Klambt C (2020) Wrapping glia regulates neuronal signaling speed and precision in the peripheral nervous system of Drosophila. *Nat Commun* 11: 4491

Kremer MC, Jung C, Batelli S, Rubin GM, Gaul U (2017) The glia of the adult Drosophila nervous system. *Glia* 65: 606-638

Lee CC, Chang CP, Lin CJ, Lai HL, Kao YH, Cheng SJ, Chen HM, Liao YP, Faivre E, Buee L *et al* (2018) Adenosine Augmentation Evoked by an ENT1 Inhibitor Improves Memory Impairment and Neuronal Plasticity in the APP/PS1 Mouse Model of Alzheimer's Disease. *Mol Neurobiol* 55: 8936-8952

Lee YM, Sun YH (2015) Drosophila as a model to study the role of glia in neurodegeneration. *J Neurogenet* 29: 69-79

Lei HT, Wang ZH, Li B, Sun Y, Mei SQ, Yang JH, Qu LH, Zheng LL (2023) tModBase: deciphering the landscape of tRNA modifications and their dynamic changes from epitranscriptome data. *Nucleic Acids Res* 51: D315-D327

Leier HC, Foden AJ, Jindal DA, Wilkov AJ, Van der Linden Costello P, Vanderzalm PJ, Coutinho-Budd J, Tabuchi M, Broihier HT (2025) Glia control experience-dependent plasticity in an olfactory critical period. *Elife* 13

Li C, Yao Y, Long D, Lin X (2021) KDELC1 and TRMT1 Serve as Prognosis-Related SARS-CoV-2 Proteins Binding Human mRNAs and Promising Biomarkers in Clear Cell Renal Cell Carcinoma. *Int J Gen Med* 14: 2475-2490

Liu J, Straby KB (2000) The human tRNA(m(2)(2)G(26))dimethyltransferase: functional expression and characterization of a cloned hTRM1 gene. *Nucleic Acids Res* 28: 3445-3451

Logan MA, Hackett R, Doherty J, Sheehan A, Speese SD, Freeman MR (2012) Negative regulation of glial engulfment activity by Draper terminates glial responses to axon injury. *Nat Neurosci* 15: 722-730

Lu JL, Zhou XL (2023) SARS-CoV-2 main protease Nsp5 cleaves and inactivates human tRNA methyltransferase TRMT1. *J Mol Cell Biol* 15

Lu TY, MacDonald JM, Neukomm LJ, Sheehan AE, Bradshaw R, Logan MA, Freeman MR (2017) Axon degeneration induces glial responses through Draper-TRAF4-JNK signalling. *Nat Commun* 8: 14355

Lyons DA, Talbot WS (2014) Glial cell development and function in zebrafish. *Cold Spring Harb Perspect Biol* 7: a020586

Macdonald JM, Doherty J, Hackett R, Freeman MR (2013) The c-Jun kinase signaling cascade promotes glial engulfment activity through activation of draper and phagocytic function. *Cell Death Differ* 20: 1140-1148

Madhwani KR, Sayied S, Ogata CH, Hogan CA, Lentini JM, Mallik M, Dumouchel JL, Storkebaum E, Fu D, O'Connor-Giles KM (2024) tRNA modification enzyme-dependent redox homeostasis regulates synapse formation and memory. *Proc Natl Acad Sci U S A* 121: e2317864121

Manaka J, Kuraishi T, Shiratsuchi A, Nakai Y, Higashida H, Henson P, Nakanishi Y (2004) Draper-mediated and phosphatidylserine-independent phagocytosis of apoptotic cells by Drosophila hemocytes/macrophages. *J Biol Chem* 279: 48466-48476

Masek P, Keene AC (2016) Gustatory processing and taste memory in Drosophila. *J Neurogenet* 30: 112-121

Masek P, Scott K (2010) Limited taste discrimination in Drosophila. *Proc Natl Acad Sci U S A* 107: 14833-14838

McLaughlin CN, Perry-Richardson JJ, Coutinho-Budd JC, Broihier HT (2019) Dying Neurons Utilize Innate Immune Signaling to Prime Glia for Phagocytosis during Development. *Dev Cell* 48: 506-522 e506

Mistry J, Chuguransky S, Williams L, Qureshi M, Salazar GA, Sonnhammer ELL, Tosatto SCE, Paladin L, Raj S, Richardson LJ *et al* (2021) Pfam: The protein families database in 2021. *Nucleic Acids Res* 49: D412-D419

Monies D, Vagbo CB, Al-Owain M, Alhomaidi S, Alkuraya FS (2019) Recessive Truncating Mutations in ALKBH8 Cause Intellectual Disability and Severe Impairment of Wobble Uridine Modification. *Am J Hum Genet* 104: 1202-1209

Motorin Y, Helm M (2010) tRNA stabilization by modified nucleotides. *Biochemistry* 49: 4934-4944

Nagayoshi Y, Chujo T, Hirata S, Nakatsuka H, Chen CW, Takakura M, Miyauchi K, Ikeuchi Y, Carlyle BC, Kitchen RR *et al* (2021) Loss of Ftsj1 perturbs codon-specific translation efficiency in the brain and is associated with X-linked intellectual disability. *Sci Adv* 7

Najmabadi H, Hu H, Garshasbi M, Zemojtel T, Abedini SS, Chen W, Hosseini M, Behjati F, Haas S, Jamali P *et al* (2011) Deep sequencing reveals 50 novel genes for recessive cognitive disorders. *Nature* 478: 57-63

Nelson N, Miller V, Broadie K (2025) Neuron-to-glia and glia-to-glia signaling directs critical period experience-dependent synapse pruning. *Front Cell Dev Biol* 13: 1540052

Nguyen Ba AN, Pogoutse A, Provart N, Moses AM (2009) NLStradamus: a simple Hidden Markov Model for nuclear localization signal prediction. *BMC Bioinformatics* 10: 202

Niederberger C, Graub R, Costa A, Desgres J, Schweingruber ME (1999) The tRNA N2,N2-dimethylguanosine-26 methyltransferase encoded by gene trm1 increases

efficiency of suppression of an ochre codon in Schizosaccharomyces pombe. *FEBS Lett* 464: 67-70

Notredame C, Higgins DG, Heringa J (2000) T-Coffee: A novel method for fast and accurate multiple sequence alignment. *J Mol Biol* 302: 205-217

Otto N, Marelja Z, Schoofs A, Kranenburg H, Bittern J, Yildirim K, Berh D, Bethke M, Thomas S, Rode S *et al* (2018) The sulfite oxidase Shopper controls neuronal activity by regulating glutamate homeostasis in Drosophila ensheathing glia. *Nat Commun* 9: 3514

Ozturk-Colak A, Marygold SJ, Antonazzo G, Attrill H, Goutte-Gattat D, Jenkins VK, Matthews BB, Millburn G, Dos Santos G, Tabone CJ *et al* (2024) FlyBase: updates to the Drosophila genes and genomes database. *Genetics* 227

Padiath QS, Saigoh K, Schiffmann R, Asahara H, Yamada T, Koeppen A, Hogan K, Ptacek LJ, Fu YH (2006) Lamin B1 duplications cause autosomal dominant leukodystrophy. *Nat Genet* 38: 1114-1123

Parks AL, Cook KR, Belvin M, Dompe NA, Fawcett R, Huppert K, Tan LR, Winter CG, Bogart KP, Deal JE *et al* (2004) Systematic generation of high-resolution deletion coverage of the Drosophila melanogaster genome. *Nat Genet* 36: 288-292

Partiot E, Hirschler A, Colomb S, Lutz W, Claeys T, Delalande F, Deffieu MS, Bare Y, Roels JRE, Gorda B *et al* (2024) Brain exposure to SARS-CoV-2 virions perturbs synaptic homeostasis. *Nat Microbiol* 9: 1189-1206

Perkins LA, Holderbaum L, Tao R, Hu Y, Sopko R, McCall K, Yang-Zhou D, Flockhart I, Binari R, Shim HS *et al* (2015) The Transgenic RNAi Project at Harvard Medical School: Resources and Validation. *Genetics* 201: 843-852

Pettersen EF, Goddard TD, Huang CC, Meng EC, Couch GS, Croll TI, Morris JH, Ferrin TE (2021) UCSF ChimeraX: Structure visualization for researchers, educators, and developers. *Protein Sci* 30: 70-82

Phillips JH, Kjellin-Straby K (1967) Studies on microbial ribonucleic acid. IV. Two mutants of Saccharomyces cerevisiae lacking N-2-dimethylguanine in soluble ribonucleic acid. *J Mol Biol* 26: 509-518

Phizicky EM, Hopper AK (2015) tRNA processing, modification, and subcellular dynamics: past, present, and future. *RNA* 21: 483-485

Pieper U, Eswar N, Webb BM, Eramian D, Kelly L, Barkan DT, Carter H, Mankoo P, Karchin R, Marti-Renom MA *et al* (2009) MODBASE, a database of annotated comparative protein structure models and associated resources. *Nucleic Acids Res* 37: D347-354

Pogodalla N, Kranenburg H, Rey S, Rodrigues S, Cardona A, Klambt C (2021) Drosophila ss(Heavy)-Spectrin is required in polarized ensheathing glia that form a diffusion-barrier around the neuropil. *Nat Commun* 12: 6357

Porat J, Vakiloroayaei A, Remnant BM, Talebi M, Cargill T, Bayfield MA (2023) Crosstalk between the tRNA methyltransferase Trm1 and RNA chaperone La influences eukaryotic tRNA maturation. *J Biol Chem* 299: 105326

Purice MD, Ray A, Munzel EJ, Pope BJ, Park DJ, Speese SD, Logan MA (2017) A novel Drosophila injury model reveals severed axons are cleared through a Draper/MMP-1 signaling cascade. *Elife* 6

Ramos J, Fu D (2019) The emerging impact of tRNA modifications in the brain and nervous system. *Biochim Biophys Acta Gene Regul Mech* 1862: 412-428

Reimand J, Kull M, Peterson H, Hansen J, Vilo J (2007) g:Profiler--a web-based toolset for functional profiling of gene lists from large-scale experiments. *Nucleic Acids Res* 35: W193-200

Rigden DJ, Fernandez XM (2024) The 2024 Nucleic Acids Research database issue and the online molecular biology database collection. *Nucleic Acids Res* 52: D1-D9

Robinow S, White K (1988) The locus elav of Drosophila melanogaster is expressed in neurons at all developmental stages. *Dev Biol* 126: 294-303

Sali A, Blundell TL (1993) Comparative protein modelling by satisfaction of spatial restraints. *J Mol Biol* 234: 779-815

Samudyata, Oliveira AO, Malwade S, Rufino de Sousa N, Goparaju SK, Gracias J, Orhan F, Steponaviciute L, Schalling M, Sheridan SD *et al* (2022) SARS-CoV-2 promotes microglial synapse elimination in human brain organoids. *Mol Psychiatry* 27: 3939-3950

Sankar A, Y SR, Singh A, Roy R, Shukla R, Verma B (2024) Next-generation therapeutics for rare genetic disorders. *Mutagenesis* 39: 157-171

Sauter C, Lorber B, Gaudry A, Karim L, Schwenzer H, Wien F, Roblin P, Florentz C, Sissler M (2015) Neurodegenerative disease-associated mutants of a human mitochondrial aminoacyl-tRNA synthetase present individual molecular signatures. *Sci Rep* 5: 17332

Savojardo C, Bruciaferri N, Tartari G, Martelli PL, Casadio R (2020) DeepMito: accurate prediction of protein sub-mitochondrial localization using convolutional neural networks. *Bioinformatics* 36: 56-64

Scott K (2005) Taste recognition: food for thought. *Neuron* 48: 455-464

Sepp KJ, Schulte J, Auld VJ (2001) Peripheral glia direct axon guidance across the CNS/PNS transition zone. *Dev Biol* 238: 47-63

Shaheen R, Al-Salam Z, El-Hattab AW, Alkuraya FS (2016) The syndrome dysmorphic facies, renal agenesis, ambiguous genitalia, microcephaly, polydactyly and lissencephaly (DREAM-PL): Report of two additional patients. *Am J Med Genet A* 170: 3222-3226

Singer P, McGarrity S, Shen HY, Boison D, Yee BK (2012) Working memory and the homeostatic control of brain adenosine by adenosine kinase. *Neuroscience* 213: 81-92

Sjostedt E, Zhong W, Fagerberg L, Karlsson M, Mitsios N, Adori C, Oksvold P, Edfors F, Limiszewska A, Hikmet F *et al* (2020) An atlas of the protein-coding genes in the human, pig, and mouse brain. *Science* 367

Snel B, Lehmann G, Bork P, Huynen MA (2000) STRING: a web-server to retrieve and display the repeatedly occurring neighbourhood of a gene. *Nucleic Acids Res* 28: 3442-3444

Sossin WS, Costa-Mattioli M (2019) Translational Control in the Brain in Health and Disease. *Cold Spring Harb Perspect Biol* 11

Stahl BA, Peco E, Davla S, Murakami K, Caicedo Moreno NA, van Meyel DJ, Keene AC (2018) The Taurine Transporter Eaat2 Functions in Ensheathing Glia to Modulate Sleep and Metabolic Rate. *Curr Biol* 28: 3700-3708 e3704

Storkebaum E (2016) Peripheral neuropathy via mutant tRNA synthetases: Inhibition of protein translation provides a possible explanation. *Bioessays* 38: 818-829

Supek F, Bosnjak M, Skunca N, Smuc T (2011) REVIGO summarizes and visualizes long lists of gene ontology terms. *PLoS One* 6: e21800

Suzuki T (2021) The expanding world of tRNA modifications and their disease relevance. *Nat Rev Mol Cell Biol* 22: 375-392

Szklarczyk D, Kirsch R, Koutrouli M, Nastou K, Mehryary F, Hachilif R, Gable AL, Fang T, Doncheva NT, Pyysalo S *et al* (2023) The STRING database in 2023: protein-protein association networks and functional enrichment analyses for any sequenced genome of interest. *Nucleic Acids Res* 51: D638-D646

Theparambil SM, Kopach O, Braga A, Nizari S, Hosford PS, Sagi-Kiss V, Hadjihambi A, Konstantinou C, Esteras N, Gutierrez Del Arroyo A *et al* (2024) Adenosine

signalling to astrocytes coordinates brain metabolism and function. *Nature* 632: 139-146

Thomas A, Lee PJ, Dalton JE, Nomie KJ, Stoica L, Costa-Mattioli M, Chang P, Nuzhdin S, Arbeitman MN, Dierick HA (2012) A versatile method for cell-specific profiling of translated mRNAs in Drosophila. *PLoS One* 7: e40276

Tushaus J, Sakhteman A, Lechner S, The M, Mucha E, Krisp C, Schlegel J, Delbridge C, Kuster B (2023) A region-resolved proteomic map of the human brain enabled by high-throughput proteomics. *EMBO J* 42: e114665

Vauti F, Goller T, Beine R, Becker L, Klopstock T, Holter SM, Wurst W, Fuchs H, Gailus-Durner V, de Angelis MH *et al* (2007) The mouse Trm1-like gene is expressed in neural tissues and plays a role in motor coordination and exploratory behaviour. *Gene* 389: 174-185

Wei N, Zhang Q, Yang XL (2019) Neurodegenerative Charcot-Marie-Tooth disease as a case study to decipher novel functions of aminoacyl-tRNA synthetases. *J Biol Chem* 294: 5321-5339

Yang AC, Kern F, Losada PM, Agam MR, Maat CA, Schmartz GP, Fehlmann T, Stein JA, Schaum N, Lee DP *et al* (2021) Dysregulation of brain and choroid plexus cell types in severe COVID-19. *Nature* 595: 565-571

Yildirim K, Petri J, Kottmeier R, Klambt C (2019) Drosophila glia: Few cell types and many conserved functions. *Glia* 67: 5-26

Zhang K, Eldin P, Ciesla JH, Briant L, Lentini JM, Ramos J, Cobb J, Munger J, Fu D (2024) Proteolytic cleavage and inactivation of the TRMT1 tRNA modification enzyme by SARS-CoV-2 main protease. *Elife* 12

Zhang K, Lentini JM, Prevost CT, Hashem MO, Alkuraya FS, Fu D (2020) An intellectual disability-associated missense variant in TRMT1 impairs tRNA modification and reconstitution of enzymatic activity. *Hum Mutat* 41: 600-607

Zhang K, Manning AC, Lentini JM, Howard J, Dalwigk F, Maroofian R, Efthymiou S, Chan P, Eliseev SI, Yang Z *et al* (2025) Human TRMT1 and TRMT1L paralogs ensure the proper modification state, stability, and function of tRNAs. *Cell Rep* 44: 115092

Chapter 3 Figures

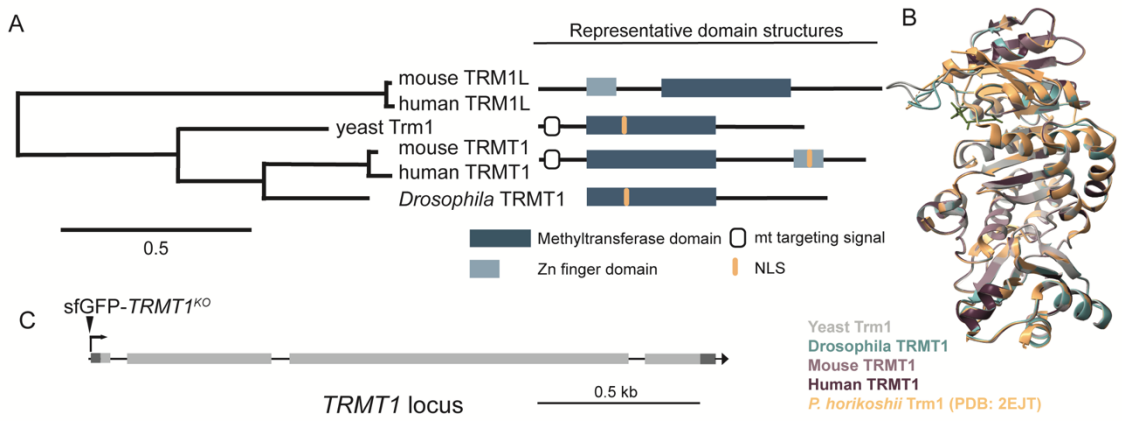

Figure 3.1. Drosophila as model to investigate TRMT1

A. Representative domains include methyltransferase domain (dark blue filled box), zinc finger (light blue filled box), mitochondrial targeting sequence schematics (white box with black outline), and nuclear targeting sequence (orange box).

B. Structural homology model of the methyltransferases domain demonstrates conserved structure between yeast Trm1 (grey), Drosophila TRMT1 (light blue), mouse TRMT1 (blue), human TRMT1 (dark blue) with *P. horiskoshii* Trm1 crystal structure (orange, PDB ID: 2EJT).

C. Schematic of the TRMT1 locus with the allele used in this study. Triangle represents insertion allele.

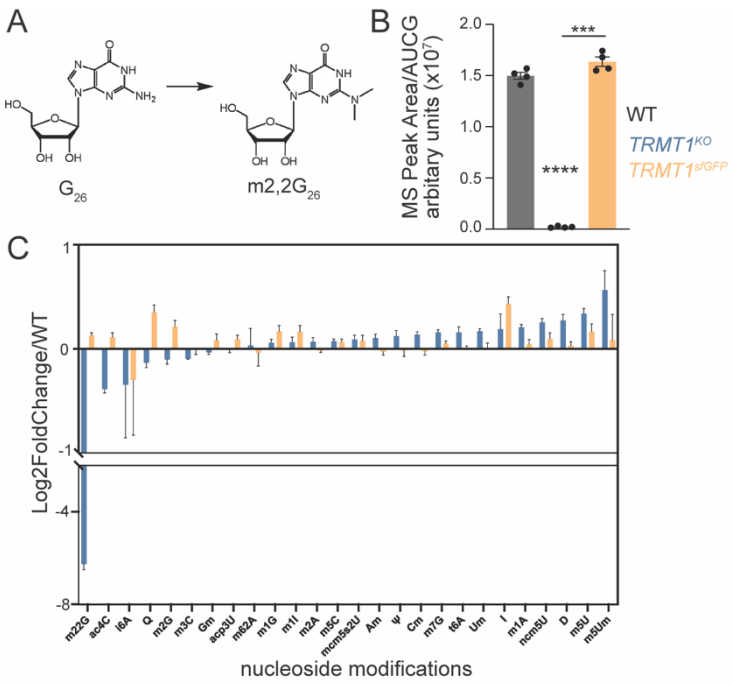

Figure 3.2. Drosophila TRMT1 is required for m2,2G tRNA modification

A. Chemical modification of guanosine 26 (G_{26}) to dimethylguanosine ($m2,2G_{26}$).

B. Peak intensity of dimethyl-guanosine normalized to the canonical nucleosides A, U, G and C measured by LC-MS in total RNA isolated from w^{1118} (grey), $TRMT1^{KO}$ (blue), and $TRMT1^{sfGFP}$ (orange) adult heads. Mean ± standard deviation is indicated. Brown-Forsythe and Welch ANOVA followed by Dunnett T3 multiple comparisons. **** $P <$ 0.0001, *** $P = 0.0001$, ns = 0.1289 (four biological replicates).

C. Comprehensive tRNA nucleotide modifications remain unchanged in the absence of *TRMT1.* Log2fold change in the levels of the indicated tRNA modifications in $TRMT1^{KO}$ (blue) and $TRMT1^{sfGFP}$ (orange) relative to w^{1118} control. Data represented as mean ± SEM (four biological replicates/genotype).

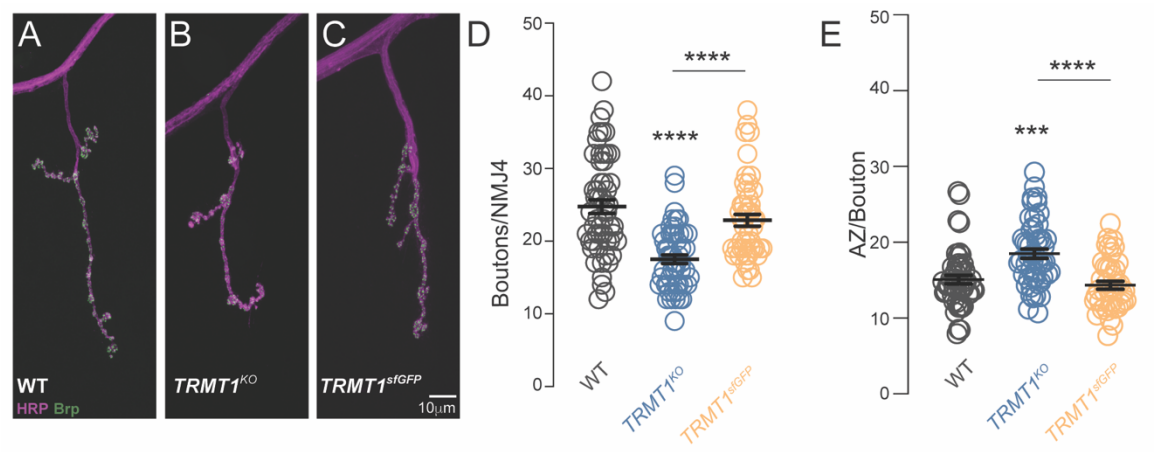

Figure 3.3. TRMT1 promotes size and synaptic growth

A-C. Representative confocal images of NMJ4 in wild type (grey), *TRMT1*^{KO} (blue), and *TRMT1*^{sfGFP} rescue (orange). Scale bar: 10 µm.

D. Quantification of bouton number per NMJ4 from A-C. Data points represent individual NMJs (*w*^{1118}: 48, *TRMT1*^{KO}: 52, *TRMT1*^{sfGFP}: 47) from 9-12 biological replicates per genotype. Mean ± SEM is indicated. Brown-Forsythe and Welch ANOVA with Dunnett T3 multiple comparison **** $p < 0.0001$, ns 0.9848.

E. Quantification of active zone number per bouton at NMJ4 from Fig2A-C. Data points represent individual NMJs (*w*^{1118}: 48, *TRMT1*^{KO}: 52, *TRMT1*^{sfGFP}: 42) from 9-12 biological replicates per genotype. Mean ± SEM is indicated.Krustal-Wallis with Dunn's multiple comparison **** *P*< 0.0001, ****P*= 00002, ns > 0.9999.

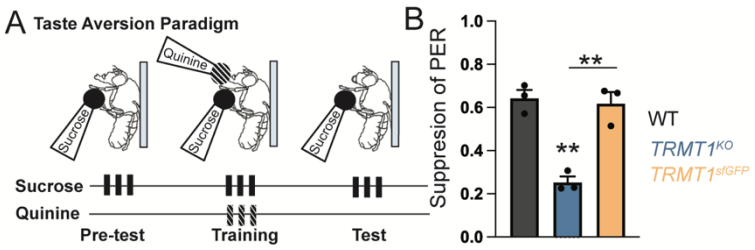

Figure 3.4. TRMT1 promotes gustatory memory

A. Representative taste aversion scheme modified from (Masek & Keene, 2016).

B. Quantification of Proboscis Extension Reflex (PER) suppression of wild type (grey), *TRMT1*^{KO} (blue), and *TRMT1*^{sfGFP} rescue (orange) flies. Data points represent average PER suppression of three biological replicates (w^{1118}: 85, *TRMT1*^{KO}: 104, *TRMT1*^{sfGFP}: 98) from > 28 biological replicates/genotype/experiment. ANOVA with Tukey's multiple comparison $^{**}P < 0.0017$, ns = 0.9105.

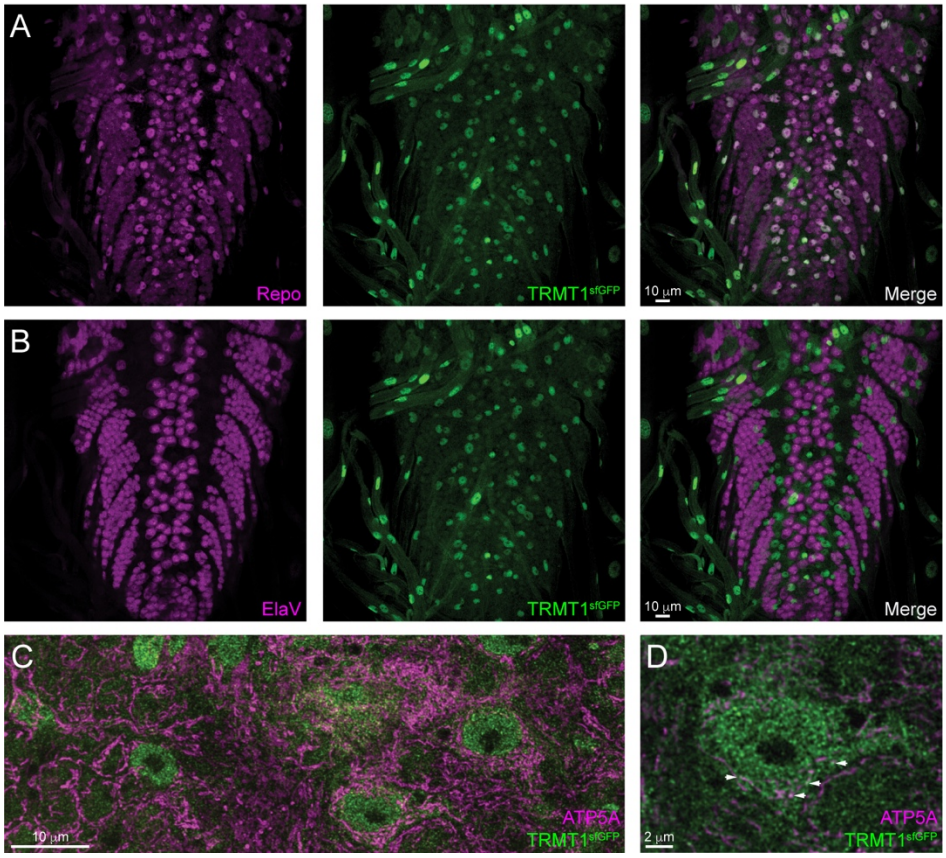

Figure 3.5. TRMT1 is expressed in glial and muscle nuclei

A. Confocal Z-projections of *TRMT1*^{sfGFP} larval ventral ganglion co-labeled with antibodies against GFP(green) and the nuclear pan-glial marker Repo (magenta) showing expression in glial nuclei.

B. Confocal Z-projections of *TRMT1*^{sfGFP} larval ventral ganglion co-labeled with antibodies against GFP(green) and the neuronal marker Elav (magenta) showing TRMT1 is not expressed in neurons.

C-D. Super resolution (C) Z-projections of *TRMT1*^{sfGFP} larval ventral ganglion co-labeled with antibodies against GFP (green) and the mitochondrial marker ATP5A (magenta) where a zoomed single Z-projection of a single glial cell (D) shows TRMT1 does colocalize with mitochondria (E, white arrows). Scale bar (C) 10 μm and (D) 2 μm.

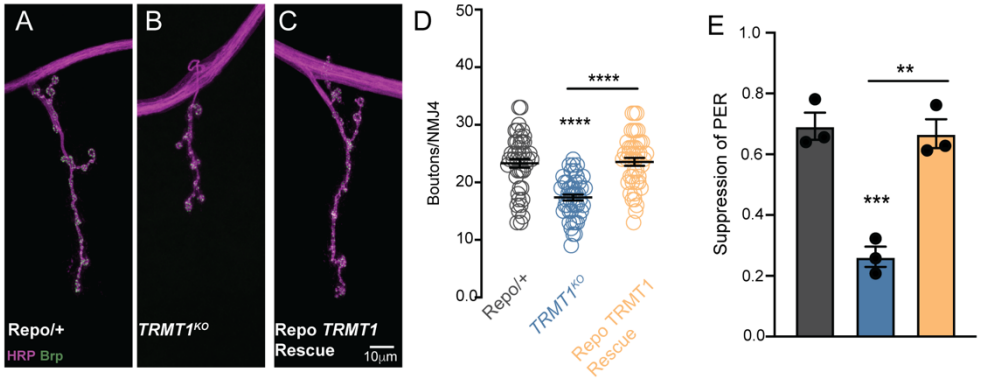

Figure 3.6. Cell-specific expression of TRMT1 in glial cells rescues synaptic growth and memory

A-C. Representative confocal images of NMJ4 in control (grey), *TRMT1*^{KO} (blue), and pan-glial rescue (orange). Scale bar: 10 μm.

D. Quantification of bouton number per NMJ4 from A-C. Data points represent individual NMJs (repo-Gal4/+: 44, *TRMT1*$^{KO/KO}$*; repo-Gal4/+*: 46, *TRMT1*$^{KO/KO}$*; repo-Gal4/UAS-TRMT1*^{KO}: 44) from 8-10 biological replicates per genotype. Mean ± SEM is indicated. ANOVA with Tukey's multiple comparison **** $P < 0.0001$, ns = 0.2688.

E. Quantification of Proboscis Extension Reflex (PER) suppression of control (grey), *TRMT1*^{KO} (blue), and pan-glial rescue (orange) flies. Data points represent average PER suppression of three biological replicates (repo-Gal4/+: 92, *TRMT1*$^{KO/KO}$*; repo-Gal4/+* 94, *TRMT1*$^{KO/KO}$*; repo-Gal4/UAS-TRMT1*^{KO}: 79) from > 25 biological replicates/genotype/experiment. ANOVA with Tukey's multiple comparison ***P = 0.0009, **P = 0.0012, ns = 0.9107.

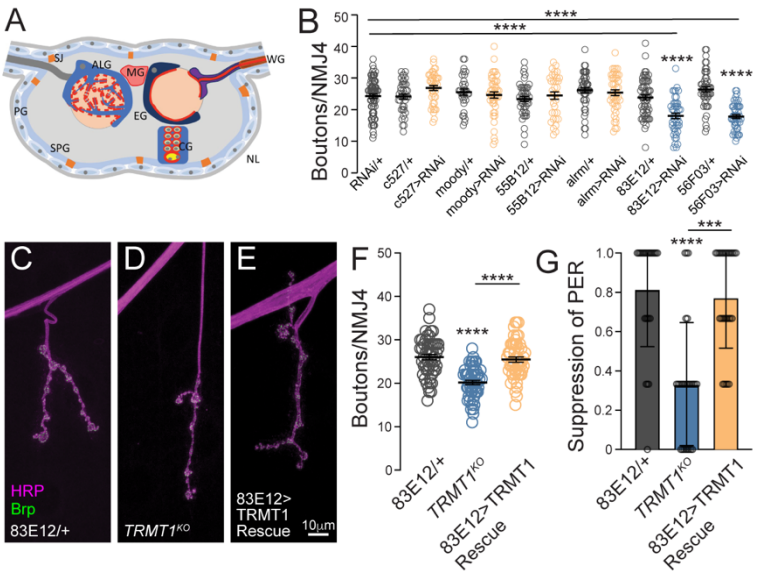

Figure 3.7. Expression of TRMT1 in ensheathing glial cell rescues synaptic growth and memory

A. Representative illustration of types of glial subtypes from an orthogonal section of the ventral nerve cord modified from (Bittern *et al.*, 2021).

B. Quantification of bouton number per NMJ4 from *TRMT1*^{RNAi} subglial cell type screen. Data points represent individual NMJs (*UAS-TRMT1*^{RNAi}*/+:* 71, *c527*-Gal4/+: 40, *UAS-TRMT1*^{RNAi}*/+; c527-Gal4/*: 40, *moody*-Gal4/+: 31, *moody-Gal4/UAS-TRMT1*^{RNAi}*/*: 43, *55B12*-Gal4/+: 44, *UAS-TRMT1*^{RNAi}*/+; 55B12*-Gal4/+: 34, *alrm*-Gal4/+: 47, *UAS-TRMT1*^{RNAi}*/+;alrm*-Gal4/+: 44,*83E12*-Gal4/+: 59, *UAS-TRMT1*^{RNAi} */+; /83E12*-Gal4/+:45, *56F03*-Gal4/+: 49, *UAS-TRMT1*^{RNAi}*/+; 56F03*-Gal4/+: 47) from 7-16 biological replicates per genotype. Mean ± SEM is indicated. ANOVA with Sidak's multiple comparison ****P = <0.0001, ns > 0.3121.

C-E. Representative confocal images of NMJ4 in control (grey), *TRMT1*^{KO} (blue), and pan-glial rescue (orange). Scale bar: 10 μm.

F. Quantification of bouton number per NMJ4 from C-E. Data points represent individual NMJs (83E12-Gal4/+: 53, *TRMT1$^{KO/KO}$; 83E12-Gal4/+*: 53, *TRMT1$^{KO/KO}$; 83E12-Gal4/UAS-TRMT1^{KO}*: 52) from 10 biological replicates per genotype. Mean ± SEM is indicated. ANOVA with Tukey's multiple comparison **** $P < 0.0001$, ns 0.7562.

G. Quantification of Proboscis Extension Reflex (PER) suppression of control (grey), *TRMT1^{KO}* (blue), and pan-glial rescue (orange) flies (83E12-Gal4/+: 25, *TRMT1$^{KO/KO}$; 83E12-Gal4/+*: 26, *TRMT1$^{KO/KO}$; 83E12-Gal4/UAS-TRMT1^{KO}*: 28) from > 25 biological replicates/genotype. ANOVA with Tukey's multiple comparison ****$P < 0.0001$, ***$P = 0.0001$, ns = 0.9107.

Figure 3-8

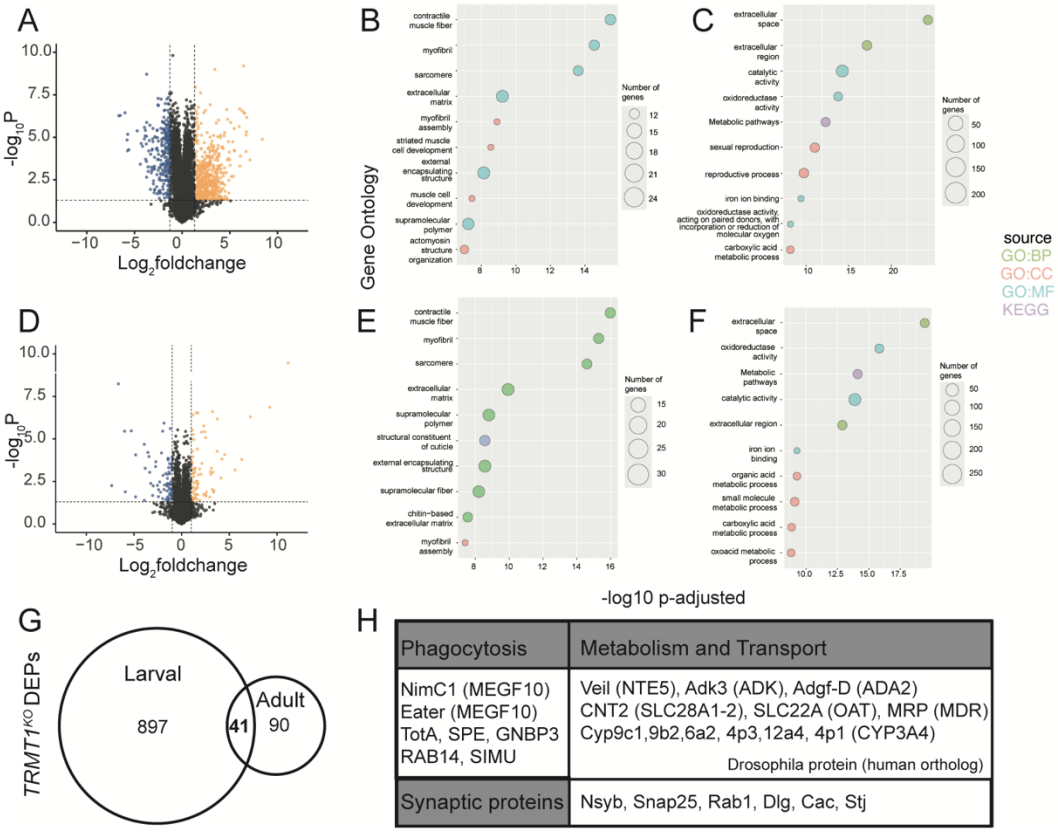

Phagocytosis	Metabolism and Transport
NimC1 (MEGF10) Eater (MEGF10) TotA, SPE, GNBP3 RAB14, SIMU	Veil (NTE5), Adk3 (ADK), Adgf-D (ADA2) CNT2 (SLC28A1-2), SLC22A (OAT), MRP (MDR) Cyp9c1,9b2,6a2, 4p3,12a4, 4p1 (CYP3A4) Drosophila protein (human ortholog)
Synaptic proteins	Nsyb, Snap25, Rab1, Dlg, Cac, Stj

Figure 3.8. Global nervous system proteomic reveal candidate pathways

A. For larval proteomics, volcano plots illustrate differentially expressed proteins from larval central nervous system and body wall. Vertical and horizontal dashed lines represented the cutoffs for upregulated proteins (orange, log2FC > 1.3 and adjusted p-value < 0.05) and downregulated (blue, log2FC < -1.3 and adjusted p-value < 0.05).

B-C. GeneOntology of molecular function, biological processes, cellular compartment, and KEGG pathways of differential expressed proteins (B) downregulated and (C) upregulated in larval *TRMT1*^{KO} proteome compared to wild-type.

D. For adult head proteomics, volcano plots illustrate differentially expressed proteins. Vertical and horizontal dashed lines represented the cutoffs for upregulated proteins

(orange, log2FC > 1 and adjusted p-value < 0.05) and downregulated (blue, log2FC < -1 and adjusted p-value < 0.05).

E-F. GeneOntology of molecular function, biological processes, cellular compartment, and KEGG pathways of differential expressed proteins (E) downregulated and (F) upregulated in adult head *TRMT1*^{KO} proteome compared to wild-type.

G. Venn Diagram represented the 41 differentially expressed proteins identified in larval and adult proteomic *TRMT1*^{KO} datasets.

H. Abbreviated summary of *TRMT1*^{KO} proteins of interest in the phagocytosis, metabolism, and known synaptic proteins.

Chapter 3 Supplemental Figures

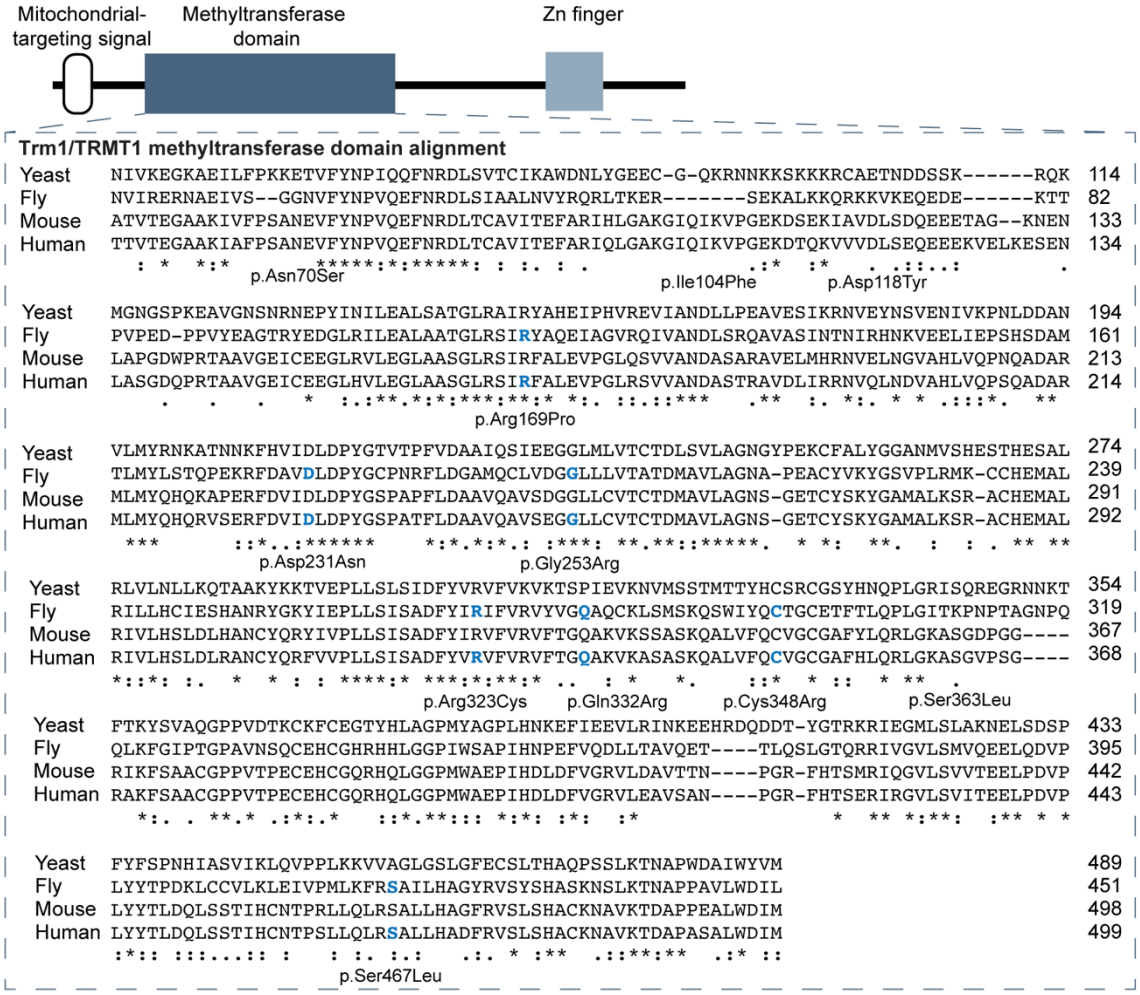

Figure 3.S1. Identified methyltransferase domain missense mutations associated with *TRMT1*-linked intellectual disability.

Human TRMT1 domains and features include mitochondrial targeting signal, methyltransferase domain, and a zinc finger. Insert denotes the sequence alignment of yeast Trm1, Drosophila (fly), mouse and human TRMT1 methyltransferase domain. Amino acids are noted as identical (*), conserved (:) and partially conserved (.). Seven of 11 *TRMT1*-associated intellectual disability variants in the methyltransferase domains reported by (Efthymiou *et al.*, 2025; Zhang *et al.*, 2020) have conserved amino acids in flies (blue font).

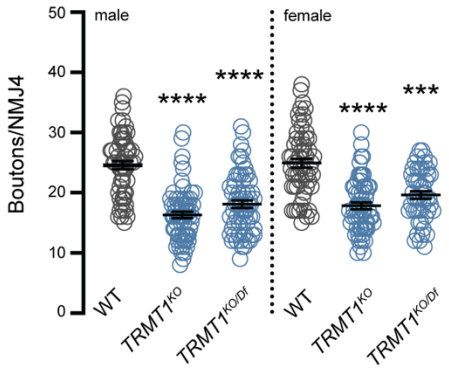

Figure 3.S2. TRMT1 promotes synaptic growth

A. Quantification of bouton number per NMJ4 in male (left) and female (right) wild type (grey) and *TRMT1* null mutants. Data points represent individual NMJs (male - w^{1118}: 56, $TRMT1^{KO}$: 64, $TRMT1^{KO/Df}$: 64; female - w^{1118}: 60, $TRMT1^{KO}$: 60, $TRMT1^{KO/Df}$: 49) from x-y biological replicates per genotype. Kruskal-Wallis test followed by Dunn's multiple ****$P < 0.0001$; *** $P = 0.0004$, ns > 0.5164.

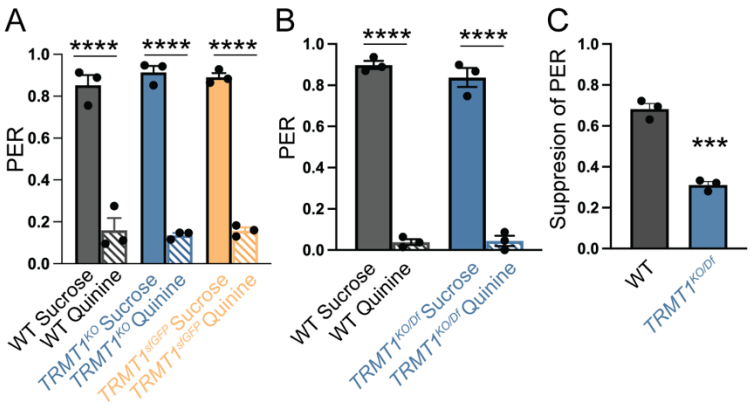

Figure 3.S3. *TRMT1* null mutants have impaired memory and normal taste preference

A-B. All genotypes show expected Proboscis Extension Reflex (PER) or preference when presented with sucrose (solid fill) or quinine (hatch fill). Data points represent the average PER of three biological replicates. (A) w^{1118}: 85, $TRMT1^{KO}$: 104, $TRMT1^{sfGFP}$: 98, ANOVA with Tukey's multiple comparison ****$P < 0.0001$. (B) w^{1118}: 82, $TRMT1^{KO/Df}$: 83) from > 19 biological replicates/genotype/experiment. Non parametric with Kruskal-Wallis multiple comparisons ***$P = 0.0003$.

C. Quantification of PER suppression of wild type (grey), $TRMT1^{KO/Df}$ (blue) flies. Data points represent average PER suppression of three biological replicates (w^{1118}: 82, $TRMT1^{KO/Df}$: 83) from > 24 biological replicates/genotype/experiment. Unpaired t-test ***$P = 0.0003$.

Fig 3.S4

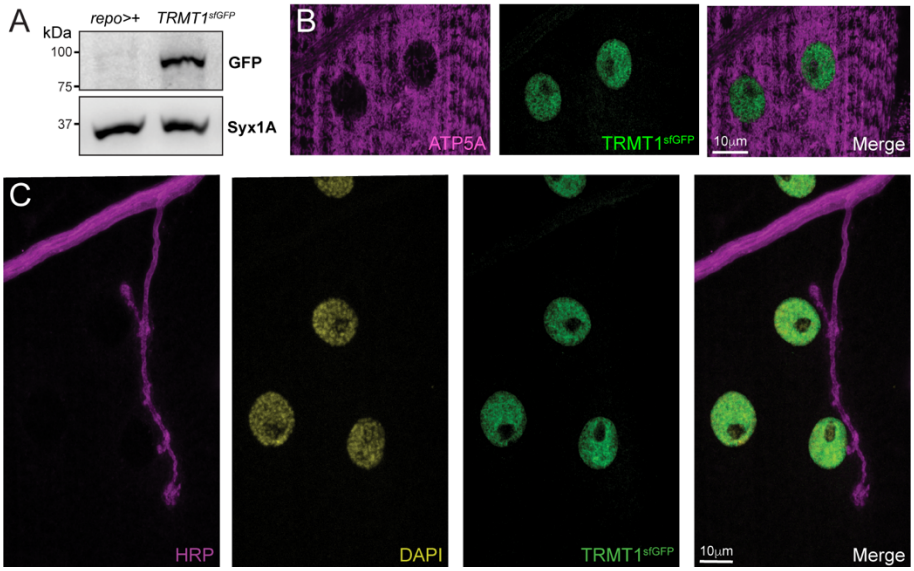

Figure 3.S4. Expression of endogenous TRMT1

A. Representative western blot of adult head extracts from control and endogenously tagged *TRMT1*^{sfGFP} stained for GFP and SyxA-1.

B. Confocal Z-projections of *TRMT1*^{sfGFP} NMJ/muscle co-labeled with antibodies against GFP (green) and the mitochondrial marker ATP5A (magenta) showing TRMT1 is expressed in muscle and accumulates in the nucleus and not mitochondria. Scale bar (A-C) 10 μm.

C. Confocal Z-projections of *TRMT1*^{sfGFP} NMJ/muscle co-labeled with antibodies against GFP (green), neuronal stain DAPI (yellow), and the neuronal membrane marker HRP (magenta) showing TRMT1 is expressed in muscle and accumulates in the nucleus. Scale bar (A-C) 10 μm.

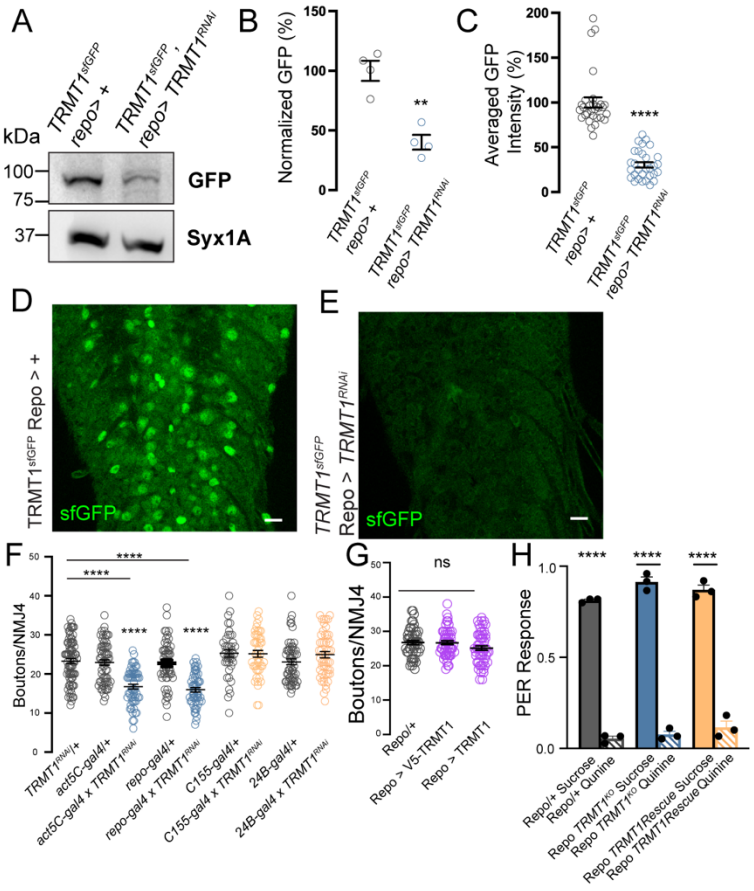

Figure 3.S5. TRMT1 cell specific rescue validation and screening experiments.

A. Representative western blot of adult head extracts from *TRMT1^{sfGFP}; repo/+* and *TRMT1^{sfGFP}; repo/UAS-TRMT1^{RNAi}* stained for GFP and Syx1A.

B. *UAS-TRMT1^{RNAi}* validation through quantification of normalized TRMT1^{sfGFP} protein expression with and without pan-glial driven *UAS-TRMT1^{RNAi}* in adult fly heads (four biological replicates). Mean ± SEM is indicated. Unpaired t-test ***P* = 0.0012.

C. Quantification of endogenously tagged TRMT1^{sfGFP} with and without pan-glial driven *UAS-TRMT1^{RNAi}* at the larval ventral ganglion (3 biological replicates/genotype). Mean ± SEM is indicated. Mann-Whitney (non-parametric) t-test, *****P* < 0.0001.

D-E. Representative confocal Z-projections of (D) *TRMT1^{sfGFP}; repo/+* and (E) *TRMT1^{sfGFP}; repo/UAS-TRMT1^{RNAi}* at the larval ventral ganglion labeled with antibodies against GFP(green) showing TRMT1^{RNAi} knocks down ~70% TRMT1 protein.

F. Quantification of bouton number per NMJ4 from *TRMT1^{RNAi}* cell specific synaptic growth screen. Data points represent individual NMJs (*UAS-TRMT1^{RNAi}/+:* 75, *act5C*-Gal4/+: 62, *act5C-Gal4/UAS-TRMT1^{RNAi}*: 57, *repo*-Gal4/+: 51, *repo-Gal4/UAS-TRMT1^{RNAi}*: 51, *C155*-Gal4/+: 40, *C155-Gal4/UAS-TRMT1^{RNAi}*: 45, *24B*-Gal4/+: 56, *24B-Gal4/UAS-TRMT1^{RNAi}*: 51) from 11-16 biological replicates per genotype. Mean ± SEM is indicated. ANOVA with Tukey's multiple comparison ****P = <0.0001, ns > 0.1478.

G. Quantification of bouton number per NMJ4 from pan-glial overexpression of TRMT1. Data points represent individual NMJs (repo-Gal4/+: 49, *repo-Gal4/UAS-V5-TRMT1*: 52, *repo-Gal4/UAS-TRMT1*: 54) from 9-10 biological replicates per genotype. Mean ± SEM is indicated. ANOVA with Tukey's multiple comparison ns > 0.1478.

H. All genotypes show expected PER or preference when presented with sucrose or quinine. Data points represent the average PER of three biological replicates from > 22 biological replicates/genotype/experiment. (repo-Gal4/+: 73, *TRMT1$^{KO/KO}$; repo-Gal4/+*: 74, *TRMT1$^{KO/KO}$; repo-Gal4/UAS-TRMT1^{KO}*: 71) Non parametric with Kruskal-Wallis multiple comparisons ***P = 0.0003.

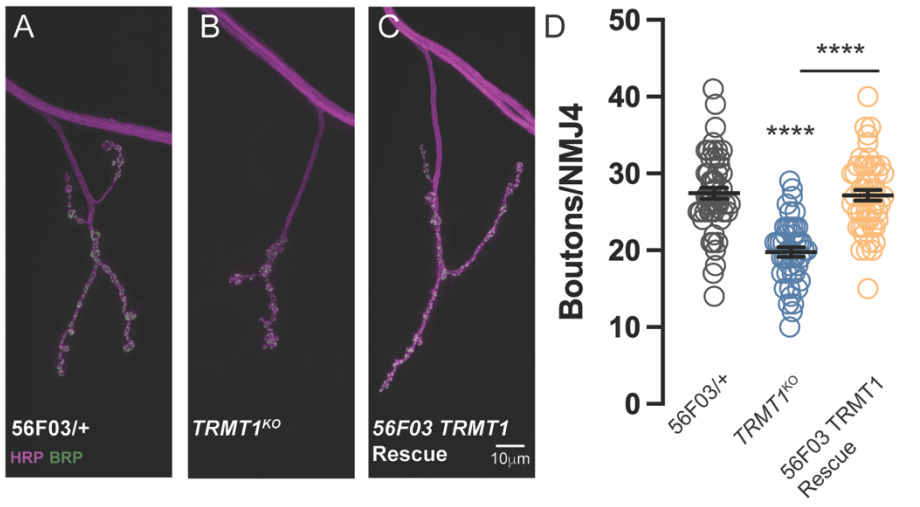

Figure 3.S6. TRMT1 reexpression using a second ensheathing glia gal4 driver rescues synaptic growth

A-C. Representative confocal images of NMJ4 in control (grey), *TRMT1*^{KO} (blue), and ensheathing glia rescue (orange). Scale bar: 10 μm.

D. Quantification of bouton number per NMJ4 from B-D. Data points represent individual NMJs (56F03-Gal4/+: 53, *TRMT1*$^{KO/KO}$*; 56F03-Gal4/+*: 53, *TRMT1*$^{KO/KO}$*; 56F03-Gal4/UAS-TRMT1*^{KO}: 52) from 9-10 biological replicates per genotype. Mean ± SEM is indicated. ANOVA with Tukey's multiple comparison **** $P < 0.0001$, ns 0.9564.

Chapter 3 Table

Table 3.1. Key Resources Table

REAGENT or RESOURCE	SOURCE	IDENTIFIER
Experimental models: Organisms/strains		
w^{1118}; ^{sfGFP}TRMT1	This study	NA
w^{1118}; TRMT1^{KO}	This study	NA
w^{1118}; UAS-TRMT1	This study	NA
w^{1118}; UAS-V5-TRMT1	This study	NA
TRMT1 Deficiency w[1118]; Df(2L)Exel6033, P{w[+mC]=XP-U}Exel6033/CyO (Rebalanced stock)	Bloomington Drosophila Stock Center	RRID:BDSC_7516
TRMT1 RNAi (y[1] v[1]; P{y[+t7.7] v[+t1.8]=TRiP.HMS06222}attP40/CyO) (Rebalanced stock)	Bloomington Drosophila Stock Center	RRID:BDSC_603563
piggyBac transposase w[1118]; CyO, P{w[+mC]=FRT(w[+])Tub-PBac\T}2/wg[Sp-1]	Bloomington Drosophila Stock Center	RRID: BDSC_8283
w^{1118}	O'Connor-Giles Lab outcrossed line	RRID:BDSC_5905
w ;; act5C-Gal4	Bloomington Drosophila Stock Center	RRID: BDSC_3954
w;; 24B-Gal4	Bloomington Drosophila Stock Center	RRID: BDSC_92172
elav^{C155}-Gal4	Bloomington Drosophila Stock Center	RRID: BDSC_458
w ;; repo-Gal4 (Rebalanced stock)	Bloomington Drosophila Stock Center	RRID: BDSC_7415
w;; alrm-Gal4 (Rebalanced stock)	Bloomington Drosophila Stock Center	RRID:BDSC_67032
w ;; GMR83E12-Gal4	Bloomington Drosophila Stock Center	RRID:BDSC_40363

w ;; GMR56F03-Gal4	Bloomington Drosophila Stock Center	RRID: BDSC_39157
w ;; GMR55B12-Gal4	Bloomington Drosophila Stock Center	RRID:BDSC_39103
w ; moody-Gal4 (Rebalanced stock)	Bloomington Drosophila Stock Center	RRID:BDSC_90883
w ;; c527-Gal4	Bloomington Drosophila Stock Center	RRID:BDSC_90391
Primers		
$TRMT1^{KO}$-gRNA	TTAACTCATCCAAATGGAAG	NA
UAS-V5 TRMT1 FP	GCAGCGGCCGCATGGGTAAGCCTATCCCTAACCCTCTCCTCGGTCTCGATTCTACGGAAGTGGACGAGGAAAAGCCG	NA
UAS-TRMT1 FP	GCAGCGGCCGCATGGAAGTGGACGAGGAA	NA
UAS-TRMT1 RP	GCATCTAGATCACGCAGTCGCCTCCAG	NA
Antibodies		
Mouse, anti-bruchpilot	Developmental Studies Hybridoma Bank	Catalog # nc82 Immunofluorescence [1:100] RRID: AB_2314866
Goat anti-mouse conjugated to Alexa Fluor 488	Thermo Fisher Scientific	Catalog # A-11029 Immunofluorescence [1:500] RRID: AB_2534088
Goat anti-HRP conjugated to Alexa Fluor 647	Jackson ImmunoResearch Laboratories, Inc	Catalog # 123-605-021 Immunofluorescence [1:500] RRID: AB_2338967
Mouse, 8D12 anti-repo	Developmental Studies Hybridoma Bank	Catalog # 8D12 Immunofluorescence [1:50] RRID: AB_528448
Rat, elaV-7E8A10 anti-elav	Developmental Studies Hybridoma Bank	Catalog # 7E8A10 Immunofluorescence [1:100] RRID: AB_525218
Mouse, anti-ATP5A, (mitochondrial marker)	Abcam	Catalog # ab14748 Immunofluorescence [1:100]

		RRID: AB_301447
Goat anti-rabbit GFP polyclonal antibody conjugated to Alexa Fluor488	Thermo Fisher Scientific	Catalog # A11077 Immunofluorescence [1:500] RRID: AB_2534121
Goat anti-rat conjugated to Alexa Fluor568	Thermo Fisher Scientific	Catalog # A11031 Immunofluorescence [1:500] RRID: AB_144696
Goat anti-mouse conjugated to Alexa Fluor647	Thermo Fisher Scientific	Catalog # A21236 Immunofluorescence [1:500] RRID: AB_2535805
Goat anti-mouse IgG AlexaFluor568	Thermo Fisher Scientific	Catalog # A11031 Immunofluorescence [1:500] RRID: AB_144696
Goat anti-mouse IgG2a conjugated to Alexa Fluor 488	Thermo Fisher Scientific	Catalog #A-21131 Immunofluorescence [1:500] RRID: AB_2535771
Mouse, anti-V5 Tag	Thermo Fisher Scientific	Catalog # R960-25 Immunofluorescence [1:500] Western Blot [1:1,000] RRID: AB_2556564
Rabbit, anti-GFP	Rockland Immunochemicals	Catalog # 600-401-215 Western Blot [1:1,000] RRID: AB_828167
Mouse, anti-beta-tubulin	Developmental Studies Hybridoma Bank	Catalog # E7 Western Blot [1:2,000] RRID: AB_2315513
Mouse, anti-syntaxin	Developmental Studies Hybridoma Bank	Catalog # 8C3 Western Blot [1:500] RRID: AB_528484
AffiniPure® Goat Anti-Mouse IgG (H+L)	Jackson ImmunoResearch Laboratories, Inc	Catalog # 115-005-003 Western Blot [1:10,000] RRID: AB_2338447
AffiniPure® Goat Anti-Rabbit IgG (H+L)	Jackson ImmunoResearch Laboratories, Inc	Catalog # 111-005-003 Western blot [1:10,000] RRID: AB_2337913
Chemicals/Commercial kits		
Bouin's fixative	Sigma Aldrich	Catalog # HT10132
Vectashield	Vector Laboratories	Catalog # H-1000-10
ProLong™ Glass Antifade	ThermoFisher Scientific	Catalog #P36980

Mountant		
DAPI Fluoromont-G®	Southern Biotech	Catalog # 0100-20
Bovine Serum Albumin	Sigma Aldrich	Catalog # A7906
Normal Goat Serum	Jackson ImmunoResearch Laboratories, Inc	Catalog # 005-000-121
Triton X-100	Fisher Scientific	Catalog # BP151-100
TRIzol Reagent	Ambion Life Technologies	Catalog # 15596018
SuperSignal™ West Femto Maximum Sensitivity Substrate	ThermoFisher Scientific	Catalog # 34095
Precision Plus Protein Dual Color Standards	BIO-RAD	Catalog # 1610374
2X Laemmli Sample Buffer	BIO-RAD	Catalog # 1610737
2-Mercaptoethanol	BIO-RAD	Catalog #1610710
30% acrylamide/Bis Solution	BIO-RAD	Catalog #1610156
Tetramethylethylene-diamine	BIO-RAD	Catalog # 1610800
Ammonium persulfate	Sigma Aldrich	Catalog # A3678
Tween-20	Fisher Scientific	Catalog # BP337-100
Ponceau S Staining Solution	Research Product International	Catalog # P56200-500
Sucrose	Fisher Scientific	Catalog # BP220-212
Quinine hydrochloride dihydrate	Sigma	Catalog # Q1125-5G
Recombinant DNA/Plasmids		
LD33880 (TRMT1 cDNA Gold Clone)	Drosophila Genomic Resource Center	Catalog # 2317 RRID: DGRC_2317
pUAST-C5	Drosophila Genomic Resource Center	Catalog # 1261 RRID:DGRC_1261
UAS-TRMT1	This study	NA
UAS-V5-TRMT1	This study	NA

Software		
Adobe Illustrator	Adobe Systems	RRID:SCR_010279
ImageJ	NIH	RRID: SCR_003070
Prism	GraphPad Software, Inc	RRID: SCR_002798
NIS-Elements	Nikon	RRID: SCR_002776
ApE Plasmid Editor	https://jorgensen.biology.utah.edu/wayned/ape/	RRID:SCR_014266

Chapter 3 Supplemental Table

Table 3.S1. Complete genotype, sample size and measured absolute values. Full genotypes, raw measurements for nucleotide LC/MSMS, synaptic growth, and gustatory memory studies (mean ± SEM) and the relevant sample size and biological replicates are provided for each panel of Figures 3.2-7, unless otherwise noted. Compared to the respective controls, p values and significance are shown for each figure while other comparisons are noted in the table.

Figure 3.2				
Panel	**Genotype**	**Mean ± SEM**	**n (independent replicates)**	**P value (significance)**
3.2B	*W*^{1118}	14975000 ± 335099	4	Normal distribution (Shapiro-Wilks), Unequal variance Brown-Forsyth ANOVA test with Dunn's multiple comparisons
	W^{1118} ; *TRMT1*^{KO}	205750 ± 40568	4	<0.0001 (****)
	W^{1118} ; *TRMT1*^{sfGFP}	16350000 ± 451848	4	0.1289 (ns) *TRMT1*^{KO} vs *TRMT1*^{sfGFP} 0.0001 (***)
Panel	**tRNA modification**	*TRMT1*^{KO} **Mean log2FC ± SD**	*TRMT1*^{sfGFP} **Mean log2FC ± SD**	**n (independent replicates)**
3.2.C	m2,2G	-6.3 ± 0.5	0.1 ± 0.1	4
	ac4C	-0.4 ± 0.1	0.1 ± 0.1	4
	i6A	-0.3 ± 1.0	-0.3 ± 1.0	4
	Q	-0.1 ± 0.1	0.4 ± 0.1	4

	m2G	- 0.1± 0.1	0.2 ± 0.1	4
	m3C	-0.9 ± 0.0	-0.0 ± 0.1	4
	Gm	-0.0 ± 0.0	0.1 ± 0.1	4
	acp3U	-0.1 ± 0.1	0.1 ± 0.1	4
	m62A	0.0 ± 0.3	-0.0 ± 0.3	4
	m1G	0.1 ± 0.1	0.2 ± 0.1	4
	m1I	0.1 ± 0.1	0.2 ± 0.1	4
	m2A	0.1 ± 0.1	-0.0 ± 0.0	4
	m5C	0.1 ± 0.0	0.1 ± 0.1	4
	mcm5s2U	0.1 ± 0.1	0.1 ± 0.1	4
	Am	0.1 ± 0.1	0.0 ± 0.1	4
	Ψ	0.1 ± 0.1	0.0 ± 0.1	4
	Cm	0.2 ± 0.1	0.0 ± 0.1	4
	m7G	0.2 ±0.1	0.1 ± 0.0	4
	t6A	0.2 ± 0.1	0.0 ± 0.0	4
	Um	0.2 ± 0.1	0.0 ± 0.1	4
	I	0.2 ± 0.3	0.4 ± 0.1	4
	m1A	0.2 ± 0.1	0.0 ± 0.1	4
	ncm5U	0.3 ± 0.1	0.1 ± 0.1	4
	D	0.3 ± 0.1	0.0 ± 0.1	4

	m5U	0.3 ± 0.1	0.2 ± 0.1	4
	m5Um	0.6 ± 0.4	0.1 ± 0.5	4

Figure 3.3

Panel	**Genotype**	**Bouton #**	**n (NMJs, animals)**	**P value (significance)**
3.3D	*W*^{1118}	23.8 ± 0.9	48, 12 animals	Non normal distribution Kruskal-Wallis ANOVA test with Dunn's multiple comparisons
	W^{1118} ; *TRMT1*^{KO}	17.6 ± 0.6	52, 12 animals	<0.0001 (****)
	W^{1118} ; *TRMT1*^{sfGFP}	23.4 ± 0.8	47, 11 animals	>0.9999 (ns) *TRMT1*^{KO} vs *TRMT1 Rescue* < 0.0001 (****)
Panel	**Genotype**	**AZ/Bouton**	**n (NMJs)**	**P value (significance)**
3.3E	*W*^{1118}	15.1 ± 0.6	48, 12 animals	Non normal distribution Kruskal-Wallis ANOVA test with Dunn's multiple comparisons
	W^{1118} ; *TRMT1*^{KO}	18.5 ± 0.6	52, 12 animals	0.0002 (***)
	W^{1118} ; *TRMT1*^{sfGFP}	14.3 ± 0.5	42, 11 animals	>0.9999 (ns) *TRMT1*^{KO} vs *TRMT1 Rescue* < 0.0001 (****)

Figure 3.4

Panel	Genotype	Suppression of PER **Mean ± SD**	n (animals, replicates)	P value (significance)
3.3B	*W^{1118}*	0.6 ± 0.1	85, 3 replicates	Normal distribution (Shapiro-Wilk) Equal variance One Way ANOVA test with Tukey multiple comparisons
	W^{1118} ; TRMT1^{KO}	0.3 ± 0.0	104, 3 replicates	0.0012 (**)
	W^{1118} ; TRMT1^{sfGFP}	0.6 ± 0.1	98, 3 replicates	0.9105 (ns) *TRMT1^{KO}* vs *TRMT1^{sfGFP}* 0.0017 (**)
Figure 3.6				
Panel	**Genotype**	**Bouton #**	**n (NMJs, animals)**	**P value (significance)**
3.6D	*W^{1118} ;; repo-Gal4 (control)*	23.3 ± 0.8	44, 10 animals	Normal distribution (Shapiro-Wilk) Kruskal-Wallis ANOVA test with Dunn's multiple comparisons
	W^{1118} ; TRMT1$^{KO/KO}$; repo-Gal4/+	17.4 ± 0.5	46, 9 animals	<0.0001 (****)
	W^{1118} ; TRMT1$^{KO/KO}$; repo-Gal4/ UAS-TRMT1	23.6 ± 0.7	44, 9 animals	0.9622 (ns) *W^{1118};TRMT1$^{KO/KO}$;repo-Gal4/+* vs *W^{1118};TRMT1$^{KO/KO}$;repo-Gal4/* UAS-TRMT1 < 0.0001 (****)
Panel	**Genotype**	Suppression of PER **Mean ± SD**	**n (animals, replicates)**	**P value (significance)**
3.6E	*W^{1118} ;; repo-Gal4 (control)*	0.6 ± 0.1	92, 3 replicates	Normal distribution (Shapiro-Wilk) Equal variance

				One Way ANOVA test with Tukey multiple comparisons
	W^{1118} ; TRMT1$^{KO/KO}$; repo-Gal4/+	0.3 ± 0.0	94, 3 replicates	0.0009 (***)
	W^{1118} ; TRMT1$^{KO/KO}$; repo-Gal4/ UAS-TRMT1	0.6 ± 0.1	79, 3 replicates	0.9107 (ns) *W^{1118};TRMT1$^{KO/KO}$;repo-Gal4/+* vs *W^{1118};TRMT1$^{KO/KO}$;repo-Gal4/* UAS-TRMT1 0.0012 (**)

Figure 3.7
TRMT1 RNAi glial sub-celltype screen comparisons are between each Gal4 control and RNAi control to the *TRMT1 ^{RNAi}* x respective Gal4 line

Panel	Genotype	Bouton #	n (NMJs, animals)	P value (significance)
3.7B	*W^{1118}; UAS-TRMT1 RNAi / +* (RNAi control)	24.3 ± 0.7	71, 16 animals	Normal distribution (Shapiro-Wilk) Equal variance One Way ANOVA test with Sidak's multiple comparisons
	W^{1118}; c527-GAL4/+	25.6 ± 1.0	40, 8 animals	*W^{1118}; c527-GAL4/+* vs RNAi control >0.9999 (ns)
	W^{1118}; UAS-TRMT1 RNAi / + ; c527-GAL4/+	24.6 ± 1.0	43, 8 animals	0.4718 (ns) *W^{1118}; UAS-TRMT1 RNAi / + ;c527-GAL4/+* vs RNAi control 0.3121 (ns)
	W^{1118}; moody-GAL4 /+	25.6 ± 1.0	31, 7 animals	*W^{1118}; moody-GAL4/+* vs RNAi control 0.9978 (ns)
	W^{1118}; UAS-TRMT1 RNAi /moody-GAL4	24.6 ±1.0	43, 9 animals	>0.9999 (ns) *W^{1118}; UAS-TRMT1 RNAi / + ; moody-GAL4/+* vs RNAi control >0.9999 (ns)

	W^{1118}; 55B12-GAL4/+	23.4 ± 0.8	44, 9 animals	*W^{1118}; 55B12-GAL4/+* vs RNAi control >0.9999 (ns)
	W^{1118}; UAS-TRMT1 RNAi / +; 55B12-GAL4 /+	24.5 ± 1.2	34, 8 animals	>0.9999 (ns) *W^{1118}; UAS-TRMT1 RNAi / + ; 55B12-GAL4/+* vs RNAi control >0.9999 (ns)
	W^{1118}; alrm-GAL4/+	26.1 ± 0.8	47, 10 animals	*W^{1118}; alrm-GAL4/+* vs *W^{1118}; UAS-TRMT1/+* 0.7707 (ns)
	W^{1118}; UAS-TRMT1 RNAi / + ; alrm-GAL4/+	25.4 ± 0.9	44, 9 animals	>0.9999 (ns) *W^{1118}; UAS-TRMT1 RNAi / + ; arlm-GAL4/+* vs RNAi control 0.9982 (ns)
	W^{1118}; 83E12-GAL4/+	23.9 ±0.8	59, 15 animals	*W^{1118}; 83E12-GAL4/+* vs RNAi control >0.9999 (ns)
	W^{1118}; UAS-TRMT1 RNAi / + ; 83E12-GAL4/+	18.0 ± 0.8	45, 13 animals	<0.0001 (****) *W^{1118}; UAS-TRMT1 RNAi / + ; 83E12-GAL4/+* vs RNAi control <0.0001 (ns)
	W^{1118}; 56F03E12-GAL4/+	26.4 ± 0.8	49, 10 animals	*W^{1118}; 56F03-GAL4/+* vs RNAi control 0.5434 (ns)
	W^{1118}; UAS-TRMT1 RNAi / + ; 56F03-GAL4/+	17.8 ±0.6	47, 10 animals	<0.0001 (ns) *W^{1118}; UAS-TRMT1 RNAi / + ; 56F03-GAL4/+* vs RNAi control <0.0001 (ns)
3.7D	*W^{1118} ;; 83E12-Gal4 (control)*	26.0 ± 0.6	53, 10 animals	Normal distribution (Shapiro-Wilk) One Way ANOVA test with Tukey's multiple comparisons
	W^{1118} ; TRMT1$^{KO/KO}$; 83E12-Gal4/+	20.2 ± 0.5	53, 10 animals	<0.0001 (****)
	W^{1118} ; TRMT1$^{KO/KO}$; 83E12-Gal4/ UAS-TRMT1	25.5 ± 0.6	52, 10 animals	0.7562 (ns) *W^{1118};TRMT1$^{KO/KO}$;83E12-Gal4/+* vs *W^{1118};TRMT1$^{KO/KO}$; 83E12-Gal4/*

				UAS-TRMT1 < 0.0001 (****)
Panel	**Genotype**	Suppression of PER **Mean ± SD**	**n (animals, replicates)**	**P value (significance)**
3.7G	*W^{1118} ;; 83E12-Gal4 (control)*	0.8 ± 0.1	25, 1 replicate	Non normal distribution Kruskal-Wallis ANOVA test with Dunn's multiple comparisons
	W^{1118} ; $TRMT1^{KO/KO}$; 83E12-Gal4/+	0.3 ± 0.1	26, 1 replicate	<0.0001 (****)
	W^{1118} ; $TRMT1^{KO/KO}$; 83E12-Gal4/ UAS-TRMT1	0.8 ± 0.1	28, 1 replicate	>0.9999 (ns) *W^{1118};$TRMT1^{KO/KO}$;83E12-Gal4/+* vs *W^{1118};$TRMT1^{KO/KO}$;83E12-Gal4/* UAS-TRMT1 0.001 (***)

Table 3.S2. Complete genotype, sample size and measured absolute values for supplemental figures. Full genotypes, log2foldchange for LC/MSMS, synaptic growth studies, western blots, and gustatory memory studies (mean ± SEM) and the relevant sample size and biological replicates are provided for each panel of Figures 3.S2-S6, unless otherwise noted. Compared to the respective controls, p values and significance are shown for each figure while other comparisons are noted in the table.

Figure 3.S2				
Figure	**Genotype**	**Bouton #**	**n (NMJs, animals)**	**P value (significance)**
3.S2	W^{1118}, male (M)	24.6 ± 0.7	56, 12 animals	Non normal distribution Kruskal-Wallis ANOVA test with Dunn's multiple comparisons W^{1118} M v W^{1118} F >0.9999 (ns)
	$TRMT1^{KO}$, M	16.3 ± 0.6	64, 12 animals	< 0.0001 (****) $TRMT1^{KO}$ M v $TRMT1^{KO/Df}$ M 0.5450 (ns) $TRMT1^{KO}$ M v $TRMT1^{KO}$ F >0.9999 (ns)
	$TRMT1^{KO/Df}$, M	18.1 ± 0.6	64, 12 animals	< 0.0001 (****) $TRMT1^{KO/Df}$ M v $TRMT1^{KO/Df}$ F 0.8485 (ns)
	W^{1118}, female (F)	24.9± 0.7	60, 12 animals	
	$TRMT1^{KO}$, F	17.8 ± 0.6	60, 12 animals	< 0.0001 (****) $TRMT1^{KO}$ F v $TRMT1^{KO/Df}$ F 0.5164 (ns)
	$TRMT1^{KO/Df}$, F	19.6 ± 0.6	49, 11 animals	0.0004 (***)
Figure 3.S3				
Panel	**Genotype**	Suppression of PER **Mean ± SD**	**n (animals)**	**P value (significance)**

3.S3A	*W*^{1118}	0.7 ± 0.0	85, 3 replicates	Normal distribution (Shapiro-Wilk) Equal variance Unpaired t-test
	W^{1118} ; *TRMT1*$^{KO/Df}$	0.3 ± 0.0	104, 3 replicates	0.0003 (***)
Panel	**Genotype, +tastant**	PER **Mean ± SD**	**n (animals)**	**P value (significance)**
3.S3B	*W*^{1118} +sucrose	0.8 ± 0.0	59, 3 replicates	Non normal distribution Kruskal-Wallis ANOVA *W*^{1118} Sucrose vs quinine < 0.0001 (****)
	W^{1118} +quinine	0.2 ± 0.1		
	W^{1118} ; *TRMT1*^{KO} +sucrose	0.9 ± 0.0	66, 3 replicates	*W*^{1118}; *TRMT1*^{KO} Sucrose vs quinine < 0.0001 (****)
	W^{1118} ; *TRMT1*^{KO} +quinine	0.1 ± 0.0		
	W^{1118} ; *TRMT1*^{sfGFP} +sucrose	0.9 ± 0.0	70, 3 replicates	*W*^{1118}; *TRMT1*^{sfGFP} Sucrose vs quinine < 0.0001 (****)
	W^{1118} ; *TRMT1*^{sfGFP} +quinine	0.2 ± 0.0		
3.S3C	*W*^{1118} +sucrose	0.9 ± 0.0	76, 3 replicates	Non normal distribution Kruskal-Wallis ANOVA *W*^{1118} Sucrose vs quinine < 0.0001 (****)
	W^{1118} +quinine	0.0 ± 0.0		
	W^{1118} ; *TRMT1*$^{KO/Df}$ +sucrose	0.8 ± 0.1	77, 3 replicates	*W*^{1118}; *TRMT1*$^{KO/Df}$ Sucrose vs quinine < 0.0001 (****)
	W^{1118} ; *TRMT1*$^{KO/Df}$ +quinine	0.0 ± 0.0		

Figure 3.S5

Panel	Genotype	Normalized GFP (%) **Mean ± SD**	n (replicates)	P value (significance)
3.S5B	*TRMT1^{sfGFP} ; repo-Gal4/+*	100 ± 16.8	4	Normal distribution (Shapiro-Wilk) Equal variance Unpaired t-test
	TRMT1^{sfGFP}/+ ; repo-Gal4/ UAS-TRMT1 RNAi	40.1 ± 12.5	4	0.0012 (**)
Panel	**Genotype**	Average GFP Intensity (%) **Mean ± SD**	**n (cells, animals)**	**P value (significance)**
3.S5C	*TRMT1^{sfGFP} ; repo-Gal4/+*	100 ± 31.3	30, 3 animals	Non normal distribution Mann Whitney t-test
	TRMT1^{sfGFP}/+ ; repo-Gal4/ UAS-TRMT1 RNAi	30.4 ± 16.1	30, 3 animals	< 0.0002 (****)

Panel 3.S5F
TRMT1 RNAi cell-type screen comparisons are between each Gal4 control and RNAi control to the TRMT1 RNAi x respective Gal4 line

Panel	Genotype	Bouton #	n (NMJs, animals)	P value (significance)
3.S5F	*W^{1118}; UAS-TRMT1 RNAi / +* (RNAi control)	23.3 ± 0.6	75, 16 animals	Non normal distribution Kruskal-Wallis ANOVA test with Dunn's multiple comparisons
	W^{1118}; act5C -GAL4 /+	22.3 ± 0.7	62, 12 animals	*W^{1118}; act5C-GAL4/+* vs RNAi control >0.9999 (ns)
	W^{1118}; UAS-TRMT1 RNAi / + ; act5C-GAL4/+	16.8 ± 0.6	57, 11 animals	< 0.0001 (ns) *W^{1118}; UAS-TRMT1 RNAi / + ;act5C-GAL4/+* vs RNAi control <0.0001 (****)
	W^{1118}; repo-GAL4 /+	22.7 ± 0.8	51, 11 animals	*W^{1118}; repo-GAL4/+* vs RNAi control >0.9999 (ns)

	W^{1118}; UAS-TRMT1 RNAi / + ; repo-GAL4/+	15.9 ± 0.6	52, 12 animals	<0.0001 (****) *W^{1118}; UAS-TRMT1 RNAi / + ;repo-GAL4/+* vs RNAi control <0.0001 (****)
	C155-Gal4/+; /+	25.3 ± 1.0	40, 12 animals	*C155-Gal4/+* vs RNAi control >0.9999 (ns)
	C155-Gal4; UAS-TRMT1 RNAi / +	25.2 ± 0.9	45, 12 animals	>0.9999 (ns) *C155-Gal4; UAS-TRMT1 RNAi /+* vs RNAi control >0.9999 (ns)
	W^{1118}; 24B-GAL4 /+	23.1 ± 0.7	56, 11 animals	*W^{1118}; 24B-GAL4/+* vs RNAi control >0.9999 (ns)
	W^{1118}; UAS-TRMT1 RNAi / + ; 24B-GAL4/+	24.9 ± 0.8	51, 12 animals	<0.0001 (****) *W^{1118}; UAS-TRMT1 RNAi / + ; 24B-GAL4/+* vs RNAi control <0.0001 (****)
3.S5G	*W^{1118} ;; repo-Gal4/+ (control)*	26.8 ± 0.6	49, 10 animals	Normal distribution (Shapiro-Wilk) Equal variance One Way ANOVA test with Tukey multiple comparisons
	W^{1118} ; UAS-V5-TRMT1 ; repo-Gal4/+	26.7 ± 0.6	52, 10 animals	0.9971 (ns)
	W^{1118} ; UAS-TRMT1 ; repo-Gal4/+	25.2 ± 0.6	54, 10 animals	0.1478 (ns) *W^{1118} ; UAS-TRMT1 ; repo-Gal4/+ vs W^{1118} ; UAS-V5-TRMT1 ; repo-Gal4/+* 0.1617 (ns)
Panel	**Genotype, +tastant**	PER **Mean ± SD**	**n (animals)**	**P value (significance)**
3.S5H	*W^{1118} ;; repo-Gal4 (control)* +sucrose	0.8 ± 0.0	73, 3 replicates	Non normal distribution Kruskal-Wallis ANOVA Tukey's multiple comparisons *W^{1118} ;; repo-Gal4 (control)* Sucrose vs quinine < 0.0001 (****)

	W^{1118} ;; repo-Gal4 (control) +quinine	0.1 ± 0.0		
	W^{1118} ; $TRMT1^{KO/KO}$; repo-Gal4/+ +sucrose	0.9 ± 0.0	74, 3 replicates	*W^{1118} ; $TRMT1^{KO/KO}$;repo-Gal4/+* Sucrose vs quinine < 0.0001 (****)
	W^{1118} ; $TRMT1^{KO/KO}$; repo-Gal4/+ +quinine	0.1 ± 0.0		
	W^{1118} ; $TRMT1^{KO/KO}$; repo-Gal4/ UAS-TRMT1 +sucrose	0.9 ± 0.0	71, 3 replicates	*W^{1118} ; $TRMT1^{KO/KO}$;repo-Gal4/* UAS-TRMT1 Sucrose vs quinine < 0.0001 (****)
	W^{1118} ; $TRMT1^{KO/KO}$; repo-Gal4/ UAS-TRMT1 +quinine	0.1 ± 0.0		

Figure 3.S6

Panel	Genotype	Bouton #	n (NMJs, animals)	P value (significance)
3.S6D	*W^{1118} ;; 56F03-Gal4 (control)*	27.4 ± 0.7	51, 10 animals	Normal distribution (Shapiro-Wilk) One Way ANOVA test with Tukey's multiple comparisons
	W^{1118} ; $TRMT1^{KO/KO}$; 56F03-Gal4/+	19.8 ± 0.6	46, 9 animals	<0.0001 (****)
	W^{1118} ; $TRMT1^{KO/KO}$; 56F03-Gal4/ UAS-TRMT1	27.2 ± 0.7	50, 10 animals	0.9564 (ns) *W^{1118};$TRMT1^{KO/KO}$; 56F03-Gal4/+* vs *W^{1118};$TRMT1^{KO/KO}$; 56F03-Gal4/* UAS-TRMT1 < 0.0001 (****)

CHAPTER 4

DISCUSSION AND FUTURE DIRECTIONS

ABSTRACT

The field of tRNA research has expanded from single-cell organisms to more complex mammalian systems to understand the dynamic role of these small adaptors that facilitate translation. Proper tRNAs function and stability is reliant on post-transcriptional modifications that can range from a single methyl group to the complex combinations of modifications that occur at the wobble position. Disrupted post-transcriptional tRNA modification has been linked to numerous cancers and neurodevelopmental disorders. While engineered tRNAs are being developed as potential therapeutics; the investigation of tRNA modifying enzymes is an exciting new area of clinical translational research. I highlighted four tRNA methyltransferases linked to disease and the potential to remodel biology through tRNA modifying enzymes (Chapter 1). In subsequent chapters, I used a CRISPR gene editing approach in Drosophila, a robust model organism, to study the impact of disrupted tRNA methylation in the nervous system. I focused on TRMT9B, a putative tRNA methyltransferase and one of two homologs of the yeast wobble uridine methyltransferase Trm9. TRMT9B negatively regulates synaptic growth and function through methyltransferase-dependent and -independent postsynaptic mechanisms, respectively, but does not methylate wobble uridines (Chapter 2). To date, its biochemical function remains a mystery. I also studied TRMT1, which has been linked to intellectual disability in a growing number of patients, and discovered that TRMT1 functions in ensheathing glia to modulate synaptic growth and memory formation (Chapter 3). Here, I will discuss both tRNA methyltransferases in the nervous system in the broader perspective of RNA biology and the contribution of glia-neuron interactions. Finally, I discuss project directions for further exploration of the role of tRNA methyltransferases in the nervous system.

THE TRMT9B PARADOX

Although enriched in the nervous system, to date TRMT9B has been primarily studied in the context of cancer outside the nervous system. High TRMT9B expression in lung, breast, ovarian, and colorectal cancer tumors correlates with improved patient survival (Begley *et al*, 2013; Chen *et al*, 2017; Flanagan *et al*, 2004; Voeghtly *et al*, 2012; Wang *et al*, 2018; Wang *et al*, 2017). Cancer cell lines expressing ectopic human TRMT9B showed decreased tumor growth under hypoxic conditions and a recent study found that TRMT9B is regulated by an mitogen-activated-protein kinase signaling cascade (Begley *et al.*, 2013; Gu *et al*, 2018). While the biochemical function of TRMT9B is unknown, the evolutionary conservation of TRMT9B from yeast to human, makes TRMT9B an attractive candidate to study in flies (Hogan *et al*, 2023; Towns & Begley, 2012). Generation of an *in vivo* genetic model opened the door to exciting new research to discover its mysterious function.

We identified and developed the first *in vivo* loss-of-function model for *TRMT9B*. We found TRMT9B to be a new regulator of synapse formation and function in Drosophila (Chapter 2, (Hogan *et al.*, 2023)). Based on mass spectrometry analysis of bulk RNA nucleosides, TRMT9B is dispensable for the canonical tRNA wobble uridine methylation carried out by its yeast homolog Trm9. Consistent with current literature, we found that this role is carried out by TRMT9B paralog ALKBH8. These results raised the question of whether TRMT9B functions as a methyltransferase or plays a non-enzymatic role. Our structural modeling studies suggest TRMT9B retains methyltransferase function and *in vivo* disruption of key methyltransferase residues prevents TRMT9B rescue of synaptic overgrowth, but not neurotransmitter release. These findings reveal two distinct roles for TRMT9B in the nervous system and point to the functional evolution of Trm9 homologs in metazoans. Our TRMT9B research provides a strong foundation to understand the

role of TRMT9B in the brain. On-going and future biochemical studies using the *in vivo* *TRMT9B*^{KO} models may also assist in solving TRMT9B's unknown biochemical function.

Loss of TRMT9B impacts neuronal translation

To investigate divergent and overlapping roles of the two metazoan Trm9 homologs in the nervous system, we conducted unbiased whole brain RNA-Sequencing (RNA-Seq) and global proteomic studies in *TRMT9B*^{KO} and *ALKBH8*^{KO} adult fly heads. Briefly, proteomics studies in adult fly heads were conducted as described in Chapter 3, while RNA-Seq was conducted through a contract research lab, Novogene using standard Illumina pair-end sequencing. For analysis, proteins were normalized to transcript levels to identify proteins with altered translation. Differentially expressed proteins were identified as those with a p-adjusted value < 0.05 and a log2fold change cut-off of > 0.5 (upregulated) and < -0.5 (downregulated). I conducted GeneOntology of differentially expressed proteins to determine which biological processes or molecular functions were impacted by loss of each protein. For a preliminary analysis, I focused on the top 5 independent GO terms for upregulated and downregulated proteins in *TRMT9B*^{KO} (Fig 4.1A) and *ALKBH8*^{KO} adult head proteomes (Fig 4.2B).

My preliminary analysis suggests that both TRMT9B and ALKBH8 regulate nervous system function through the regulation of translations. Specifically, upregulation of known regulators of synaptic plasticity and neurotransmission (Arc1, VGAT, Futsch), phototransduction signaling opsins (Rh6), and increased sensory perception markers (odorant binding proteins Obp19a, Obp83a) were observed in the absence of *TRMT9B* (Fig 4.C). Similar to yeast Trm9 (Begley *et al*, 2007; Deng *et al*, 2015), *ALKBH8*^{KO} showed downregulation of biological processes and components associated with translation, including many ribosomal subunit proteins. These changes were not

observed in *TRMT9B* mutants, indicating a divergent role. Based on the RNA-Seq and proteomic differences, it will be of interest to also investigate if ALKBH8 rescues TRMT9B phenotypes described in Chapter 2.

We further explored the proteomic datasets for evidence that TRMT9B methylates a subset of Trm9-dependent codons. In yeast lacking *Trm9*, dysregulated proteins are enriched for GAA and AGA codons and GAA/AGA clusters (Deng *et al.*, 2015). For proteins exhibiting decreased translation in our $TRMT9B^{KO}$ samples, I analyzed codon enrichment to identify potential TRMT9B-dependent tRNAs using a previously reported approach (Begley *et al.*, 2007). Interestingly, my preliminary analysis showed that GGA (Z-score of 0.198, p-value of 0.0043) and AAA (Z-score of 0.106, p-value < 0.0006) are over-represented in proteins downregulated in the absence of *TRMT9B* (Fig 4.1D). Refined codon analysis will be required to investigate the impact of clusters of specific codons. This analysis will complement on-going research which supports tissue-specific codon enrichment (Allen *et al*, 2022). Alternative methods to identify codons dependent on TRMT9B include codon reporters in Drosophila (Hudson *et al*, 2021; Stewart *et al*, 2024).

This preliminary codon analysis supports a model in which TRMT9B methylates a small subset of tRNAs that we were unable to observe in our bulk RNA analysis. Excitingly, our endogenously tagged line provides the opportunity to determine if TRMT9B interacts with specific tRNA isodecoders or tRNA fragments *in vivo*. Preliminary RNA-immunoprecipitation studies using a 3XFLAG-tagged TRMT9B line did not detect RNA (data not shown). In contrast, 3XFLAG-tagged TRMT9B system efficiently immunoprecipitated TRMT112, the homolog of obligate yeast Trm9 co-factor Trm112, in protein immunoprecipitation mass spectrometry (IP LC-MS) experiments (Gu *et al.*,

2018). RNA immunoprecipitation studies using a different tagged approach (endogenous C-terminal sfGFP TRMT9B) may provide improved pull-down efficiency for future studies. Alternatively, future sequencing approaches with improved library preparation that take into account steric hindrances from to tRNA modifications (Behrens & Nedialkova, 2022; Behrens *et al*, 2021; Hu *et al*, 2021; Scheepbouwer *et al*, 2023). To complement the multi-omics approach, I would also conduct cell-specific ribosomal profiling (Chen & Dickman, 2017, 2021) in neurons. I expect to identify proteins associated with synapse formation that may open new avenues for *in vivo* genetic interaction studies.

A mysterious methyltransferase with unknown biochemical function

It is also possible that TRMT9B has evolved to methylate a non-tRNA substrate. Recent research has shown broad substrate expansion for Class I S-adenosyl-L-methionine (SAM)-dependent methyltransferases (Abbasi-Moheb *et al*, 2012; Chellamuthu & Gray, 2020; Chen *et al*, 2011; Xu *et al*, 2017). For example, DNA methyltransferase 2 and tRNA methyltransferases 10A methylate both DNA/RNA and mRNA/tRNA, respectively (Jeltsch *et al*, 2017; Ontiveros *et al*, 2020). Additionally, lysine methyltransferase 9, a SAM-dependent methyltransferase that methylates a tRNA mimic, was recently found to also methylate H4 lysine 12 with the co-factor TRMT112 (Metzger *et al*, 2019). We have established collaborations with Dr. Kevin Clark at Tufts University and Dr. Simone Sidoli and Dr. Chandan Guha at Albert Einstein College of Medicine to assess if TRMT9B methylates ribosomal RNA or small proteins through high resolution mass spectrometry approaches, respectively.

While evolution of a non-tRNA substrate is an exciting possibility to examine; TRMT9B may also serve as scaffolding-protein. Our genetic studies elucidated that TRMT9B

regulates synaptic growth and neurotransmission through a methyltransferase domain dependent and independent postsynaptic mechanisms, respectively (Chapter 2, (Hogan *et al.*, 2023)). In Drosophila, careful coordination of pre- and post-synaptic proteins are required to maintain synapse plasticity and function (Ataman *et al*, 2006). If TRMT9B acts as a post-synaptic scaffolding protein, identifying and evaluating protein partners from the pilot protein IP LC-MS data collected using the 3XFLAG-tagged TRMT9B system and which pulled-down TRMT112, triaging for any known post-synapse proteins or signaling mechanisms. This proteomics data set could also be reinforced with IP LC-MS data from pan-neuronal overexpression of our V5-tagged wild-type TRMT9B or V5-TRMT9B with a disrupted methyltransferase domain ($TRMT9B^{MTD}$) transgene system to distinguish protein partners specific to synaptic growth and neurotransmission. Improved Drosophila adult head sample preparation strategies, ranging from adult brain dissections to detergents, may enrich proteomics obtained from central nervous system tissue from cuticle/fat body (Depner *et al*, 2014; Lutzkendorf *et al*, 2025; Nuwal *et al*, 2011; Owald *et al*, 2010; Perlegos *et al*, 2022; Zhang & Nezis, 2022).

The role of TRMT9B in the central nervous system

Future genetic and biochemical studies will be important for further explore the distinct role of TRMT9B in the central nervous system compared to ALKBH8. In flies, mice and human, ALKBH8-driven tRNA methylation modulates selenoprotein synthesis and promote cellular homeostasis (Fu *et al*, 2010; Madhwani *et al*, 2024; Songe-Moller *et al*, 2010). Previous work from our lab demonstrates that ALKBH8 regulates oxidative stress to promote synapse development and memory (Madhwani *et al.*, 2024).

A recent study demonstrate that the disordered C-terminal domain of TRMT9B is a downstream substrate of the oxidative stress-activated mitogen-activated protein kinase

kinase-extraceullar signal regulated kinase-ribosomal protein S6 kinase (MEK-ERK-RSK) signaling cascade (Gu *et al.*, 2018). While mammals have four RSK isoforms, Drosophila have one (SK6II), which has been used as a model system to study the X-linked intellectual disability disorder Coffin-Lowry syndrome (Fischer & Raabe, 2018; Putz *et al*, 2004; Zeniou *et al*, 2002). Notably, SK6II was found to be required for restraining synaptic growth (Beck *et al*, 2015), similar to TRMT9B, and promoting learning and memory (Putz *et al.*, 2004).

To assess memory in the absence of *TRMT9B,* I turned to the aversive gustatory memory assay, described in Chapter 3. Under basal conditions, all lines demonstrate preference for sweet tastants over bitter tastants as expected (Fig 4.2A). I trained flies to associate sweet tastants presented to their tarsi (legs) with a bitter tastant to their proboscis. Following training, wild-type flies exhibit a low proboscis extension reflex (PER) when tested with a sweet tastant (Amrein & Thorne, 2005; Kirkhart & Scott, 2015; Madhwani *et al.*, 2024; Masek & Scott, 2010; Scott, 2005). In *TRMT9B*^{KO} flies, the PER was not suppressed, indicating impaired learning and/or memory compared to wild-type (Fig 4.2B). Reexpression through our endogenous tag (*TRMT9B*^{HA}) approach or through expression of either wild-type TRMT9B or TRMT9B^{MTD} in all neurons restored memory formation (Fig 4.2B-C). These preliminary experiments suggest that TRMT9B's role in learning and memory is methyltransferase-independent. To assess conservation from flies to human, we generated a human TRMT9B transgene. Excitingly, reexpression of human TRMT9B also restored memory in preliminary experiments (Fig 4.2C), and supports conservation of function. Future genetic interaction studies to determine if TRMT9B functions in a pathway with S6KII/RSK to regulate memory will be of interest. Overall, the genetic tools and findings detailed in Chapter 2 and here demonstrate

TRMT9B's key roles in the nervous system and exciting new opportunities for further exploring underlying cellular mechanisms and defining TRMT9B's biochemical function.

TRMT1-DRIVEN TRANSLATION IN GLIA MODULATES NERVOUS SYSTEM DEVELOPMENT AND FUNCTION

The emergence of links between the tRNA methyltransferase, TRMT1, and disrupted neurodevelopmental in humans led us to study its *in vivo* role in the nervous system using a Drosophila model. I found that loss of *TRMT1* in ensheathing glia leads to reduced synapse formation and memory impairment (Chapter 3). Global nervous system proteomic changes in the absence of *TRMT1* point to dysregulated translation of glial pathways, including metabolic homeostasis and phagocytosis. Our data demonstrate Drosophila as a tractable *in vivo* model system to understand TRMT1's role in the nervous system and suggest disrupted glia-neuron interactions may underpin clinical *TRMT1*-linked intellectual disability. Building on our foundational studies, it will be of interest to assess synaptic plasticity through electrophysiological assays and to define TRMT1 protein localization in the adult central nervous system. While synaptic growth and memory impairment observed in *TRMT1* null alleles were linked to ensheathing glia through $TRMT1^{RNAi}$ screens and UAS/Gal4 system for glial subcell types; further localization studies to determine if TRMT1 drives translation in other cell types will be of interest. I would use a genetic approach to co-express our endogenous tagged $TRMT1^{sfGFP}$ with a UAS-mCherry reporter with glial subcell Gal4 drivers.

Glia-neuron interactions modulating synapse function

Drosophila ensheathing glia are similar to mammalian oligodendrocytes and microglia (Freeman & Doherty, 2006). Ensheathing glia are critical for the formation of a diffusion

barrier around synaptic neuropils (Pogodalla *et al*, 2021). While ensheathing glia were recently shown to regulate neuronal activity, through glutamate homeostasis (Otto *et al*, 2018), their primary function is phagocytosis. These specialized cells engulf synapse to maintain function and connectivity through phagocytosis pathways during injury (Bittern *et al*, 2021; Freeman & Doherty, 2006; Logan *et al*, 2012; Macdonald *et al*, 2013; McLaughlin *et al*, 2019; Purice *et al*, 2017; Yildirim *et al*, 2019) and critical periods in development (Hilu-Dadia & Kurant, 2020; Jindal *et al*, 2023; Manaka *et al*, 2004; McLaughlin *et al.*, 2019; Nelson *et al*, 2025). Based on the *TRMT1*^{KO} proteomics and endogenous TRMT1 localization studies, future evaluation of upregulated phagocytic receptors, NimC1 and Eater, would add value to understanding ensheathing glia and glia-neuron communication that regulates synapse formation and memory.

We obtained an overexpression line of an upregulated phagocytic receptor, Eater from the Bloomington Drosophila Stock Center. Future investigations could investigate if overexpression of Eater phenocopies TRMT1 synaptic growth or memory phenotypes. Recent work in Drosophila has also linked disruption of another phagocytic receptor Draper to neurodegeneration and dysregulation of the innate immune system by monitoring vacuolization in the adult brain (Elguero *et al*, 2023; Liu *et al*, 2024). The *TRMT1*^{KO} proteomics dataset supports dysregulation of the immune system, further evaluating morphology changes in the brain in the absence or overexpression of TRMT1 could provide further insight into TRMT1-linked phagocytosis. To study synapse pruning in *TRMT1*^{KO} adult flies, we have also established collaborations with Dr. Heather Broilier at Case Western University.

TRMT1-dependent modifications impact neuronal translation

In addition to understanding genetic interactions and potential molecular mechanisms, it would be of interest to further understand TRMT1-driven translation. TRMT1 is responsible for the m2,2G modifications on many nuclear and mitochondrial tRNAs; however, in flies we see only partial localization with mitochondria at the ventral nerve cord. It would be of interest to determine which mitochondrial tRNAs are modified by Drosophila TRMT1 by primer extension assays. Reverse transcriptase extension is blocked based on the steric hindrance of tRNA modifications. In RNA isolated from *TRMT1*^{KO} adult fly heads compared to control, I would expect to see reverse transcription read through for tRNAs associated with TRMT1 driven m2,2G modifications. Recently 22 mitochondrial tRNAs in Drosophila were identified and annotated; reported 2-dimensional structures are mostly unknown (Marygold *et al*, 2022). Alternative to generation of multiple primers per each tRNA containing a guanosine at position 26, we could investigate modified Drosophila tRNAs through an RNA-Seq approach aimed at improved tRNA library preparation (Behrens & Nedialkova, 2022; Behrens *et al.*, 2021; Hu *et al.*, 2021; Lucas *et al*, 2024; Scheepbouwer *et al.*, 2023; Zhang *et al*, 2025).

To complete the investigation of TRMT1's effect on global mRNA translation, I would complement whole brain proteomics data with RNA-Seq studies and cell-specific ribosomal profiling (Chen & Dickman, 2017, 2021) in glia. I expect identified proteins will provide further insight into how the regulation of translation in ensheathing glia impacts synaptogenesis and memory. Finally, we established a collaboration with Dr. Erik Storkebaum in Radboud University to further understand global changes in proteomics in the absence of *TRMT1* using fluorescent non-canonical amino acid tagging (FUNCAT) approach (Niehues *et al*, 2015).

Using Drosophila a model organism to investigate *TRMT1*-associated intellectual disability

Drosophila is a flexible model system to study human disease (Chow, 2016; Chow & Reiter, 2017). Studies conducted in the *TRMT1* null model are robust and 7 of 11 reported TRMT1 methyltransferase domain missense mutations are conserved in flies (Fig 3.S1, (Efthymiou *et al*, 2025)). To determine the impact of the human pathological variants on nervous system development, I would generate (1) human *TRMT1* transgenes for cell-specific rescue and (2) introduce TRMT1 patient mutations into the Drosophila *TRMT1* locus along with an endogenous tag for following protein localization. I would determine how patient variants impact (1) synaptic growth, synapse function, and short-term memory, (2) TRMT1-patient variant protein stability and localization, and (3) tRNA modifications, tRNA binding, and translation. Work in a *TRMT1* null and *TRMT1*-linked patient mutations could also be used to evaluate other phenotypic changes in flies. My preliminary characterization of *TRMT1* null flies indicates smaller body size (data not shown) and increased lifespan (Fig 4.3A-B). With age, I find that $TRMT1^{KO}$ flies demonstrate a seizure-like phenotype (data not shown). Further evaluation of seizure through mechanical or temperature sensitivity assays (Mituzaite *et al*, 2021) as well as baseline activity through Drosophila Activity Monitors (DAM) (Pfeiffenberger *et al*, 2010; Vecsey *et al*, 2024) will be of interest. At the larval stage, no changes in locomotion were observed (data not shown). As adults, at 1 week old *TRMT1* null flies show impaired locomotor function (climbing ability), although over time, *TRMT1* null flies show improved climbing compared to wild-type flies (Fig 4.3C-D). We established a collaboration with Dr. Dragony Fu to translate our insights from Drosophila to human iPSC-derived cells and organoids. Together, these experiments will yield critical insight into the role of tRNA modification in the nervous system and may identify candidate targets for therapeutic intervention in *TRMT1*-associated intellectual disability.

CONCLUSIONS

Despite their size, ~70-90 nucleotides, tRNA are small but mighty. A growing number of rare tRNA-linked neurodevelopmental disorders have been reported (Abbasi-Moheb *et al.*, 2012; Blocquel *et al*, 2019; Chujo & Tomizawa, 2025a, b; Efthymiou *et al.*, 2025; Monies *et al*, 2019; Nagayoshi *et al*, 2021; Sauter *et al*, 2015; Storkebaum, 2016; Suzuki, 2021; Zhang *et al*, 2020). The underlying molecular mechanisms and reasons for the disproportionate effect on nervous system development and function are poorly understood. tRNA modifying enzymes are highly conserved between Drosophila and humans, providing an exciting opportunity to study how tRNA function is critical to nervous system development. Drosophila studies benefit from extensive genetic tools and a compact nervous system that regulates complex behaviors. Our findings provide insights to the role of a putative tRNA methyltransferase, TRMT9B, which promotes synapse development and function through independent mechanisms. We also found that TRMT1-driven glia-neuron communication is critical for synapse and memory formation. The findings, genetic tools, and multiple-omic datasets in this study advance our understanding of the role of tRNA methyltransferases in the nervous system and establish a path for future *in vivo* investigations of tRNA modifying enzymes.

Chapter 4 References

Abbasi-Moheb L, Mertel S, Gonsior M, Nouri-Vahid L, Kahrizi K, Cirak S, Wieczorek D, Motazacker MM, Esmaeeli-Nieh S, Cremer K *et al* (2012) Mutations in NSUN2 cause autosomal-recessive intellectual disability. *Am J Hum Genet* 90: 847-855

Allen SR, Stewart RK, Rogers M, Ruiz IJ, Cohen E, Laederach A, Counter CM, Sawyer JK, Fox DT (2022) Distinct responses to rare codons in select Drosophila tissues. *Elife* 11

Amrein H, Thorne N (2005) Gustatory perception and behavior in Drosophila melanogaster. *Curr Biol* 15: R673-684

Ataman B, Budnik V, Thomas U (2006) Scaffolding proteins at the Drosophila neuromuscular junction. *Int Rev Neurobiol* 75: 181-216

Beck K, Ehmann N, Andlauer TF, Ljaschenko D, Strecker K, Fischer M, Kittel RJ, Raabe T (2015) Loss of the Coffin-Lowry syndrome-associated gene RSK2 alters ERK activity, synaptic function and axonal transport in Drosophila motoneurons. *Dis Model Mech* 8: 1389-1400

Begley U, Dyavaiah M, Patil A, Rooney JP, DiRenzo D, Young CM, Conklin DS, Zitomer RS, Begley TJ (2007) Trm9-catalyzed tRNA modifications link translation to the DNA damage response. *Mol Cell* 28: 860-870

Begley U, Sosa MS, Avivar-Valderas A, Patil A, Endres L, Estrada Y, Chan CT, Su D, Dedon PC, Aguirre-Ghiso JA *et al* (2013) A human tRNA methyltransferase 9-like protein prevents tumour growth by regulating LIN9 and HIF1-alpha. *EMBO Mol Med* 5: 366-383

Behrens A, Nedialkova DD (2022) Experimental and computational workflow for the analysis of tRNA pools from eukaryotic cells by mim-tRNAseq. *STAR Protoc* 3: 101579

Behrens A, Rodschinka G, Nedialkova DD (2021) High-resolution quantitative profiling of tRNA abundance and modification status in eukaryotes by mim-tRNAseq. *Mol Cell* 81: 1802-1815 e1807

Bittern J, Pogodalla N, Ohm H, Bruser L, Kottmeier R, Schirmeier S, Klambt C (2021) Neuron-glia interaction in the Drosophila nervous system. *Dev Neurobiol* 81: 438-452

Blocquel D, Sun L, Matuszek Z, Li S, Weber T, Kuhle B, Kooi G, Wei N, Baets J, Pan T *et al* (2019) CMT disease severity correlates with mutation-induced open conformation of histidyl-tRNA synthetase, not aminoacylation loss, in patient cells. *Proc Natl Acad Sci U S A* 116: 19440-19448

Chellamuthu A, Gray SG (2020) The RNA Methyltransferase NSUN2 and Its Potential Roles in Cancer. *Cells* 9

Chen C, Huang B, Anderson JT, Bystrom AS (2011) Unexpected accumulation of ncm(5)U and ncm(5)S(2) (U) in a trm9 mutant suggests an additional step in the synthesis of mcm(5)U and mcm(5)S(2)U. *PLoS One* 6: e20783

Chen HM, Wang J, Zhang YF, Gao YH (2017) Ovarian cancer proliferation and apoptosis are regulated by human transfer RNA methyltransferase 9-likevia LIN9. *Oncol Lett* 14: 4461-4466

Chen X, Dickman D (2017) Development of a tissue-specific ribosome profiling approach in Drosophila enables genome-wide evaluation of translational adaptations. *PLoS Genet* 13: e1007117

Chen X, Dickman D (2021) Tissue-Specific Ribosome Profiling in Drosophila. *Methods Mol Biol* 2252: 175-188

Chow CY (2016) Bringing genetic background into focus. *Nat Rev Genet* 17: 63-64

Chow CY, Reiter LT (2017) Etiology of Human Genetic Disease on the Fly. *Trends Genet* 33: 391-398

Chujo T, Tomizawa K (2025a) Mitochondrial tRNA modifications: functions, diseases caused by their loss, and treatment strategies. *RNA* 31: 382-394

Chujo T, Tomizawa K (2025b) Neurological Diseases Caused by Loss of Transfer RNA Modifications: Commonalities in Their Molecular Pathogenesis. *J Mol Biol*: 169047

Deng W, Babu IR, Su D, Yin S, Begley TJ, Dedon PC (2015) Trm9-Catalyzed tRNA Modifications Regulate Global Protein Expression by Codon-Biased Translation. *PLoS Genet* 11: e1005706

Depner H, Lutzkendorf J, Babkir HA, Sigrist SJ, Holt MG (2014) Differential centrifugation-based biochemical fractionation of the Drosophila adult CNS. *Nat Protoc* 9: 2796-2808

Efthymiou S, Leo CP, Deng C, Lin SJ, Maroofian R, Lin R, Karagoz I, Zhang K, Kaiyrzhanov R, Scardamaglia A *et al* (2025) Bi-allelic pathogenic variants in TRMT1 disrupt tRNA modification and induce a neurodevelopmental disorder. *Am J Hum Genet* 112: 1117-1138

Elguero JE, Liu G, Tiemeyer K, Bandyadka S, Gandevia H, Duro L, Yan Z, McCall K (2023) Defective phagocytosis leads to neurodegeneration through systemic increased innate immune signaling. *iScience* 26: 108052

Fischer M, Raabe T (2018) Animal Models for Coffin-Lowry Syndrome: RSK2 and Nervous System Dysfunction. *Front Behav Neurosci* 12: 106

Flanagan JM, Healey S, Young J, Whitehall V, Trott DA, Newbold RF, Chenevix-Trench G (2004) Mapping of a candidate colorectal cancer tumor-suppressor gene to a 900-kilobase region on the short arm of chromosome 8. *Genes Chromosomes Cancer* 40: 247-260

Freeman MR, Doherty J (2006) Glial cell biology in Drosophila and vertebrates. *Trends Neurosci* 29: 82-90

Fu D, Brophy JA, Chan CT, Atmore KA, Begley U, Paules RS, Dedon PC, Begley TJ, Samson LD (2010) Human AlkB homolog ABH8 Is a tRNA methyltransferase required for wobble uridine modification and DNA damage survival. *Mol Cell Biol* 30: 2449-2459

Gu C, Ramos J, Begley U, Dedon PC, Fu D, Begley TJ (2018) Phosphorylation of human TRM9L integrates multiple stress-signaling pathways for tumor growth suppression. *Sci Adv* 4: eaas9184

Hilu-Dadia R, Kurant E (2020) Glial phagocytosis in developing and mature Drosophila CNS: tight regulation for a healthy brain. *Curr Opin Immunol* 62: 62-68

Hogan CA, Gratz SJ, Dumouchel JL, Thakur RS, Delgado A, Lentini JM, Madhwani KR, Fu D, O'Connor-Giles KM (2023) Expanded tRNA methyltransferase family member TRMT9B regulates synaptic growth and function. *EMBO Rep* 24: e56808

Hu JF, Yim D, Ma D, Huber SM, Davis N, Bacusmo JM, Vermeulen S, Zhou J, Begley TJ, DeMott MS *et al* (2021) Quantitative mapping of the cellular small RNA landscape with AQRNA-seq. *Nat Biotechnol* 39: 978-988

Hudson AM, Szabo NL, Loughran G, Wills NM, Atkins JF, Cooley L (2021) Tissue-specific dynamic codon redefinition in Drosophila. *Proc Natl Acad Sci U S A* 118

Jeltsch A, Ehrenhofer-Murray A, Jurkowski TP, Lyko F, Reuter G, Ankri S, Nellen W, Schaefer M, Helm M (2017) Mechanism and biological role of Dnmt2 in Nucleic Acid Methylation. *RNA Biol* 14: 1108-1123

Jindal DA, Leier HC, Salazar G, Foden AJ, Seitz EA, Wilkov AJ, Coutinho-Budd JC, Broihier HT (2023) Early Draper-mediated glial refinement of neuropil architecture and synapse number in the Drosophila antennal lobe. *Front Cell Neurosci* 17: 1166199

Kirkhart C, Scott K (2015) Gustatory learning and processing in the Drosophila mushroom bodies. *J Neurosci* 35: 5950-5958

Liu G, Bandyadka S, McCall K (2024) Protocol to analyze 3D neurodegenerative vacuoles in Drosophila melanogaster. *STAR Protoc* 5: 103017

Logan MA, Hackett R, Doherty J, Sheehan A, Speese SD, Freeman MR (2012) Negative regulation of glial engulfment activity by Draper terminates glial responses to axon injury. *Nat Neurosci* 15: 722-730

Lucas MC, Pryszcz LP, Medina R, Milenkovic I, Camacho N, Marchand V, Motorin Y, Ribas de Pouplana L, Novoa EM (2024) Quantitative analysis of tRNA abundance and modifications by nanopore RNA sequencing. *Nat Biotechnol* 42: 72-86

Lutzkendorf J, Matkovic-Rachid T, Liu S, Gotz T, Gao L, Turrel O, Maglione M, Grieger M, Putignano S, Ramesh N *et al* (2025) Blobby is a synaptic active zone assembly protein required for memory in Drosophila. *Nat Commun* 16: 271

Macdonald JM, Doherty J, Hackett R, Freeman MR (2013) The c-Jun kinase signaling cascade promotes glial engulfment activity through activation of draper and phagocytic function. *Cell Death Differ* 20: 1140-1148

Madhwani KR, Sayied S, Ogata CH, Hogan CA, Lentini JM, Mallik M, Dumouchel JL, Storkebaum E, Fu D, O'Connor-Giles KM (2024) tRNA modification enzyme-dependent redox homeostasis regulates synapse formation and memory. *Proc Natl Acad Sci U S A* 121: e2317864121

Manaka J, Kuraishi T, Shiratsuchi A, Nakai Y, Higashida H, Henson P, Nakanishi Y (2004) Draper-mediated and phosphatidylserine-independent phagocytosis of apoptotic cells by Drosophila hemocytes/macrophages. *J Biol Chem* 279: 48466-48476

Marygold SJ, Chan PP, Lowe TM (2022) Systematic identification of tRNA genes in Drosophila melanogaster. *MicroPubl Biol* 2022

Masek P, Scott K (2010) Limited taste discrimination in Drosophila. *Proc Natl Acad Sci U S A* 107: 14833-14838

McLaughlin CN, Perry-Richardson JJ, Coutinho-Budd JC, Broihier HT (2019) Dying Neurons Utilize Innate Immune Signaling to Prime Glia for Phagocytosis during Development. *Dev Cell* 48: 506-522 e506

Metzger E, Wang S, Urban S, Willmann D, Schmidt A, Offermann A, Allen A, Sum M, Obier N, Cottard F *et al* (2019) KMT9 monomethylates histone H4 lysine 12 and controls proliferation of prostate cancer cells. *Nat Struct Mol Biol* 26: 361-371

Mituzaite J, Petersen R, Claridge-Chang A, Baines RA (2021) Characterization of Seizure Induction Methods in Drosophila. *eNeuro* 8

Monies D, Vagbo CB, Al-Owain M, Alhomaidi S, Alkuraya FS (2019) Recessive Truncating Mutations in ALKBH8 Cause Intellectual Disability and Severe Impairment of Wobble Uridine Modification. *Am J Hum Genet* 104: 1202-1209

Nagayoshi Y, Chujo T, Hirata S, Nakatsuka H, Chen CW, Takakura M, Miyauchi K, Ikeuchi Y, Carlyle BC, Kitchen RR *et al* (2021) Loss of Ftsj1 perturbs codon-specific translation efficiency in the brain and is associated with X-linked intellectual disability. *Sci Adv* 7

Nelson N, Miller V, Broadie K (2025) Neuron-to-glia and glia-to-glia signaling directs critical period experience-dependent synapse pruning. *Front Cell Dev Biol* 13: 1540052

Niehues S, Bussmann J, Steffes G, Erdmann I, Kohrer C, Sun L, Wagner M, Schafer K, Wang G, Koerdt SN *et al* (2015) Impaired protein translation in Drosophila models for Charcot-Marie-Tooth neuropathy caused by mutant tRNA synthetases. *Nat Commun* 6: 7520

Nuwal T, Heo S, Lubec G, Buchner E (2011) Mass spectrometric analysis of synapsins in Drosophila melanogaster and identification of novel phosphorylation sites. *J Proteome Res* 10: 541-550

Ontiveros RJ, Shen H, Stoute J, Yanas A, Cui Y, Zhang Y, Liu KF (2020) Coordination of mRNA and tRNA methylations by TRMT10A. *Proc Natl Acad Sci U S A* 117: 7782-7791

Otto N, Marelja Z, Schoofs A, Kranenburg H, Bittern J, Yildirim K, Berh D, Bethke M, Thomas S, Rode S *et al* (2018) The sulfite oxidase Shopper controls neuronal activity by regulating glutamate homeostasis in Drosophila ensheathing glia. *Nat Commun* 9: 3514

Owald D, Fouquet W, Schmidt M, Wichmann C, Mertel S, Depner H, Christiansen F, Zube C, Quentin C, Korner J *et al* (2010) A Syd-1 homologue regulates pre- and postsynaptic maturation in Drosophila. *J Cell Biol* 188: 565-579

Perlegos AE, Shields EJ, Shen H, Liu KF, Bonini NM (2022) Mettl3-dependent m(6)A modification attenuates the brain stress response in Drosophila. *Nat Commun* 13: 5387

Pfeiffenberger C, Lear BC, Keegan KP, Allada R (2010) Locomotor activity level monitoring using the Drosophila Activity Monitoring (DAM) System. *Cold Spring Harb Protoc* 2010: pdb prot5518

Pogodalla N, Kranenburg H, Rey S, Rodrigues S, Cardona A, Klambt C (2021) Drosophila ss(Heavy)-Spectrin is required in polarized ensheathing glia that form a diffusion-barrier around the neuropil. *Nat Commun* 12: 6357

Purice MD, Ray A, Munzel EJ, Pope BJ, Park DJ, Speese SD, Logan MA (2017) A novel Drosophila injury model reveals severed axons are cleared through a Draper/MMP-1 signaling cascade. *Elife* 6

Putz G, Bertolucci F, Raabe T, Zars T, Heisenberg M (2004) The S6KII (rsk) gene of Drosophila melanogaster differentially affects an operant and a classical learning task. *J Neurosci* 24: 9745-9751

Sauter C, Lorber B, Gaudry A, Karim L, Schwenzer H, Wien F, Roblin P, Florentz C, Sissler M (2015) Neurodegenerative disease-associated mutants of a human mitochondrial aminoacyl-tRNA synthetase present individual molecular signatures. *Sci Rep* 5: 17332

Scheepbouwer C, Aparicio-Puerta E, Gomez-Martin C, Verschueren H, van Eijndhoven M, Wedekind LE, Giannoukakos S, Hijmering N, Gasparotto L, van der Galien HT *et al* (2023) ALL-tRNAseq enables robust tRNA profiling in tissue samples. *Genes Dev* 37: 243-257

Scott K (2005) Taste recognition: food for thought. *Neuron* 48: 455-464

Songe-Moller L, van den Born E, Leihne V, Vagbo CB, Kristoffersen T, Krokan HE, Kirpekar F, Falnes PO, Klungland A (2010) Mammalian ALKBH8 possesses tRNA methyltransferase activity required for the biogenesis of multiple wobble uridine modifications implicated in translational decoding. *Mol Cell Biol* 30: 1814-1827

Stewart RK, Nguyen P, Laederach A, Volkan PC, Sawyer JK, Fox DT (2024) Orb2 enables rare-codon-enriched mRNA expression during Drosophila neuron differentiation. *Nat Commun* 15: 5270

Storkebaum E (2016) Peripheral neuropathy via mutant tRNA synthetases: Inhibition of protein translation provides a possible explanation. *Bioessays* 38: 818-829

Suzuki T (2021) The expanding world of tRNA modifications and their disease relevance. *Nat Rev Mol Cell Biol* 22: 375-392

Towns WL, Begley TJ (2012) Transfer RNA methytransferases and their corresponding modifications in budding yeast and humans: activities, predications, and potential roles in human health. *DNA Cell Biol* 31: 434-454

Vecsey CG, Koochagian C, Reyes M, Sitaraman D (2024) Neural Stimulation during Drosophila Activity Monitor (DAM)-Based Studies of Sleep and Circadian Rhythms in Drosophila melanogaster. *Cold Spring Harb Protoc* 2024: pdb prot108180

Voeghtly LM, Mamula K, Campbell JL, Shriver CD, Ellsworth RE (2012) Molecular alterations associated with breast cancer mortality. *PLoS One* 7: e46814

Wang S, Liu X, Huang J, Zhang Y, Sang C, Li T, Yuan J (2018) Expression of KIAA1456 in lung cancer tissue and its effects on proliferation, migration and invasion of lung cancer cells. *Oncol Lett* 16: 3791-3795

Wang SL, Huang JA, Liu XQ (2017) Mechanism of action of KIAA1456 gene on the proliferation and apoptosis of alveolar epithelial cells. *Eur Rev Med Pharmacol Sci* 21: 600-605

Xu L, Liu X, Sheng N, Oo KS, Liang J, Chionh YH, Xu J, Ye F, Gao YG, Dedon PC *et al* (2017) Three distinct 3-methylcytidine (m(3)C) methyltransferases modify tRNA and mRNA in mice and humans. *J Biol Chem* 292: 14695-14703

Yildirim K, Petri J, Kottmeier R, Klambt C (2019) Drosophila glia: Few cell types and many conserved functions. *Glia* 67: 5-26

Zeniou M, Ding T, Trivier E, Hanauer A (2002) Expression analysis of RSK gene family members: the RSK2 gene, mutated in Coffin-Lowry syndrome, is prominently expressed in brain structures essential for cognitive function and learning. *Hum Mol Genet* 11: 2929-2940

Zhang K, Lentini JM, Prevost CT, Hashem MO, Alkuraya FS, Fu D (2020) An intellectual disability-associated missense variant in TRMT1 impairs tRNA modification and reconstitution of enzymatic activity. *Hum Mutat* 41: 600-607

Zhang K, Manning AC, Lentini JM, Howard J, Dalwigk F, Maroofian R, Efthymiou S, Chan P, Eliseev SI, Yang Z *et al* (2025) Human TRMT1 and TRMT1L paralogs ensure the proper modification state, stability, and function of tRNAs. *Cell Rep* 44: 115092

Zhang Y, Nezis IP (2022) Label-free quantitative proteomic analysis of adult Drosophila heads. *STAR Protoc* 3: 101830

Chapter 4 Figures

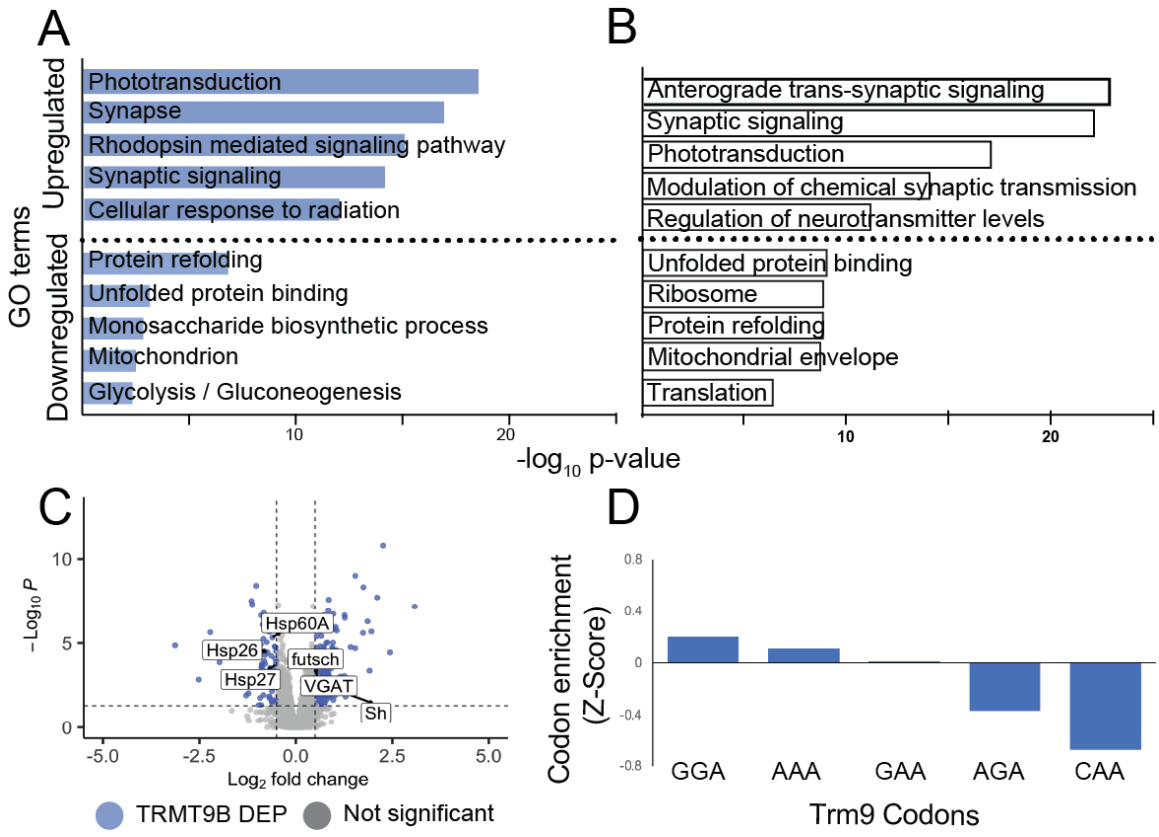

Figure 4.1. Multi-omics approach to study ALKBH8 and TRMT9B in the nervous system

A-B. Trimmed top 5 distinct GeneOntology categories for differentially expressed proteins (|log2fold change| > 1, p-adj < 0.05) in *TRMT9B*^{KO} (A, blue) and *ALKBH8*^{KO} (B, black) adult heads.

C. Volcano plot of differentially expressed proteins (DEP) in TRMT9B^{KO} adult heads.

D. Preliminary Trm9 codon enrichment of downregulated proteins in *TRMT9*^{KO} heads.

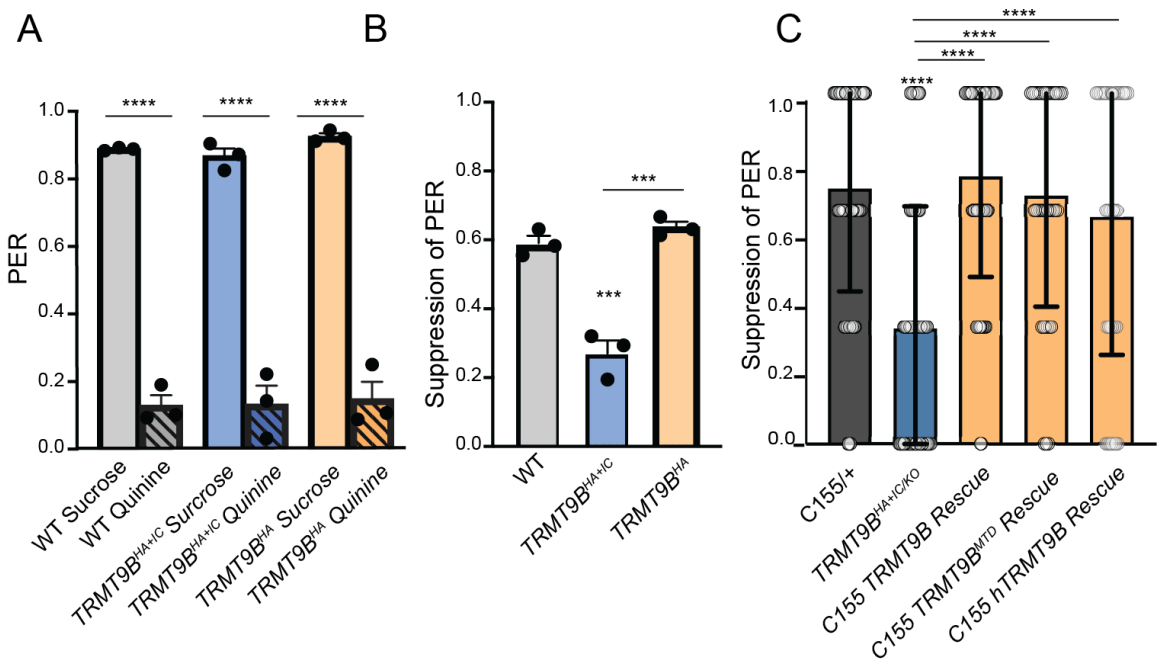

Figure 4.2. TRMT9B promotes short-term memory in a methyltransferase domain independent mechanism

A. All genotypes show expected Proboscis Extension Reflex (PER) or preference when presented with sucrose (solid fill) or quinine (hatch fill). Data points represent the average PER of three biological replicates (w^{1118}: 69, $TRMT1^{HA+IC}$: 63, $TRMT1^{HA}$: 68) from > 20 biological replicates/genotype/experiment. Non parametric with Kruskal-Wallis multiple comparisons ***P < 0.0001 and ns > 0.9999.

B. Quantification of PER suppression of wild type (light grey), $TRMT1^{HA+IC}$ (light blue), and $TRMT1^{HA}$ rescue (light orange) flies. Data points represent average PER suppression of three biological replicates (w^{1118}: 57, $TRMT1^{HA+IC}$: 54, $TRMT1^{HA}$: 56) from > 12 biological replicates/genotype/experiment. ANOVA with Tukey's multiple comparison ****P < 0.0004, ns = 0.4778.

C.Quantification of PER suppression of C155/+ (dark grey), $TRMT1^{HA+IC/KO}$ (dark blue), and pan-neuronal TRMT9B rescue, pan-neuronal TRMT9B methyltransferase dead and pan-neuronal human TRMT9B rescue (dark orange) flies. Data points represent PER

suppression of two independent experiments (C155/+: 85, C155/+;; *TRMT1*$^{HA+IC/KO}$ 67, C155/+;; *TRMT1*^{KO}*/ UAS-TRMT9B, TRMT9B*$^{HA+IC}$ 65, C155/+;; *TRMT1*^{KO}*/ UAS-TRMT9B*^{MTD}*, TRMT9B*$^{HA+IC}$ 39; C155/+;; *TRMT1*^{KO}*/UAS-human TRMT9B, TRMT9B*$^{HA+IC}$ 38) from > 15 biological replicates/genotype/experiment. Non parametric with Kruskal-Wallis multiple comparisons ****P < 0.0001 and ns > 0.9999.

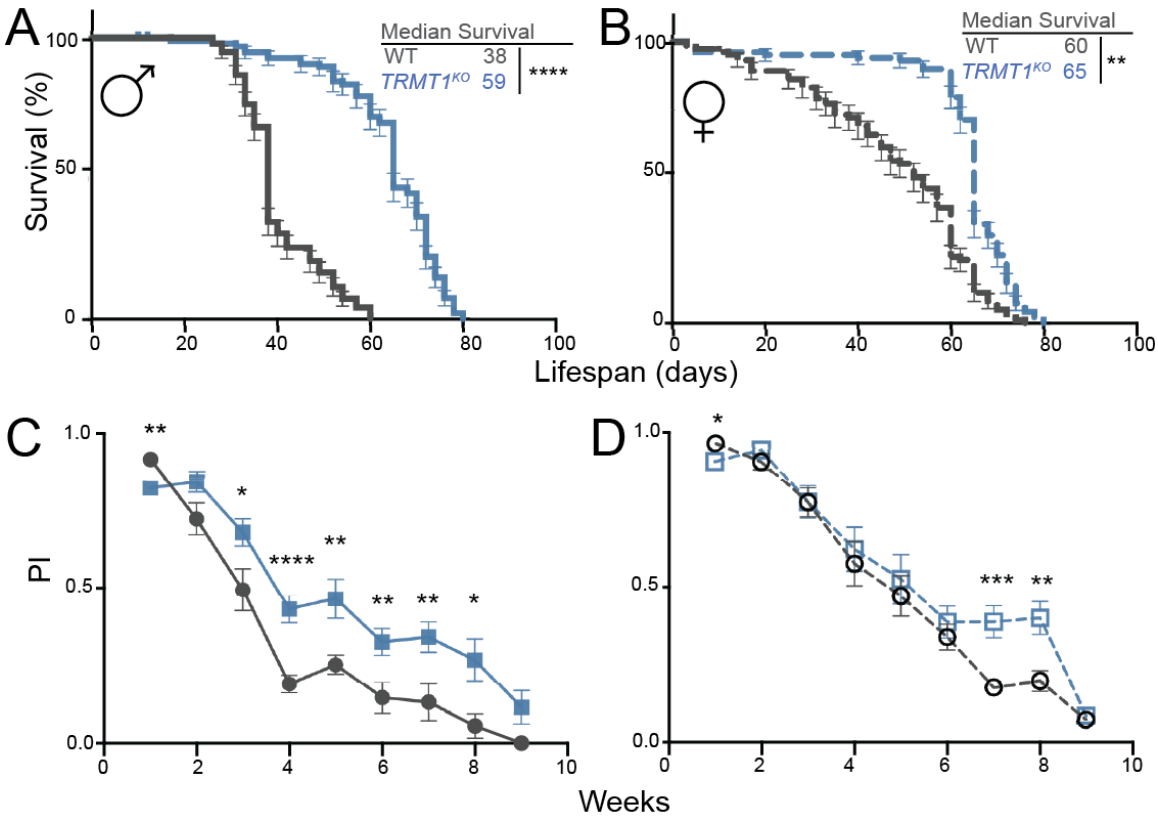

Figure 4.3. TRMT1 impacts lifespan and adult locomotor function

A-B. (A) *TRMT1*^{KO} in males (blue, solid line, N = 284, mean survival of 59 days) extends lifespan by 55% compared to wild-type (grey, solid line, N = 294, mean survival of 38 days; Log-rank ****P <0.0001). (B) *TRMT1*^{KO} in females (blue, dashed line, N = 291 flies, mean survival of 65 days) shows an 8% change in lifespan compared to wild-type (grey dashed line, N = 286 flies, mean survival of 65 days; Log-rank **P = 0.0044)

C. Quantification of adult locomotor function by a climbing performance index (PI). At 1 week *TRMT1*^{KO} flies show decreased climbing ability at week 1 and improved climbing with age in males (C) and females (D) compared to controls. (Males: Multiple Man-Whitney tests ****P <0.0001, **P <0.0091, *P <0.0171, and ns = 030646; Females: Multiple Man-Whitney test ***P = 0.0009, **P =0.0056, *P = 0.0157, and ns >0.2072).